

Electrostimulation Contingencies and Attention, Electrocortical Activity and Neurofeedback

By

Jean-Lon Chen

A thesis submitted to

Goldsmiths, University of London

For the degree of

DOCTOR OF PHILOSOPHY

Psychology Department

Goldsmiths, University of London

March 2013

ABSTRACT

There is a growing body of evidence for diverse ways of modulating neuronal processing to improve cognitive performance. These include brain-based feedback, self-regulation techniques such as EEG-neurofeedback, and stimulation strategies, alone or in combination. The thesis goal was to determine whether a combined strategy would have advantages for normal cognitive function; specifically operant control of EEG activity in combination with transcutaneous electro-acustimulation.

In experiment one the association between transcutaneous electro-acustimulation (EA) and improved perceptual sensitivity was demonstrated with a visual GO/NOGO attention task (Chen et al, 2011). Furthermore reduced commission errors were related to an electrocortical motor inhibition component during and after alternating high and low frequency EA, whereas habituation in the control group with sham stimulation was related to different independent components.

Experiment two applied frequency-domain ICA to detect changes in EEG power spectra from the eyes-closed to the eyes-open state (Chen et al, 2012). A multiple step approach was provided for analysing the spatiotemporal dynamics of default mode and resting state networks of cerebral EEG sources, preferable to conventional scalp EEG data analysis. Five regions were defined, compatible with fMRI studies.

In experiment three the EA approach of Exp I was combined with sensorimotor rhythm (SMR) neurofeedback. SMR training improved perceptual sensitivity, an effect not found in a noncontingent feedback group. However, non-significant benefits resulted from EA. With ICA spectral power analysis changes in frontal beta power were associated with contingent SMR training. Possible long-term effects on an attention network in the resting EEG were also found after SMR training, compared with mock SMR training.

In conclusion, this thesis has supplied novel evidence for significant cognitive and electrocortical effects of neurofeedback training and transcutaneous electro-acustimulation in healthy humans. Possible implications of these findings and suggestions for future research are considered.

ACKNOWLEDGEMENTS

I would first like to thank my supervisor Professor John Gruzelier for his continuous guidance, sound advice and prompt responding whenever his input was necessary. I would also like to thank Professor Jane Powell, Professor Pamela Heaton, and Dr. Karina Linnell for their important help in the early stages of my research.

Many thanks to Dr. Tomas Ros and Dr. Trevor Thompson for the statistical and technical programming assistance, and also to Professor Juri Kropotov for sharing his WinEEG expertise with me and for the fruitful collaboration we had in the first experiment of this thesis. Special thanks to all the members of the ITC lab and mostly to Tony Steffert, Beverly Steffert, David Mayor, and Joseph Leach for their assistance in understanding the important aspects of neurofeedback practice and EEG research.

I have to express my sincere thanks to all my participants. Without their help, this thesis would not have been possible. Of course, I appreciate all special support from my colleagues and bosses in the Department of Physical Medicine and Rehabilitation of Chang Gung Memorial Hospital in Taiwan. All experiments were supported by Grants from School of Medicine, Chang Gung University & Department of Physical Medicine and Rehabilitation, Chang Gung Memorial Hospital, Taiwan (CMRPG350811, CMRPG350812, CMRPG350813, CMRPG350814).

Lastly, but more importantly, I would like to thank my family, Carl Chen and all my friends who supported me and kept me on track throughout the course of my studies.

LIST OF ABBREVIATIONS

ADHD	attention deficit hyperactivity disorder
AE	electro-acustimulation with alternating high and low frequencies
ANOVA	analysis of variance
BSS	Blind source separation
CNS	Central nervous system
COM	commission errors
CPT	Continuous Performance Test
<i>d</i>	Cohen's <i>d</i>
<i>d'</i>	D Prime
DMN	default mode network
DAN	dorsal attention network
EA	transcutaneous electro-acustimulation
EC	Eyes closed
EEG	Electroencephalogram
EO	Eyes open
EOG	Electro-oculogram
ERP	Event-related potential
Exp I	Experiment one
Exp II	Experiment two
Exp III	Experiment three
FFT	Fast Fourier transform
Hz	hertz

ICA	Independent component analysis
ICs	Independent components
ISC	instrumental SMR conditioning
LE	electro-acustimulation with low frequency
min	minute
ms	millisecond
MNI	Montreal Neurological Institute
NFT	neurofeedback training
NSP	Normalized spectral power
OM	omission errors
Post	post-treatment
PR	Power ratio
Pre	pre-treatment
QEEG	Quantitative EEG
RSNs	resting state networks
RT	Reaction time
RTV	Reaction time variability
SD	Standard deviation
SE	sham electro-acustimulation
sec	second
SMR	sensorimotor rhythm
SP	Spectral power
μ V	microvolt

CONTENTS

Abstract	2
Acknowledgement	3
List of Abbreviations	4
CHAPTER 1 BACKGROUND	12
1.1 Overview of Research Aims	13
1.2 Physiological Basis of the Electroencephalography (EEG)	17
1.2.1 Brief History of the Discovery of the EEG	17
1.2.2 EEG generation	18
1.2.2.1 A. Post-synaptic potentials in cortical pyramidal neurons	18
1.2.2.2 B. Thalamocortical networks	19
1.2.2.3 C. Local-scale and large-scale synchronization	20
1.2.3 Normative EEG Spectrum	21
1.2.3.1 Delta band (1-4 Hz)	22
1.2.3.2 Theta band (4-8 Hz)	22
1.2.3.3 Alpha band (8-12 Hz)	23
1.2.3.4 Sensorimotor rhythm (SMR, 12-15 Hz)	24
1.2.3.5 Beta band (15-36 Hz)	25
1.2.3.6 Gamma band (36-44 Hz)	26
1.2.4 Artefacts	26
1.2.4.1 Muscle artefact	27
1.2.4.2 Skin artefact	30
1.2.4.3 Eye movement and eye blinking artefacts	31
1.2.4.4 ECG artefact (electrocardiogram, ECG or EKG)	33
1.2.4.5 Respiration artefact and tongue movement	33
1.2.4.6 Electrical interference from the environment	33
1.2.5 Summary	34
1.3 From Quantitative Analysis of EEG to Source Localization Techniques	35
1.3.1 Quantitative EEG (QEEG)	37
1.3.1.1 Spectral analyses	38
1.3.1.2 Coherence analyses	39
1.3.1.3 Time-frequency analyses	41
1.3.2 Blind Source Separation (BSS)	42
1.3.3 Independent Component Analysis (ICA)	43

1.3.3.1 Statistical independent	45
1.3.3.2 Nongaussian distribution	46
1.3.3.3 Infomax ICA algorithm	46
1.3.3.4 Application of ICA in EEG and ERP	48
1.3.4 Source Localization Techniques	50
1.3.4.1 Equivalent dipole approaches (Dipole Source Modelling)....	50
1.3.4.2 Linear distributed source localization techniques	51
1.3.4.2.1 Minimum norm solutions	52
1.3.4.2.2 Weighted Minimum norm solutions	53
1.3.4.2.3 Low resolution Electromagnetic Tomography (LORETA)	54
1.3.4.2.4 Variable resolution electromagnetic tomography (VARETA)	57
1.3.4.2.5 Simulation studies comparing different distributed inverse solutions	57
1.3.5 Summary	59
1.4 Event-related potential (ERP)	61
1.4.1 Late positive components in ERPs	63
1.4.1.1 P3a component	65
1.4.1.2 P3b component	66
1.4.1.3 Visual continuous performance task (VCPT)	67
1.4.2 ERP components in the selective attention and executive control ...	68
1.4.2.1 ERP components in the engagement and disengagement operations	69
1.4.2.1.1 Sensory comparison component	70
1.4.2.1.2 Motor inhibition component	71
1.4.2.1.3 Action suppression	71
1.4.2.2 ERP components in the monitoring operation	72
1.4.2.2.1 P400 monitoring component	73
1.4.2.2.2 Function of ACC	73
1.4.3 Summary	74
1.5 Brief History of Acupuncture	75
1.5.1 General application of acupuncture and electroacustimulation (EA)	76
1.5.2 Effects of EA stimulation on EEG/ERP and attention	79
1.6 Introduction of functional connectivity and functional networks	82
1.6.1 Resting state networks (RSNs) and default mode network (DMN)...	84
1.6.2 Dorsal attention network (DAN)	86
1.7 Neuroplasticity and learning	87
1.7.1 Activated states for learning	88

1.7.2 A neurochemical for motor learning – Dopamine	88
1.7.3 Exogenous stimulation for the release of dopamine to enhance learning	91
1.7.4 Attention and vigilance	94
CHAPTER 2 AIMS	96
CHAPTER 3 EXPERIMENT ONE	101
3.1 Introduction	101
3.1.1 Proposed Mechanisms of Acupuncture	101
3.1.2 Proposed Mechanisms of EA and TENS	102
3.1.2.1 Short-term effects of EA and TENS	103
3.1.2.2 Long-term effects of EA and TENS	104
3.1.3 Hypotheses for Experiment One	106
3.2 Materials and Methods of Experiment One	108
3.2.1 Subjects	108
3.2.2 Experimental Design	109
3.2.3 Procedure	111
3.2.3.1 Attention paradigm	111
3.2.3.2 EEG recordings and pre-treatment of EEG	113
3.2.3.3 Data management: ICA and standardized low-resolution brain electromagnetic tomography (sLORETA)	113
3.2.3.4 Data management: Behavioural dependent variables	115
3.2.3.5 Statistical analysis	115
3.3 Results of Experiment One	117
3.3.1 Hypothesis 1: Sustained effects on perceptual sensitivity in attention	117
3.3.1.1 Perceptual sensitivity	117
3.3.1.2 Sustained stimulation effects	121
3.3.2 Hypotheses 2 and 3: Sustained effects on visual attention	
ERP latency and amplitude	125
3.3.2.1 Visual attention ERP latency and amplitude	125
3.3.3 Hypothesis 4: Decomposed independent components (ICs) of visual attention ERPs	129
3.3.3.1 Components of visual attention ERPs	129
3.3.3.2 Sustained stimulation effects	129
3.3.4 Hypothesis 5: Decomposed components will correlate with habituation after the repetition of the visual attention task	134
3.3.4.1 Decomposed components correlated with habituation	134
3.3.4.2 Components with significant differences due to task repetition	136

3.4 Discussion of Experiment One	141
3.5 Summary	151
CHAPTER 4 EXPERIMENT TWO	152
4.1 Introduction	152
4.1.1 The introduction of experiment two	152
4.1.2 Aims for experiment two	156
4.2 Methods of Experiment Two	159
4.2.1 Subjects	159
4.2.2 Design	159
4.2.3 Procedure	160
4.2.3.1 Independent component (ICA) and spectral power analysis	160
4.2.3.2 EEG recordings and pre-processing of EEG	162
4.2.3.3 Source localization analysis	163
4.2.3.4 Computation of Mean Regional Correlation Matrix and Graph Analysis	166
4.2.3.5 Clustering of ICA components	168
4.3 Results of Experiment Two	170
4.3.1 Aim 1: The application of group ICA to extract independent components (ICs) from epoch-wise alpha-band power	170
4.3.1.1 Extract independent components	170
4.3.1.2 Epoch-wise alpha-band power	170
4.3.2 Aim 2: The application of sLORETA for cortical source localization of the ICs	171
4.3.2.1 sLORETA and cortical source localisation	171
4.3.3 Aim 3: The application of graph theory for functional connectivity estimation	173
4.3.3.1 Graph theory	173
4.3.3.2 Functional connectivity	174
4.3.4 Aim 4: circumscribing IC similarity measures via hierarchical cluster analysis	176
4.3.4.1 Hierarchical cluster analysis	176
4.3.4.2 Circumscribing IC similarity	179
4.3.5 Aim 5: circumscribing IC similarity measures via multi-dimensional scaling (MDS)	181
4.3.5.1 Multi-dimensional scaling (MDS)	181

4.4	Discussion of Experiment Two	183
4.5	Summary	194
CHAPTER 5 EXPERIMENT THREE		196
5.1	Introduction	196
5.1.1	Neurofeedback	196
5.1.2	EEG-based neurofeedback	199
5.1.3	Neurofeedback and Attention	203
5.1.4	The effect of neurofeedback and electrostimulation on attention and the EEG	208
5.1.5	Assessment of Neurofeedback Learning	209
5.1.6	Aims and hypotheses for Experiment Three	211
5.2	Methods of Experiment Three	214
5.2.1	Subjects	214
5.2.2	Design	215
5.2.3	Procedure	217
5.2.3.1	Instrumental Conditioning Procedure (SMR training) and associated apparatus	217
5.2.3.2	The setting of non-contingent SMR training in the control group	220
5.2.3.3	Visual Attention Task -- the Test of Variables of Attention (T.O.V.A)	220
5.2.4	Resting EEG recordings, pre-processing of EEG, independent component (ICA) and spectral power analysis	222
5.2.5	Source localization analysis, Graph Analysis and Clustering of ICA components	225
5.2.6	Statistical analysis	226
5.2.6.1	Behavioural measurements of attention performance in 4 groups (hypothesis 1)	226
5.2.6.2	EEG outcome measurements of SMR training in 4 groups (hypotheses 2-4)	227
5.3	Results of Experiment Three	229
5.3.1	Hypothesis 1	229
5.3.1.1	Perceptual sensitivity	229
5.3.2	Hypothesis 2	237
5.3.2.1	EEG measurements in the baseline period	237
5.3.3	Hypothesis 3	247

5.3.3.1 EEG measurements in the feedback period	247
5.3.4 Hypothesis 4	255
5.3.4.1 Relative SMR and theta activity	255
5.3.5 Hypothesis 5	260
5.3.5.1 Conventional EEG comparisons for 19 channels, pre- vs. post- SMR training	260
5.3.5.2 Group ICA as a valid method for extracting ICs in the resting state EEG	264
5.3.6 Hypothesis 6	269
5.3.6.1 The five circumscribed functional regions, across subjects ...	269
5.3.6.2 A comparison of the changes in spectral power in the relevant regions of the resting EEG state, pre- and post- SMR training	271
5.3.6.3 Beta power in the frontal region	271
5.3.6.4 Theta and SMR power in the central region	276
5.4 Discussion of Experiment Three	282
5.4.1 Limitations and future studies	293
5.5 Summary	295
CHAPTER 6 GENERAL DISCUSSION AND CONCLUSIONS	296
6.1 Evaluation of Results in Relation to the Aims of the Thesis	296
6.1.1 Transcutaneous electrical acustimulation and frequency modulation	296
6.1.2 ICA-based EEG functional connectivity in the resting state	299
6.1.3 The effect of Neurofeedback training and electrocortical findings refined by the ICA-based approach	301
6.1.4 Does EA stimulation have a measurable effect in assisting SMR training?	303
6.2 Implications of this Thesis	306
6.2.1 Transcutaneous Electrical Acustimulation and its application ...	306
6.2.2 SMR training	308
6.2.3 The combination of NF assisted by EA	314
6.3 Methodological Limitations and Future Directions	317
6.4 Final Conclusions	320
REFERENCES	321
APPENDICES (The Publication List)	359

CHAPTER 1 BACKGROUND

This chapter will serve to introduce a knowledge base of the historical origin and significantly developed analytic methods, including the topics of the electroencephalograph (EEG), EEG rhythm and current quantitative methods for analysing the EEG. This chapter also provides the concepts of EEG artefact rejection, quantitative EEG (qEEG), and then the independent component analysis (ICA) method, developed in order to optimize clinical and research applications of the EEG. Other relevant background issues of the three experiments, for example, acupuncture, electroacustimulation (EA), and neurofeedback training (NFT), will be introduced in the next three chapters respectively.

1.1 Overview of Research Aims

The thesis rests upon the principle that the brain, and the central nervous system (CNS) as a whole, has an extraordinary capacity to be changed by exogenous stimulation, and endogenously regulate itself. Moreover, as is well-known plasticity is an essential characteristic par excellence in the evolution of the brain for which it relies on its basic constituents, the neurons. The flexibility of the CNS provides an advantage in the most important brain function: the principle of adaptation to local conditions. In fact, to learn is ultimately to adapt.

Firstly, the ‘hardware’ or neural circuitry of brain will be considered, describing the generation of ‘brain electrophysiological activity’ within brain regions. Following this, the way in which exogenous and endogenous factors are thought to enhance or inhibit this hardware to influence brain function or behavioural performance will be considered along with consideration of ‘reliable functional imaging suited to address the dynamics of brain source activity’. The EEG provides a non-invasive method of recording the voltage differences of scalp potentials created by cerebral sources. Only the EEG has the sufficient time resolution (sampled at a high rate, typically 256 Hz or more) to capture the macroscopic dynamics of brain activation and synchronization (Delorme et al., 2002).

Furthermore, the EEG inverse technique, known by the mathematical method for recovering the locations and activities of brain processes from these locations, has been developed to face the problem of reconstructing the intracranial brain sources from the observed EEG signals, and to separate the generated EEG processes which overlap both in time and space, becoming inextricably mixed in EEG recordings. Here in the thesis the new statistical technique, ICA, is applied to separate EEG mixed

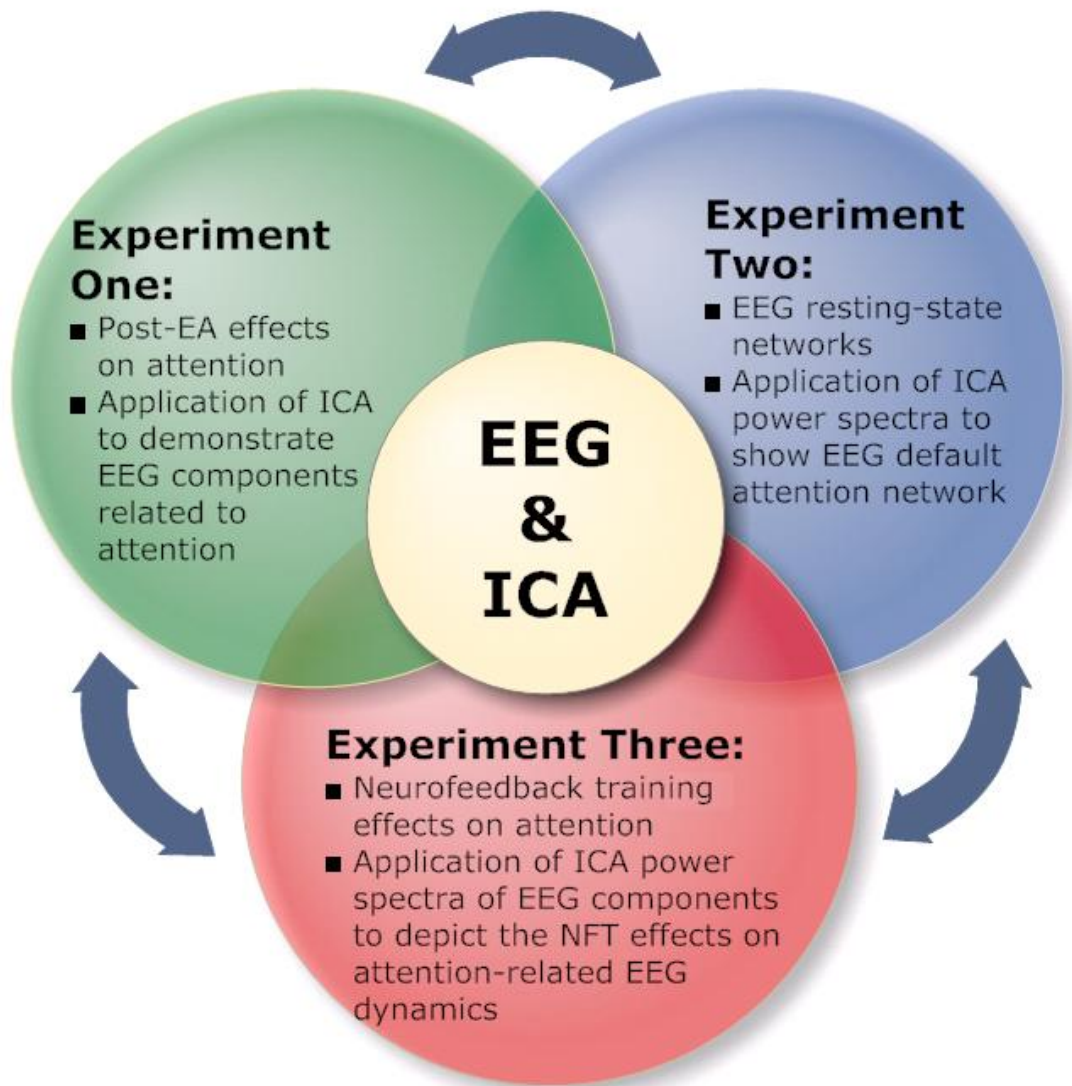
sources and artefacts at scalp electrodes (Bell and Sejnowski, 1995; Makeig, et al., 1996).

Recently, the functional organization of the brain's resting state is conceived of in terms of resting state networks (RSNs) and default mode networks (DMNs), clusters of mostly cortical regions, inter-connected anatomically and functionally (e.g., Damoiseaux et al., 2006; Mantini et al., 2007). In addition, the study of RSNs has shifted its focus from the localization of specialized brain activations to the interpretation of inter-relationships in brain dynamics (e.g., Mantini, et al., 2007). A main advantage of eyes-closed (EC) and eyes-open (EO) resting state protocols is that they may be carried out without requiring subjects to perform a specific task, and therefore be easily deployed in clinical settings. The EEG-alpha rhythm is the predominant component in the resting states. Therefore, EEG alpha power correlation-based RSNs, resolved with ICA and power spectral analysis, may provide a useful measure of functional connectivity, since resting-state connectivity has been shown to correlate with behavioural performance and cognitive measures (for a review, see Greicius, 2008).

Then, the last experiment focuses on combining exogenous stimulation and endogenous self-regulation strategies EA and NFT. The aim of this thesis is to provide a framework of converging evidence which logically supports the use of a variety of modern neuromodulation techniques such as neurofeedback towards “optimizing” the neurocognitive mechanisms and functional networks responsible for the enhanced performance of cognitive function.

Three designed experiments with their relationship and explicit aims are depicted by the Venn diagram.

The correlation of three experiments



The thesis is organized into six chapters. Chapter 1 provides the background information about the EEG and the analytic methods with which to deal with offline EEG. Chapter 2 gives the aims of each experiment, towards the main goal of this thesis namely the validation of the enhanced cognitive function by exogenous and endogenous stimulations. Chapter 3 for Exp I depicts the EA (exogenous) stimulation effects on attention, and the benefit of using the ICA method for analysing EEG components of repetitive attention tasks. Chapter 4 presents EEG-alpha associated networks in the resting states, compared with current fMRI research for RSN and DMN, in order to demonstrate the functional networks found in the EEG recordings. The applications of EEG RSNs found in the neurological signals and research are also mentioned. In Chapter 5, the theory of neurofeedback training (NFT) for enhancing cognitive function (the endogenous factor) and the role of EA for assisting NFT are analysed by ICA power spectra and QEEG ratio studies. Chapter 6 provides the general discussion and conclusions according to the results obtained by the three experiments.

1.2 Physiological Basis of the Electroencephalography (EEG)

This section provides the brief history of the discovery of the EEG, an introduction to the electrophysiology of the EEG, and the various types of electrical activity that are generated in the brain (commonly referred to as “brain waves”). Importantly, the study of the basic mechanism of brain rhythms informs our understanding of the underlying processes of neuronal networks within the human brain.

1.2.1 Brief History of the Discovery of the EEG

Richard Caton, discovered electrical brain signals by probing directly on the surface of exposed brains of animals, and published his results in 1875 (Caton, 1875; Haas, 2003). In 1924, Hans Berger, a German psychiatrist, performed the first EEG recording in humans (Haas, 2003; Jasper and Carmichael, 1935), and discovered the existence of rhythmic activity oscillating at approximately 10 Hz, particularly during relaxed wakefulness, and described the alpha waves for the first time. Berger was also the first researcher to suggest that the periodic fluctuations of the human EEG may be associated with mental processes and consciousness. Over the years, because of developments in data collection (EEG recording) and analyses, the EEG has become one of the prime techniques for studying the human brain. To understand these developments in the EEG field it will first be necessary to detail the physiological basis of the EEG signal. Subsequently, important issues associated with data acquisition, signal processing, artefact rejection, and quantitative analyses will be introduced.

1.2.2 EEG generation.

The brain's neurons transmit electrical currents to each other along dendrites and axons. Electrical current is a flow of charged particles through chemical conduction that make up the current in a nerve impulse. However, even if the current has not yet occurred, the potential for a current flow is still there. The term "potential" is a technical term here and refers to the separation of charges between two places. In other words, the greater the initial potential, the stronger the current will be when it is released. In contrast, if there is no potential, no current will flow. EEG records summated extracellular field potentials from large pyramidal neurons in the cerebral cortex.

1.2.2.1 A. Post-synaptic potentials in cortical pyramidal neurons

The "field potentials" reflected in the scalp-recorded EEG mainly originate from oscillations in dendritic transmembrane currents. The neural membrane can be either excited (depolarized) or inhibited (hyperpolarized), resulting in excitatory post-synaptic potentials (EPSP) or inhibitory post-synaptic potentials (IPSP) respectively (Cantor, 1999). For example, excitation of the neural membrane caused by excitatory neurotransmitters, such as acetylcholine, changes the neural cell membrane's permeability to sodium ions in the extracellular fluid. The resulting influx of positive charge creates an EPSP. Enough inputs from a summation of EPSPs are sufficient to trigger a corresponding axonal action potential (Cantor, 1999; W. J. Freeman, 1999). However, inhibitory neurotransmitters, such as gamma amino butyric acid (GABA), work by increasing the membrane's permeability to negatively charged ions, which causes the intracellular negativity. Thus, neural cells become inhibited from firing and an IPSP is created (Cantor, 1999; W. J. Freeman, 1999).

Billions of individual action potentials, the summation of IPSP and EPSP field potentials from large groups of cortical neurons, make up the rhythmic EEG phenomena (Niedermeyer, 1987).

The oscillatory activity recorded at the scalp is the sum of electrical field potentials generated by cortical neurons in the proximity of the electrode site (Nunez, 1995). Moreover, random fluctuating electrical potentials will not be detected by the scalp electrode due to the counterbalancing of their haphazard fluctuations. Therefore, only when synchronous activity of a large number of neurones occurs, is the electrical activity detectable at the scalp. Some types of neurons can display spontaneous oscillatory behaviour and enable them to generate rhythmic activity in vitro (Llinas, 1988; Steriade and Llinas, 1988). However, the autorhythmic neuronal activity in the functional brain is dependent upon modulation through interaction with a large pool of neurons and by projections from neuromodulator systems (Steriade and Llinas, 1988). These “pacemakers”, both autorhythmic neurons and interactions in local neuronal networks, can produce summed oscillations at very different frequencies and result in propagation of global rhythmic activity (Steriade et al., 1990; Thompson and Thompson, 2003).

1.2.2.2 B. Thalamocortical networks

The rhythmic cycles observed in scalp-recorded EEGs are generally agreed to be the result of neural activity between the thalamus and the cortex. Interactions between thalamocortical neurons in specific and non-specific nuclei of the thalamus have been demonstrated. The thalamic reticular nucleus formed by a sheath of inhibitory feedback neurons around the thalamus works with cortical neuronal populations. Hence, they can elicit and modulate rhythmic activity in cortex effectively (Contreras

et al., 1996; Steriade, et al., 1993). In other words, the thalamus is a central subcortical structure displaying characteristic functional states, which relays signals to the cortical level and relays signals between ascending and descending tracks to multiple brain areas. Cortical rhythmicity results from complex feedback and interactions between thalamocortical circuitry and both local and global cortico-cortical circuitry (Thatcher, et al., 1986).

1.2.2.3 C. Local-scale and large-scale synchronization

The diameter of the EEG electrode is about 1cm and the area (about 0.79 cm²) of an electrode covers approximately 250,000 neurons (Baillet et al., 2001). Therefore, the signal recorded at the scalp is due to spatial summation of the induced current density from the post-synaptic potential of excited large clusters of neurons. It is clear that many neurons must be activated synchronously to form an EEG signal at the scalp.

Animal studies have already described substantial synchronization among adjacent neurons, called “local-scale synchronization” (e.g., Llinas, 1988), while for neuronal assemblies of distant brain regions, this is known as “large-scale synchronization” (e.g., Bressler and Kelso, 2001). The temporal interaction among neural activities, synchronization of oscillations, is a key mechanism for neuronal communication between spatially distributed brain networks (Schnitzler and Gross, 2005). Animal studies also show that oscillatory processes might temporally bind neurons into assemblies and foster synaptic plasticity (Buzsaki and Draguhn, 2004). Interestingly, low frequency oscillations need larger neuronal populations, and higher frequency oscillations originate from smaller neuronal assemblies (Buzsaki and Draguhn, 2004). Furthermore, large-scale neuronal synchronization has an important

role in information processing that relies on constructed neuronal networks (e.g., language processing; Weiss and Mueller, 2003). Through EEG coherence analysis, those networks can be studied, and the particular methods for analysing EEG will be discussed further below.

1.2.3 The Normative EEG Spectrum

This section will briefly introduce common brain activities (rhythms) and their putative functional roles for the EEG frequency band from EEG scalp recordings in the resting state. The “electroencephalograph” (EEG) is an instrument to detect and amplify the electrical activity in the brain. Therefore, the scalp-recorded EEG generated by the pooled activity of billions of cortical neurons is easily influenced by shared activity between cortical and subcortical regions, and each EEG electrode site records rhythmic activity from multiple generators of EEG activity.

The range of frequencies may be divided into six bands: Delta (1-3 Hz), Theta (4-7 Hz), Alpha (8-12 Hz), SMR (12-15 Hz), Beta (13-20 Hz), High Beta (20-33 Hz), and Gamma (36-44 Hz). This definition of frequency band components has been chosen in order to accommodate the bandwidths which have typically been applied in the NFT literature. Moreover, this definition merges the traditional frequency designation in other EEG literatures as well. Different oscillating patterns of the EEG (such as theta, alpha and beta rhythms) are thought to reflect distinct processes of modulation of information processing in neuronal networks.

Not only to differentiate between functional inhibitory and excitatory activities but also to investigate fluctuations (increases/decreases) of EEG activity, the temporal

resolution at the millisecond level has allowed scientists to explore the minute changes due to task demands or between conditions. Low frequencies (delta and theta) originate from larger neuronal populations and show large synchronized amplitudes. However, higher EEG frequencies (e.g., beta and gamma) demonstrate small amplitudes due to a high degree of degree of desynchronization in the underlying neuronal activity (e.g., Pfurtscheller, et al., 2006; Pfurtscheller and Neuper, 1992; Pfurtscheller, et al., 1996).

1.2.3.1 Delta band (1-4 Hz)

The delta wave, often referred to as “slow wave” activity is related to restorative processes of repair, especially during deep sleep (Niedermeyer, 2005). Delta is also the predominant activity in infants during the first two years of life. In addition, slow delta and theta activity generally diminish with increasing age, whereas the faster alpha and beta bands linearly increase across the life span of adults (e.g., John et al., 1980). Pathologically, increased delta waves will be found in a variety of serious disorders including head injury, coma and major depression (Laibow, 1999). In adults, delta power has been shown to increase in the proximity of brain lesions (Gilmore and Brenner, 1981) and tumors (Fernandez-Bouzas, et al., 1999). Delta activity reflects mostly an inhibitory rhythm.

1.2.3.2 Theta band (4-8 Hz)

Theta activity is prominently seen during sleep. However during wakefulness, two different types of theta activity have been described in healthy adults (Schacter 1977). The first type, which is linked to the decreased alertness condition (drowsiness), shows a widespread scalp distribution of theta waves, indicating

impaired information processing. The second one, so-called frontal midline theta (FMT) activity, is generated in the middle prefrontal area, and it has been associated with anterior cingulate cortex activation (ACC, Brodmann area 24/32; Asada, et al., 1999; Luu, et al., 2003). The ACC is the largest region with significant positive correlations between theta current density and glucose metabolism (Pizzagalli, et al. 2003).

Physiologically, activation in the septo-hippocampal circuit reveals functional relationships with hippocampal theta generators (Gaztelu and Buno, 1982), although theta has also been recorded in numerous other limbic regions, including the ACC, entorhinal cortex, and the medial septum (Vinogradova, 1995; Bland and Oddie, 1998). In encoding information into episodic memory and memory-related tasks, the theta rhythm plays an integral role in the timing of action potentials of hippocampal neurons reacting to components of any given task (Hasselmo, 2005; Hyman et al., 2005). In other words, these theta oscillations facilitate transmission between different limbic structures, and it has been speculated that theta activity may subserve a gating function on the information processing flow in limbic regions (Vinogradova, 1995).

However, pathologically increased theta waves often are seen in psychotic states, delusions, and other states connected with poor reality testing and with seizure disorders. Theta may also appear excessively in head trauma cases (Laibow, 1999).

1.2.3.3 Alpha band (8-12 Hz)

In healthy adults, alpha activity can be predominantly recorded during a state of relaxed wakefulness and the unfocused state, “often characterized by creativity and dreamy thoughtfulness” (Laibow, 1999). Although large individual differences in

alpha amplitudes are not uncommon (Niedermeyer, 2005), alpha rhythms typically show their greatest amplitude over posterior regions, particularly posterior occipito-temporal and parietal regions during the eyes-closed (EC) state. In fact, a phenomenon, known as “alpha blockage” or “alpha desynchronization”, is defined by the greatly diminished or abolished alpha rhythm with opening the eyes, sudden alerting, and mental concentration. However, the physiological role of the alpha rhythm remains largely unclear. Some authors have suggested that alpha synchronization may demonstrate an electrophysiological correlate of cortical “idling” or cognitive inactivity (e.g., Pfurtscheller, et al., 1996). In recent years, this conjecture has been heavily discussed in the literature, particularly in studies investigating evoked EEG activity described during information processing (event-related potentials, ERPs; e.g., Cooper, et al., 2006; Klimesch, 1999).

It may be pathologically decreased in all stress-related disorders, anxiety and attention deficit disorders (Laibow, 1999).

1.2.3.4 Sensorimotor rhythm (SMR, 12-15 Hz)

The SMR (sensorimotor rhythm) normally is associated with a resting body but active mind, an external focus of attention, paying attention, sequencing, and information storage and retrieval. It is often decreased in attention deficit disorders, anxiety and stress-related disorders (Laibow, 1999). In the study of Onton et al (2005) theta components worked strongly with SMR (12-15 Hz, or named a low-beta rhythm) activity during memorising-letter trials. Their results showed that low-beta activity reflected harmonic energy in continuous, sharp-peaked theta wave trains as well as independent low-beta bursts (Onton, et al., 2005). The observed theta and SMR

relation may index dynamic adjustments in medial frontal cortex to trial-specific behavioural context and task demands.

1.2.3.5 Beta band (13-36 Hz)

The beta rhythm is normally associated with higher cognitive processes and rational analytical, problem-solving thinking and with focused concentration (Laibow, 1999). Moreover, the beta rhythm has been shown to increase with attention (Murthy and Fetz, 1992) and vigilance (Bouyer, et al., 1987) in animal studies. In adults, beta activity presents mainly a symmetrical fronto-central distribution, and typically replaces the alpha rhythm during cognitive activity. Collectively, these findings suggest that increased beta activity generally reflects increased excitatory activity, particularly during diffuse arousal and focused attention (Steriade, 1993). In the research of Tallon-Baudry et al. (2004) their findings suggest that the successful performance of a visual short-term memory task depends on the strength of oscillatory synchrony in the beta range (13-20 Hz) during the maintenance of the object in short-term memory, which matches behavioural performance (Tallon-Baudry, et al., 2004).

Consistent with this view of increased beta activity for attention, the high beta rhythm, also named the beta2-frequency (20-36 Hz) oscillation, is normally associated with states of physiological arousal. Beta2 frequency oscillation occurs over somatosensory and motor cortices during motor preparation. It can be coherent with muscle electrical activity (Roopun et al., 2006).

However, pathologically it is elevated in all stress-related disorders, some mood disorders, with panic and anxiety (Laibow, 1999).

1.2.3.6 Gamma band (from 36 Hz to > 80 Hz)

Gamma oscillations have recently received great attention given their role in cognition (Tiitinen, et al., 1993). Various findings indicate that gamma activity is directly associated with brain activation, for example, attention, arousal, object recognition, top-down modulation of sensory processes (e.g., Engel, et al., 2001; for learning, Miltner, et al., 1999). Gamma oscillations with high frequencies span from roughly gamma (30–80 Hz) to high gamma (>80 Hz). These oscillatory activities can be obtained at many levels, ranging from single cell to local field potentials in animals, to large-scale synchronized activities in human scalp. Gamma is often the first component in response to a sensory stimulus, interestingly not only in auditory but also in visual, somatosensory, and olfactory or even cellular levels (Moran and Hong, 2011). Dose-dependent decreases of gamma activity have also been described during anaesthesia (Uchida et al., 2000). In addition, systematically decreased gamma activity has been described throughout the sleep-wake cycle (the highest during wakefulness and the lowest during slow wave sleep; Gross and Gotman, 1999).

1.2.4 Artefacts

How to obtain "clean" data from cerebral activity without contaminated signals by non-cerebral artefacts? It is a substantial problem in the procedure of EEG recording. Physiological artefacts, such as muscular activity of scalp muscles, eye movements and blinks, are generated by subjects, and even extra-physiological artefacts from environmental electrical signals are recorded from sources outside the body. Nevertheless, two complementary approaches can substantially decrease or

eliminate artefacts. The first one, of course, is to minimise movement artefacts during EEG recording. The second one requires computational methods to remove artefacts within the EEG data. The following paragraphs will consider some of the artefacts, how to identify such artefacts, and introduce methods to minimise those artefacts (Please see a number of good sources, Beaussart and Guieu, 1977; Rowan and Tolunsky, 2003; Schachter and Schomer, 2005). The important computational methods for artefact removal will be considered in the next section.

1.2.4.1 Muscle artefact

Muscular contraction elicits myogenic potentials and that kind of potential is a major source of EEG artefact, so-called electromyographic (EMG) artefact. Consequently, muscular activity with high amplitudes can mask neural potentials altogether. For example, a historical problem with monitoring of EEG in epileptic patients, where there are strong spikes which can obscure the detection of epileptic spikes (Panych, et al., 1989). In the worst case, the fact that muscle artefact can totally conceal EEG activity may potentially limit EEG applications.

EMG consists of a series of spiked discharges from underlying motor units, and the frequency of muscular discharges can range from 20 to 1000 Hz due to recruited muscle fibres for different degrees of muscular contraction (Andreassi, 2000). Importantly, the dominant frequency of muscular discharges is in the 50–150 Hz band, whereas more than 90% of the EEG's spectral power lies within 1–30 Hz frequency. Therefore, the brain activity of interest lies below 15 Hz, and then we can simply use a low-pass filter to avoid the directly contaminated electrodes with many muscular artefacts, in order to facilitate adequate signal detection.

Indeed, muscle artefact also tends to occur in specific places and these should be examined. The scalp locations most affected are the temporal areas T3 and T4 which lie in close proximity to the bilateral temporalis muscle due to jaw tension, a particularly common muscle artefact. Figure 1-1 shows with increased power of muscular contraction and recorded at T3 and T4 on the topographical scalp map. To reduce this artefact, chewing should be discouraged and showing subjects how the effects of muscle tension on the EEG recordings is a good way to allow them to learn to reduce the artefact's impact. In addition, frontal sites Fp1, Fp2, F7 and F8 lie in the region of the activity of the bilateral frontalis muscle (the 'frowning' muscle) of the forehead. Figure 1-2 illustrates the topographical map with strong muscular signals over the frontal region.

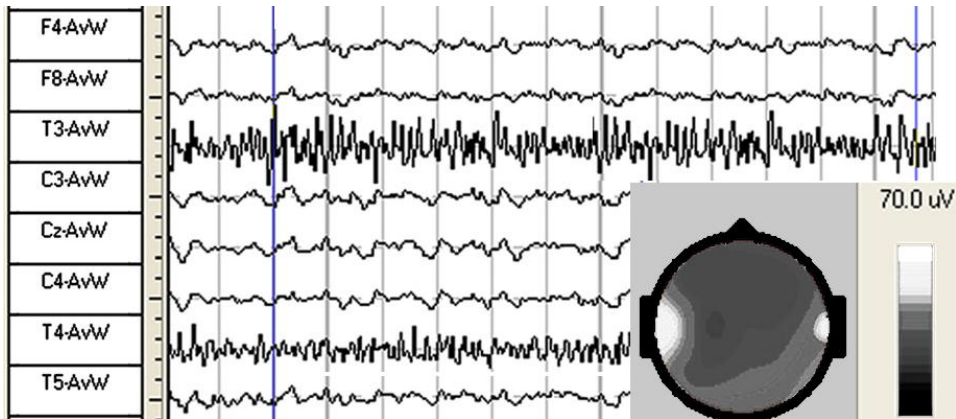


Figure 1-1. EEG signal and topographical map indicate jaw tension.

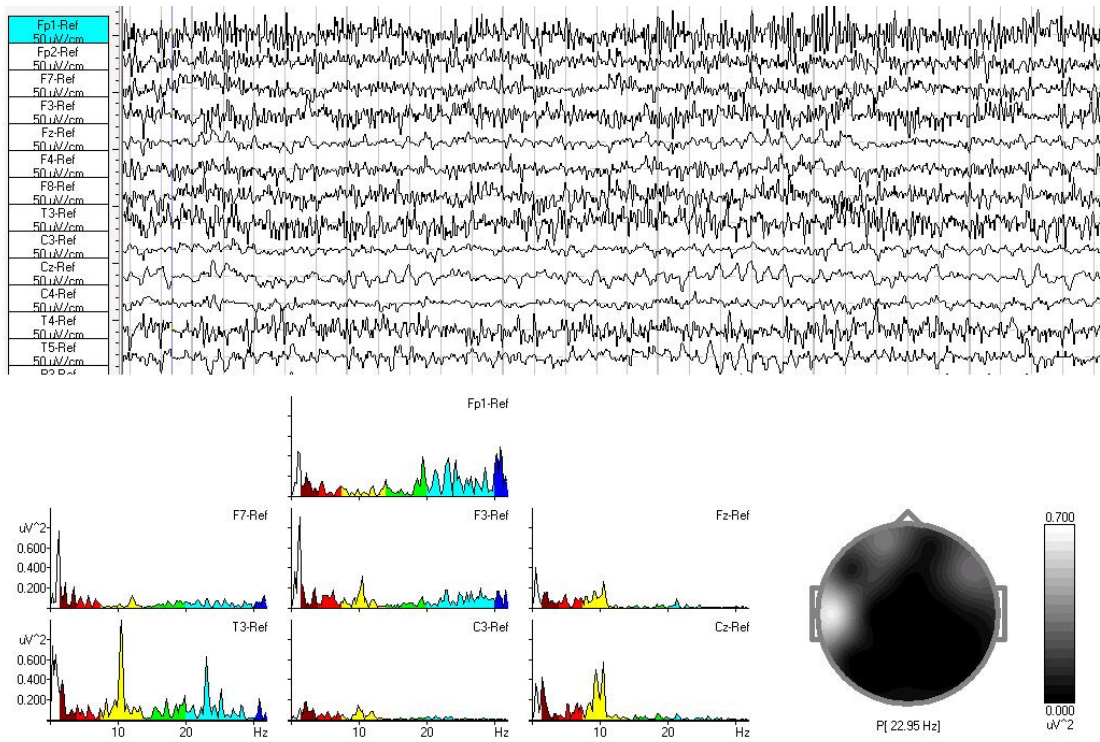


Figure 1-2. EEG topographical map and spectral analysis indicate possible frowning and jaw tension.

What can be done for eliminating EMG artefact? Fortunately, it becomes easy to distinguish between substantial EMG and EEG from the raw EEG recordings after the developed methods of quantitative EEG (qEEG) for spectral distribution and independent component analysis (ICA) for signal morphology and scalp location (please see the next sections). Of course, a common way of eliminating overt EMG (and other types of) artefact is to simply reject (delete) the contaminated portions of the EEG. However, when the degree of contamination is considerable, it can be the case that the rejection procedure results a considerable loss of hard-earned EEG data with perhaps unfortunate results. In this instance, more advanced post-processing methods such as ICA can be attempted to separate the EMG signal from the raw EEG signals. ICA has shown its benefit in isolating muscle artefact. ICA and other methods are described in the later section on computational analysis of EEG data.

1.2.4.2 Skin artefact

Sweat with sodium chloride and lactic acid can react with the metal of the electrodes and then alter impedance and signal amplitudes. Therefore, exercise is naturally more likely to cause sweating and produce this type of artefact. However, such artefact is generally found at very low frequencies below 1 Hz and subjects may be instructed how to reduce the influence of this skin artefact, for example, with lower body temperature to minimise that artefact, and the avoidance of exercise before EEG recording. It is also important to monitor impedances of all channels to ensure that differences across active and reference sources are minimal, ideally by ensuring all impedances are kept low (Thompson et al., 2008).

1.2.4.3 Eye movement and eye blinking artefacts

Both eye blinks and lateral eye movements are universal sources of artefact. During an eye-blink the eyeball turns upwards, which primarily affects the frontal electrodes, with a large positive deflection seen at Fp1 and Fp2 (a peak amplitude of around 50–200 μ V, lasting 200–400 ms). The peak generally presents a large wave recorded by other electrodes. In addition, lateral eye movement with sharply contoured potentials is recognisable in the fronto-temporal areas (Rowan and Tolunsky, 2003). There is some evidence that increased visual load decreases the rate of eye blinks (e.g., Bynum and Stern, 1970; Veltman and Gaillard, 1996). As dealing with EMG, eye blink is easily recognised in the EEG because of its signal morphology and amplitude with a distinctive pattern. It may contaminate delta (1–4 Hz) and theta (4–8 Hz) bands predominantly at frontal sites (see Figure 1-3). Many modern techniques, such as ICA, can ameliorate/correct this problem caused by eye blinks.

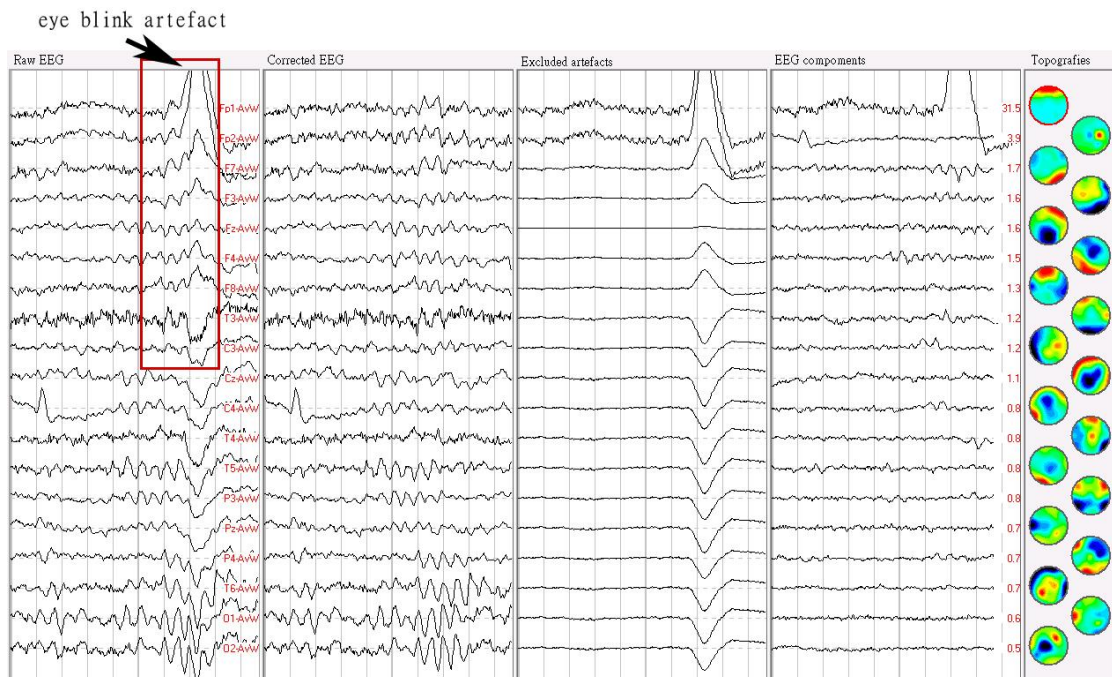


Figure 1-3. Removal of eye blink artefact using ICA. Five columns (from left to right) show the raw EEG, corrected EEG, excluded artefact, along with EEG components and topographies

1.2.4.4 ECG artefact (electrocardiogram, ECG or EKG)

The electrical activity of the heart can be measured by the ECG. If the electrical field from each cardiac pulse is very large, the signal can be measured by the scalp EEG recording. ECG artefact is more likely to be seen in people with wide necks, but it generally does not become a big problem due to its contamination with only low frequencies of around 1–2 Hz (Thompson et al., 2008). This artefact can be common in channels connected to the ears. In addition, the rhythmic and distinct morphology of ECG also means that it is generally easily removed by the post-processing computational methods, which will be discussed in the next section.

1.2.4.5 Respiration artefact and tongue movement

Respiration artefact arises from the rhythmic body movement of inhalation and exhalation. This sort of artefact may be initially observed with high amplitude deflections as a delta frequency. As with ECG, this type of artefact is highly suitable for removal by post-processing methods.

Regarding tongue movement, it is created by the potential difference between the tip and base of the tongue and gives rise to slow potentials. This type of artefact usually does not occur frequently enough to cause a significant loss of data. The main reason for tongue movement is the need to swallow.

1.2.4.6 Electrical interference from the environment

Electrical noise from the environment is normally eliminated by common mode rejection as previously described. A very large discrepancy exists due to a poor quality of connection, and noise will appear commonly at the 50 Hz frequency (Europe) or 60 Hz in the USA. Ensuring a good quality connection and checking

impedance online during EEG recording may help to minimise this artefact. Active shielding can be used to reduce electrical noise (Thompson et al., 2008).

1.2.5 Summary

Overall, the reviewed research on EEG generation, spectrum, and artefacts suggests that those related explanatory mechanisms can be simulated and analysed by computational methods. Fortunately, solutions to the inverse problem can be found by postulating physiologically and anatomically sound assumptions about supposed EEG sources and by mathematically applying established laws of electrodynamics. The main purpose of the present section of introducing EEG is to review recent advances in the EEG field. To understand these developments it will first be necessary to describe the physiological basis of the EEG signal. Subsequently, important issues associated with data acquisition (please see the methodology part in the chapter 3), signal processing and quantitative analyses (for more comprehensive reviews of these topics, please see the next section) will be presented.

Regarding emerging source localization techniques that have been shown to localize EEG activity, perhaps the greatest advancements in the EEG field in the last 5-10 years has been the development of these localization techniques (for details of this method, please see the chapter 3), particularly when used in concert with EEG recording, realistic head models, and other functional neuroimaging techniques. These achievements reveal that the spatial resolution of the EEG may be substantially and mathematically exact enough to open exciting opportunities for investigating spatio-temporal dynamics of brain mechanisms and functional networks underlying

mental processes (for details of EEG functional networks, please see the following section).

1.3 From Quantitative Analysis of EEG to Source Localization Techniques

EEG involves the measurement, amplification, and registration of differences between fluctuating electrical field potentials as a function of time (Kamp and da Silva, 1999). The signals recorded at the scalp primarily reflect cortical activity which is the neuro-electrical activity of underlying brain cortical structures. This classical method for reading EEG relies on the visual analysis by a qualified specialist to analyse the recording of the electrical signals obtained from electrodes placed on the skull. It is still the first step and remains the gold standard in analysing any type of EEG. However, Coburn et al (2006) have described the obvious advantages of quantitative EEG (qEEG) when compared with other imaging methods in their comprehensive review (Coburn et al., 2006).

Quantitative analysis of the EEG involves computer-assisted imaging and statistical analysis of the EEG, and therefore, many methodological problems have to be solved with caution (Kaiser, 2000). The development of several methods to investigate EEG signals with respect to various parameters includes waveform frequencies, amplitudes, phase, and coherence. The EEG analyses can be divided into linear and nonlinear approaches. The most widely used linear methods to quantify spontaneous or task-related EEG activity are spectral and coherence analyses. However, nonlinear approaches incorporating higher order statistics, information

theory, or chaos theory, started to emerge in the 1990s, and have demonstrated their usefulness to analyse transient and irregular EEG patterns (see Thakor et al., 2004 for a review).

The advent of multi-channel EEG systems has enriched the development of EEG mapping techniques. Unlike traditional EEG waveform approaches, EEG mapping consider data in the spatial domain first, and then in the temporal domain, providing a display of the constantly changing spatial distribution of brain activity (Maurer and Dierks, 1992). For topographic mapping, at minimum the complete 10-20 system should be used (Nuwer et al., 1999). One of the main advantages of space-oriented EEG analysis is that, at any given time point, activity from all electrodes is considered simultaneously. A second main advantage is that, unlike waveform analyses, space-oriented analysis is independent from the reference electrodes. When examining the unfolding of momentary potential distributions over time, different configurations of scalp potentials are assumed to index different functional brain states because different scalp potential distribution must have been generated by different neural sources (Fender, 1987), and different neural sources likely subserve different functions (Kühnpast, 2008; Pizzagalli, 2007). Although EEG mapping represents a powerful and unambiguous approach for scalp EEG data, it is important to stress that this technique does not provide any additional information about the generating sources underlying scalp measurements (Pivik et al., 1993). Thus source localization techniques are required for estimating the sources of scalp-recorded electromagnetic activity in order to localise intra-cerebral sources.

In general these solutions of localisation can be divided into two broad categories, “equivalent dipole approaches” and “linear distributed approaches”. The first

approach typically assumes that EEG signals are generated by a relatively small number of focal disconnected sources, presented as fixed or moving dipoles (e.g., Scherg and Ebersole, 1994). However, the numbers of dipoles, unfortunately in many experimental situations, cannot be determined a priori (e.g., Phillips, et al., 2002a; Rao, et al., 2002). In contrast the second approach, linear distributed approaches consider all possible source locations simultaneously. The distributed approaches typically allow researchers to limit the solution space by means of anatomical and functional constraints; for example, anatomical constraints assume that some specific compartments or regions of the brain (e.g., cortical structures) have a higher likelihood of generating scalp-recorded EEG signals than others. Various source localization techniques will be presented in the following sections (for more technical reviews, see Baillet et al., 2001; Hamalainen and Ilmoniemi, 1994; Grave de Peralta and Gonzalez Andino, 2000; Phillips, et al., 2002a; Phillips, et al., 2002b; Pascual-Marqui, et al., 2002; Trujillo-Barreto, et al., 2004).

1.3.1 Quantitative EEG (QEEG)

In comparison with other techniques of brain imaging, although qEEG has a weaker spatial resolution, qEEG offers many advantages with, for example, no ionizing radiation and an ideal temporal resolution in the millisecond time domain for the processing of neuronal information. Of course, qEEG also produces non-invasive images from both excitatory and inhibitory cortical neuronal activity, but not from circulatory (e.g., the measurement of cerebral cortical blood flow) nor from metabolic activity (the measurement of regional cerebral cortical metabolic rate of oxygen and carbon dioxide) (Gleichmann et al., 1962). Furthermore, a variety of factors can

display their effects on EEG patterns, including metabolic rate of oxygen, biochemical, hormonal, neuroelectric, and behavioural factors (Bronzino, 1995). Therefore, the standard procedure of EEG recordings is the essential element in order to validate EEG changes under standard conditions. Thus EEG signals can be computerized and analysed by software for specific frequencies at specific sites without controversy. Calculations can be obtained, including ratios, standard deviations and other statistics.

1.3.1.1 Spectral analyses

Probably the most common method of frequency analysis to analyse EEG signals is the spectral analysis. The algorithm of fast Fourier transform (FFT) to study the frequency of the spectrum of EEG is used for the spectral analysis (Thompson and Thompson, 2003). FFT is a mathematical calculation to transform the raw EEG from the time related domain to the frequency domain. The principal rationale is that any signal can be analysed and redrawn as a combination of sine and cosine waves of various phases, frequencies and amplitudes (Fisch, 1999). When FFT is applied to EEG recordings containing rhythms, these rhythms appear in the corresponding spectra in the form of peaks (Cantor, 1999), and the root-mean-square average amplitude or the power (the square of the amplitude) is used to quantify its contribution to the measured EEG signal.

Spectral analyses assume that the EEG is a stationary signal. Accordingly, segments entered in FFT analyses cannot be too long because of potential violation of the stationary assumption of EEG (Gasser and Molinari, 1996). At least 60 seconds of artefact-free data should be used for spectral analyses (Nuwer et al., 1999; Pivik, et al., 1993), in order to obtain reliable estimation of spectral features and to reduce the

impact of second-to-second variability in EEG signals. Furthermore, the window approach is used for abrupt changes in EEG signals at the beginning and the end of the EEG segments. The Hanning (cosine) window has been commonly utilized. This window tapers the beginning and end of the EEG segment to zero, whereas the middle of the segment retains 100% of its amplitude (see Dumermuth and Molinari, 1987 for a review of various windowing approaches), and overlapping segments (e.g., 50%) are often used to restore the amount of data for spectral analyses.

Importantly, several methodological points should be highlighted in this section. First, the frequency range for a given oscillatory activity (e.g., alpha activity) can show considerable individual differences (Klimesch, 1999), indicating substantial effects from specific bands on the findings. Second, measures of absolute or relative power can be derived from spectral analyses. Absolute power reflects the amount of a given frequency within the EEG, and relative power is calculated as the amount of EEG activity in a given frequency band divided by the total power. Generally speaking, absolute power should be preferred as it is more easily interpreted. Third, transformations (e.g., log) are often used before statistical analyses to estimate a Gaussian distribution (Davidson et al., 2000). Fourth, many ratios have been used to investigate left-right (L-R) differences or the parameters of neurofeedback training (please see the chapter 5). Those ratios allow a straightforward interpretation in terms of asymmetry or tendency to be normally distributed (Pivik, et al., 1993).

1.3.1.2 Coherence analyses

In EEG studies, the investigation of large-scale neuronal synchronization becomes particularly important in hypothesized experimental situations for recruiting distributed neuronal networks (e.g., Llinas, 1988). Therefore, the *coherence measures*

are developed and computed in order to quantitatively measure the dynamic functional interactions among EEG signals from different scalp locations.

Based on the frequency-dependent dataset, coherence computation is similar to a correlation algorithm, and it can be mathematically obtained by dividing the cross-spectrum between two time series by the root of the two spectra (Pizzagalli, 2007). In addition, cross-power spectrum is from the multiplied Fourier transform of one signal with the complex conjugate of another signal, allowing the quantification of relationships between different EEG signals (Pizzagalli, 2007).

In other words, coherence estimates the linear cross-correlation between two signals as a function of frequency. EEG coherence estimates the degree of synchrony between the electrical activities of the two brain regions, focusing on a certain frequency or EEG band as well (Cvetkovic and Cosic, 2009). Accordingly, the estimated coherence ranges from 0, indexing the absence of any synchrony (the activities of the signals with the minimum linear correlation for this frequency), to 1, indicating maximal synchrony between the frequency components of two signals (the maximum linear correlation for this frequency), irrespective of their amplitudes (Cvetkovic and Cosic, 2009; Pizzagalli, 2007). In general, synchronized brain regions are assumed to show increased coherence during a given cognitive process ("neuronal synchronization within specific EEG frequency bands"), depending on the nature and difficulty of the task (Weiss and Mueller, 2003).

It is important to note that coherence analyses show a promising approach to assess the degree of synchronization between different brain regions, but they cannot inform us about the causality of these interactions or the direction and speed of the information transferred. However in recent years, advanced methods for assessing

these important aspects of brain function have been described, for example, the Directed Transfer Function (DTF) and the Directed Mutual Information (DMI) (for a review, see Thakor and Tong, 2004).

1.3.1.3 Time-frequency analyses

Although spectral analyses can provide essential information about how many frequency compositions within EEG oscillations, they cannot give any information about when such frequency shifts occur. Therefore, the approaches allowing the exploration of dynamic and time-varying changes in the frequency domain of EEG oscillations appear particularly important. Many time-frequency analyses methods have been developed, for example, short-time Fourier Transform (STFT) and wavelet analysis. STFT allows to compute an FFT-based spectrogram, and wavelet analysis allow a approach with more adaptive time-frequency resolution to resolve EEG waveforms into specific time and frequency components (for a conceptual tutorial, see Samar, et al., 1999), rather than a composition of sine waves with varying frequencies as in the FFT (Pizzagalli, 2007).

Compared to the Fourier transform in the spectral analysis, the STFT evaluates the frequency and possibly the phase change of a signal over time. However, the Fourier transform cannot show us these changes of frequency over time. To achieve the STFT, the signal is cut into blocks of finite length, and then the Fourier transform of each block is computed. To improve the result, blocks are overlapped using overlap add or overlap save method and each block is multiplied by a window that is tapered at its end points (for a conceptual tutorial, see Proakis, 2003).

1.3.2 Blind Source Separation (BSS)

Blind source separation (BSS), is a technique for estimating individual source components from their mixtures at sensors. This is called “blind” because, the estimation is done without prior information on the sources, that is their spatial location and time activity distribution; and on the mixing function, i.e. information about the mixing process. Several BSS algorithms estimate the source signals from observed mixtures (Cardoso, 1998). The solutions of BSS have become increasingly important in the area of signal processing due to their prospective application in medical signal processing, brain imaging (for example, EEG and fMRI), and audio signal separation (Hyvarinen, et al., 2001). In these applications, signals are mixed and make blind source separation difficult (Benesty, et al., 2005). Many reports have been studying the problem of BSS and numerous ways have been proposed to solve the problem. Recently attention has been drawn to Independent Component Analysis (ICA), which is a very important statistical tool for solving the BSS problem. ICA transforms the observed signals into mutually statistically independent signals (Hyvarinen and Oja, 2000) (see details in the next section).

Let us imagine that there are two persons in a room speaking simultaneously, let us denote the signal emitted from Speaker1 with $S1(t)$ and Speaker2 with $S2(t)$ correspondingly, and there are two microphones placed at different locations in the same room. These microphones will produce two time signals which we can call $X1(t)$ and $X2(t)$, where t is the time index. Each of these recorded signals is a sum of the speech signals from the two speakers, because each microphone is “hearing” the two speakers at the same time. We could express this as a linear equation as shown below

$$x1 = a11 * s1 + a12 * s2$$

$$x2 = a21 * s1 + a22 * s2$$

Where * represents convolution and a_{ij} are some parameters that depend on the distances of the microphones from the speakers and on the room properties, these parameters are referred to as the room impulse response.

This scenario is normally refer to as the cocktail-party problem, it would be very useful if the original speech signals $S1(t)$ and $S2(t)$ could be estimated. What it then means is that if we knew the values of $a11$, $a12$, $a21$, $a22$ (i.e. the impulse responses), $X1(t)$ and $X2(t)$ (the two time signals), we could easily solve the linear equation above with any of the classical methods available. ICA can be used to estimate these values and allow us to separate the two original signals $S1(t)$ and $S2(t)$ from their mixtures $X1(t)$ and $X2(t)$. Even we have N source signal $Si(t)$ that are mixed and observed (see details in the next section).

1.3.3 Independent Component Analysis (ICA)

ICA was introduced as a statistical model to express a linear transformation of non-Gaussian, mutually-independent variables in signals processing (Sanchez and David, 2002). Applications of BSS/ICA methods have contributed to the popularity of this field of study and their application, for example, the blind separation of EEG, electrocardiographic (ECG), magnetoencephalographic (MEG), and fMRI data for separating neurologic signal components. Moreover, the BSS/ICA has been applied on analysing biological modelling of feature extraction, speech enhancement, data mining, communications, as well as exploratory data analysis (Sanchez and David,

2002). ICA is a powerful higher order statistical technique used to separate independent sources that were linearly mixed together through a medium and received at several sensors.

Let us assume that we observe N source signal $S_i(t)$ (linear mixtures) that are mixed and observed at M sensors (independent components) as $X_j(t)$: $X_1(t)$, $X_2(t)$, $X_N(t)$ of M independent components. It's always assumed that the number of sources N is known or can be estimated and the number of sensors M is equal to or greater than N; $M \geq N$. Thus mathematically we can write the linear mixing model of ICA is given as:

$$\mathbf{X}_j = a_{j1}S_1 + a_{j2}S_2 + \dots + a_{jN}S_N \quad \text{for } j = 1, 2, 3 \dots, M$$

Where $S_i(t)$ is the N dimensional vector of unknown source signals, $X_j(t)$ is the M dimensional vector of observed signals. Assuming no noise, the matrix representation of mixing model is written as:

$$\mathbf{X} = \mathbf{A}\mathbf{S}$$

, or graphically as:

$$\begin{bmatrix} x_1 \\ \vdots \\ \vdots \\ \vdots \\ x_M \end{bmatrix} = \begin{bmatrix} a_{11} & \cdots & a_{1N} \\ \vdots & \ddots & \vdots \\ a_{M1} & \cdots & a_{MN} \end{bmatrix} \begin{bmatrix} s_1 \\ \vdots \\ \vdots \\ \vdots \\ s_N \end{bmatrix}$$

Here X and S are M×T and N×T matrices whose column vectors are observation vectors $x(t_1), \dots, x(t_T)$ and sources $s(t_1), \dots, s(t_T)$, A is an M×N full column rank

matrix A , called mixing matrix. Then the objective of ICA is to find the separating matrix W which inverts the mixing process such that

$$Y = WX$$

Where Y is an estimate of original source matrix S and W is the (pseudo) inverse of the estimate of the matrix A . An estimate of the sources with ICA can be obtained up to a permutation and a scaling factor. There are different approaches for estimating the ICA model using the statistical properties of signals. Some of these methods are: ICA by maximization of nongaussianity, by minimization of mutual information, by maximum likelihood estimation, by tensorial methods (Choi, et al., 2005; Gursoy and Niebur, 2009; Hyvarinen, et al., 2001; Lee, et al., 2000).

1.3.3.1 Statistical Independence

First, the concept of statistical independence can easily be explained with an example. Let us assumed that y_1 and y_2 are scalar valued random variables, y_1 and y_2 are said to be independent if the information of the value of y_1 does not give any information of the values of y_2 and vice versa. It's important to note that we are referring this to the sources (s_i) alone and not the mixtures (x_i), which generally are highly dependent. In probability theory, independence can be defined by the probability densities. Let $P_1(y_1)$ denote the Marginal Probability Density Function (i.e. the probability density function when y_1 is considered alone) and let $P(y_1, y_2)$ denote the Joint Probability Function (i.e. considering y_1 and y_2 together).

$$P_1(y_1) = \int P(y_1, y_2) dy_2$$

$$P_2(y_2) = \int P(y_1, y_2) dy_1$$

We say y_1 and y_2 are independent if and only if the Joint Probability Density Function can be factorised in the following way:

$$P(y_1, y_2) = P_1(y_1)P_2(y_2)$$

In other words, two events are statistically independent if the probability of their occurring jointly equals the product of their respective probabilities (Cao and Murata, 1999; Choi, et al., 2005).

1.3.3.2 Nongaussian Distribution

Second, the fundamental restriction or assumption in ICA is that the independent component must be nongaussian or at most may have one Gaussian distribution, for ICA to be possible; the reason is because the joint probability densities of Gaussian random variables are completely symmetric (Hyvärinen, et al., 2002; Hyvarinen, 1999; Hyvarinen and Oja, 2000). Nevertheless if not more than one of the components are Gaussian it is still possible to identify the nongaussian independent components as well as the corresponding columns of the mixing matrix. In other words without nongaussianity, estimation of the ICA model is not possible at all.

1.3.3.3 Infomax ICA algorithm

In this present thesis, for example how to apply the method of BSS/ICA on analysing EEG data, the details of the **Infomax ICA algorithm** can be found in (Bell and Sejnowski, 1995). This Infomax algorithm was implemented in EEGLAB

software (Delorme and Makeig, 2004), and successfully applied for both analysis of independent components of EEG, ERP (for review see (Onton, et al., 2006), and for artefacts correction procedures (Delorme, et al., 2007). The same Infomax algorithm was also implemented in WinEEG software (WinEEG 2.83 software, Mitsar, Ltd. <http://www.mitsar-medical.com>), applied in the thesis, for analysing all raw EEG and ERPs of all experiments in the thesis.

Briefly, the method implemented in this thesis is as follows. The input data are the collection of individual EEGs arranged in a matrix \mathbf{W} of 19 channels (rows) by N time points (columns). The ICA finds an ‘‘unmixing’’ matrix \mathbf{W} that, when multiplied by the original data \mathbf{X} causes the matrix \mathbf{S} of the sources (independent components or activation curves).

$$\mathbf{S} = \mathbf{W}\mathbf{X}.$$

Where \mathbf{S} and \mathbf{X} are $19 \times N$ matrices, and \mathbf{W} is 19×19 matrix (19 channels EEG recording). $\mathbf{S}(t)$ are maximally independent. In the present study, matrix \mathbf{W} is found by means of **infomax algorithm**, which is an iteration procedure that maximizes the mutual information between \mathbf{S} . According to the linear algebra,

$$\mathbf{X} = \mathbf{W}^{-1} \mathbf{S}.$$

Where \mathbf{W}^{-1} is the inverse matrix of \mathbf{W} (also called mixing matrix). Further, according to the linear algebra,

$$\mathbf{X} = \sum \mathbf{W}_i^{-1} \mathbf{S}_i,$$

where \mathbf{W}_i^{-1} is the i -th column of the mixing matrix \mathbf{W}^{-1} (represents the topography of independent component, IC), and \mathbf{S}_i , is the row of \mathbf{S} (i.e. time course of the

independent component). As mentioned in the section 1.3.3, where X is an estimate of original source, and matrix W^{-1} is the inverse of the estimate of the mixing matrix. In other words, each column of the (W^{-1}) mixing matrix represents the relative projection weight at each electrode of a single component source (IC topography). Mapping these weights to corresponding electrodes on a cartoon head model allows visualization of the scalp projection or scalp map of each source. The source locations of the components are presumed to be stationary for the duration of the training data. That is, the brain source locations and projection maps (W^{-1}) are assumed to be spatially fixed, while their ‘activations’ (S) reveal their activity time courses throughout the input data. Thus, the IC activations (S), can be regarded as the EEG waveforms of single sources, although obtaining their actual amplitudes at the scalp channels requires multiplication by the inverse of the unmixing matrix (W^{-1}). Then the statistically independent component with corresponding EEG topography can be obtained mathematically (e.g., Grin-Yatsenko, et al., 2010).

1.3.3.4 Application of ICA in EEG and ERP

ICA can be used for the analysis of encephalographic signals like EEG and ERP only if certain conditions are satisfied, at least approximately:

1. Statistical independency of the brain sources involved in the generation of the EEG signal. This independence criterion considers solely the statistical relations between the amplitude distributions of the signals involved, and not the morphology or the physiology of neural structures.

2. Instantaneous mixing at the electrodes. Because most of the energy in EEG signals lies below 1kHz, the so-called quasi-static approximation of the Maxwell equations holds, and each time instance can be considered separately (Bossetti, et al., 2007). Therefore, the propagation of the signals is immediate, there is no need for introducing time-delays, and the instantaneous mixing is valid.

3. Linear mixing. Because the volume conduction through the cerebrospinal fluid, skull, and scalp is thought to be linear, the EEG and the ERP are assumed to be a linear mixture of the potentials associated with synchronous activation of neuropil (a synaptically dense region) in each stimulated area (Alonso-Nanclares, et al., 2008; Makeig, et al., 1997).

4. Stationarity of the mixing and the independent components. Stationarity is generally assumed in the analysis of the EEG and related signals.

Another common application of ICA is the separation of ERP components (details in the next section 1.4). Several studies (e.g., Makeig, et al., 1997; Marco-Pallares, et al., 2005) have shown that ICA is able to obtain a blind decomposition of the ERP without imposing any a priori structure on the measurements. Those studies concluded that ICA can successfully detect ERP components in a single trial and grand averaged paradigms what are very difficult to achieve using traditional methods. Thus, ICA allows the study of the brain dynamics arising from intermittent changes in subject's state and/or from complex interaction between task events.

1.3.4 Source Localisation Techniques

Estimating the source of scalp-recorded electromagnetic activity has attracted considerable interest, and various solutions have been described. The solutions of localisation can be divided into two broad categories, “equivalent dipole approaches” and “linear distributed approaches”.

1.3.4.1 Equivalent dipole approaches (Dipole Source Modelling)

The equivalent current dipole (ECD) model is the most basic source localization technique and assumes that scalp EEG potentials are generated by one or few focal sources (for review, see (Fuchs, et al., 2004). A dipole does not reflect the presence of a unique and discrete source (Baillet et al., 2001). In fact, the position of a dipole can provide clues about the extent and configuration of the activated cortical area: superficial dipoles typically reflect localized cortical activity, whereas deeper dipoles reflect the activity of an extended cortical area (Lopes da Silva, 2004). Focal sources are modelled by an ECD through six parameters: three location parameters (X, Y, Z), two orientation parameters, and one strength (amplitude) parameter.

In general, some caution should be exerted when interpreting dipole modelling solutions because user’s interventions and decisions about the number of underlying sources are required in dipole fitting. The method, called multiple signal classification (MUSIC), attempts to decompose the signal to identify underlying components in the time series data (Mosher and Leahy, 1998; Mosher and Leahy, 1999; Mosher, et al., 1992). Furthermore, substantial progress has been made to extend the original dipole fitting approach implemented using simplified spherical head models to more realistic geometry head model constructed from single subject’s MRI images in recent years,

in particular using boundary element methods (BEM) or finite element methods (FEM). The best average localization that could be achieved with spherical head model was 10 mm (Cuffin, et al., 2001), and a more accurate localization can be achieved by using realistic head models (e.g., Fuchs, et al., 2001).

Moreover, studies combining electrophysiological and hemodynamic measures have further extended dipole source localization approaches by using PET- or fMRI-identified activation loci, providing informed guess about the putative location of sources (e.g., Heinze, 1994; Woldorff, et al., 2002). A more promising (and potentially less biased) approach involves independent EEG/MEG source modelling, which is then weighted based on hemodynamic findings to select the most likely solution (e.g., Dale and Halgren, 2001; Liu, et al., 1998).

Although dipole source modelling has been successfully used to localize spatially restricted and focal sources, its main limitation is that the exact number of dipoles often cannot be determined a priori. Further, since intracranial recordings have provided very little support for the notion that only a few sites in the brain are active in generating ERP or spontaneous EEG recording (e.g., Towle, et al., 1998), dipole fitting results should be interpreted with caution.

1.3.4.2 Linear distributed source localization techniques

Considering the intrinsic limitation of dipole modelling (the number of underlying sources), distributed source modelling approaches have been developed considerably. These approaches are based on the estimation of brain electric activity at each point within a 3-dimensional solution space. Each point, in turn, can be

considered a dipole. Unlike equivalent dipole models, these “dipoles” have fixed positions (e.g., Pascual-Marqui, et al., 1999) and sometime fixed orientations (e.g., Phillips et al., 2002a; Phillips et al., 2002b), which are determined by anatomical and physiological constraints implemented within the localization algorithms. As these methods are used to estimate the strengths (and in some cases, the orientation) of the source, the equations describing distributed solutions are linear.

Mathematically, so-called “regularization methods” can be understood as mathematical representations of the physiological/structural assumptions implemented in a given method, in order to limit the range of allowable solutions and identify the “optimal” or “most likely” solution. Various regularization methods have been developed and utilized in many researches. Some of the most widely used include minimum norm solution (Hamalainen and Ilmoniemi, 1994), maximal smoothness (Pascual-Marqui, et al., 1994), structural/functional priors (Phillips et al., 2002a; Phillips et al., 2002b), and fMRI-weighted solution space (Dale, et al., 2000). In the following section, a review of distributed source localization techniques is presented. Especially, the LORETA algorithm has been used extensively by researchers in the field (e.g., Kropotov, 2008; Lavric, et al., 2001; Pascual-Marqui, 2002; Pascual-Marqui, et al., 2002; Pascual-Marqui, et al., 1999; Pizzagalli, et al., 2005), and therefore, a more extended discussion as well as limitations of LORETA will be in the relevant section.

1.3.4.2.1 Minimum norm solutions

The Minimum norm (MN) solution (Hamalainen and Ilmoniemi, 1994) was one of the first linear inverse solutions. In the MN approach, the head model is first

mapped onto a 3D grid, and three mutually perpendicular dipole current sources are placed at each grid point (Koles, 1998). The goal of the MN approach is to estimate the distribution and strengths of these tens of thousands of dipole. The MN approach selects the least energy, i.e., minimal overall current density within the brain, and MN does not incorporate any prior information. In particular, MN solutions do not impose any spatial correlation among sources, but other methods do (e.g., Pascual-Marqui et al., 1994; Phillips et al., 2002a; Phillips et al., 2002b). In fact, simulation studies have shown that the MN solution typically favours weak and localized activation patterns, and can misplace deep sources onto the outermost cortex (Pascual-Marqui, 1999). Accordingly, MN does not completely fulfil the promise of a 3D source localization technique. However, LORETA, as we will see in the following section, was the first approach that successfully extended the good localization properties of the 2D MN solution to 3D solution space.

1.3.4.2.2 Weighted Minimum norm solutions

Then to compensate for the depth dependency of MN solution, in particular the tendency to favour superficial sources, various weighting factors have been suggested. The weighted MN solution uses a lead field normalization for compensating for the lower representation of deeper sources (e.g., Jeffs, et al., 1987). One more solution, called FOCUSS (Focal Underdetermined System Solution; (Gorodnitsky, et al., 1995), is a nonparametric algorithm, in which the weights are iteratively modified according to the solution estimated in a previous step. Although these weighted MN approaches gave some promising results for reducing the low spatial resolution (blurring) of all MN solutions and for reducing the depth-dependency of sources (Michel, et al., 2004),

it is important to point out that weighting is selected based on mathematical operations rather than physiological assumptions.

1.3.4.2.3 Low resolution Electromagnetic Tomography (LORETA)

LORETA (Pascual-Marqui et al., 1994), a form of Laplacian-weighted MN solution, assumes that: (1) neighbouring neurons are synchronously activated and display only gradually changing orientations; and (2) the scalp-recorded signal originates mostly from cortical gray matter. The first assumption is mathematically implemented by computing the “smoothest” of all possible activity distributions (consistent with neurophysiological studies in animals; e.g., (Haalman and Vaadia, 1998; Vaadia, et al., 1995). The smoothest solution is assumed to be the most plausible one giving rise to the scalp-recorded EEG signal. Furthermore, the second assumption constrains the solution space to cortical gray matters (and also hippocampi), as defined by a standard brain template.

LORETA uses a three-shell spherical head model registered to the Talairach brain atlas (available as digitized MRI from the Brain Imaging Centre, Montreal Neurological Institute, MNI; (Evans, et al., 1993) in recent implementations (Pascual-Marqui et al., 1999). EEG electrode coordinates derived from cross-registrations between spherical and realistic head geometry (Towle et al., 1993).

The solution space is restricted to cortical gray matters and hippocampi, as defined by a digitized probability atlas provided by the MNI. Under these constraints, the solution space includes 2394 voxels at 7 mm spatial resolution. For analyses in the frequency domain, LORETA computes current density as the linear, weighted sum of

the scalp electrical potentials, and then squares this value for each voxel to yield power of current density in units proportional to amperes per square meter (A/m^2).

Furthermore, Pascual-Marqui (in 2002) introduced a variant of the LORETA algorithm, in which localization inferences are based on standardized current density (standardized LORETA, or sLORETA). Conceptually using a two-step process, Dale et al. first estimated current density using the MN solution (Dale, et al., 2000); subsequently, current density was standardized using its expected standard deviation, which was assumed to fully originate from measurement noise. Although sLORETA uses a slightly different implementation that considers simultaneously two sources of variations (variations of the actual sources and variations due to noisy measurements), its localization inference is also based on standardized values of current density estimates (Pizzagalli, 2007). Compared to LORETA, sLORETA does not introduce Laplacian-based spatial smoothness and does not compute current density but rather statistical scores. In initial simulations, sLORETA was reported to have zero-localization error (Pascual-Marqui, 2002). Independent simulations replicated that sLORETA had higher localization accuracy than LORETA or MN solutions (Wagner, et al., 2004).

In more recent years, important cross-modal validation has come from studies directly combining LORETA with functional fMRI (Mulert, et al., 2004; Vitacco, et al., 2002), structural MRI (Worrell, et al., 2000), PET (Dierks, et al., 2000; Gamma, et al., 2004), and intracranial recordings (Krakow, et al., 1999; Seeck, et al., 1998). In two recent EEG/fMRI studies LORETA localizations were, on average 16 mm (Mulert et al., 2004) and 14.5 mm (Vitacco et al., 2002) from fMRI activation loci, a discrepancy that is in the range of the spatial resolution of LORETA (~1-2 cm). Although substantial consistency between LORETA findings and other traditional

neuroimaging techniques has been reported, some controversy in the field about the localization capability of LORETA (Grave de Peralta Menendez and Gonzalez Andino, 2000).

The LORETA algorithm has received important cross-modal validation, but however it is important to highlight three factors of the spatial resolution of this method and the limitation of LORETA. First, the vast majority of LORETA studies have used a three-shell spherical head model, and a more complex head model that better represents the geometry of gray and white matter regions (e.g., FEM) can substantially improve the spatial resolution of LORETA (Ding, et al., 2004). Second, most of the studies have used a general (average) brain template (Evans et al., 1993). Clearly, use of individual anatomical MRI scans is expected to improve the precision of the solution space. Third, digitization of electrode positions for individual subjects is expected to further improve the spatial resolution of LORETA. In addition to three factors, some more conceptual limitations should be mentioned. First, due to the smoothness assumption, LORETA is incapable of resolving activity from closely spaced sources. The generating source is known to be well-represented by a single dipole (e.g., early sensory ERPs), and dipole fitting procedures might be preferred, when LORETA will tend to blur the solution (e.g., Fuchs, et al., 1999; Moffitt and Grill, 2004). Second, some authors have argued that the electrophysiological and neuroanatomical constrains used by LORETA are somewhat arbitrary. In particular, concerns have been raised about whether the assumption of maximal synchronization between neighbouring neuronal populations can be appropriately extended to adjacent voxels (Kincses, et al., 1999).

1.3.4.2.4 Variable resolution electromagnetic tomography (VARETA)

Frequency-domain VARETA has been used to estimate sources of EEG frequency bands (Bosch-Bayard, et al., 2001; Valdes-Sosa, et al., 2000). Conceptually, it belongs to the family of weighted MN solutions. VARETA utilizes different amounts of spatial smoothness for different types of generators. This is achieved by a data-driven procedure that estimates the spatial covariance matrix through the scalp cross-spectra, which ultimately selects the amount of spatial smoothness required at each voxel in the brain (Valdes-Sosa, et al., 2000). A further key difference between LORETA and VARETA algorithm is that VARETA is able to estimate discrete and distributed sources with equal accuracy (Fernández-Bouzas, et al., 1999; Fernández-Bouzas, et al., 2001).

In VARETA, current sources are also restricted to gray matter, as defined by a probabilistic brain atlas. However, a limited number of studies have used VARETA, although encouraging results have been reported for localizing EEG current density during normative mental processes (e.g., Fernández, et al., 2000) as well as in pathological conditions (e.g., Fernandez-Bouzas et al., 1999). Additional testing from independent laboratories will be important to assess the validity of this promising approach.

1.3.4.2.5 Simulation studies comparing different distributed inverse solutions

As evident from the previous sections, the past decade has witnessed substantial progress in developing distributed source localization techniques. Although these approaches have similarities and an identical goal, they often differ in the nature and extent of the anatomical, physiological, and/or statistical assumptions they implement.

Ultimately, no matter how sophisticated their mathematical and biophysical implementations are, the validity and reliability of any of these methods should be exclusively evaluated by their ability to provide physiologically meaningful solutions, in relations to other neuroimaging techniques (e.g., fMRI, PET).

Over the years, several simulations have been published. Pascual-Marqui (1999) reported that only LORETA was capable of correct localization with, on average, localization error of 1 voxel resolution, whereas the other methods showed large localization errors, in particular with deep sources. Although LORETA showed the best 3D localization accuracy, it is important to stress that LORETA tended to underestimate deep sources and that correct localization was achieved with some degree of blurring. In a later simulation, Pascual-Marqui et al. (2002) compared the localization error and spatial dispersion (i.e., resolution) of sLORETA, MN (Hamalainen and Ilmoniemi, 1994), and a new tomographic method described by Dale et al. (2000). Findings showed that sLORETA had smaller localization error and higher spatial resolution, irrespective of the presence or absence of noise and source orientation. Indeed, sLORETA was the only algorithm achieving zero-error localization. Moreover, the spatial blurring of sLORETA was smaller than the one achieved by the method employed by Dale et al. (2000).

Recently, Ding et al. (2004) recently evaluated the localization accuracy of LORETA using a realistic geometry head model (BEM). As expected, the LORETA localization error was lower when using the BEM compared to the spherical head model (approximately 10 mm vs. 20-30 mm) (Ding, et al., 2004). Yao and Dewald (2005) compared the performance of moving dipoles, MN solution, and LORETA using simulated EEG data and real ERP data. Compared to the other methods, LORETA had the smallest localization error, as well as the smallest percentage of

undetected sources and falsely-detected sources in simulated EEG data, but however LORETA, as well as the other methods, was unable to separate two discrete sources spaced only by 5 mm (Yao and Dewald, 2005).

Other simulations, however, have challenged the localization accuracy of LORETA. For example, Trujillo-Barreto et al. (2004) compared LORETA with an extension of the Bayesian model incorporating probabilistic maps derived from segmentation of standard brain template within 71 separate brain regions, and found that the latter method gave higher localization accuracy and less spatial distortion (i.e., higher spatial resolution), particularly when subcortical regions were implicated (Trujillo-Barreto, et al., 2004). Better localization accuracy of a Bayesian model incorporating structural and physiological priors compared to LORETA was also reported by Phillips et al. (2002a, b).

In fact, as mentioned above, distributed source localization techniques have been developed to resolve multiple and spatially distributed sources, and thus physiological validation through other techniques is necessary. Encouraging cross-modal validity has started to emerge for the LORETA algorithm, particularly in studies comparing LORETA with functional fMRI, structural MRI, PET, and intracranial recordings (details in the section 1.3.4.2.3). Similar cross-modal validity will be necessary for evaluating the localization accuracy of new-developed distributed source localization techniques.

1.3.5 Summary

The main goal of any quantitative EEG analysis and EEG source imaging technique is to draw reliable conclusion about sources underlying scalp-recorded signals, in order to find the accurate localization in situations of highly focal

activations. Importantly, the choice of the relevant method depends on the experimental situation. Dipole fitting method, for example during somatosensory stimulation or epileptic discharges (Michel et al., 2004; Fuchs et al., 2004), can provide accurate localization in situations of highly focal activations. On the other hand in more complex cognitive or pathological conditions that likely recruit widespread neuronal networks, distributed source localization imaging techniques, for example LORETA and sLORETA, are expected to perform better.

To sum up, a given example with a specific selected EEG record, the event-related potential (ERP, details in the next section 1.4), can generally present how to deal with the EEG data from quantitative analysis to EEG source localization (e.g., Marco-Pallares, et al., 2005). The ERP gives an electrophysiological index capable of detecting changes, and it has a temporal resolution of milliseconds but appear to result from mixed neuronal contributions whose spatial location is not fully understood. Thus, it is important to separate these sources in space and time. To tackle this problem, a designed approach combining the ICA and LORETA algorithms has been reported to analyze the spatiotemporal dynamics of ERP and cerebral sources. First, ICA separated signals' statistically independent contributions, which was used to find temporally independent and spatially fixed components of ERPs. The Infomax ICA algorithm, in which components are obtained through minimization of mutual information among output components, has recently been used to separate mixed information into spatially stationary and temporally independent sub-components in some ERP studies (Jung et al., 2001; Makeig et al., 1999, 2002). Second, the spatial maps associated with each ICA components,

statistically independent components, were analyzed, with use of LORETA (Pascual-Marqui, 1999; Pascual-Marqui et al., 1994), to locate its cerebral sources.

1.4 Event-related potential (ERP)

ERP was introduced in cognitive neuroscience more than 40 years ago (in 1960s) in order to assess the neural information processing of cognition. A wide variety of ERPs can be elicited by repeated occurrences of cognitive, motor or sensory events. Sensory evoked potentials, which are perhaps the most extensively studied type of ERPs, can be elicited by taste, somatic, auditory, various types of visual detection and recognition tests in different modalities (e.g. details in the visual GO/NOGO test, please see the following section and (Kropotov, 2009b)).

The majority of EEG research has focused on electrical responses, which are time- and phase-locked to an event, thus termed ERPs. ERPs do not represent activity generated from a single nerve cell; instead, they reflect the summed postsynaptic potentials. Due to their relatively small amplitude (usually in the range of μV) and to the high levels of environmental and biological noise in the EEG signal, ERPs only become distinguishable after averaging of multiple repetitions. They are typically characterized in terms of polarity, peak latency and scalp topography. The neurophysiological mechanisms which underlie the generation of the ERPs are still under debate. Importantly, those mechanisms are associated with a group of distinct psychological operations, for example, detecting stimuli, updating working memory, initiating and suppressing action, monitoring the results of actions and so on. In addition, the involved temporal activation/inhibition patterns of neurons locate in certain brain areas. The classical view supports the existence of an “evoked model”,

according to which the ERPs are independent from the ongoing cortical rhythms and are simply superimposed over the background oscillatory activity and noise (e.g., Jervis, et al., 1983). An alternative and more recent view suggests that the ERPs are generated by phase resetting of the ongoing cortical rhythms without any amplitude modulation (pure phase resetting) (Sayers, et al., 1974) or with a parallel increase in amplitude (phase resetting with enhancement) (Basar, et al., 1980). However, although increasing evidence supports the existence of a phase resetting mechanism (Hanslmayr, et al., 2005; Hanslmayr, et al., 2007), the important role of stimulus-evoked activity in ERPs generation cannot be disregarded (Sauseng, et al., 2007; Shah, et al., 2004).

At the early years of ERP studies the components were associated with peaks and troughs on ERPs themselves or on ERPs difference waves. The difference waves were obtained by subtraction of ERPs in a task condition that presumably did not involve a studied psychological operation from ERPs in another task condition that presumably included this operation (e.g., Bechtereva and Kropotov, 1984). Potential deflections at difference waves could be divided into classes on the basis of their latency and direction of positive or negative deviation, such as P100, N100, N200, P200, P300, N400, where P stands for positivity and N for negativity. The number stands for the peak latency in milliseconds. However, latency of peaks and troughs does not really capture the essence of a component. Therefore, for example the detected peak latency of a so-called P3b component (details in the following section) may vary by hundreds of milliseconds among subjects depending on the difficulty of the target–non-target discrimination. Even polarity of a certain components may depend on conditions of recording.

Another type of classification of components presumes their functional meaning. There are several ERP components that are elicited in certain type of behavioural paradigms and that have specific names according to their presumed function (e.g., the mismatch negativity, MMN, as an indicator of change detection in repetitive sound by Marco-Pallares, et al., 2005). The first attempts to decompose ERPs into separate components were made in 1970 by means of factor analysis and principle component analysis (e.g., Brown, et al., 1979). Recently emerged methods of objective separation of components, for example ICA (details in the section 1.3.3), lack this disadvantage of old methods without accurate presentation of ERP components, and open a new horizon in this field. Accumulating knowledge shows a diagnostic power of independent ERP components as endphenotypes of brain dysfunctions (e.g., Grin-Yatsenko, et al., 2010). The separated ERP components are presumed to reflect distinct psychological operations carrying out in distinct systems of the brain. The all studied independent ERP components in the present thesis are based on their functional meaning and the same ICA method for decomposing ERPs as well.

1.4.1 Late positive components in ERPs

From ERP studies the time interval of 250–400 ms is associated with a family of late positive components, usually called “P300” or “P3” components (Polich, 2007). The P300 components are elicited by behaviourally meaningful stimuli. The traditional two-stimulus oddball presents an infrequent target in a background of frequent standard stimuli. The subject is instructed to respond mentally or physically to the target stimulus, but not to respond to the non-target. The P300 component is measured by assessing its amplitude and latency. The definition of amplitude (μV) is

the difference between the mean pre-stimulus baseline voltage and the most robust positive peak of the ERP waveform within a time window. Latency (ms) is defined as the time from the onset of the stimulus to the peak point of the maximum positive amplitude within a time window (Polich, 2007). Therefore, ERP data are analysed in the time domain by assessing the amplitudes and latencies of eminent and robust peaks. From current neuroelectric and neuroimaging data analysis, the understanding of the P300 derived primarily from functional analysis is now thought to be constructed of various parts that reflect the cognitive processing flow when attentional and memory mechanisms are involved (Polich, 2007). There are two neuropsychological subcomponents in the P300, P3a and P3b.

An earlier component with relatively short peak latency, P3a component, stems from “stimulus-driven” frontal attention mechanisms. It is enhanced in response to a sudden and noticeable change in sensory stimulation and is associated with orienting to the stimulus change and shift of attention (Polich, 1989; Polich, 2007). The frontal/central P300 can be extracted when an infrequent distracter stimulus is inserted randomly into the target/standard sequence. The P3a is elicited by the non-target distracter, and therefore it is not a task relevant potential but an indicator of an involuntary switch of attention (Polich, 2007).

In contrast, P3b, the task relevant potential, is elicited during target stimulus processing (Polich, 2007; Snyder and Hillyard, 1976). The P3b stems from temporal–parietal activity, and P3b component is enhanced in response to targets, such as pressing a button or counting the number of targets for responding a rare stimulus or tone. Therefore, it is associated with attention and appears related to subsequent memory processing, as an index of updating working memory (Kropotov, 2009b; McCarthy, et al., 1989; Polich, 2007). These reports favour a relation between

P300 and the attentional processing of target events and the results appear connected to memory processing. Attention and working memory are interconnected operations: to keep the item in working memory one must attend to it, and vice versa to attend to some expected stimulus one must keep it in memory. PET and fMRI studies in humans indicate that neuronal networks for these operations are similar. A network consisting of areas in the parietal and frontal cortex has been found to be activated in a variety of visuospatial tasks that require attention and working memory (Buschman and Miller, 2007; Ungerleider, 2000).

1.4.1.1 P3a component

When a sudden change occurs in the environment an inside sensory system detects this new event and shifts attention toward the new object with a goal of exploring it more closely. This mechanism of this kind of involuntary nature “orienting response” enables humans and animals to adapt in constantly changing situations. The brain constructs this sort of model to sense surrounding environment and maintains this model in the sensory system. An ERP component associated with the orienting response – the P300a or P3a – was first described in 1967 (Sutton, et al., 1967).

In a typical P3a experiment, a subject performs an auditory target detection task with simple pure tone stimuli, and occasionally hears a contextually novel sound. Then these novel sounds repeatedly elicit a scalp-recorded potential that peaks about 200–300 ms after the stimulus and that is largest over the central and frontal scalp electrodes (Polich, 2007). It should be stressed here that neuronal circuits for generators of P3a are not only limited by the premotor areas, but also found in a variety of cortical and subcortical structures, including prefrontal, parietal, lateral

temporal, and medial temporal cortical areas as well as subcortical structures such as the basal ganglia and thalamus (Halgren, et al., 1994; Kropotov, 2009a). Obviously this heterogeneous network includes several systems with different functions. Importantly, some of these structures, such as anterior cingulate and prefrontal cortex, are responsible for orienting attention in order to process the deviations from the background simulation (Patel and Azzam, 2005; Posner and Dehaene, 1994).

1.4.1.2 P3b component

The experimental evidence in humans indicate that the P3b appears show features: (1) P3b appears after target stimuli in oddball paradigms, and (2) it depends on the behavioural significance and attention paid to eliciting stimuli, (3) P3b is greater for hits than for false alarms or misses in a signal-detection task (Kropotov, 2009a; Polich, 2007). In 1990s P3b was studied by using intracranial recordings in patients with implanted electrodes, and the evoked P3b-like components were found in the frontal and parietal cortical areas (including lateral, medial parts, and anterior cingulate) as well as the basal ganglia and thalamic nuclei only in the active condition when deviant stimuli required actions (pressing a button) (Kropotov and Etlinger, 1999; Kropotov, et al., 1995). These intracranial ERPs components were in the latency range of P3b scalp recorded component, but in contrast to the positive deflections in scalp were both of positive or negative polarities in intracranial recordings.

P3b component is the most studied in the scientific literature component both in theoretical and clinical fields. There were several reasons for that: First, the P3b is elicited in the odd ball task which is quite simple to perform for almost all categories of neurological or psychiatric patients. Second, the P3b is a relatively large

component which is quite easy to discriminate as a difference wave between responses to target deviants and non-target standards. Third, the P3b seems to have a diagnostic power because the impairments of the P3b were found in several executive dysfunctions such as schizophrenia (e.g., Neuhaus, et al., 2010; Olbrich, et al., 2005) and attention deficit hyperactivity disorder (ADHD) (e.g., Becker and Holtmann, 2006; Gow, et al., 2012).

1.4.1.3 Visual continuous performance task (VCPT)

Based on the traditional two-stimulus oddball with target and non-target stimuli, the VCPT condition consists of a typical visual GO/NOGO (GNG) paradigm, reflecting the electrophysiological characteristics of selective attention mechanisms (Polich and Herbst, 2000; Polich and Kok, 1995). Subjects are required to attend and respond to certain target stimuli by pressing a button in a typical “active oddball paradigm” with “GO” pictures of visual stimuli, but not to respond to the non-target, “NOGO” pictures of visual stimuli. It has been documented that “on-task” measures during attention-requiring activities reproduce reliably between testing session (McEvoy, et al., 2000). The on-task measures can induce more homogeneous arousal levels and cognitive processing demands across subjects and repeated testing.

The GNG task is also a useful behavioural model for studying executive functions, which are needed for optimizing behaviour. The term “executive functions” refer to the coordination and control of motor and cognitive actions to attain specific goals. The relevant ERP components associated with selection of attention and action in executive control are in the following section.

Basically in the VCPT, the electrophysiological signature of selective attention mechanisms is investigated by comparisons between ERP components to “GO” and to

“NOGO” stimuli in attended visual tasks. “GO” stimuli require attention and response to certain stimuli for the assessing of voluntary attention. Of particular interest in relation to the demand-characteristics of GNG attention measures is the “P3GO”, the P300 (P3b) ERP component. This P3GO component reflects a positive deflection in the ERP wave around 300 ms at the parietal site (Pz) after presenting a target stimulus in the GNG task (Kirmizi-Aslan, et al., 2006; Pfefferbaum, et al., 1985). However, the “P3NOGO” ERP component occurs around 400 ms with a centro-parietal maximum in a semantic GNG paradigm (Kirmizi-Aslan et al., 2006; Pfefferbaum, 1985). The P3GO has the same characteristics as the traditional oddball-P3, but the P3NOGO has a different topography, which implies that it corresponds to a separate neuronal process from the P3GO.

Furthermore, considering the N2 component elicited in the NOGO condition in a visual task, the difference in ERPs between the NOGO and the GO conditions is a negative wave with a frontocentral distribution, peaking around 200-260 ms which is labelled as the N200 motor inhibition component (Bekker, et al., 2005; Kropotov, 2009b; Pfefferbaum, 1985) (details in the following section). However, in the auditory modality, this N200 component in some variants of the GO/NOGO paradigm was either absent or reduced (Falkenstein, et al., 1995). Briefly, the N2-P3 component in the GO/NOGO paradigm has been reported in association with response inhibition (Bekker, et al., 2005; Falkenstein, et al., 1999b; Smith, et al., 2008) and conflict monitoring (Nieuwenhuis, et al., 2003).

1.4.2 ERP components in the selective attention and executive control

The term “executive functions” has long been used as a synonym for frontal lobe function in neuropsychology. The need for the executive control mechanism has been

postulated for selecting an appropriate action from variety of options, inhibition of inappropriate actions, and keeping in working memory the plan of action as well as the results of actions (Kropotov, 2009b). A modern view with several sub-components in the presumed executive mechanisms is from Smith and Jonides (1999). They distinguished between mechanisms relating to (a) attention and inhibition, (b) task management, (c) planning, (d) monitoring, and (e) coding (Smith and Jonides, 1999). Recent research has been concentrated on those sub-processes and distinguished the following operations on actions: (1) selection operations such as engagement and disengagement procedures, (2) working memory, and (3) monitoring operations (Kropotov, 2009b; Smallwood, et al., 2004) (details in the following sections). These operations are well defined at psychological level. It is assumed that these different functions are sub-served by different neuronal mechanisms and are reflected in different components evoked by actions.

1.4.2.1 ERP components in the engagement and disengagement operations

In the typical GNG paradigm, Gemba and Sasaki found a specific premotor/motor cortical circuit involved in motor suppression (Gemba and Sasaki, 1990; Sasaki, et al., 1993). They showed in monkeys that excitation of cells in the principle sulcus during regular responses yielded a decrease of activity in primary motor cortex and either a delay or the complete suppression of responses while direct electric stimulation of this area suppressed a prepared response to GO stimulus (Sasaki, et al., 1989). In humans a frontally distributed negative ERP component, called **N200 NOGO**, peaks at about 200–260 ms poststimulus has been observed in numerous studies (Falkenstein, et al., 1999a; Kopp, et al., 2007). This component had greater amplitude for NOGO in comparison to GO stimuli and was associated with

response inhibition in GNG paradigms. Note that in all classical studies the N2 component was separated simply as a difference between ERPs for GO and NOGO cues.

To sum up, N2 NOGO ERP component (N200 motor inhibition component) is elicited after NOGO cues and expressed in frontally distributed negativity. NOGO cues elicit a strong negative wave with peak latency at 260 ms, and the negative fluctuation is followed by a positive component with the frontal distribution.

Furthermore according to recent ICA-based ERP analyse, the negative fluctuation in the raw ERP (N200 motor inhibition component) is actually a sum of negative fluctuations generated in three different components (sensory comparison, motor inhibition, and action suppression components) revealed by ICA in the engagement and disengagement operations (Kropotov, 2009b). This association between raw ERPs and their independent components shows us that the ICA provides decomposition of ERPs into several independent components each of them having specific temporal–spatial pattern and specific functional meaning. In addition, the power of ICA in discriminating separate psychological operations is superior to conventional methods of ERP analysis. Moreover, independent components may represent with a better success in diagnosis of different brain dysfunctions associated with impairments in specific operations such as comparison, motor inhibition, and action suppression operations (details in the following sections).

1.4.2.1.1 Sensory comparison component

The inhibition of prepared action is performed by a complex brain circuit with the lateral prefrontal cortex (PFC) as a part. The PFC receives the sensory information from the sensory systems (visual, auditory, and somato-sensory) and is in position to

make decision whether to GO or NOGO depending on the results (Hester, et al., 2004; Kropotov, 2009b; Swainson, et al., 2003). One can speculate that to inhibit a prepared action, the brain must first compare the current sensory situation with the sensory model and to detect the mismatch.

Then the result of these comparison operations is transferred to the PFC to activate the circuits responsible for inhibition of the prepared action. This thinking process is supported by results of ICA performed on ERPs computed for GO and NOGO cues in the two stimulus GO/NOGO task (Kropotov, 2009b). In the temporal cortex, NOGO cues evoke an additional component in comparison to GO cues while in the left premotor cortex NOGO and GO cues elicit opponent reactions. The difference in time dynamics of the two components for GO and NOGO cues shows that the components are functionally different.

1.4.2.1.2 Motor inhibition component

The second component generated in the left premotor cortex is associated with motor suppression, and this motor inhibition component is negative in the frontal areas (Kropotov, 2009b). Neuronal mechanisms of motor inhibition involve the basal ganglia circuits. The inhibition of the prepared action seems to be performed by means of the indirect pathway of the basal ganglia thalamo-cortical loop with a cortical location in the premotor cortex.

1.4.2.1.3 Action suppression component

The existence of the third component elicited by NOGO cues is the intriguing part of ICA of ERPs data in a GO/NOGO task. Spatial distribution, temporal pattern, and contrast to GO cues are different from the previous two components. This action

suppression component has only one prominent peak with latency of 340 ms, and it is a symmetrical component with generators widely distributed over premotor and motor cortical areas (Kropotov, 2009b). However, it is present only in NOGO condition, and decreased in amplitude and increased in latency with aging. The action suppression component is almost three times larger than the motor inhibition component, and then it may have a superior diagnostic power than the motor inhibition component.

1.4.2.2 ERP components in the monitoring operation

Experimental findings indicate that the function of the dorsal part of the ACC is to monitor actions (e.g., Hester, et al., 2004; Van Veen and Carter, 2002). Flexible adjustments of human and animal behaviour require the continuous assessment of ongoing actions and the outcomes of these actions. The ability to monitor and compare ongoing actions and performance outcomes with internal goals and standards is critical for optimizing decision making. This ability is called action monitoring.

In addition, the ventral part of the ACC is suggested of being involved in this cognitive operation (Luu, et al., 2003). The concept of monitoring must be distinguished from the concept of attentional control. Attentional control refers to a top-down, limited resource cognitive mechanism modulating sensory information processing, while the monitoring of actions refers to a cognitive mechanism that evaluates the quality of executive control and activates the executive system in the case of mismatch between expected and executed action (Kropotov, 2009b).

Three requirements allow certain ERP components for the function of monitoring. First, the component has to be of a long latency for action initiation because the activation of the executed action has to be compared with the planned one. Second, the component has to be generated in a particular area that receives

information from both the planned action and the executed one in order to compare these two signals. Third, the component has to occur in conflict situations when a prepared action has to be withheld because the current situation does not match the expected one or when an action has been executed but its outcome does not match the planned one. The late positive P400 component that occurs in NOGO trials, generated in the ACC fulfils these requirements and therefore can be considered as a “monitoring” component in GO/NOGO Paradigm (Kropotov, 2009b).

1.4.2.2.1 P400 monitoring component

The P400 monitoring component is the largest NOGO ERP component in amplitude in medial prefrontal and anterior cingulate cortical areas. It is a symmetrical positive component located centrally in the 2D space with maximum at Cz–Fz site. The latency of the P400 monitoring component changes with age significantly – from 370 ms at middle age to 420 ms at early age and 460 ms at older age (Kropotov, 2009b).

1.4.2.2.2 Function of ACC

The P400 monitoring component is the one that is generated in the ACC. So, it is important to present the anatomy and physiology of the ACC in details. First of all, the ACC includes motor areas that receive inputs from the primary motor cortex, premotor, and supplementary motor areas. These motor areas thus store the precise image of a planned action. This part of the cingulate is also in position to initiate a new action. Second, the ventral part of the ACC receives inputs mostly from the affective (limbic) system directly (such as from amygdala) or indirectly (via the anterior nucleus of the thalamus). Therefore, the ventral portion of the ACC is called

“limbic” part. Third, the dorsal part of the ACC has strong reciprocal connections with the lateral, anterior, and medial prefrontal cortical areas – areas presumably involved in cognitive functions, and therefore, the dorsal portion of the ACC is called “cognitive” part (Kropotov, 2009b).

1.4.3 Summary

The executive control is needed for optimizing behaviour. Therefore, the need for an executive control mechanism has been postulated for non-routine situations requiring a supervisory system, in order to select an appropriate action from variety of options, inhibit inappropriate actions, and keep in working memory the plan of the action as well as the results of the action at the same time. The executive functions are implemented by a complex brain system that consists of several cortical and subcortical structures interconnected with each other. Together with the basal ganglia the prefrontal areas perform executive functions associated with engagement, disengagement, monitoring operations as well as with working memory. These operations are reflected in ERP components evoked in a GNG paradigm as well as in working memory tasks. The recently developed ICA provides a powerful tool for separating the components associated with executive functions overlap in time and space. The following executive components can be separated by ICA in the two stimulus GO/NOGO task: the motor and action suppression components associated with frontal negativities at 200 ms (the conventional N2 inhibition component), the engagement component associated with parietal positivity at 300 ms (the conventional P3b component), the monitoring component associated with frontal–central positivity at 400 ms. Those decomposed ERP components with functional meanings and ICA

will be applied to study the effect of electroacustimulation (EA) on the sustained attention and electrocortical activity (details in the chapter 3).

1.5 Brief History of Acupuncture

Acupuncture has been used for thousands of years. The first document that depicts the use of acupuncture dates to 200 B.C. It is based on a concept of inner power and the ancient established theory of Qi, an energy that flows through the body^{*1}. Over years, acupuncture has become a standard treatment modality in Chinese medicine. Acupuncture therapy has been practiced in Chinese medicine for more than three thousand years with applications including treating headache, recovering from stroke and controlling pain (Han, 2004; He, et al., 2004; Huang, et al., 2002; Wong, et al., 1999).

The history of acupuncture in the West began as early as the 17th century. In fact, for a short-lived period in the early 19th century, it was introduced in scientific journals. In one Lancet publication in 1823, the author discussed its uses and offered a brief description of the variations of technique at that time^{*2}. However, acupuncture eventually achieved acceptance in the USA when an NIH consensus conference reported positive evidence for the effectiveness of acupuncture treatment, at least in a limited range of conditions (Marwick, 1997).

^{*1} The Chinese medical text that first describes acupuncture is The Yellow Emperor's *Classic of Internal Medicine (History of Acupuncture)*, which was compiled around 305–204 B.C.

^{*2} Acupuncturation. Lancet. 1823. Nov. 9: 200-1

Acupuncture can now be considered an important complementary medicine practice, with increasing interest from the public, and both the National Institute of Health (USA) and the World Health Organization have summarized guidelines on acupuncture therapy (Berman, 2001; Bonnerman, 1979). The traditional theories of acupuncture have been challenged in the West, and ancient concepts of Qi flowing in meridians have been replaced by a neurological model, based on the evidence of stimulation, from changes of peripheral nerve endings to changes of brain function, particularly the intrinsic pain inhibitory mechanisms (Han and Terenius, 1982; Mann, 2000; Ulett, 1992). (Please see the following sections). Recent years have seen increased interest in acupuncture therapy in neuroscience including (a) mechanisms of action (Kaptchuk, 2002), (b) respondent brain areas (Biella, et al., 2001; Dhond, et al., 2007; Uchida, et al., 2003), and (c) temporal dynamics such as immediate and/or delayed effects (Chen, et al., 2006; Dhond, et al., 2008). With the increasing development of acustimulation methods for cognition, reliability requirements have become more critical.

1.5.1 General application of acupuncture and electroacustimulation (EA)

Peripheral electrical stimulation may be elicited via electrodes located on the skin (transcutaneous electrical nerve stimulation, TENS), and the process is usually named electroacupuncture stimulation or acustimulation (Han, 2003). Wang et al (1992) have demonstrated that TENS operates through very similar mechanisms to traditional acupuncture (Wang, et al., 1992), with the mechanism of therapeutic action thought to involve neurotransmitter and opioid peptide systems in order to facilitate the release of neuropeptides in the central nervous system (CNS) (Cheng and

Pomeranz, 1979; Han, 2003; Han, 2004; Mayer, et al., 1977; Wang, et al., 1992). The stimulus parameters of electroacupuncture (intensity, mode, frequency, etc.) can be controlled more precisely than by manual acupuncture. Furthermore, the uncomfortable pain sensation induced by needle manipulation is undesirable and an invasive procedure may also carry the risks of hematoma formation and infection. Electroacupuncture has been the procedure of choice for its comfort, convenience and high repeatability during an individual stimulus program.

Different types of endorphins for analgesia have been selectively released by low- and high-frequency acustimulation (Han, 2003; Shen, 2001). Low-frequency stimulation has induced the release of enkephalins, whereas high frequency stimulation has increased the release of dynorphins in both animal and human experiments (Han, 2003; Ulett, et al., 1998). Therefore acustimulation in specific frequencies can facilitate the release of specific endogenous opioid peptides for acupuncture-induced analgesia in the central nervous system. Furthermore, through increases in the level of enkephalins and serotonin in the CNS and plasma acupuncture could affect psychological processes, hence applications for the treatment of depression and anxiety (Cabyoglu, et al., 2006; Ulett, 1996; Ulett, et al., 1998) (Acupuncture mechanisms, details in the chapter 3)

Regarding the temporal effects, both short-term and long-term impact has been examined. It has been proposed that the basic mechanism of the former involves immediate frequency modulation of neuroplasticity (Kaptchuk, 2002), and of the latter gene transformation of protein synthesis in specific cortical areas as shown with neuroimaging (Biella, et al., 2001; Uchida, et al., 2003). Dhond et al (2008) have claimed that acupuncture can “enhance the post-stimulation spatial extent of resting

brain networks to include anti-nociceptive, memory, and affective brain regions” (Dhond, et al., 2008). There is a likely impact of acustimulation on cognitive functions aside from therapeutic outcome. There has been limited research showing differential effects between low versus high frequency stimulation on cognitive function. With the electroencephalograph (EEG), scalp maps of high versus low-frequency effects have been investigated in a resting eyes-closed condition, but not in cognitive tasks (e.g., Chen, et al., 2006). In general the relationship between acustimulation and task evoked brain activity is a neglected area.

In fact by using powerful non-invasive fMRI (Wu, et al., 2002), positron emission tomography (PET) (Pariente, et al., 2005), and the electroencephalogram (EEG) (Chen, et al., 2006), not only pain related cortical regions, but more acupuncture-induced sites associated with other systems in the CNS have also been confirmed. These brain imaging techniques provide evidence supporting the effect of acupuncture manipulation on cortical networks and subcortical limbic and paralimbic structures in the human brain (Dhond, et al., 2007; Hui, et al., 2000). Recently, a broad search through nine electronic bibliographic databases (PubMed, Cochrane Library, Web of Science, ERIC, PsychINFO, Psyn dex, Cinahl, Biological Abstracts, Rehabdata) was accomplished to evaluate the effects of Transcutaneous Electrical Nerve Stimulation (TENS) on non-pain related cognitive and behavioural functioning in patients, for example with stroke, Alzheimer's disease (AD), or coma due to traumatic brain injury (van Dijk, et al., 2002). Electrostimulation with TENS was also reported to have a moderate beneficial influence particularly on executive function and improvement in behavior in studying children with ADHD (Jonsdottir, et al., 2004), showing the proved hypotheses of cortical plasticity and intracranial

modulation in TENS stimulation effects on cognition. Theoretical and neuroimaging studies of acupuncture modulating neuronal functional networks in relation to multiple physiological systems with diverse cortical effects have only emerged since 2008 (e.g., Bai, et al., 2009; Dhond, et al., 2008) (mechanism of EA stimulation, details in the chapter 3).

Applying acupuncture as a tool for alleviating pain and for modulating cognitive performance in patients and healthy subjects is developing and although acupuncture practice has found a niche in clinics, acupuncture is far from being accepted. There is a need for more scientific progress in delineating the neurobiology of acupuncture. Based on published scientific articles it has been shown that the effect of acupuncture is not just due to a so-called placebo effect (e.g., Bai, et al., 2009; Dhond, et al., 2008). Careful scientific studies have presented evidence of the neurochemical basis of acupuncture (e.g., Chen, et al., 2006; Han, 2003). Moreover, electrical stimulation has presented a more scientific and powerful mode of acupuncture treatment via frequency modulation (e.g., Chen, et al., 2006; Han, 2003). Thus, the electroacustimulation mode with different frequencies has been the chosen modality for use in this thesis.

1.5.2 Effects of EA stimulation on EEG/ERP and attention

Although there are recent publications demonstrating significant associations between acupuncture and the neuroimaging (fMRI), little information has been reported in the literature concerning EA stimulation (or acupuncture) and the resting EEG. There is also limited research related to electrocortical activity and EA in

revealing distinguishable influences between low versus high frequency stimulation on cognitive function. Rosted et al. (2001) concluded that there were no changes in the resting EEG in the frequency range from 2 Hz to 30 Hz after very short periods (0.5, 1.0 and 2.0 min) of manual acupuncture stimulation. However, specific comparisons of high- vs. low-frequency effects have been investigated in the study of Chen et al. and they reported that the activity of theta power significantly decreased during high-frequency (100 Hz) EA stimulation in a resting eyes-closed condition and the localization of the decreased theta EEG power was near the frontocentral midline sites (Chen, et al., 2006).

These findings and others have led to two main methodological implications. First, sufficient stimulation time is important to generate detectable changes in EEG, as also seen with the sustained hypoalgesic effect for 30 min post-stimulation in the study of changed pain threshold after TENS stimulation (Chesterton, et al., 2002). This led us to ensure that EA tested for at least 15 minutes. The second concerns the site of stimulation. Short-term cortical dynamic changes occurred in theta, notably at the frontocentral midline site, and this cortical plasticity was modulated by EA stimulation at the HeGu acupoint. Furthermore, the significant effects of acupuncture at the NeiGuan acupoint on the electroencephalogram and attenuating nausea and vomiting have also been studied extensively (e.g., Chang, et al., 2009; Streitberger, et al., 2006). Therefore, we chose these two acupoints located on the hands for our stimulation sites (see the methods section in the chapter 3).

Considering the acupuncture effects on ERPs, some articles of auditory ERPs together with acupuncture have been published with various results (Abad-Alegria, et al., 1995; Bray, et al., 2005; Liao, et al., 1993). Liao et al. concluded that acupuncture

may promote middle latency auditory evoked potentials (MLAEPs) activity, while decreased P50 potential amplitude after EA stimulation was reported by Bray et al. (2005). Regarding a possible change in the auditory P300 amplitude after acupuncture stimulation, Abad-Alegria et al. (1995) reported that the real action of ShenMen acupoint, reflecting possible neuropsychological processes after stimulation, but no changes were detected in a non-acupuncture point stimulation. Additionally, the anatomical structure difference in the acupoints and non-acupoints may explain the specific acupoint-brain correlation. P150 located in bilateral anterior cingulate cortex and it was also observed after EA stimulation on acupoints but not non-acupoints, indicating a characteristic activation in response to acupoint afferent (Yu, et al., 2009; Zeng, et al., 2006).

However, there are very few articles related to visual ERPs. Recently, Chae et al. (2010) concluded a significant effect of acupuncture on selective attention for smoking-related visual cues in smokers. The relevant fMRI studies on acupuncture effects on visual and auditory cortex activations (Beissner and Henke, 2009) showed that activations, deactivations or both in some part of the visual cortex (Brodmann areas 17, 18 and 19)(Gareus, et al., 2002). For hearing-related acupoints the situation is similar, and Cho et al. (in 2000 and 2001) also published positive results on hearing-related acupoints in two books. Even in the view of treatment in the various diseases related to hyperactivity, acupuncture has been reported that it might be effectively mediated through the central nervous system, especially through the forebrain, shown in EEG changes in theta band power by acupuncture stimulation, increased during acupuncture stimulation and post-acupuncture stimulation period (Hori, et al., 2010; Sakai, et al., 2007).

Therefore based on the suggestions of prior publication in ERPs EEG and fMRI, two more implication can be noted. First, a new analysis method for ERPs may play an important role to enhance different neuropsychological processes after stimulation. For instance, the ICA together with sLORETA in studying cortical activity of ERPs and their components may reveal effects (details in the previous section 1.3), superior to the results from the traditional ERPs, after repeated visual attention tasks, and when compared with a control baseline meaning of attention before EA stimulation. Second, in line with the expectations of changed attention after stimulation, visual continuous attention task seems to be a valuable behavioural outcome measurement and a method to measure cortical electrophysiological activity in evaluating EA stimulation effect on attention (details in the chapter 3).

1.6 Introduction of functional connectivity and functional networks

“Functional connectivity” refers to many possible relationships that might exist between the activation of distinct and often well separated neuronal populations (Ioannides, 2007). It may go with or without any reference to physical connections or an underlying causal model. In contrast with functional connectivity, “effective connectivity” refers to causal effects that one neuronal population applies to another, and it is based on an underlying way of connecting the different neuronal populations (Ioannides, 2007). There are diverse methodologies which have proven useful for the study of functional and effective connectivity, such as PET and fMRI, and electrophysiological and magnetic recordings, EEG and MEG, taken directly from multiple brain areas.

MEG and EEG record the magnetic or electrical fluctuations that occur when a population of neurons is active. These methods are excellent for measuring the time-course of neural events (in the order of milliseconds), but however generally poor at detecting the locations of the happening events. On the other hand, PET and fMRI measure changes in the composition of blood near a neural event, and those changes are slow (in the order of seconds). Therefore, these imaging methods are much worse at measuring the time-course of neural events, but are generally better at detecting the location. Nowadays “brain activation studies” focus on determining distributed patterns of brain activity associated with specific tasks according to the interaction of distinct brain regions. As a great deal of neural processing is performed via a network of several cortical regions, scientists are able to thoroughly understand information flow back and forth in the brain.

Therefore, examining functional connectivity is to validate the interregional neural interactions during particular cognitive or motor tasks or merely from spontaneous activity during rest. fMRI and PET enable creation of functional connectivity maps of distinct spatial distributions of temporally correlated brain regions called ‘functional networks’. Recent studies of functional brain connectivity by neuroimaging have used graph-theory-based tools for describing large-scale brain networks (for a review, Ioannides, 2007), and this refined technology is well developed for describing the connectivity of distinct brain areas at the level of anatomy and function. Furthermore, some direct methods to measure functional connectivity involve observing how stimulation of one part of the brain region will affect other cortical areas. Noninvasively in humans, combining transcranial magnetic stimulation (TMS) or EA with one of the neuroimaging tools such as PET, fMRI, or

EEG have been investigated (e.g., Hui, et al., 2010; Napadow, et al., 2005; Ros, et al., 2010).

1.6.1 Resting state networks (RSNs) and default mode network (DMN)

Typically fMRI experiments focus on the acquisition of MR images during periods of increased oxygen consumption, blood-oxygen level dependent (BOLD) signal (according to neuronal response to experimental conditions), and then the measured image intensities are compared with recordings obtained from a ‘rest’ condition. Therefore, such suitable definition of this baseline/rest signal is of particular importance in exhibiting complex fMRI ‘activation maps’ identified under the rest condition and under external stimulation (Beckmann, et al., 2005). Recently, this resting state activity has been termed the default-mode of brain activity to indicate a state in which an individual is awake and alert, but not actively involved in an attention demanding or goal-directed task (Raichle, et al., 2001). RSNs depict the neuronal baseline activity of the human brain in the absence of stimulated neuronal activity, reflecting functionally basic networks.

RSNs have been identified in the motor system (Biswal, et al., 1995), the language system (Hampson, et al., 2002), and the dorsal and ventral attention systems (Fox, et al., 2006). Not only has the hemodynamic footprint been well investigated, but also the underlying electrophysiological signature (e.g., Laufs, et al., 2003; Mantini, et al., 2007). Using simultaneously acquired EEG combined with fMRI data under a rest condition, at least two research teams have shown that the variation in alpha rhythm in the EEG (8–12 Hz) is correlated with the fMRI measurements, including multiple regions of occipital, superior temporal, inferior frontal and

cingulate cortex (Goldman, et al., 2002; Laufs, et al., 2003). These results show some important implications for the interpretation of RSNs and the correlation between RSNs and EEG-alpha dynamics.

Since Marcus Raichle first coined the term “default-mode” in relation to resting state brain function (Raichle, et al., 2001), the DMN concept has rapidly become a central theme in cognitive and clinical neuroscience. This DMN concept comes from an emergent body of evidence showing a consistent pattern of deactivation across a network of brain regions which includes precuneus/posterior cingulate cortex (PCC), medial prefrontal cortex (MPFC) and medial, lateral and inferior parietal cortex (see a review, Broyd et al., 2009). This DMN consists of two relatively independent major regions – the frontal and parietal lobes. The DMN is active in the resting brain with a high degree of functional connectivity between regions. Although the DMN is characterized as a homogenous single network, each brain area participating in the DMN has its own functional role. For example, attenuation of the ventral MPFC occurred with tasks involving judgments that were self-referential; activity in the dorsal MPFC increased for self-referential stimuli, suggesting the dorsal MPFC is associated with introspective orientated thought (Gusnard, et al., 2001); working memory tasks differentially deactivate the PCC (see a review, Broyd, et al., 2009).

However, some mental disorders show DMN abnormalities and atypical patterns of DMN activity. These altered patterns of DMN activity are typically characterised by dysfunction of introspective mental processes. For example in schizophrenia, positive symptom severity was correlated with increased deactivation in the MFG and precuneus in an oddball task (Garrity, et al., 2007). In autism however, atypical or reduced self-referential, affective and introspective thought is associated with low

activation of the DMN in the resting state (see a review, Broyd, et al., 2009). In ADHD, reductions in the resting state anti-correlation between dorsal ACC and PCC/precuneus have been reported in an adult ADHD group. In addition, the anterior component of the DMN was markedly absent, with significant reduced resting state functional connectivity in medial PFC, superior frontal gyrus and also in PCC/precuneus, indicating a relationship between working memory deficits and attentional lapses in ADHD (Castellanos, et al., 2008). That the DMN may become a potentially significant clinical tool warrants further research.

1.6.2 Dorsal attention network (DAN)

Attention is not a unitary function, and it includes perception, action, language, and memory (Pashler, 1999). One of the better studied forms of attention is visual orienting, i.e., the ability to select stimuli for action, and a model has been proposed for different attentional operations during sensory orienting. These operations are carried out by two separate frontoparietal systems, a dorsal attention system and a ventral attention system (for a review, see Corbetta and Shulman, 2002). The dorsal system, also called the Dorsal Attention Network (DAN), is involved in voluntary (top-down) orienting and shows activity increases after presentation of cues indicating where, when, or to what subjects should direct their attention (Corbetta, et al., 2000; Shulman, et al., 2003). The DAN is bilateral and composed of the intraparietal sulcus (IPS) and the junction of the precentral and superior frontal sulcus (frontal eye field, FEF) in each hemisphere (Fox, et al., 2006). On the other hand, the ventral system is right-lateralized and composed of the right temporal-parietal junction (TPJ) and the right ventral frontal cortex (VFC). This ventral system shows activity increases upon

detection of salient targets appearing in unexpected locations (Corbetta, et al., 2000; Kincade, et al., 2005). These two systems appear to cooperate and interact during normal behaviour.

1.7 Neuroplasticity and learning

Neuroplasticity, which refers to the ability of the brain and nervous system to change structurally and functionally as a result of input from the environment, occurs on a variety of levels, ranging from learning and memorizing to cortical remapping in response to injury and recovery from brain damage (Shaw, et al., 2001). Although for most of the 20th century neuroscientists generally believed that brain structure is relatively immutable after early childhood, this belief has been challenged by recent findings, which reveal that many aspects of the brain remain plastic even in adulthood (Rakic, 2002). In other words, it is this inherent flexibility of the central nervous system (CNS) that gives the more complex organisms their most important advantage: their ability to adapt, because to learn is ultimately, to adapt.

To investigate the behavioural and neurophysiological processes and the EEG dynamics that are commonly associated with the concept of “neuromodulation” and the ability to appropriately adjust the nervous system for optimal function, the third experiment provides a feasible framework with converging evidence which logically supports the use of a variety of modern neuromodulation techniques – culminating in neurofeedback assisted by electroacustimulation – to promote or “optimize” the neurocognitive mechanisms responsible for the acquisition of improved levels of attention and enhanced perceptual sensitivity (details in the chapter 5).

1.7.1 Activated states for learning

Learning during different behavioural states may lead to different outcomes. Since the neurobiological functions of an organism serve to assist its adaptation to behaviourally challenging environments, it becomes critical to survival when it is necessary to accelerate and more profoundly distil the learning and refinement of proper skills. It seems logical to ask which clinical processes actually characterise the neurobiological states that appear to be beneficial to learning and/or performance in general? Historically speaking, previous studies have noted that the neurochemical and neuroelectric (EEG) operation of specific functional systems is upregulated, during so-called ‘activated’ states of behaviour, and references have often been made to increased states of ‘arousal’ (Gruzelier, et al., 2006; Neiss, 1988; Paisley and Summerlee, 1984). Details of this will be presented in the succeeding sections. In the operational sense, such states may be regarded as ‘activated’, in light of evidence that they require a concerted upregulation of the central nervous system (CNS) and metabolic activity (Ursin and Eriksen, 2004). Furthermore, it has recently been shown that exogenous stimulation of such systems, via magnetic and electrical methods, can successfully modulate and enhance learning and its associated behavioural performance (Hirshberg, et al., 2005). Details of this will be presented in the succeeding sections. It is this poignant combination of several behavioural and neurophysiological processes that allows a more integrated understanding of the phenomenon.

1.7.2 A neurochemical for motor learning – Dopamine

Neurochemicals, such as serotonin and dopamine, are organic molecules that participate in neural activity. The brain exploits the neuromodulatory property of

neurochemicals to manipulate neural activity on a more global or distributed scale. The common neuromodulatory transmitters are usually secreted by a small group of neurons located in the sub-cortex (brainstem or basal forebrain regions), whose axons diffuse through large areas of the nervous system and, therefore, have long-lasting effects on multiple neurons. In addition, the structure of sub-cortical regions enables the nervous system to flexibly tune the level of its overall activity and those regions' particular functional subsystems. For example, activity in corticostriatal circuits alters during the learning of new actions, but the plastic changes observed during the early stages of learning a new action are different to those observed after extensive training. Accordingly, dopamine, a critical modulator of short- and long-term plasticity in corticostriatal circuits, is involved differently in the early and late stages of action learning. (Costa, 2007).

The dopaminergic system arises from the ventral mesencephalic neurons which are located in two main aggregations: the substantia nigra and ventral tegmental area (VTA), which is believed to be involved in reward-dependent behaviours and to be activated by rewards. Other reports have also documented that the dopaminergic system is mainly driven by craving and reward (Berridge, 2004; Hollerman and Schultz, 1998; Schultz, et al., 1997). Moreover, the dopaminergic system strongly innervates the frontal cortical regions (Briand, et al., 2007). Their axons ascend through the medial forebrain bundle and the synapse in the striatum (comprising the nigro-striatal pathway), the basal forebrain and the neocortex. In primates, the greatest density of dopaminergic fibres occurs in the primary motor cortex (Lewis, et al., 1987). The neurons of the dopaminergic system may fire in both tonic and phasic modes and this determines the dynamics of DA release in the prefrontal cortex and

striatum, where relatively prolonged and frequency-dependent effects can occur, indicating their role as a neuromodulator of these structures (Garris and Wightman, 1994; Lapish, et al., 2007; O'Reilly, et al., 2002).

In pharmacological and pathological views, firstly, pharmacological stimulation of the VTA is positively rewarding in animals and results in repetitive self-stimulation (Ikemoto and Wise, 2002). One study has reported the release of dopamine in the nucleus accumbens of the ventral basal ganglia (Fiorino, et al., 1993), a nucleus that has been implicated in addictive behaviours (Niehaus, et al., 2009). In contrast, cytotoxic lesion of the VTA induces behavioural akinesia (Jones, et al., 1973) and leads to a reduction in the fast EEG activities that are related to attentional arousal (Montaron, et al., 1982). Parkinson's disease (PD), which occurs due to a depletion of DA in the nigro-striatal pathway, is behaviourally less characterised by motor paralysis, but rather by the inability to initiate or select certain motor actions (Kropotov and Etlinger, 1999). Moreover, children with attention deficit hyperactivity disorder (ADHD) have been found to have genetic mutations in their dopamine transporters, which indicates an impaired performance for dopamine reuptake at the synapse (Sharp, et al., 2009).

DA has also been observed to regulate neuronal excitability, since direct VTA stimulation decreases the spontaneous firing of prefrontal pyramidal neurons, through local excitation of interneurons (Lewis and O'Donnell, 2000). Owing to the lateral-inhibition of neighbouring cells, a winner-takes-all mechanism predominates (Durstewitz, et al., 2000). Therefore a phasic release of DA could render the prefrontal cortex more reactive to behaviourally relevant stimuli.

As well as ensuring efficient attention and motor performance, dopamine regulation is also essential during perceptuo-motor learning (Eckart, et al., 2010). Analogously, DA release in the basal ganglia should enable more effective inhibition of competing motor programs and improve the speed of action selection (Mink, 1996). During positron emission tomography (PET) of subjects playing a video game (Koepp et al., 1998), performance improvements were associated with the decreased binding of a radiolabeled DA antagonist, suggesting an increase in the amount of dopamine released in the striatum, relative to a control condition. This study is compatible with research in animals that demonstrates a role for dopamine in stimulus-response learning (Packard and White, 1991).

1.7.3 Exogenous stimulation for the release of dopamine to enhance learning

Prior studies have been replicated noninvasively in human subjects with the help of PET neuroimaging methods, whereby a selective release of dopamine in the striatum was observed following high frequency rTMS of the primary motor cortex and dorsolateral prefrontal cortex (Strafella, et al., 2001; Strafella, et al., 2003). Similarly, the clinical efficacy of electroacupuncture (EA) and moxibustion, is dependent on functional alterations in cerebral dopaminergic and serotonergic neurons, especially because of their anti-stress and psychosomatic actions (Yano, et al., 2004). Furthermore, long-term high-frequency EA has also been demonstrated to be effective in halting the degeneration of dopaminergic neurons in the substantia nigra and in up-regulating the levels of brain-derived neurotrophic factor (BDNF) mRNA in the subfields of the ventral midbrain (Liang, et al., 2002; Liang, et al., 2003). The activation of endogenous neurotrophins by EA may be involved in the

regeneration of the injured dopaminergic neurons, which may explain the effectiveness of EA in the treatment of PD (Liang, et al., 2003). EA might regulate the biosynthesis of DA by altering the tyrosine hydroxylase (TH) gene transcription (Liang, et al., 2002; Wang, et al., 1999).

Evidently, the dopamine precursor, Levodopa, is able to induce a significant boost in the performance of a serial reaction-time task for stroke patients (Rössler et al., 2008). Hence, the combination of rTMS or EA intervention with the usual rehabilitative treatments could improve the outcome of neurorehabilitation in real-life situations. A simple explanation may be that sustained rTMS or EA gives rise to a cumulative release of neuromodulators (e.g., serotonin, dopamine), which then modulate cortical excitability and practice-dependent plasticity that is necessary for learning. The neuro-anatomical correlates of successful reaction-time task performance implicate the basal ganglia as a key structure that seems to be necessary, as well as being sufficient for procedural learning, which indicates that dopamine is crucial to motor sequence learning and synaptic plasticity in the primary motor cortex (Eckart, et al., 2010; Molina-Luna, et al., 2009).

However, there is a possibility that neurofeedback training (NFT) may also upregulate dopaminergic tone in the motor cortex and/or basal ganglia. An animal study that examined the EEG dynamics, using the spectral power densities (SPDs) of the alpha and theta rhythms, found that the spiking frequency of supposedly dopaminergic (DA) neurons from the ventral tegmentum directed changes in the EEG characteristics, in the course of neurofeedback sessions (Kulichenko, et al., 2009). While the animals learned to correlate changes in the intensity of the sound signal and power of the EEG rhythms and to control the latter, in a conditioned-reflex mode, the

α/θ ratio changed, in the course of neurofeedback sessions, due to an increase in the SPD of the alpha EEG component and a noticeable drop in the SPD of the theta oscillations. Meanwhile, in a similar manner, augmentation of the spike activity of DA neurons was observed, which indicates the probable mechanisms for the involvement of the cerebral DA system in the results of neurofeedback sessions (Kulichenko, et al., 2009). Thus the method of combining and integrating NFT and stimulation strategies may enhance learning and performance, based on the likely system for neuromodulation. Intriguingly, the combination of feedback techniques and stimulation strategies may facilitate neurofeedback training (Hirshberg, et al., 2005; Ros, et al., 2010). Electroacupuncture (EA) stimulation has also been found to enhance alpha power, a non-specific change, or to inhibit theta rhythmic activity, during high frequency EA stimulation (Chen, et al., 2006), and to enhance attention levels (Chen, et al., 2011). The real-time emergent pattern of the EEG may be assisted by other successive non-invasive brain stimulation techniques, such as rTMS or EA, resulting in enhanced learning and performance (e.g., stimulation to enhance rhythmic activity), which implies that these combined stimulation and feedback approaches may be more effective than either alone (Hirshberg, et al., 2005; Keck, et al., 2002).

The close relationship between the basic modulation of the nervous system, the DA system and an associated improvement in attention, reward and learning has been extensively covered in the previous paragraphs. In addition, the probable mechanism that describes the effect of NFT on the cerebral DA system is based on the premise that neurofeedback sessions which direct change in the EEG characteristics may cause up-regulation of dopaminergic tone, because of the observed augmentation of the spike activity of DA neurons (Kulichenko, et al. 2009). It is therefore pertinent to

review the literature pertaining to EEG oscillation, which is relevant to particular enhancement and inhibition of EEG rhythms due to neurofeedback that produces an improvement in attention (details in the chapter 5). Most neurofeedback research to date has concentrated on the improvement of cognitive functions, such as attentional skills, and mood.

1.7.4 Attention and vigilance

Attention refers to the ability to focus on a specific thing, without becoming distracted, and also to a more focused activation of the cerebral cortex that enhances information processing (Mesulam, 1990; Oken, et al., 2006; Posner, 1989). Attention is different from simply being alert, because alertness refers to basic arousal, which refers to the state of simply being awake. For example, an alert but inattentive patient is attracted to any novel stimulus, but cannot screen out irrelevant stimuli in the environment (Oken, et al., 2006). However, one state, termed sustained attention, is synonymous with the most common usage of vigilance (Parasuraman, et al., 1998). Although there are several activation states of the cerebral cortex that impact the ability to process information globally or locally, no terms which have been used to describe these states of arousal, alertness, vigilance, or attention perfectly describe these states of cortical activation, since most terms are used broadly, with various associations, and there are no perfect physiological markers. In particular, the term, vigilance, has been used in many different ways by different groups of scientists. For example, psychologists and cognitive neuroscientists use the term specifically to describe an ability to sustain attention during a task and a performance that requires attention for a period of time (Davies and Parasuraman, 1982; Mackworth, 1964; Parasuraman, et al., 1998). However, clinical neurophysiologists use the term,

vigilance level, as well as arousal level, in the sleep–wake spectrum, without reference to cognition or behavioural responsiveness, because of an EEG’s great sensitivity to the activity of the corticothalamic networks that are fundamental to the sleep–wake dimension (Steriade, 1999, 2000).

Vigilance is a term that has various definitions, but the most common scientific usage is to define a state of sustained attention or tonic alertness (Oken, et al., 2006). Vigilance implies both a degree of arousal in the sleep–wake cycle and in the level of cognitive performance over time. The EEG is the most common physiological measure of vigilance, and various measures of eye movement and of autonomic nervous system activity have also been used (Oken, et al., 2006). Attention tasks can be made progressively more complicated, but the evaluation of more complex functions requires vigilance (Gillig and Sanders, 2011). Problems with vigilance are indicated by the omission of a letter, or by signalling when the letter is not presented, which is called a commission error. The GNG test is also a popular format for testing vigilance (Gillig and Sanders, 2011; Sander, 2010).

Interestingly, subjects who are uninterested in the environment are not as vigilant as those people with high motivation. In other words, the underlying brain system that impacts sustained attention is motivation. The motivational system includes much of the dopamine system and portions of the frontal lobes (e.g., anterior cingulate), as well as the limbic and subcortical structures (striatum, nucleus accumbens and amygdala) (Robbins and Everitt, 1996). The dopamine system may be related to reward (Schultz, 2002). Conceptually, effort (Kahneman, 1973) and motivation are related to sustained attention.

The studies in the thesis have been conducted to provide reasonable evidence to validate enhanced cognitive function through a combination of exogenous and endogenous stimulations. Following a review of the research literature and theoretical thought on the application and understanding of SMR neurofeedback training and electrical acustimulation protocols, it is possible to identify three major goals for three experiments, in accordance with the literature examined.

Exp I – Beneficial effects of electrostimulation contingencies on sustained attention and electrocortical activity

With regard to the change in sustained attention, an improvement in behavioural results (perceptual sensitivity) and their ERP is modulated by real EA stimulation with specific frequency (alternating frequency vs. low frequency vs. sham stimulation). Certainly, whether or not traditional EEG and ERP methods show significant changes in electrophysiology, the ICA-based EEG analysis provides significant results in the EEG and ERP studies.

The aim of the first experiment in the thesis is also to compare the results of the stimuli-produced cortical activities for three conditions (before, during and after EA stimulation), to identify whether the attentional ERPs and performance are altered by EA stimulation, even in the period of post stimulation (the outlasting effect after EA stimulation). Meanwhile, the presumed components, reflecting synchronous cortical local field activity of connected networks, can be decomposed from ERP data, via ICA decomposition, using spatial filters for each group and each time period. Therefore, based on the results of the experiment, EA can be used in the later experiment as an assisting modality in the SMR NF training.

The ICA method for the analysis of EEG data is a very important issue, not only for ERP, but also for the existing resting state EEG networks. Furthermore, the idea from previous studies indicates that the general effect of NFT may be better described by its action on the resting EEG (Egner, et al., 2004; Ros, et al., 2010), which is

highly correlated with the dorsal attention network (Laufs, 2008; Mantini, et al., 2007; Uddin, et al., 2009). Therefore, in order to provide more evidence of enhanced attentional performance, using NFT and NFT assisted by EA, the following experiment focuses on exploring the default and attentional networks. In order to improve the application of ICA, the methods of the second experiment serve to validate that any improvement to the attention network is correlated with trained oscillations (in the third experiment).

Exp II – Dynamic changes of ICA-derived EEG functional connectivity in the resting state

EEG epochs, as fMRI volumes of individual-subject data, can be concatenated across subjects, along the time axis to apply the ICA algorithm to group data. Furthermore, combining ICA with time-frequency and cross-correlation analyses performed on the power spectra of selected ICs at the group-level reveals information about resting EEG networks, with regard to neural synchronization (Chen et al., 2009; Grin-Yatsenko, et al., 2010).

This experiment focuses on the steps to model and examine the effective resting EEG networks established by similarity in the components' alpha power, in order to investigate: (a) the topographical maps of EEG components in both EC and EO states; (b) the associated EEG sources according to their alpha power correlation coefficients in both states; (c) the localization of circumscribed groups associated with relevant EEG components, from the EC to the EO state; (d) the alpha power-associated functional connectivity between ICs and the difference between EC and EO states and (e) the changes in spectral power in the circumscribed groups, from the EC to the EO state. Then, based on the previous two experiments' results, the third experiment investigates the effect of a combination of NF training and EA stimulation on the attention performance, the enhanced and inhibited oscillation after NFT and the improvement in spectral power, within circumscribed regions of attention network.

Exp III –The increased perceptual sensitivity in attention performance and the enhanced beta power of the attention network in the resting state caused by a combination of neurofeedback self-regulation and electroacupuncture stimulation.

It is plausible to utilize the lasting effect of post-EA stimulation outlasting to boost the improvement in attention performance, while undertaking NF training to increase SMR and decrease theta activity, during the post-EA interval. This improvement does not occur in the non-contingent (sham feedback) group. However, superior cognitive benefits result from NF training assisted by EA stimulation, as validated by the increase in regional attention-related spectral power of the formerly developed EEG attention network.

Finally ICA-based EEG power spectra are used to study the differences between pre- and post- NF training. Comprehensive data for the identified EEG components and networks is collected, to identify the source of differences in attentional performance between the four groups (AE+SMR, LE+SMR, SMR, and non-contingent SMR). To the best of the author's knowledge, no studies have specifically investigated a potential improvement in attentional performance and the EEG dynamics of the dorsal attention network, due to a combination of NFT and EA. Importantly, no study to date has studied the differences in attentional performance due to SMR and the non-contingent SMR (pseudo-feedback) NF training, or in EEG dynamics. The third experiment attempts to validate the possible long-term effects of NF training.

Beneficial Effects of Electrostimulation Contingencies on Sustained Attention and Electrocortical Activity

3.1 Introduction

3.1.1 Proposed Mechanisms of Acupuncture

As acupuncture has evolved from the realm of traditional Chinese medicine towards an adjuvant role in the western medicine, scientists have tried to understand its basic mechanism and its efficiency in treating disorders in accordance with modern scientific principles. The first magnetic resonance imaging (fMRI) study on acupuncture represented a major first step toward understanding oriental acupuncture in relationship to brain function (Cho, et al., 1998). Several fMRI reports on manual acupuncture and electroacupuncture stimulation have also been published (e.g., Kong, et al., 2002; Wu, et al., 2002). There are some suggested mechanisms of action of acupuncture, for instance, involving the gate control theory of pain ^{*3} and neurohormonal theory (Ulett, et al., 1998b) (details in the section 3.1.2).

The theory of central pain blockade in the brain via stimulating the release of endogenous opioid neurohormones, such as endorphins and enkephalins (naturally occurring morphines), has been demonstrated in a series of acupuncture studies (Han, 2003, 2004; Han and Terenius, 1982; Ulett, et al., 1998a; Ulett, et al., 1998b).

^{*3} Melzack, R., Wall, P.D., 1965. Pain mechanisms: a new theory. *Science* 150, 971-979.

Similar results were also obtained in animal experiments showing that the effect is not from a so-called placebo effect, but from a real physiological phenomenon (Takeshige, et al., 1992; Takeshige, et al., 1990). In the past ten years, systematic reviews and studies have provided more reliable evidence of acupuncture's value in treating nausea (e.g., Ezzo, et al., 2006; Streitberger, et al., 2006), back pain (e.g., Haake, et al., 2007; Itoh, et al., 2006), osteoarthritis of the knee (Itoh, et al., 2008; Miller, et al., 2009), headache (Wang, et al., 2007), and selective attention (Chae, et al., 2010; details in the section 1.5.2). To sum up, such pain pathways in the central nervous system (CNS), including the peri-aqueductal gray, thalamus, and the feedback pathways from the cortex back to the thalamus, can be modulated by acupuncture stimulation, reflecting the potential role of acupuncture and electro-acustimulation in investigating the functional areas of the human brain.

3.1.2 Proposed Mechanisms of EA and TENS

TENS has the advantage of fewer side effects than traditional invasive needle acupuncture (details in the section 1.5.1). Furthermore the main concern for research in this thesis was its combination with neurofeedback training without interruption from painful sensation. As used in clinics as one of EA types, TENS has fewer side effects than manual acupuncture and the frequency of stimulation has been extensively studied as an important parameter of stimulation (e.g., Chen, et al., 2006; Napadow, et al., 2005; Ulett, et al., 1998b; Zeng, et al., 2006; Zhang et al., 2003).

Published studies during the past few decades have provided scientific evidence for EA and TENS usage and have greatly facilitated their widespread application. It is

now known that the effects of EA and TENS may be mediated via multiple mechanisms at peripheral and central sites. Mechanisms involved are summarised below (Kotz and Simpson, 2008).

3.1.2.1 Short-term effects of EA and TENS

Gate control: Stimulation of A β fibres activates inhibitory neurons in the substantia gelatinosa (lamina II) of the dorsal horn. This causes release of non-opioid inhibitory neurotransmitters, leading to inhibition of the upward transmission of painful C-fibre impulses (Sluka and Walsh, 2003). The "gate control theory of pain" (developed by Ronald Melzack and Patrick Wall) (Melzack and Wall, 1967) proposed that pain perception is not simply a direct result of activating pain fibres, but is modulated by the interplay between excitation and inhibition of the pain pathways. According to the theory, the "gating of pain" is controlled by inhibitory action on the pain pathways. That is, the perception of pain can be altered (gated on or off) by a number of means physiologically, psychologically and pharmacologically. The gate-control theory was developed in neuroscience independent of acupuncture and the gate theory as a mechanism to account for the hypothesized analgesic action of acupuncture in the brainstem reticular formation was proposed in Germany in 1976 (Melzack, 1976). Furthermore, this development led to the theory of the central control of pain gating, i.e., pain blockade in the brain (a central pain control system in the brain rather than at the spinal cord or periphery) via the release of endogenous opioid neurotransmitters (peptides), such as endorphins, enkephalins and dynorphins (naturally occurring morphines), described in the next paragraphs.

3.1.2.2 Long-term effects of EA and TENS: (e.g., sustained analgesia after acupuncture)

Production of endogenous opioids: Several studies support this mechanism, including animal and human studies (Lin, 2006; Sluka and Walsh, 2003; Ulett, et al., 1998b). Acupuncture and TENS are partially reversed by naloxone and cross-tolerance develops between opioids and regular TENS (Watkins and Mayer, 1982). It is hypothesized that differential neurotransmitters and neuromodulatory effects are released (e.g., enkephalin, endorphin and dynorphin) by high- vs. low-frequency stimulation and this hypothesis of neurochemical induction in the brain by differential frequency modulations has gained strong support (Han, 2003, 2004). Both high- and low-frequency stimulation-induced analgesia are mediated by opioid peptides via different receptor effects and the low-frequency stimulation exerts effects on the central hypothalamus, which has descending inhibition via enkephalin at PAG, medulla, and dorsal horn of spinal cord on mu receptors. However, the high-frequency stimulation exerts effects directly on parabrachial nuclei, periaqueductal gray, medulla, and dorsal horn via dynorphin on kappa receptors (Chen, et al., 2006) and see review, (Han, 2003). In fact, even EA stimulation with the dense-disperse mode (mixed or alternating frequencies) may produce differential release of met-enkephalin and dynorphins into the spinal fluid and has suggested a synergistic effect with exogenously administered opioid analgesics without interference from each other (Han and Sun, 1990).

Two issues of importance have been introduced in recent reports. First, gate control seems to be less important than the production of endogenous opioids at the spinal cord and in the limbic system (Cabyoglu, et al., 2006; Han, 2003). Secondly,

the role of endogenous opioid peptides in the mediation of the effects of acupuncture is not only on pain relief, but also on mental functions (Sher, 1998). The endogenous opioid system is involved in various mental processes and regulates activity in different neurotransmitter pathways, and for instance, effects of acupuncture on mood, behaviour, learning, and memory (Sher, 1998, 2001). The action of acupuncture on mental functions involves interactions among different neurotransmitter systems, which is consistent with the complexity of the brain. Moreover, the endogenous opioid system may be one of the key mediators. Prior studies have produced substantial evidence that the endogenous opioid system has significant effects on memory and learning (Schulteis and Martinez, 1992; Shen and Li, 1995). The endogenous opioid system is closely linked to different neurotransmitter systems in the brain, including dopaminergic, noradrenergic, serotonergic, GABAergic, and glutamatergic systems (see a review, Zhao, 2008), with effects on learning and memory (see a review, Bodnar, 2008).

Impact on functional connectivity: Based on prior fMRI findings of EA stimulation, studies with resting fMRI data taken before and after verum and sham acupuncture have been undertaken to explore impact on functional connectivity (Dhond, et al., 2008; Hui et al., 2009). Following verum, but not sham, acupuncture there was increased default mode network (DMN) connectivity with pain (anterior cingulate cortex (ACC), periaqueductal gray), affective (amygdala, ACC), and memory (hippocampal formation, middle temporal gyrus) related brain regions, and increased sensorimotor network (SMN) connectivity as well. This is an important approach for demonstrating that acupuncture can enhance the post-stimulation spatial extent of resting brain networks (Dhond, et al., 2008). In addition, the default mode

network (task-negative) and the anti-correlated task-positive network in response to stimulation were also reported, indicating that acupuncture mobilizes the two anti-correlated functional networks of the brain to mediate its actions, and that the effect is dependent on the psychophysical response (Hui, et al., 2009) (DMN will be described in chapter 4).

3.1.3 Hypotheses for Experiment One

The first experiment was conducted in order to (a) confirm the findings from prior research of improved visual attention with EA stimulation (detail in the section 1.5.2 and the page 80), and (b) to compare subjects of experimental and control groups on other putative correlates with behavioural tasks (e.g., perceptual sensitivity) and brain electrophysiological activity (e.g., ERPs and ERP components). On the basis of the prior research in EA stimulation and opioid analgesics (details in the section 3.1.2.2; Han and Sun, 1990), enhanced attention with alternating frequency electro-stimulation (AE) was expected to be greater than with low frequency electro-stimulation (LE), and effects on attention would be superior to sham electro-stimulation (SE). In addition, inclusion of three conditions (pre-, during, and post-stimulation) enabled a test of whether effects on attention would outlast TENS and inform whether this was a useful and effective modality of exogenous stimulation to enhance cognitive performance.

Hypothesis 1: sustained effects on perceptual sensitivity in attention.

That attention will improve with EA and this improvement will outlast stimulation which behaviourally will be indexed by an increase in d-prime, largely

due to a reduction in errors of commission, for young adults tend to make few omission errors (Egner and Gruzelier, 2001). That improvement in attention will be greater with alternating than lower frequency stimulation.

Hypothesis 2: sustained effects on visual attention ERP latency.

Improvement in attention with EA will have a counterpart in ERP components, with shorter ERP latencies in the stimulation groups than the control group. Correspondingly, subjects in the AE group would have the shortest ERP latencies, and the LE group would have shorter latencies than the SE group.

Hypothesis 3: sustained effects on visual attention ERP amplitude.

That improvement in attention will also coincide with increased ERP amplitudes in the different stimulation groups. Correspondingly, subjects in the AE group would have the most robust ERP amplitudes, and the LE group would have more robust amplitudes than the SE group.

Hypothesis 4: Decomposed independent components (ICs) of visual attention ERPs.

Application of the ICA method to decompose visual attention ERPs into ICs was expected to reveal changes in ERP components related to cognitive activation after

the sustained attention task. This may disclose the benefit of applying ICA to conventional ERP methods of analysis.

Hypothesis 5: Decomposed components will correlate with habituation after the repetition of the visual attention task.

That the control group through an absence of EA effects will show habituation across the three conditions as measured by particular component amplitudes. In line with this hypothesis, the ICA and decomposed components may explain subjects' enhanced attention performance following EA stimulation due to the absence of a habituation effect of EA stimulation on important components, which are associated with working memory, motor inhibition, and visual discrimination processes.

3.2 Materials and Methods of Experiment One

3.2.1 Subjects

Data were recorded from 30 individuals, but because of technical problems or excessive artefacts, three data sets were excluded from further analysis. 27 healthy volunteers (20 female, 7 male), mean age = 22.5 (SD = 1.56, range 18-30 years) from Goldsmiths, University of London, participated in the study. Subjects were excluded if they had any history of epilepsy, drug abuse, head injury, or psychiatric disorders. Those participants currently having any sore, pain, cut, skin problems on the hands or receiving psychoactive medication were also screened out. All subjects had not experienced acustimulation before our testing. All had normal hearing and normal (or corrected-to-normal) eyesight. Written consent was obtained prior to the start of the

experiment in accordance with the Helsinki Declaration, and the current investigation received the ethical approval from the College Research Ethics Committee.

Participants were randomly assigned to one of three experimental groups of equal size (N=9) with the method of randomly permuted blocks <http://www.randomization.com>. Group 1 (alternating frequency electrostimulation, AE) who received stimulation with alternating low (5 Hz) and high (100 Hz) frequencies; Group 2 (low frequency electrostimulation, LE) received stimulation with the low frequency (5 Hz) only; Group 3 (sham electrostimulation, SE) received a control condition with the minimal intensity for electroacupuncture.

3.2.2 Experimental Design

Each subject was asked to perform a continuous performance visual attention task and sat in a comfortable armchair throughout the duration of the experiment in a quiet room. They were seated facing a computer screen, 100 cm in front of them, and were instructed to press a response button whenever a visual target stimulus picture occurred and to withhold responses to other stimuli. Detection accuracy and response time were recorded during the repetitive tasks. All subjects were blind to the stimulation mode and effect. They were told that the machine could stimulate acupuncture points through high-frequency or low-frequency stimulation, and this may or may not give a sensation. Transcutaneous electric acupoint stimulation (HANS: Han's acupoint nerve stimulator, Wearnes Technology, Singapore) was applied. The selected acupoints were LI-4 (HeGu point) and P-6 (NeiGuan point) of

both hands. The HeGu point is located at the first inter-interosseous muscle of the hand. The NeiGuan point is located on the anterior surface of the wrist between the tendons of the flexor carpi radialis and the palmaris longus, next to the median nerve, and on average 3-5 cm proximal to the flexor crease. The two acupoints of each hand were stimulated at the same time as a circuit in one output channel of HANS (Figure 3-1.) in order to prevent unusual current overflowing across the body inducing arrhythmia. Subjects received stimulation via four adhesive surface electrodes (size: 4 cm × 5 cm) at the aforementioned bilateral acupoints. The stimulation intensity for the real acustimulation was adjusted to a maximal but comfortable level, slightly below the pain or discomfort threshold, ranging from 7 to 15 mA. For the sham acustimulation the intensity was set at less than 5 mA (Chao, et al., 2007). Based on a literature review (Chao, et al., 2007; Hsieh, et al., 2001; Itoh, et al., 2006; Lund and Lundberg, 2006; Shen et al., 2000; White, et al., 2004; Wu, et al., 2002; Zhang, et al., 2003), we selected sham acustimulation applied to the same points with minimal intensity as our control placebo model, and only the intensity parameter of stimulation was different from the real stimulation groups.

Each subject was instructed to pay no attention to the sensation induced at the stimulated site, and to focus on the attention task. All 27 subjects were assessed by evaluating their behavioural results from the attention task and the event-related EEG measures in the three study stages (before stimulation, during stimulation and 5 minutes post-stimulation). Each study stage consisted of 5 minutes eyes closed baseline EEG, 5 minutes eyes open baseline EEG and 20 minutes of the attention task.

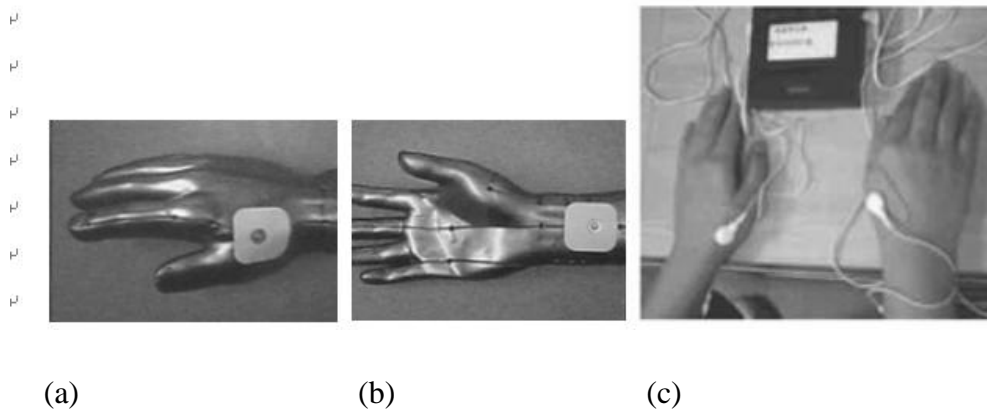


Figure 3-1. The location of two acupoints: HeGu (a), NeiGuan (b), and the application of the stimulator device on both acupoints (c).

3.2.3 Procedures

3.2.3.1 Attention paradigm

The two-stimuli go and nogo task is a subtype of the general go and nogo paradigm. When the “go” stimulus is presented a manual response is required whereas when a “nogo” stimulus is presented the response is to be withheld. The purpose of this design is to examine two types of errors, namely those representing inattentiveness and impulsivity. The task presents stimuli in pairs so that the subject would implicitly be ready to make a decision after the first stimulus in the pair and to respond as fast as possible after the second stimulus is shown on the screen. Here the images were flashed on the screen in pairs within 3 seconds with the instruction to press a button when the target pair occurred. The stimuli were non-language based and consisted of a total of 20 different images of animals (A), plants (P) or humans (H). In addition, each human picture was presented together with a pure tone of 500 Hz of 20 ms duration. Four different categories of trials were shown: “Animal-Animal

(A-A)”, “Animal-Plant (A-P)”, “Plant-Plant (P-P)”, and “Plant-Human (P-H)”. The duration of the stimuli was 100 ms, and trials were presented in a random order with equal probability. Inter-stimulus intervals were 1400ms, and long enough for subjects to prepare their responses; the total interval between trials was 3100ms. The task consisted of 400 trials, divided into 4 sessions with 100 trials each, and took around 20 minutes. The subject had to press a button as fast as possible when the A-A pairs were presented on a screen and ignore other pairs of stimuli (A-P, P-P, P-HS, Figure 3-2.) (Psytask user manual, <http://www.mitsar-medical.com>) (Kropotov, 2009b).

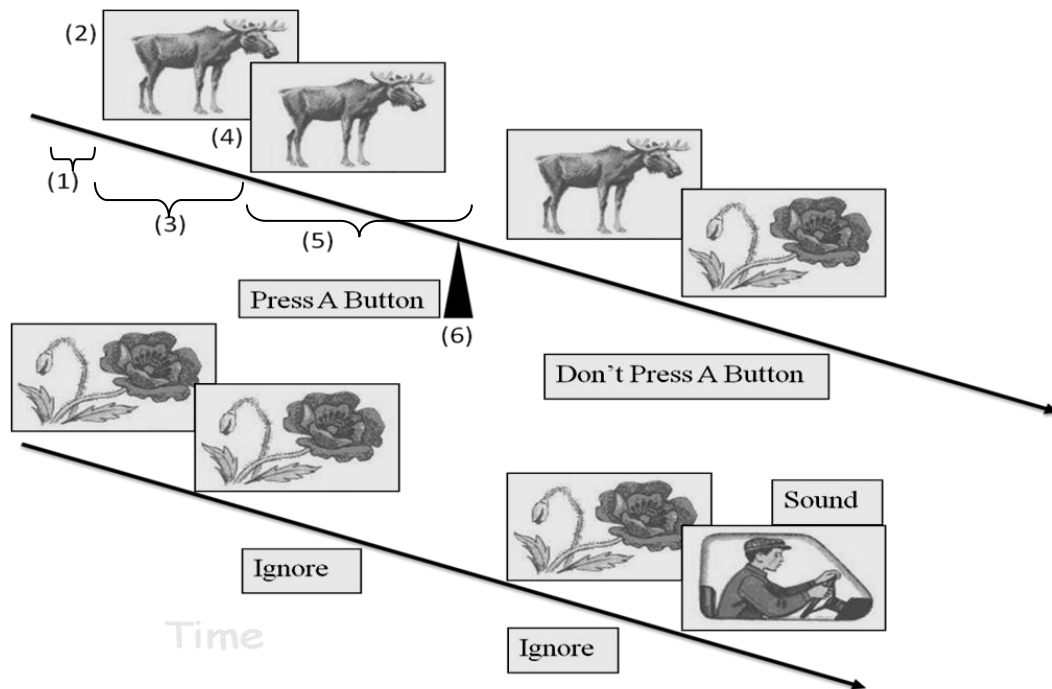


Figure 3-2. Stimulus presentation in the visual attention task. (1) Pre-stimulus interval, (2) First stimulus, (3) Inter-stimulus interval, (4) Second stimulus, (5) Post-stimulus interval, (6) Subject response. Two arrows and lines represent the continuous time axis during the task with four pairs of pictures randomly shown. The first pair, the Animal-Animal (A-A) pair, represents the “go” cue, to which the subject should press the button. The second pair, the Animal-Plant (A-P) pair, represents a “nogo” cue, and the subject should not respond. The remaining two Plant-Plant (P-P) and Plant-Human (P-H) pairs are control condition trials, and the subject should ignore them.

3.2.3.2 EEG recordings and pre-treatment of EEG

Topographical EEG and ERP data of all participants were recorded during the attention task. All neuroelectric data were recorded using the Mitsar 21-channel EEG system, the “Mitsar-201” (CE 0537) manufactured by Mitsar, Ltd. (<http://www.mitsar-medical.com>), with a 19-channel electrode cap with silver-chloride electrodes that included Fz, Cz, Pz, Fp1/2, F3/4, F7/8, T3/4, T5/6, C3/4, P3/4, O1/2. The cap was placed on the scalp according to the standard 10-20 system (Electro-cap International, Inc. <http://www.electro-cap.com/caps.htm>). Electrodes were referenced to linked earlobes (off-line) and the input signals were sampled at a rate of 250 Hz (bandpass 0.5–30 Hz). The ground electrode was placed on the forehead. Impedance was kept below 5 k Ω . Electro-oculogram (EOG) data were recorded from electrodes (Fp1/2) placed above the frontal muscles to monitor eye blinking or movements. An EOG correction procedure (by ICA, details in the sections 1.2.4.1, 1.2.4.3 and 1.3.3) to remove artefacts was performed and non-specific artefacts were rejected offline. ERP waveforms were averaged and computed off line. All participants performed the attention task three times: before, during and 5 minutes post-stimulation.

3.2.3.3 Data management: ICA and standardized low-resolution brain electromagnetic tomography (sLORETA)

EEG data analysis was performed using WinEEG 2.83, the commercial software from the Mitsar, Ltd. (<http://www.mitsar-medical.com>). First, data were digitally filtered using a linear filter to minimize drifts and line noise (bandwidth 0.5 - 30 Hz; notch filters 45-55 Hz). ERP data epochs were extracted (0 to 3000 ms) and baseline corrected (-100 to 0 ms). Epochs containing unique, non-stereotyped artefacts (e.g.,

swallowing, extreme muscle activities with amplitudes over 35 μ V, electrode cable movements, etc.) were automatically rejected from further analysis, whereas epochs containing repeatedly occurring artefacts (e.g., eye blinks, heart beat artefacts, etc.) were corrected using the ICA method (Jung, et al., 2000; Jung, et al., 2000). It was implemented in the software (<http://scn.ucsd.edu/eeglab>) (Makeig, et al., 1997), WinEEG, and written by Valery A. Ponomarev (Kropotov, 2009a).

The independent components of average ERPs are computed using selected in ERP database array of individual (subject or observation) ERPs as a source data. The parts of ERP waveforms corresponding to specified time intervals are merged to continuous time series and then this data are decomposed to independent components. Grand average ERPs are computed separately for each independent component. Individual ERP component waveforms, grand average ERP components and component topographies are displayed in ICA window and are available for analysis. Additional assumption is also suggested that cortical localization of components is similar between subjects due to performing the same task, so that it is viable to implement the ICA on array of ERPs.

sLORETA is a method that computes images of electric neuronal activity from EEG. EEG measurements do not contain enough information for the unique estimation of the electric neuronal generators. sLORETA imaging is one of methods for locating cortical generators provided source computations for the independent components (ICs) using freeware provided by the Key Institute for Brain-Mind Research in Zurich, Switzerland (http://www.uzh.ch/keyinst/_loreta.htm) (Pascual-Marqui, 2002).

3.2.3.4 Data management: Behavioural dependent variables

The behavioural parameters included errors of omission (indicative of inattentiveness), errors of commission (indicative of impulsivity), reaction time (RT) and reaction time variability (RTV). We also introduced the parameter “d-prime” (d') derived from signal detection theory (Green and Swets, 1966; McNicol, 1972). This takes into account both the ratio of hit rate (H) and the false alarm rate (F) and is used as measure of perceptual sensitivity. Conventionally in calculating d' , H is defined as [$H' = 1 - (\text{number of omission errors} / \text{number of targets})$], and F as [$F' = \text{number of commission errors} / \text{number of non-targets}$]. From these formulae, however, the d' is not simply $[H - F]$, rather, it is the difference between the z-transforms of these two rates and was calculated as [$d' = z(H) - z(F)$]. In other words, d' measures both of these two error types as an index of perceptual sensitivity (Egner and Gruzelier, 2001, 2004).

3.2.3.5 Statistical analysis

To evaluate the effectiveness of acustimulation relative to the sham procedure, a mixed-design ANOVA was used to examine the effects of Group (AE, LE, SE) and Time (before, during, after acustimulation) on behavioural measures. Separate ANOVAs were performed on each of the five measures: omission errors, commission errors, RT and RTV and d' with the Bonferroni correction for post-hoc comparisons. Given the exploratory nature of the study, an uncorrected significance threshold of $p=0.05$ was used for each of the five ANOVAs in order to preserve a reasonable sensitivity for detecting real effects (i.e. to maintain a reasonable type I error rate).

Given this, caution must be used in interpreting each effect, with greater credence given to those effects specifically predicted a priori, as outlined in the Introduction. So that the reader can judge which effects would survive a harsher significance criterion, an adjusted alpha of 0.01 was also calculated using a Bonferroni adjustment based on the number of tests (i.e. $0.05 / 5$). The nature of any significant interactions that emerged were explored using contrast tests comparing mean scores across time periods (i.e. before vs. after, before vs. during, after vs. during) for each of the three groups, in line with the primary goals of the study, including parameters of ERP and ICs (latencies and amplitudes) in both conditions (go and nogo cues).

3.3 Results of Experiment One

3.3.1 Hypothesis 1: Sustained effects on perceptual sensitivity in attention.

3.3.1.1 Perceptual sensitivity

Here it was hypothesised that young adults would have improvement of perceptual sensitivity in repetitive visual attention tasks due to EA stimulation, indexed by an increase in d-prime. Correspondingly, with a significant reduction in errors of commission and few omission errors, the improvement in attention would be greater with alternating (the AE group) than lower frequency stimulation (the LE group) and sham stimulation (the SE group) after stimulation.

Table 3-1 shows the means and standard deviations of the d', commission errors, omission errors, RT and RTV scores of the attention task for the three groups, and in Table 3-2 the results of ANOVA with repeated measures.

Table 3-1

Scores (mean \pm standard deviations) for attention test measures before, during and after electrostimulation (3 groups)

Group	GO/NOGO Variables	Before	During	After
AE	Omission errors	1.22 \pm 0.83	1.67 \pm 1.66	1.33 \pm 1.87
	Commission errors	1.22 \pm 0.67	0.11 \pm 0.33	0.22 \pm 0.67
	d' (d-prime)	5.09 \pm 1.01	6.63 \pm 1.36	6.88 \pm 1.47
	RT (ms)	401.00 \pm 62.92	372.56 \pm 65.28	358.22 \pm 52.94
	RTV (ms)	8.68 \pm 2.23	8.23 \pm 2.30	8.64 \pm 2.65
LE	Omission errors	4.33 \pm 3.94	1.89 \pm 1.69	4.11 \pm 3.95
	Commission errors	1.44 \pm 1.33	0.56 \pm 0.88	1.00 \pm 0.71
	d' (d-prime)	4.47 \pm 1.03	6.27 \pm 1.13	4.79 \pm 1.12
	RT (ms)	379.00 \pm 53.70	379.67 \pm 54.35	378.89 \pm 56.37
	RTV (ms)	9.51 \pm 3.22	10.67 \pm 3.16	9.90 \pm 3.15
SE	Omission errors	5.67 \pm 5.05	4.78 \pm 3.96	5.67 \pm 4.36
	Commission errors	0.33 \pm 0.71	0.67 \pm 0.71	0.89 \pm 1.17
	d' (d-prime)	5.79 \pm 1.41	5.15 \pm 1.23	5.23 \pm 1.27
	RT (ms)	349.22 \pm 70.76	345.78 \pm 44.53	353.67 \pm 56.49
	RTV (ms)	8.58 \pm 4.46	9.56 \pm 2.94	9.97 \pm 4.18

AE, alternating frequency electrostimulation; LE, low frequency electrostimulation; SE, sham electrostimulation; RT, response time; RTV, response time variability.

Table 3-2

The effects of Group (AE, LE, SE) and Time (before, during, after electrostimulation) on attention task with repeated measures ANOVA with baseline as a covariate.

	Source	<i>df</i>	<i>F</i>	<i>P</i>
<i>d'</i> (d-prime)	Group	2	9.236	0.001**
	Change	1	0.124	0.728
	Group × Change	2	1.997	0.159
Commission errors	Group	2	5.255	0.013*
	Change	1	1.764	0.197
	Group × Change	2	0.251	0.780
Omission errors	Group	2	1.673	0.210
	Change	1	1.745	0.199
	Group × Change	2	0.862	0.435
RT (ms)	Group	2	3.256	0.057
	Change	1	0.102	0.752
	Group × Change	2	1.331	0.284
RTV (ms)	Group	2	1.404	0.266
	Change	1	0.103	0.751
	Group × Change	2	0.933	0.408

Group × Change indicates the interaction between group and change (between baseline and during stimulation and post stimulation); *, significance level: $P < 0.05$; **, significance level: $P < 0.01$; according to Bonferroni correction. AE, alternating frequency electrostimulation; LE, low frequency electrostimulation; SE, sham electrostimulation.

The groups were first examined for differences at baseline (before stimulation) with a one-way ANOVA, followed by Bonferroni post-hoc tests. There was a significant Group effect for omission errors ($F(2,26)=3.368$, $P=0.051$) due to lower error rates in the AE group than the controls ($p=0.055$, Bonferroni; for LE $p=1$, Bonferroni); for commission errors ($F(2,26)=3.429$, $P=0.049$) due to fewer errors in the control group than the LE group ($p=0.062$, Bonferroni; for AE $p=0.178$, Bonferroni), the opposite to the omission error difference. D-prime yielded a Group effect that approached significance at the $P<0.05$ level, with a lower-d-prime in the LE group than the control group ($F(2,26)=2.860$, $P=0.077$; for LE $p=0.075$, Bonferroni; for AE $p=0.646$, Bonferroni). As omission and commission errors make an equal contribution to d-prime, and because the differences between the AE and control groups for the two variables were in the opposite direction their indices were accordingly not differentially affected. There were no baseline differences in the RT measures (for AE $p=0.280$ and for LE $p=0.975$, Bonferroni).

The effects of task repetition with or without EA stimulation were examined with repeated measures ANOVA with baseline as a covariate in the case of d-prime, omission and commission errors in view of the baseline differences, and with the change between baseline (before stimulation) and during stimulation and post stimulation as the within subject factor (Table 3-2). Considering first d-prime there was a highly significant group difference ($F(2,23)=9.236$, $P=0.001$) with no difference between stimulations ($F(2,23)=1.997$, $P=0.159$). Post-hoc analysis indicated that the increment in d-prime differed significantly between the control and AE groups, during and post stimulation (for during stimulation $p=0.043$ and for post stimulation $p=0.043$, Bonferroni). For the increment in d-prime differed significantly between the control

and LE groups, post-hoc analysis only indicated that the effect in the during stimulation period significantly (for during stimulation $p=0.021$ and for post stimulation $p=1$, Bonferroni). For omission errors there were no effects of group ($F(2,23)=1.673$, $P=0.210$) or of stimulation ($F(2,23)=0.862$, $P=0.435$). For commission errors there was a significant groups effect ($F(2,23)=5.255$, $P=0.013$) but no difference between stimulations ($F(2,23)=0.251$, $P=0.780$). The findings of increased perceptual sensitivity in both AE and LE groups were consistent with the hypothesis.

Furthermore turning to the RT measures, the effects of task repetition with or without EA stimulation were examined with repeated measures ANOVA with baseline as a covariate in the case of RT and RTV in view of the baseline differences, and with the change between baseline (before stimulation) and during stimulation and post stimulation as the within subject factor (Table 3-2). For RT there was approaching effect of group ($F(2,23)=3.256$, $P=0.057$) but no effect of stimulation ($F(2,23)=1.331$, $P=0.284$). For RTV there was no groups effect ($F(2,23)=1.404$, $P=0.266$) and no difference between stimulations ($F(2,23)=0.933$, $P=0.408$).

3.3.1.2 Sustained stimulation effects

In line with supporting the hypothesis that attention will improve with EA and this improvement will outlast stimulation, the sustained improvement of perceptual sensitivity post stimulation is found only in the AE group.

With AE the increase in d' with stimulation ($t(24)=2.532$, $p=0.018$; in Figure 3-3, t1) was sustained post stimulation ($t(24)=2.932$, $p=0.007$; in Figure 3-3, t2), whereas

with LE the increase with stimulation ($t(24)=3.494$, $p=0.002$; in Figure 3-3, t3) was not sustained post stimulation ($t(24)=-2.884$, $p=0.008$; in Figure 3-3, t4; non-significant before vs. after stimulation, $t(24)=0.611$, $p=0.547$; in Figure 3-3, t5). Moreover, the consequent difference between the AE and SE groups post stimulation showed higher d' scores following AE stimulation ($t(24)=2.695$, $p=0.013$, contrast test).

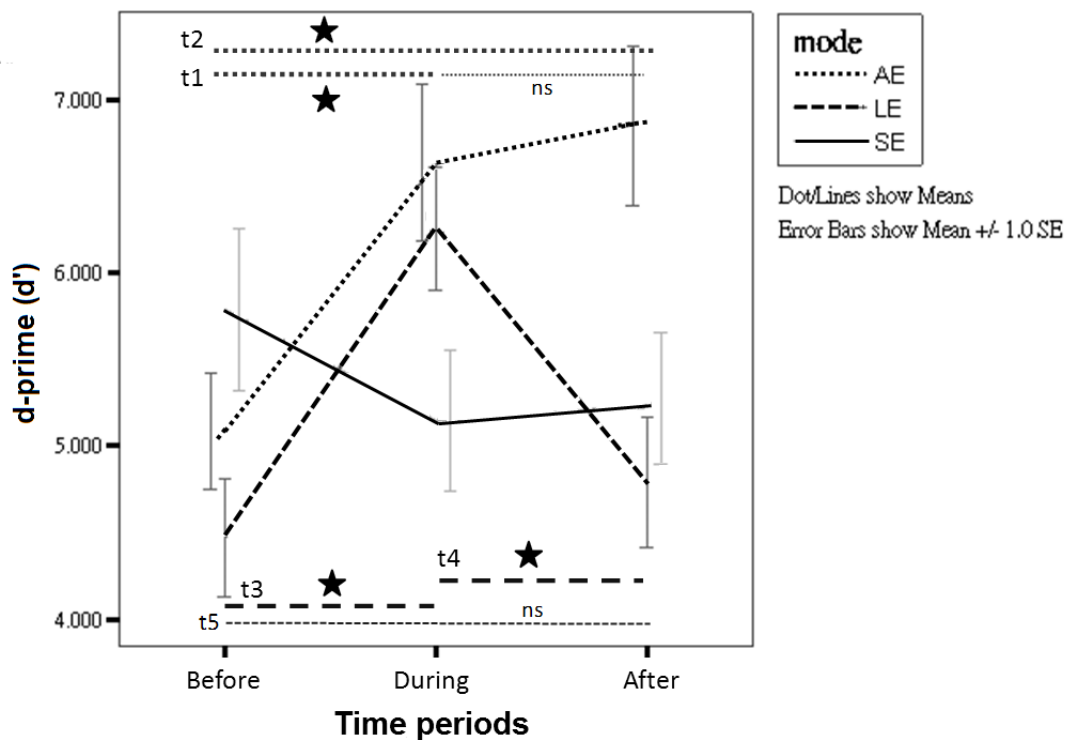


Figure 3-3. Electrostimulation changes on mean d' scores (\pm SEM) in the attention task for both AE and LE groups relative to the SE control group (\star denotes $P < 0.05$; AE, alternating frequency electrostimulation; LE, low frequency electrostimulation; SE, sham electrostimulation; t1, the contrast test during vs. before stimulation in the AE group; t2, the contrast test after vs. before stimulation in the AE group; ns, not significant during vs. after stimulation in the AE group; t3, the contrast test during vs. before LE stimulation; t4, after vs. during LE stimulation; t5, before vs. after LE stimulation, ns, not significant).

The finding of increased perceptual sensitivity largely due to reductions in commission errors in the AE group post stimulation was consistent with the hypothesis. Underscoring the pattern of results with d' , whereas with AE stimulation there was a decrease in commission errors (contrast test, $t(24)=-4.082$, $p=0.0004$, in Figure 3-4, t1) which was sustained post stimulation (contrast test, $t(24)=-3.674$, $p=0.001$, in Figure 3-4, t2), with LE there was a tendency towards a decrease in errors with stimulation (contrast test, $t(24)=-1.868$, $p=0.074$, in Figure 3-4, t3) which was not sustained post-stimulation (contrast test, $t(24)=-0.934$, $p=0.360$, in Figure 3-4, t4). However, the absence of such an effect in the LE group post stimulation was unexpected. In contrast to the hypothesis, there was not sustained improvement in commission errors post-stimulation in the LE group.

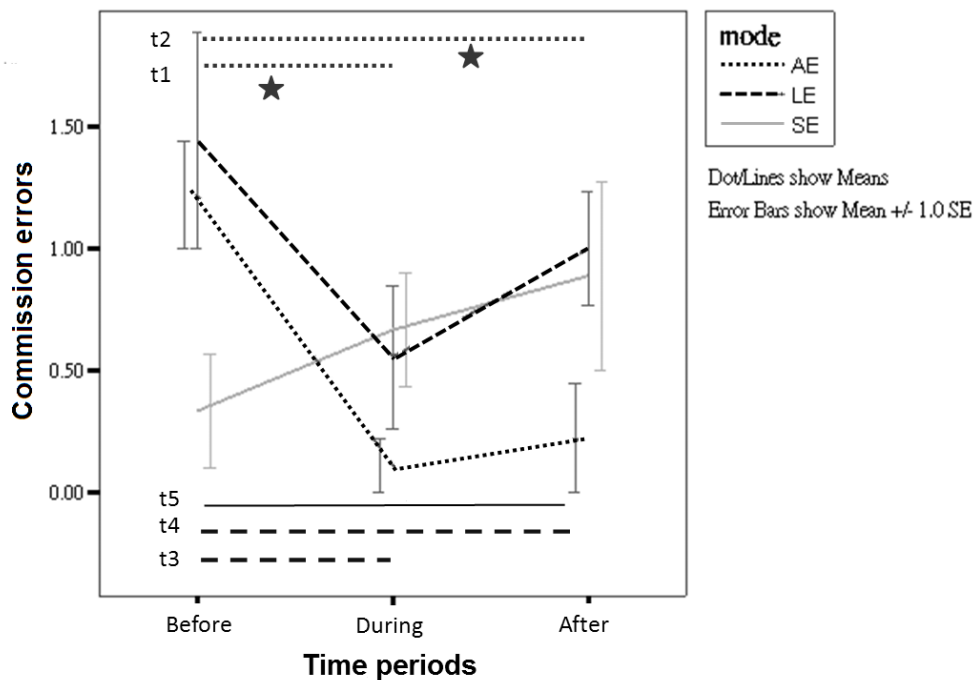


Figure 3-4. Electrostimulation changes on mean commission errors (\pm SEM) in the attention task for both AE and LE groups relative to the SE control group (\star denotes $P < 0.05$; t1, the contrast test during vs. before stimulation in the AE group; t2, the contrast test after vs. before stimulation in the AE group; t3, the contrast test during vs. before LE stimulation; t4, after vs. before LE stimulation; t5, after vs. before SE stimulation).

Furthermore turning to the RT measures, there was a mean reduction in RTs post stimulation in the AE group compared with the SE group (Figure 3-5). Although exploratory post hoc analyses with the Bonferroni correction indicated that the reduction in RT differed significantly between the SE and AE groups post stimulation ($p=0.023$), however according to repeated measures ANOVA with baseline as a covariate, there was approaching effect of group ($F(2,23)=3.256$, $P=0.057$) but no effect of stimulation ($F(2,23)=1.331$, $P=0.284$) for the RT measure (Table 3-2). Therefore, the RT change post stimulation may reflex the group difference but not the real stimulation effect.

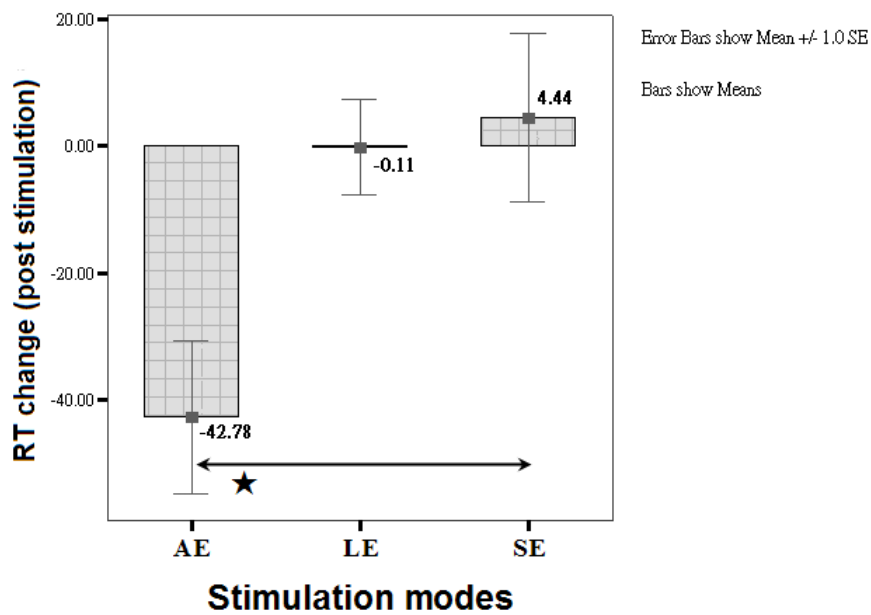


Figure 3-5. Post electrostimulation changes on mean response times (\pm SEM) in the attention task for the AE, LE and SE control groups (★ denotes $P < 0.05$; RT, response time).

3.3.2 Hypotheses 2 and 3: Sustained effects on visual attention ERP latency and amplitude.

3.3.2.1 Visual attention ERP latency and amplitude

Here it was hypothesised that improvement in attention with EA would have a counterpart in ERP components, with shorter ERP latencies and more robust amplitudes in the stimulation groups than the control group. The shortest ERP latency would coincide with the most robust ERP amplitude in the AE group, and the LE group would have more robust amplitude and shorter latency than the SE group. However, All three groups showed no statistically reliable changes in the early ERP components (with latencies of 80-180 ms), or in the late positive components (180-420 ms), and all groups displayed a trend of decreasing amplitude, but with no statistically significant findings (see also Tables 3-3 and 3-4). The group grand averages of the two conditions (go and nogo) in the attention task for the midline electrodes for each time period (before, during and after stimulation) are illustrated in Figure 3-6.

The hypotheses of increased ERP amplitude and shortened latency and such sustained stimulation effects on improvement in attention post EA stimulation were not supported. There was no improvement in attention revealed by a counterpart in ERP components. In addition, a further unexpected finding was a trend of decreasing amplitude in repetitive visual attention tasks (of three time periods, before, during and after stimulation, respectively) in all three groups. Therefore, the following hypothesis with the application of ICA to decompose attention ERPs into ICs would become critical.

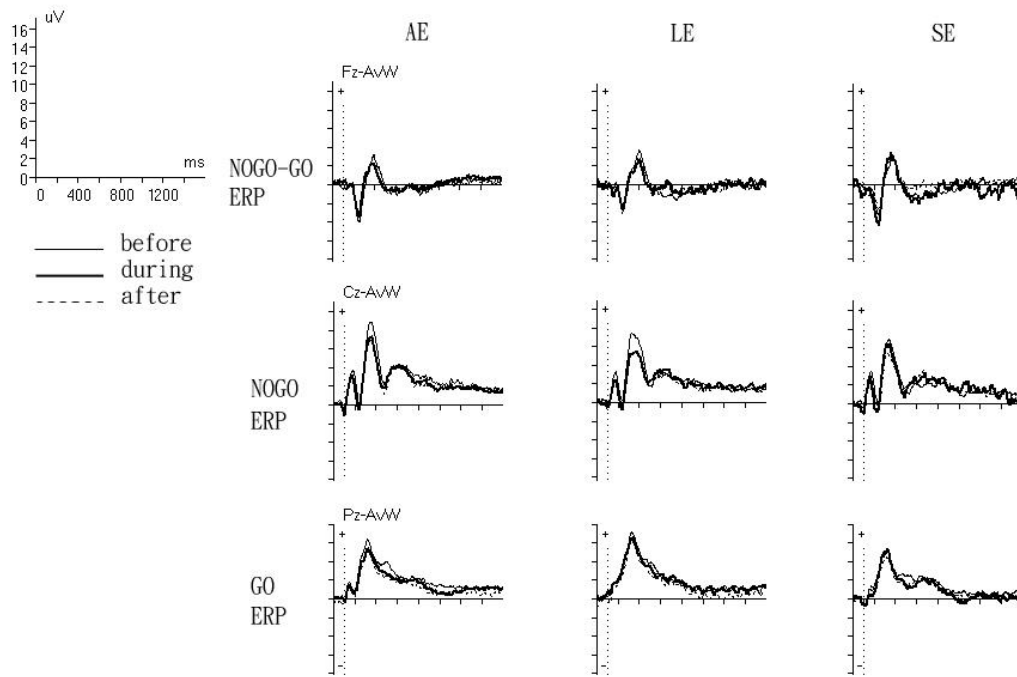


Figure 3-6. Grand average ERPs for each group and time block for the midline electrodes in the attention paradigm. A frontally distributed negative ERP component had greater amplitude for NOGO in comparison to GO stimuli and was associated with response inhibition in GO-NOGO paradigms (upper panel). No significant changes in amplitudes and latencies among three groups and three time periods (before, during and after stimulation, repeated measures ANOVA) were found. (See also Tables 3-3 and 3-4.)

Table 3-3

Means and standard deviations for the visual attention ERP measures in each group before, during and after electrostimulation

Group	GO/NOGO Variables	Before	During	After
AE	Pz GO amplitude	6.07 ± 2.20	4.96 ± 2.28	4.77 ± 2.12
	Pz GO latency	323.78 ± 10.60	321.56 ± 13.33	322.44 ± 8.82
	Cz NOGO amplitude	9.22 ± 3.59	7.23 ± 2.49	7.21 ± 2.19
	Cz NOGO latency	348.67 ± 17.89	348.22 ± 16.38	344.67 ± 24.49
LE	Pz GO amplitude	7.10 ± 3.23	6.39 ± 2.78	6.24 ± 2.95
	Pz GO latency	321.56 ± 21.49	320.22 ± 24.13	317.56 ± 24.29
	Cz NOGO amplitude	8.39 ± 5.35	6.37 ± 4.33	6.76 ± 3.81
	Cz NOGO latency	362.44 ± 31.52	363.78 ± 31.31	355.33 ± 33.97
SE	Pz GO amplitude	5.20 ± 2.95	5.40 ± 2.28	4.36 ± 1.80
	Pz GO latency	324.44 ± 16.49	328.67 ± 19.34	326.22 ± 24.05
	Cz NOGO amplitude	7.01 ± 4.52	6.71 ± 3.88	5.37 ± 4.27
	Cz NOGO latency	354.00 ± 15.17	351.33 ± 22.05	342.44 ± 15.61

AE, alternating frequency electrostimulation; LE, low frequency electrostimulation; SE, sham electrostimulation.

Table 3-4

The effects of Group (AE, LE, SE) and Time (before, during, after electrostimulation) on attention ERP with repeated measures ANOVA.

	Source	<i>df</i>	<i>F</i>	<i>P</i>
GO amplitude (μ V)	Group	2	2.571	0.091
	Time	2	1.038	0.359
	Group \times Time	4	0.177	0.949
GO latency (ms)	Group	2	2.011	0.191
	Time	2	0.186	0.831
	Group \times Time	4	0.171	0.953
NOGO amplitude (μ V)	Group	2	1.008	0.370
	Time	2	1.534	0.223
	Group \times Time	4	0.177	0.949
NOGO latency (ms)	Group	2	2.371	0.101
	Time	2	0.813	0.448
	Group \times Time	4	0.070	0.991

Group \times Time indicates the interaction between group and time period; *, significance level: $P < 0.05$; according to Bonferroni correction. AE, alternating frequency electrostimulation; LE, low frequency electrostimulation; SE, sham electrostimulation.

3.3.3 Hypothesis 4: Decomposed independent components (ICs) of visual attention ERPs.

3.3.3.1 Components of visual attention ERPs

It was hypothesised that application of the ICA method to decompose visual attention ERPs into ICs was expected to reveal changes of ERP components related to cognitive activation. Importantly, analysis of the grand mean ERPs in response to the difference between go and nogo cues revealed a relatively large frontocentral positive deflection in all groups, especially in the AE group (left columns of Figure 3-7(A)). For the AE group at Fz, Cz and Pz, the motor inhibition component extracted by the ICA method and spatial filters had a significantly decreased peak from 372 ms to 396 ms, compared with the pre-stimulation stage (during vs. before stimulation, $p=0.0156$ in Figure 3-7) (Bekker, et al., 2005; Bokura, et al., 2001a; Smith, et al., 2008). Whereas there were no differences in the LE group, the hypothesis of expected changes of ERP components related to cognitive activation during LE stimulation was not supported.

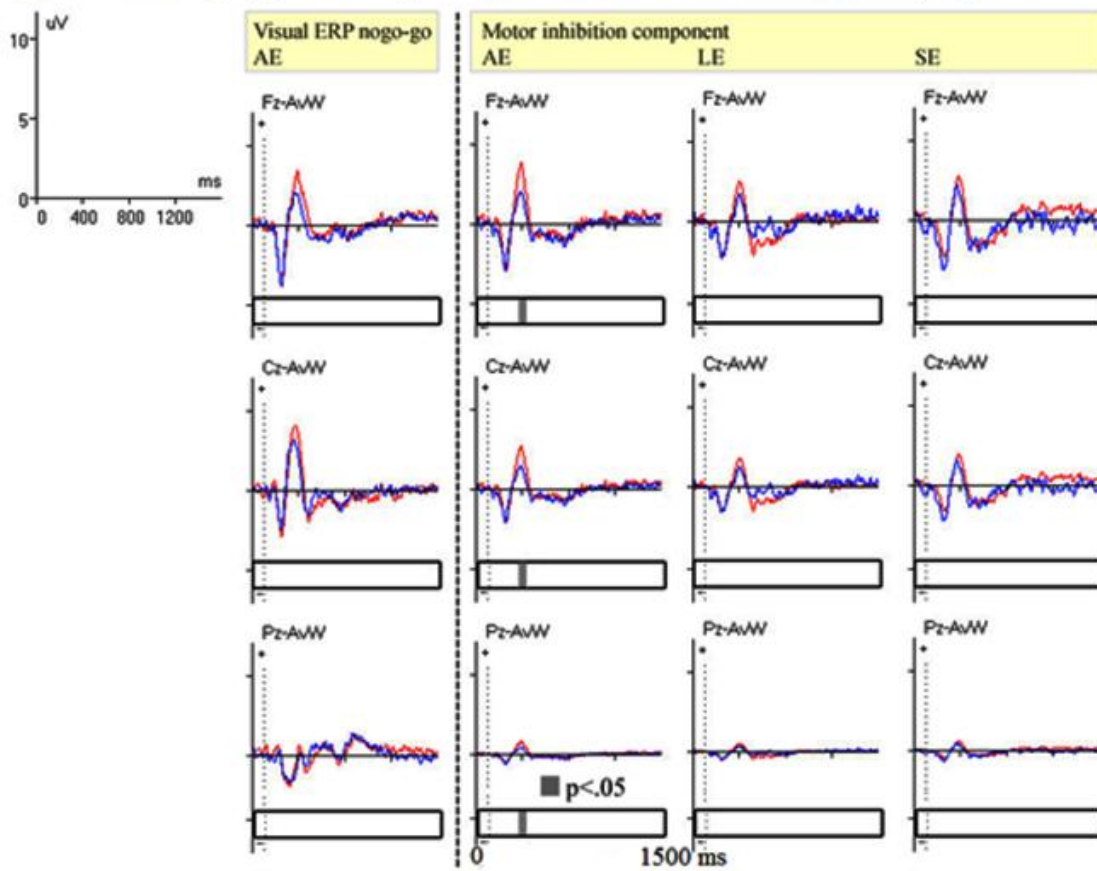
3.3.3.2 Sustained stimulation effects

Again, for disclosing the benefit of applying ICA to conventional ERP methods of analysis, it was hypothesised that the decomposed visual attention ICs was expected to correlate with cognitive activation post stimulation. Only in the AE group at Fz, Cz and Pz channels, the motor inhibition component extracted by the ICA method and spatial filters had a significantly decreased peak from 372 ms to 396 ms, compared with the pre-stimulation stage (after vs. before stimulation, $p=0.0143$ in

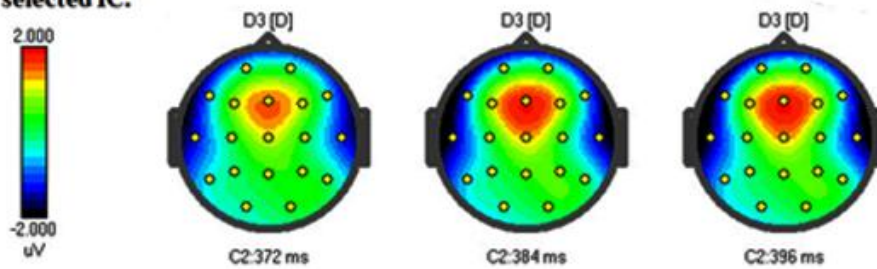
Figure 3-8) (Bekker, et al., 2005; Bokura, et al., 2001a; Smith, et al., 2008). However, the sustained stimulation effects on the motor inhibition component were not found in the LE group, and the hypothesis of expected changes of ERP components related to cognitive activation post LE stimulation was not supported.

During vs. before stimulation

(A) The curves display grand average visual ERPs and the motor inhibition IC in 3 groups.



(B) The 2D topographies of the selected IC.



(C) The perspective views of the selected IC in sLORETA.

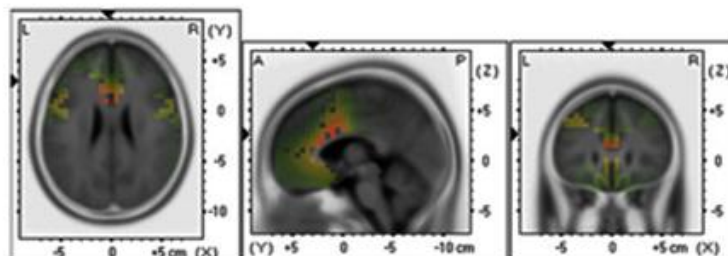
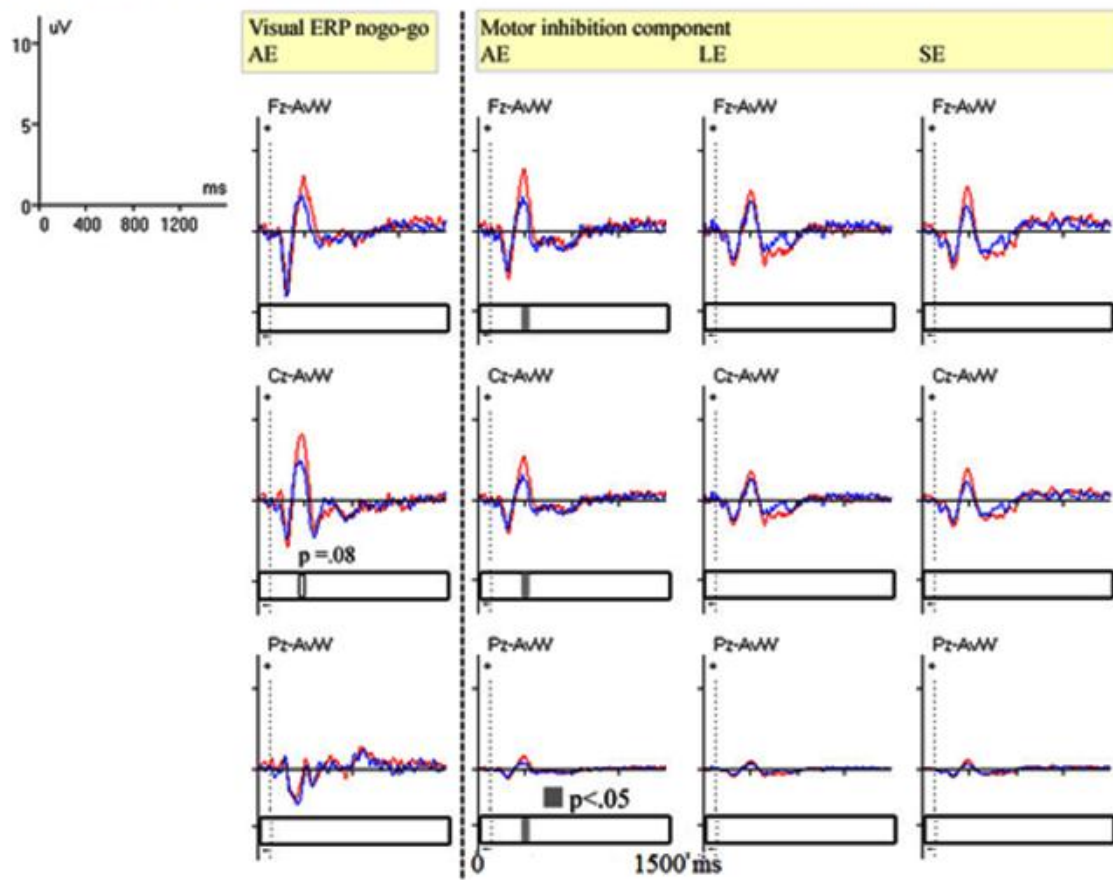


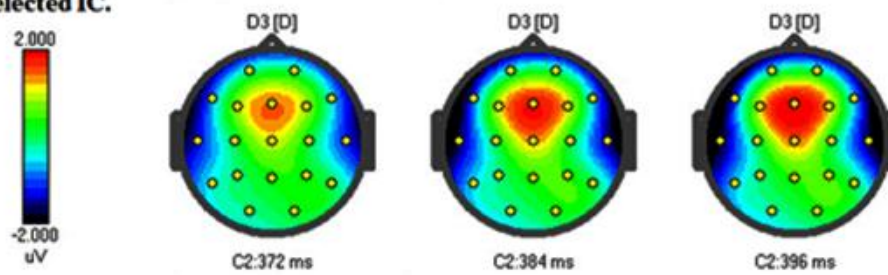
Figure 3-7. (A) Grand mean extracted motor inhibition ICs at midline scalp sites and correlated ERP of nogo-go cues, during stimulation (blue lines) compared with pre-stimulation (red lines) in the three groups. Red lines showed the pre-stimulation baseline of grand mean ERPs and grand mean motor inhibition components in the three groups. The animal pairs were the targets of the manual responses (GO cues), and nogo-go means the component difference between GO and NOGO cues. Superimposed blue lines gave the grand mean ERPs and grand mean motor inhibition components during electrostimulation in the three groups. (B) Horizontal bars below each trace represent t-test results from 0-1500 ms after the second stimulus onset, with values $p < 0.05$ represented in grey between 372 ms and 396 ms. The corresponding time courses are presented at the electrodes (indicated by letters Fz, Cz, and Pz) at which the projected components reach their maximums or minimums. (Y-axis, amplitude in μV at the corresponding electrode; X-axis, time in ms) (e.g., Kropotov, et al., 2011; Kropotov, 2009a). (C) The perspective views (top, sagittal and coronal views) showed the highest density of the motor inhibition component, according to sLORETA images for cortical generators.

After vs. before stimulation

(A) The curves display grand average visual ERPs and the motor inhibition IC in 3 groups.



(B) The 2D topographies of the selected IC.



(C) The perspective views of the selected IC in sLORETA.

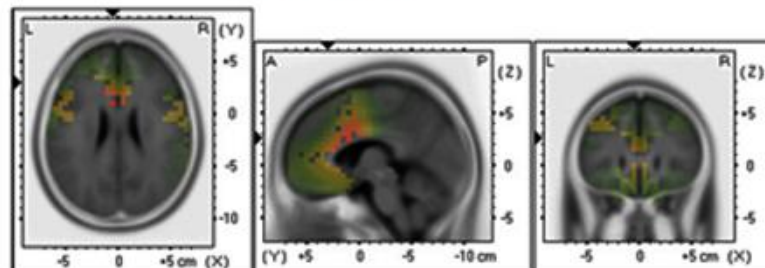


Figure 3-8. (A) Grand mean extracted motor inhibition ICs at midline scalp sites and correlated ERP of nogo-go cues, after stimulation (blue lines) compared with pre-stimulation (red lines) in the three groups. Layout as for Figure 3-7(A), 3-7(B), and 3-7(C).

3.3.4 Hypothesis 5: Decomposed components will correlate with habituation after the repetition of the visual attention task.

3.3.4.1 Decomposed components correlated with habituation

Here it was hypothesised that the control group through an absence of EA effects will show habituation across the three conditions as measured by particular component amplitudes. These decomposed particular components may explain subjects' enhanced attention performance following EA stimulation due to the absence of a habituation effect of EA stimulation on such important components. Thus to evaluate if a putative habituation effect in controls would be inhibited by the stimulation with task repetition, we used the ICA method to reveal the fundamental components in the ERPs. The related ICs of ERPs were compared for the first and last task in each group. Of eleven components that were identified by the spatial filters based on the ICA from the Human Brain Indices (HBI) reference database. (<http://www.mitsar-medical.com>) (Kropotov, 2009c), seven components responding to the “go and nogo” cues were meaningfully related to the visual attention task as follows: visual comparison component at the left temporal area, visual comparison component at right temporal area, P400 working memory component at the frontal area, P300b component at the parietal area, slow wave component at the hippocampus,

P300 suppression component at the frontal area and P400 action monitoring component at the anterior cingulate cortex (ACC) (Kropotov, 2009c).

However, only significantly changed ICs were considered further, as the goal of this report to describe and investigate the ICA features that significantly changed by applying electroacupuncture and/or attention task repetition (details in the next paragraphs).

The ICA decomposition of the attention task revealed similar components in the three conditions. Between-group differences in mean IC topographies in the pre-stimulation stage were barely visible, suggesting a good reproducibility of the component characteristics (Olofsson and Polich, 2007). However, only with the control group did the differences between the first and the third repetition in mean IC topographies show fatigue according to time-on-task effects showing significantly decreased amplitudes of the ICs (Gonsalvez and Polich, 2002; Kato, et al., 2009; Polich, 1989; Ravden and Polich, 1998). Four ICs showed obvious differences, including the left visual comparison component, the P400 action monitoring component, the P400 working memory component, and the passive auditory P300 component. The average characteristics of the ICs as identified in the control group from the beginning to the end of the three tasks are shown in Figures. 3-9 and 3-10, with details in the next paragraphs. Then there were findings in line with the hypothesis to explain the enhanced attention performance following EA stimulation due to the absence of the habituation effect of EA stimulation on important components.

3.3.4.2 Components with significant differences due to task repetition

Visual comparison component, left

The normalized grand-mean component in Figure 3-9, (Figure 3-9A, upper row), revealed a large negative deflection between 100 and 400 ms post second stimulus onset, peaking around 236ms ($p < 0.05$), with a left temporal topography. The significant change of this component in left temporal topography was also projected on to a mean-MRI brain image (Montreal Neurological Institute, Canada), according to the sLORETA images of the components (Figure 3-9A, bottom row) (Kropotov, 2009; Protzner, et al., 2009).

P400 action monitoring component

As illustrated in Figure 3-9B, the second IC of interest was labelled the P400 action monitoring component in the ACC area due to its time course and topography, which was characterized by a later and slower ERP positivity from 260 ms to 520 ms with a peak latency around 400 ms (Figure 3-9B, upper row). The P400 action monitoring component location was in deep brain frontocentral regions through the ACC area (Figure 3-9B, bottom row) (Kaufman, et al., 2003; Kropotov, 2009). Briefly, the characteristics of the significantly decreased amplitude of P400 action monitoring component ($p < 0.05$, around the peak) outlined in Figure 3-9B strongly suggested a relation between fatigue with task repetition, and the declined amplitude of the P400 action monitoring component as a function of a time-on-task effect (Kato, et al., 2009; Olofsson and Polich, 2007).

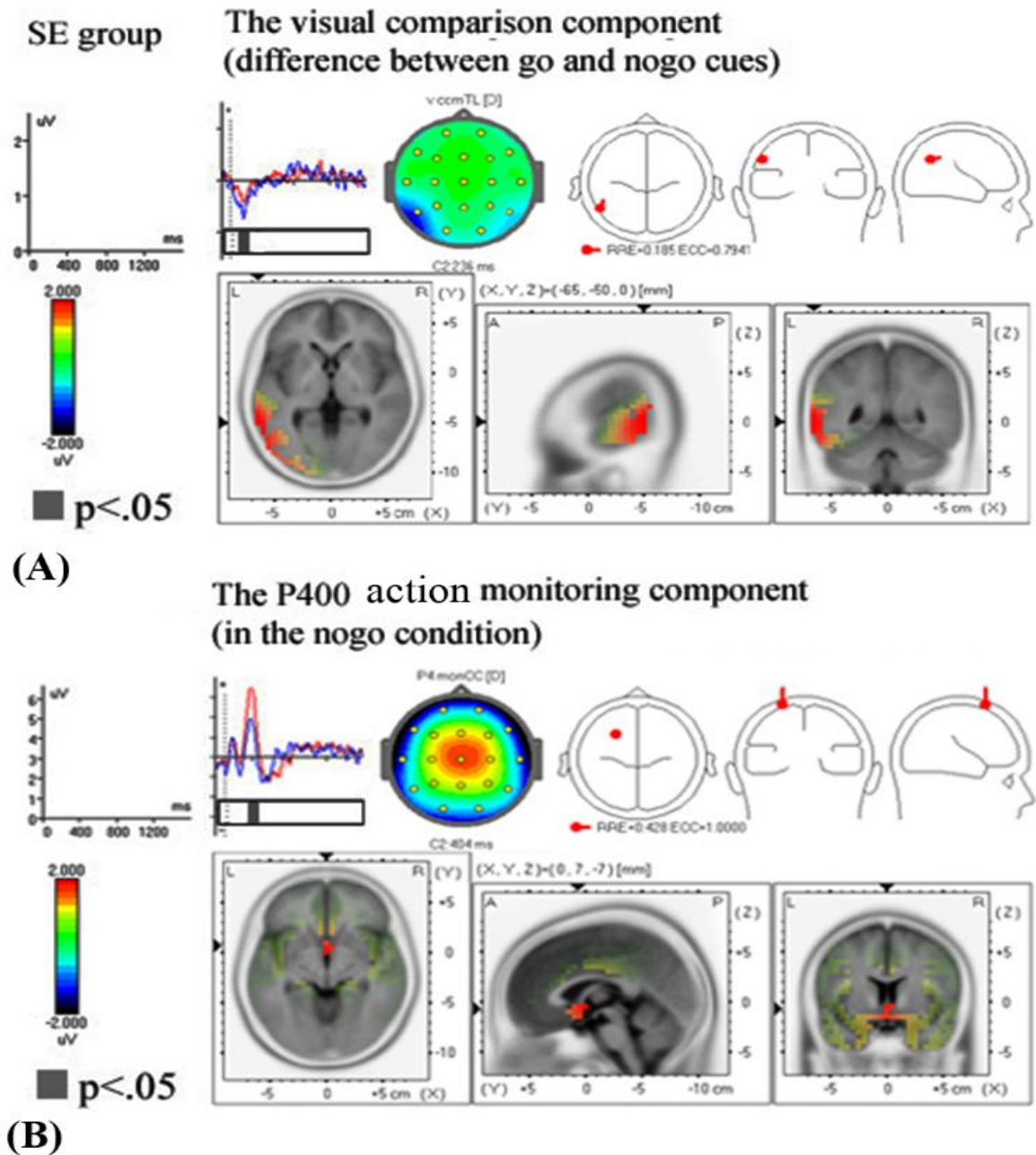


Figure 3-9: The independent components difference between the first and third task repetition in the sham stimulation group: (A) the visual comparison component difference between go and nogo cues; (B) the P400 action monitoring component in the nogo condition. The upper row of the panel for each component shows the grand mean component in amplitude-time plot at Cz (upper left), the scalp topographic map (upper middle), and the single equivalent current dipole locations for each component (upper right). The lower row shows the highest density of each component, according to sLORETA images, from three different perspectives (top, sagittal and coronal views). Each red line shows the grand mean component of the first attention task. Each superimposed blue line gives the grand mean component of the repeated

third task. Horizontal bars below each trace represent t-test results from 0-1500 ms post second stimulus onset, with values $p < 0.05$ represented in grey. The corresponding time courses are presented at the electrodes (3-9A, T5; 3-9B, Cz) at which the projected components reach their maximums or minimums, in order to illustrate significant differences between the first and the third repeated tasks. (Y-axis, amplitude in μV at the corresponding electrode; X-axis, time in ms) (e.g., Kropotov, et al., 2011; Kropotov, 2009a)

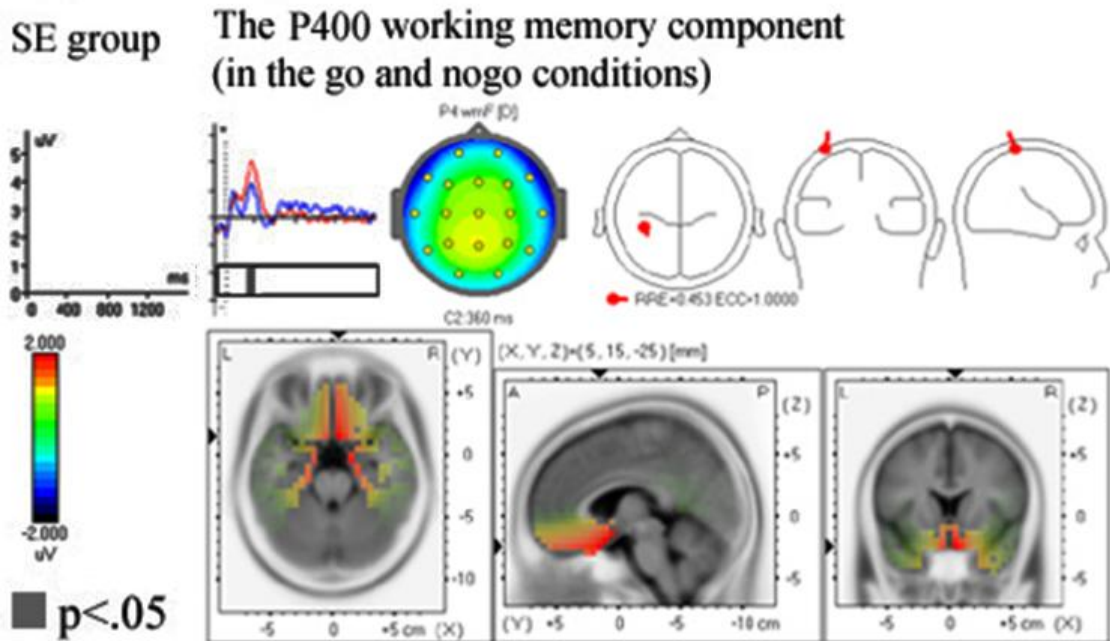
P400 working memory component

The P400 working memory component was presented with positive double-peak morphology between 148 ms and 540 ms post second stimulus onset (peak latency around 360 ms; Figure 3-10A, upper row). This projected component on sLORETA images appeared to be more accurate than the 2D scalp map for assessing the spatial distributions of current density in the deep sources. The P400 working memory component location was in the deep inferior prefrontal region (Figure 3-10A, bottom row) (Kropotov, 2009; Muller and Knight, 2006). To come to the point of related findings, the characteristics of the P400 working memory component mostly demonstrated a relation between fatigue with task repetition and the declined amplitude of the P400 working memory component ($p < 0.05$, around the peak) in the current study, also as a function of time-on-task (Kato, et al., 2009; Olofsson and Polich, 2007).

Passive auditory P300 component

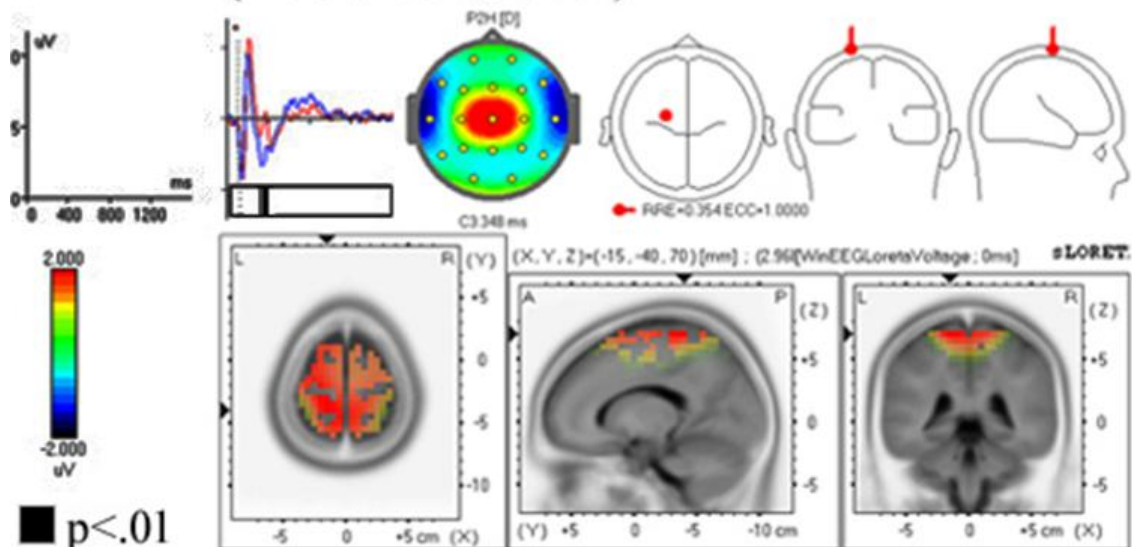
As illustrated in Figure 3-10B, the passive auditory P300 component includes auditory N1/P2 peaks (Polich, 2007), thus serving as a good indicator of the functioning of the auditory attention system in the attention task. The peak of the passive auditory P300 component is around 348 ms and lasting roughly 900 ms. The passive auditory P300 responding to deviant auditory stimuli can be elicited without active attention. The 2D topography and the sLORETA images showed the highest density over the central scalp electrodes (Figure 3-10B, bottom row) (Kropotov, 2009; Polich, 2007; Polich and McIsaac, 1994). In addition, the characteristics of the passive auditory attention P300 component possibly showed a significant relation between

fatigue with repetition and the strongly declined amplitude of the passive auditory P300 component ($p < 0.01$, around the peak) in the present study, also as a function of time-on-task (Kato, et al., 2009; Olofsson and Polich, 2007).



(A)

The passive auditory P300 component (in the control condition)



(B)

Figure 3-10: The independent components difference between the first and third task repetition in the sham stimulation group: (A) the P400 working memory component in both the go and nogo conditions; (B) the passive auditory P300 component in the control condition. Same layout as for the panels in Figure 3-9(A) and 3-9(B) with values $p < 0.05$ and $p < 0.01$ represented in grey and black. The corresponding time courses are presented at the electrodes (3-10A, Pz; 3-10B, Cz) at which the projected components reach their maximums or minimums, in order to illustrate significant differences between the first and the third repeated tasks. (Y-axis, amplitude in μV at the corresponding electrode; X-axis, time in ms) (e.g., Kropotov, et al., 2011; Kropotov, 2009a)

3.4 Discussion of Experiment One

The primary purpose was to explore the effects of electroacupuncture stimulation on a repetitive visual continuous performance attention test and accompanying attention-related ERPs using behavioural performance indices and ERP components extracted by the ICA method. Whereas a number of EEG studies have explored acupuncture effects without the popular ERP methodology (Chen, et al., 2006; Litscher, 2004; Pilloni, et al., 1980; Rosted, et al., 2001; Tanaka, et al., 2002), our current investigation was designed to complement these through the neglected field of topographical EEG, and also to learn more about the recent development of electrical stimulation. It was of particular interest to determine whether putative benefits would outlast stimulation, and whether stimulation with alternating high and low frequencies would be superior to low frequency stimulation. It was hypothesized that stimulation would result in a significant behavioural change with increased sensory sensitivity (d'), largely due to a decrease in errors of commission, as found previously with university students performing the visual continuous performance task (Egner and Gruzelier, 2001; Gruzelier, et al., 2006). Students tend to be highly motivated to attend,

producing few errors of omission, whereas the motivation to achieve may lead to over eagerness, resulting in impulsive errors of commission. It was further hypothesized that their performance would be reflected in ERP components with different types of ERPs generated on 'go' versus 'nogo' trials. Another purpose of this study was to examine if a putative habituation effect in controls would be inhibited by stimulation with task repetition. For this purpose response synchronized ICs of ERPs were compared for the first and last task in each group.

Behavioural results – compatible with hypothesis 1: sustained effects from EA stimulation on perceptual sensitivity in attention.

There was some suggestion of differences in commission errors, but given that the p-value was not significant with the conservative Bonferroni adjustment, caution must be applied and further research is warranted. However, d' was significantly changed differentially by parameters of stimulation (Table 3-2), particularly in relation to attention during and after stimulation with alternating frequencies (Figure 3-3).

The findings overall indicated that stimulation with alternating frequencies was superior to low frequency stimulation in having sustained effects during the task, benefits which continued post-stimulation. In contrast, low frequency stimulation while effective during stimulation did not produce sustained benefits. These effects on the visual sustained attention task were disclosed through higher d' scores (Green and Swets, 1974; Lloyd and Appel, 1976). As anticipated, the improved d' score was largely due to a reduction in commission errors. Reaction time was less definitively

influenced, though exploratory post-hoc tests confirmed shorter RTs following alternating frequency stimulation in the post-stimulation condition when compared with sham stimulation.

ERPs to the go- and nogo-stimuli – incompatible with hypotheses 2 and 3: sustained effects on visual attention ERP latency and amplitude.

Compared to the pre stimulation stage, the grand average ERPs showed a trend of decreasing peak amplitudes of the late components because of task repetition, but no changes in those early components having latencies between 80 to 180 ms. Previous studies using non-affective targets have reported decreased P300 amplitudes at fronto-central sites both as a function of time-on-task and with sequence repetition, (Gonsalvez and Polich, 2002; Polich, 1989; Ravden and Polich, 1998). Another study employing unpleasant, neutral and pleasant stimuli has reported that P300 amplitude decreased with repetitive picture processing (Codispoti, et al., 2006). In the current study the stimuli were mainly non-emotional and hence the results were in line with previous studies, notwithstanding the novel introduction of acustimulation

Application of ICA, spatial filter and sLORETA

Applying ICA with spatial filtration disclosed a variety of interesting results which confirm and extend efforts to decompose ICs of ERPs recorded during the visual attention task (Li, et al., 2009). Mathematically, ICs are often characterized by scalp maps fitting the projection of a single equivalent current dipole, which is compatible with each presumed IC reflecting synchronous cortical local field activity

of a connected network. However, only a few ICs can be approximately calculated by a single dipole because some ICs are most likely to be generated by distributed neuronal circuits. Therefore standardized low resolution electromagnetic tomography (sLORETA) images were used instead of dipole approximations. Overall the present findings strongly suggest that the main features of averaged ERP ICs can be successfully decomposed from ERP data via ICA decomposition combined with spatial filters (from HBI database) for each group and each time period, especially for the pre vs. post stimulation comparison. The components reflected motor inhibition, visual comparison, P400 action monitoring, working memory, and passive auditory P300 components.

Acupuncture effect induced by stimulation in the real vs. the sham group

The typical HeGu and NeiGuan (LI-4 and P-6) acupoints are among the traditional points used in modulating cortical plasticity, relieving pain and treating nausea and vomiting (Chao, et al., 2007; Chen, et al., 2006; Streitberger, et al., 2006). The HeGu acupoint lies at the midpoint between the first and second carpal bones of the first web space on the dorsal side, and the NeiGuan acupoint is located on the anterior surface of the wrist, approximately 3 cm proximal to the wrist between the tendons of the flexor carpi radialis and the palmaris longus, next to the median nerve. These junctures are full of peripheral nerve extensions from the sensory nerve and muscle tendons (Lu, 1983), and with lower focal transcutaneous resistance they can provide effective electrical stimulation without much current. In contrast, the sham (fake) electroacupuncture at the same acupoints (placebo electrostimulation), generates insufficient sensory input to cortex. Thus the observed changes of behaviour

and the motor inhibition component in the ERP could be due to the differences in the nerve conduction and excitability of stimulated acupoints of the two real electroacupuncture groups and the selected minimal stimulation in the sham group (Chao, et al., 2007). Certainly the differential stimulation effects between real vs. sham stimulation on the same sites in behavioural performance and changes in independent components encourage the use of sham stimulation as a control for the study of brain function and associated acupuncture effects.

Acupuncture effect induced by stimulation in alternating frequency mode vs. low-frequency mode – compatible with hypotheses 1 and 4: sustained effects from EA stimulation on perceptual sensitivity in attention, expected to reveal the ERP component related to cognitive activation after the repetition of attention tasks.

Our study confirmed that only stimulation with alternating frequencies (5/100Hz), but not with a low-frequency delivered at 5 Hz, had the sustained post stimulation effect in improving d' scores and decreasing mean commission errors. Low stimulation at 5 Hz had only short lived benefits. In addition, compared to the baseline without stimulation, alternating stimulation induced a significantly decreased motor inhibition component during stimulation and post stimulation, which theoretically was compatible with improvements in commission errors which reflect motor impulsivity (Bekker, et al., 2005; Bokura, et al., 2001a; Smith, et al., 2008).

For clinical practice, the result of a prolonged effect due to alternating high and low frequencies has become an important issue for treatment (Tong, et al., 2007). A recent study with resting functional Magnetic Resonance Imaging (fMRI) data using a

probabilistic ICA method demonstrated for the first time that the post-stimulation effects of acupuncture can enhance the spatial extent of resting brain networks (Dhond, et al., 2008). Interestingly, such sustained post-stimulation effects have been hypothesized to alleviate pain by altering neurotransmission in the CNS in both animals and man (Han, 2004; Somers and Clemente, 2009). Differential release of opioid peptides in the CNS by electroacupuncture stimulation has been noted, with a low frequency of 2-15 Hz triggering the release of enkephalins and Beta endorphins, and a high frequency of 100 Hz stimulation increasing the release of dynorphin at the spinal cord level (Han, 2004). A combination of both frequencies with an alternating current of 2 and 100 Hz may allow synergistic interaction among the neurotransmitters and so provide a more powerful effect than sham stimulation (Chao, et al., 2007; Streitberger, et al., 2006). Napadow et al. (2005) with fMRI have claimed that the limbic system is central to acupuncture effects regardless of the specific acupuncture modality, although some differences do exist in the underlying neurobiologic mechanisms for different modalities. The findings may also provide hints for optimising acupuncture in clinical applications (Napadow, et al., 2005).

Further potential clinical applications – compatible with hypotheses 4 and 5: expected to reveal the ERP component related to cognitive activation. This may disclose the benefit of applying ICA to conventional ERP methods of analysis.

Although most of the studies of electroacupuncture stimulation have explored the role of acupuncture in analgesia, neuroimaging research has also revealed possible brain networks and regions for potential influence on attention and memory (Chen, et al., 2006; Dhond, et al., 2008; Napadow, et al., 2005; Wu, et al., 2002; Zhang, et al.,

2003). Manual stimulation showed increased regional cerebral blood flow (rCBF) mainly in the parahippocampal gyrus, premotor area, frontal and temporal areas bilaterally and the ipsilateral globus pallidus (Lee et al., 2003). In a recent report of electroacupuncture-induced analgesia examined by fMRI, several areas with positive correlation of analgesic effects for low-frequency stimulation included the contralateral motor area, the supplementary motor area, and the ipsilateral superior temporal gyrus. In contrast with high-frequency stimulation the response occurred in the contralateral inferior parietal lobule, ipsilateral anterior cingulate cortex (ACC), nucleus accumbens, and pons (Zhang, et al., 2003; Zhang, et al., 2004). Functional MR imaging has demonstrated the CNS pathways involved in acupuncture stimulation. Even the subcortical gray structures, hypothalamus-limbic system and hypothalamus-pituitary-adrenal axis (HPA axis) have been related to electroacupuncture stimulation (Cho, et al., 2006; Wu, et al., 2002; Zeng, et al., 2006). In the case of low-frequency stimulation, high activation has been elicited over the hypothalamus and primary somatosensory-motor cortex, with deactivation over the rostral segment of anterior cingulate cortex (Wu, et al., 2002).

The findings of our study also support the assumption that electroacupuncture stimulation has an effect on specific brain areas, and the improved performance in cognition is possibly related to enhanced cortical activity. While previous studies have demonstrated a sustained post stimulation effect for pain relief, gastric mobility and heart rate variability (HRV) (Chesterton et al., 2002; Claydon, et al., 2008; Imai, et al., 2008), to our knowledge no prior published research has examined sustained attention during stimulation and post-stimulation periods in healthy young adults. This conclusion followed a search of nine bibliographic databases for the effects of

transcutaneous electrical nerve stimulation (TENS) on non-pain related cognitive and behaviour which found only reports on patients (van Dijk, et al., 2002).

The guidelines for electroacupuncture safe practice in dual-site electroacupuncture stimulation of the experimental design

In clinical practice, the more distal acupoint location of the electrodes on hands and wrists seems much more practical than the proximal location of the limbs, paraspinal muscles, and neck or head regions. Our design with a pair of acupoints on each hand followed the guidelines for safe practice recommended by the British Medical Acupuncture Society (BMAS) to avoid adverse events. Especially, electroacupuncture should not be applied such that the current is likely to traverse the heart. If the application of electrostimulation is likely to cross the heart (for example, from one shoulder to the other shoulder (Thompson and Cummings, 2008), this placement is prohibited. A study has also reported that electrical fields generated by pairs of needles below the knee or elbow do not create a detectable spread of the currents along the limb or into the chest (Thompson and Cummings, 2008). The safety guidelines are rarely mentioned in scientific reports.

Limitations and recommendations for future research

Notwithstanding the beneficial outcome on sustained attention that we have demonstrated, our study has potential limitations or at least issues warranting further examination. First, an optimal washout period of the neurobiological effects generated by stimulation remains unknown. The effective post stimulation period was for a

minimum of 30 minutes in our study, similar to the report of Claydon et al. (2008) using pressure pain threshold (Claydon, et al., 2008). Second, the optimal sites for influencing cognition have not been systematically examined. HeGu (Li4) and NeiGuan (P6) are the well studied acupoints, but other acupoints such as Zusanli (St36) and Taichong (Liv3) might be helpful adjuncts for improving cognitive function. Third, the relative contribution of the mechanism for the synergistic action produced by different combinations of neuropeptides is still not well understood, and therefore, the effectiveness of alternating frequency stimulation must be verified with neuroimaging. Meanwhile, various stimulation frequencies may involve different mechanisms. Several neurotransmitters such as serotonin and dopamine are also believed to contribute to attention and memory systems (Boulougouris and Tsaltas, 2008; McNab, et al., 2009; Muller and Carew, 1998). It is not clear, however, to what extent these neurotransmitters are involved and how they are coordinated with each other during and after electrical stimulation. Further research should be conducted to combine the behavioural, electrophysiological and neurochemical modulation data.

The risk of unblinding and the limitations of a single blind study include the interaction between subjects and the researchers. First, we asked participants to perform and focus on the repetitive visual attention task, and not pay attention to the sensation induced at the stimulated site, in order to blind any effect from the interaction between subject and the researcher. Second, the requirement of recruiting subjects was that all subjects had no experience about electroacupuncture prior to our testing. Complying with ethical considerations, although all subjects were blind to the stimulation mode and effect, they were told that the machine could generate transcutaneous stimulation on the acupoints of the hands with various frequencies,

which may or may not give a sensation. However, because subjects had no experience of electrostimulation, they were blinded to the relationship of stimulation modes and effects. Importantly, only the intensity parameter of stimulation in the sham group was different from the real electroacupuncture groups, and possibly any emotional reaction to the thought of minimal tactile sensation was unlikely to influence responding; as mentioned earlier the sham stimulation itself has been shown not to affect sensory cortex (Chao, et al., 2007; Wu, et al., 2002).

Finally, electroacupuncture stimulation presented in this study is one method for modulating neuronal processing in order to improve cognitive performance. This may be useful in the range of neurological and psychopathological conditions mentioned above where the continuous performance paradigm has disclosed deficits (Arns, et al., 2009; Lubar, et al., 1995; van Dijk, et al., 2002). Two studies related to the effects of TENS on cognition and behaviour showed a moderate beneficial influence on cognitive functions in children with ADHD (Jonsdottir, et al., 2004) and in aging (Scherder, et al., 2000).

EEG-neurofeedback is another approach (Gruzelier, 2009; Gruzelier, et al., 2006; Lubar, et al., 1995). In addition, combining feedback techniques with stimulation strategies has become a potential method for exploring brain function and effective protocols than either alone (Hirshberg, et al., 2005; Ros, et al., 2010). Studies of the neurofeedback training to improve attention and memory performance have implied the promising evidence for employing electroacupuncture stimulation as an assisting tool, according to the fundamental cortical electrophysiological activities (Egner and Gruzelier, 2001, 2004; Vernon et al., 2003). The prospective approach in combining these two techniques will be valuable and will be investigated in our future studies.

3.5 Summary

This single-blind randomized placebo-controlled study showed that electroacupuncture stimulation with alternating frequencies on pairs of acupoints of both hands resulted in significantly better sustained behavioural performance and sustained cortical activation with decreased motor inhibition component in a repeated visual continuous attentional performance task than low frequency stimulation, which in turn was superior to placebo. No obvious adverse effect in healthy subjects was noted. Evidence was provided that ICA with spatial filtration, applied to ERP data, successfully decomposed the spatiotemporally overlapping ERPs into a range of underlying EEG processes whose localization was congruent with a range of behavioural functions: visual comparison, P400 action monitoring, working memory and passive auditory P300. The alternating frequency stimulation could be an adjunct for helping adults successfully enhance their sustained attention and inhibit competing motor responses both during and post stimulation, indicating its potential therapeutic benefit for psychiatric disorders with compromised attention and cognition. When the baseline was compared with the pre-stimulation and post-stimulation period in the control group with the placebo stimulation, the IC-derived ICs disclosed evidence of habituation. The absence of habituation in the experimental groups suggests a potentially successful activation for preventing fatigue. Further randomized trials with a larger sample size will be conducted to compare and combine electroacupuncture stimulation with a more established modality, such as EEG-biofeedback. Interestingly, these further trials will clarify the role of applied acustimulation on self-regulation, cognitive function, and cortical activation.

Dynamic changes of ICA-derived EEG functional connectivity in the resting state

4.1 Introduction

4.1.1 The introduction of experiment two

The identification of a resting baseline state is an essential issue in neuroscience in order to interpret brain activation and to disentangle the mechanisms behind neuronal cooperative activity, which form the core of all cognitive, perceptive and motor-driven activities. Since its discovery by Hans Berger in the 1930s, electroencephalography (EEG) has been a reliable method for monitoring brain dynamics, contributing an early focus on the electrophysiological changes from the eyes-closed (EC) to the eyes-open (EO) resting condition. This transition has traditionally been characterized by a suppression of occipital alpha activity through visual stimulation in the EO state, classically termed “alpha blocking” (Pollen and Trachtenberg, 1972), or more recently “alpha desynchronization” (Klimesch, et al., 2000; Klimesch, et al., 2007; Klimesch, et al., 2007; Neuper and Pfurtscheller, 1992; Neuper, et al., 2006; Pfurtscheller, et al., 1996). Both EC and EO resting conditions, either alone or in combination, have commonly served as a standard baseline estimate in cognitive tasks as well as resting (or “spontaneous”) conditions.

Recently however, the study of RSNs has shifted its focus from the localization of specialized brain activations to the interpretation of interrelationships in brain dynamics. In parallel, a host of EEG rhythms has been documented in the network

operations of corticothalamic systems (Steriade, 2006), where several rhythms have been found to coexist in the same area or interact among different structures (Steriade, 2001). These discoveries have led to the suggestion that the EEG could be combined with fMRI to study baseline functions and oscillations within a more dynamic architecture of the human brain (Gusnard, et al., 2001; Laufs, 2008; Mantini, et al., 2007), with the goal of spatio-temporally decomposing the complex dynamics associated with multiple EEG frequencies simultaneously (Laufs, et al., 2003; Mantini, et al., 2007).

A main advantage of EC and EO resting-state protocols is that they may be carried out without requiring subjects to perform a specific task, and therefore be easily deployed in clinical settings. Barry et al. examined the possible arousal or processing differences and topographies between EC/EO resting conditions in adults (Barry, et al., 2007) and children (Barry, et al., 2009). They demonstrated that significant reductions in mean activity in the delta, theta and alpha bands were accompanied by increased beta activity in frontal hemispheric regions, analyzed by spectral energy and topographic changes in the traditional frequency domain from the EC to the EO state. Others such as Chen et al. (2008) have introduced scalp EEG spectral regional field power to study the distribution of RSN activity at rest. However, the possibility exists that the apparent disparities (for example, to construct functional networks shown by fMRI studies) between the above EEG and fMRI studies may be due to the well-known inadequacy of conventional scalp recordings to resolve EEG source locations, for scalp voltage is a mixture of underlying source activity and volume conduction (Congedo, et al., 2009; Nunez, 1987; Nunez et al., 1997; Winter, et al., 2007).

The utility of MEG, a neuroimaging modality bypassing the hemodynamic response and measuring the magnetic fields associated with electrophysiological brain activity, as a means to investigate RSNs has been shown in recent papers. de Pasquale et al (2010) showed correlation between resting state temporal MEG signals originating in nodes of the DMN and the "task positive" or DAN. Brookes et al. (2005) used seed-based envelope correlation in conjunction with beamformer spatial filtering methods to show interhemispheric motor cortex connectivity in source space. These reports showed that RSNs measured using fMRI are mirrored in MEG data. Brookes et al. (2011) used a unique combination of beamformer spatial filtering and ICA and required no prior assumptions about the spatial locations or patterns of the networks. They reported their results in RSNs with significant similarity in their spatial structure compared with RSNs derived independently using fMRI. They also concluded that the DMN was identified using alpha-band data whereas all other networks were identified in beta-band data (Brookes, et al., 2011).

Hipp et al. (2012) also found that spontaneous oscillatory neuronal activity exhibited frequency-specific spatial correlation structure in the human brain in their MEG research. They concluded that correlation of power across cortical regions was strongest in the alpha to beta frequency range (8–32 Hz) and correlation patterns depended on the underlying oscillation frequency, for examples, in the medial temporal lobe in the theta frequency range (4–6 Hz), in lateral parietal areas in the alpha to beta frequency range (8–23 Hz) and in sensorimotor areas for higher frequencies (32–45 Hz). The strongest correlation of alpha to beta activity may be a generic signature of intrinsic neuronal interactions (Hipp, et al., 2012).

As a solution, an approach termed Blind Source Separation (BSS) has been developed and which originated in the engineering field of signal processing (Bell and Sejnowski, 1995; Comon, 1994; Hyvarinen and Oja, 2000). Independent component analysis (ICA) is a special case of BSS methods that has been applied to EEG and fMRI data (Calhoun, et al., 2001; Calhoun, et al., 2004; Makeig, et al., 1996; Makeig, et al., 2002) as a tool to remove artefacts (e.g., Jung, et al., 2000) and to separate physiological sources (e.g., Makeig, et al., 2004). One of the advantages of ICA is that individual-subject EEG epochs (or fMRI voxels) can be concatenated across subjects along the time axis to apply the ICA algorithm to group data (e.g., Calhoun, et al., 2001; Calhoun, et al., 2004).

Therefore, it is proposed here to utilise group ICA as a valid approach to decompose resting EEG signals into a number of independent components (ICs). Then, after spectral power analysis and estimating the cross-correlation of (alpha-band) EEG power between different ICs within subjects, a functional relationship between such source “nodes” can be established, analogous to approaches that have been adopted to calculate functional connectivity from BOLD signal strength in fMRI data (e.g., Buckner, et al., 2009). Finally, using an inverse localization tool such as sLORETA, the cortical location of these ICs may be resolved into spatially well-defined “sources” (Pascual-Marqui, et al., 2002).

As will be shown results demonstrate the feasibility of studying neuronal resting-state networks according to the existence of functional relationships between ICA components in EEG data. The present study also replicates the previously reported spectral power changes in the EEG–alpha band from the EC to the EO state.

4.1.2 Aims for experiment two

Therefore the second experiment was conducted to explore EEG functional connectivity between eyes closed (EC) and eyes open (EO) states, which have been two traditionally used EEG baseline indices, in order to elucidate direct neuronal (electrophysiological) RSNs in healthy subjects. The source-derived EEG functional connectivity maps may be a valuable method to (a) identify EEG baseline states and accompanying networks termed “EEG resting state networks (RSNs)”, and (b) provide a means to compare the findings of ICs from fMRI studies with current EEG research, thereby elucidating synchronous spatiotemporal patterns during resting states.

On the basis of prior fMRI research in both EC and EO states, the current EEG research employs a pipeline with which to analyse the EEG resting and default mode networks. A four-step analytic approach was undertaken in order to depict five statistically clustered groups having frontal, central, parietal occipitotemporal, and occipital cortical sources, and networks involving those sources.

In addition, the salient electrophysiological clustered groups in the healthy EEG decomposed by the ICA method may disclose differences between EC and EO resting states. This approach could subsequently be applied to validate evidence of enhanced cognitive performance as shown in Exp I, for example, and the improved attention found after NF training with or without exogenous stimulation as will be outlined in Exp III.

Aim 1: The application of group ICA to extract independent components (ICs) from epoch-wise alpha-band power.

One of the advantages of ICA is that individual-subject EEG epochs (as with fMRI voxels) can be concatenated across subjects along the time axis to apply the ICA algorithm to group data (e.g., Calhoun, et al., 2001; Calhoun, et al., 2004). ICA may be utilized as a valid approach to decompose resting EEG signals into a number of ICs.

Aim 2: The application of standardized low-resolution tomography analysis (sLORETA) for cortical source localization of the independent components.

Using an inverse localization tool such as sLORETA, the cortical location of these ICs may be resolved into spatially well-defined “sources” (Pascual-Marqui, et al. 2002).

Aim 3: The application of graph theory for functional connectivity estimation.

After spectral power analysis and estimating the cross-correlation of (alpha-band) EEG power between different ICs within subjects, a functional relationship between such source “nodes” can be established, analogous to approaches that have been adopted to calculate functional connectivity from BOLD signal strength in fMRI data (e.g., Buckner, et al. 2009). It was hypothesized that graph analysis may reveal EEG functional networks with fronto-parietal connectivity: a more medial network with nodes in the mPFC/precuneus which overlaps with the “default-mode network” (DMN), which has been found in several fMRI studies. Moreover, putatively a more lateralized network comprised of the middle frontal gyrus and the inferior parietal lobule may coincide with the “dorsal attention network” (DAN) during the EO

compared to the EC state, hypothesized to result from engagement of the visual attention system in the EO state.

Aim 4: Circumscribing IC similarity measures via hierarchical cluster analysis.

Several statistically clustered groups by the cross-correlation of (alpha-band) EEG power may be found and considered as cortical grouped sources, indicating similarities between EC and EO resting states.

Aim 5: Circumscribing IC similarity measures via multi-dimensional scaling (MDS).

MDS analysis calculates a distance matrix of ICs which supported the emergence of a pattern of increased proximity (mutual information) between frontal and parietal clusters specifically for the EO state.

In summary, the aims of the second experiment will be to demonstrate the feasibility of studying neuronal resting-state networks according to the existence of functional relationships between ICA components in EEG data, and the previously reported spectral power changes in the EEG–alpha band from the EC to the EO state. Since resting-state connectivity has been shown to correlate with behavioural performance and cognitive measures in several published studies (for a review, see Greicius, 2008), EEG spectral-power based RSNs, resolved with ICA, may provide a useful measure with which to directly quantify neuronal functional connectivity during activated brain conditions, for example, NF training for improving attention.

4.2 Methods of Experiment Two

4.2.1 Subjects

Participants were twenty-seven healthy volunteers from Goldsmiths, University of London (20 females and 7 males) with ages ranging from 18 to 30 years, mean = 22.5. All subjects had normal hearing and normal or corrected-to-normal vision and were not receiving psychoactive medication. Subjects were excluded if they had any history of epilepsy, drug abuse or head injury. They were recruited by advertisement and signed an informed consent form before the start of the experiment in accordance with the Helsinki Declaration. The current investigation received ethical approval from the College Research Ethics Committee.

4.2.2 Design

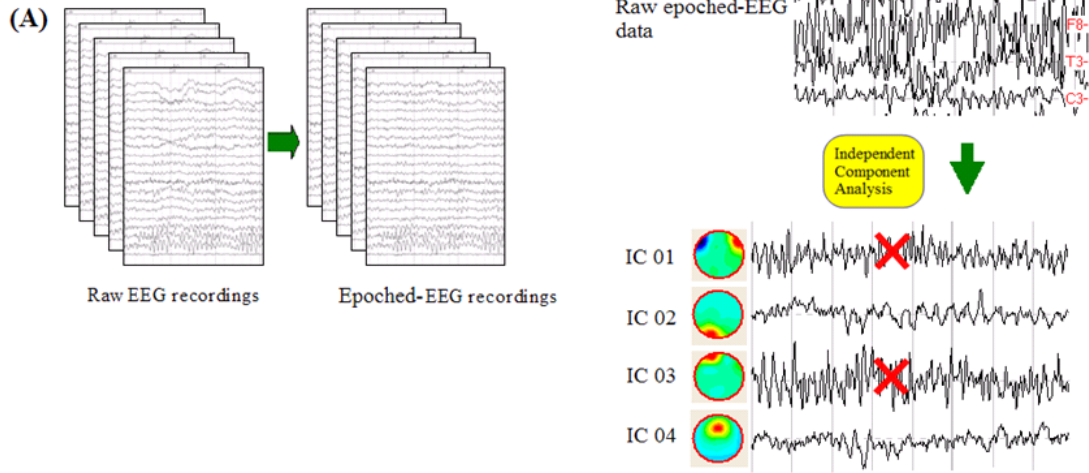
Each subject was asked to sit in an armchair in a quiet room with stable temperature and shaded daylight. The experiment began for all subjects with a 3 minute eyes-closed (EC) condition, followed by 3 minutes with eyes open (EO). Each subject was not given any instruction but asked to stay fully relaxed without eye movements to avoid motion artefacts in the eyes-closed condition. During the eyes-open condition, participants were instructed to visually fixate on a small cross presented on a table below eye level in front of them to reduce eye blinking and lateral eye movement artefacts.

4.2.3 Procedure

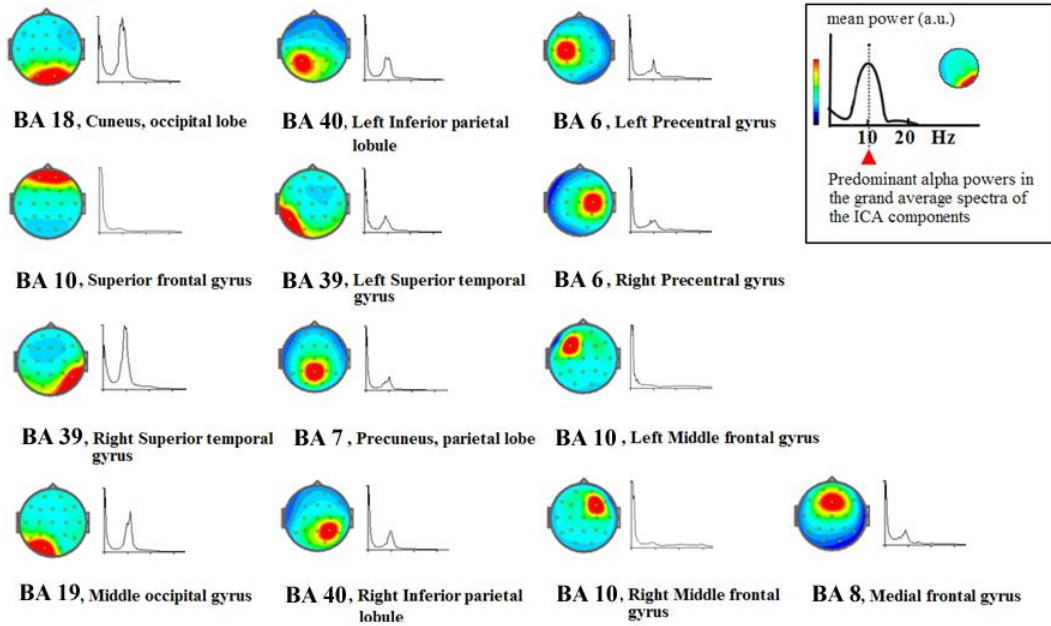
4.2.3.1 Independent component (ICA) and spectral power analysis

The general scheme of this approach is illustrated in Figure 4-1. Artefact-free EEG epochs from EC and EO conditions (and from all subjects) were concatenated into one file, which was then decomposed into independent brain sources by the group ICA procedure (Jung, 2001; Makeig, 1996) using WinEEG 2.83 software (Mitsar, Ltd. <http://www.mitsar-medical.com>), which utilises the Infomax ICA algorithm (Bell and Sejnowski 1995). Theoretically, ICA is able to separate N source components from N channels of EEG signals in each subject. This is represented by the rows of an inverse unmixing matrix, W in $u=Wx$, where u is the source matrix and x is the scalp-recorded EEG (details in the section 1.3). The time courses of the sources are assumed to be statistically independent. Then, for each subject, the alpha-band (8-12 Hz) power spectra of the back-reconstructed ICs were computed by short-time Fourier Transform (STFT) for each selected time interval (4-second epochs with a 50% overlapping Hanning time window). As may be seen in Figure 4-1(C), the predominant frequency of ICs is alpha (8-12 Hz) in almost 70% or 9 ICs/13 ICs. Finally, for both EC and EO conditions, the present study cross-correlated the 13 IC alpha-band powers across all epochs and within subjects. The individual within-subject connectivity matrix r^2 values were then averaged across subjects to give a group-wise matrix for each condition. Through this time-frequency analysis the present study showed that several grouped components oscillate synchronously with alpha-frequency dynamics in the resting state.

(B) Steps in EEG decomposition using Infomax ICA



(C) Topographies and grand average power spectra of selected (valid) independent components of EEG, across cases



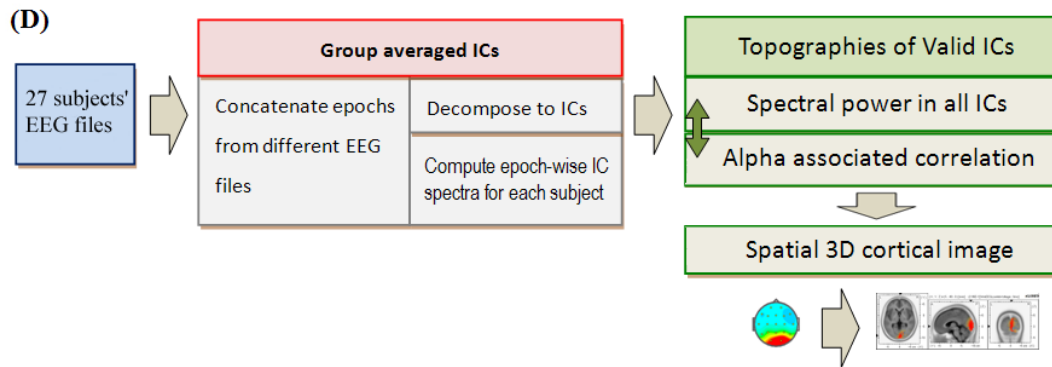


Figure 4-1. Schematic representation of the different pipeline steps from (A) raw EEG to epoched-EEG recordings, from a single subject's EEG, (B) EEG concatenation and decomposition using Infomax ICA and artefact rejection, which excludes large amplitudes from muscular activity and eye-blinking, C) the construction of mean power spectra of each valid independent component (IC) and its topography. (D) General schema of deriving the alpha power correlation matrices from back-reconstructed Fourier spectra of all ICs to estimate functional connectivity in both EC and EO states. Then, 3D cortical images are presented for visualizing related ICs within the cortical source-level map.

4.2.3.2 EEG recordings and pre-processing of EEG

Scalp voltages were recorded using a 19 Ag/AgCl electrode cap according to the 10-20 international system: Fp1, Fp2, F7, F3, Fz, F4, F8, T3, C3, Cz, C4, T4, T5, P3, Pz, P4, T6, O1, O2. (Electro-cap International, Inc. <http://www.electro-cap.com>). The ground electrode was placed on the scalp, at a site equidistant between Fpz and Fz. Electrodes were referenced to linked earlobes, and then the common average reference was calculated off-line before further analysis. Electrode impedance was kept under 5 K Ω . Electro-oculogram (EOG) data were recorded from electrodes (Fp1/2) placed to monitor eye movements and eye blinking. Electrical signals were

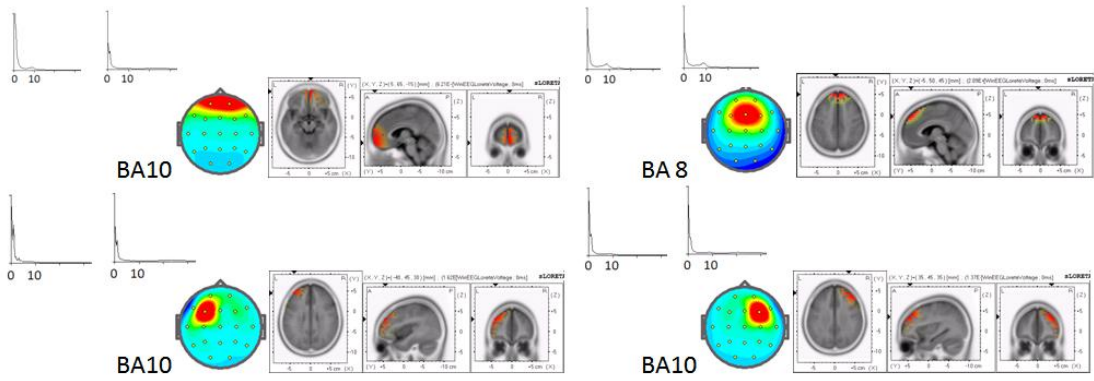
amplified with the Mitsar 21-channel EEG system (Mitsar-201, CE0537, Mitsar, Ltd. <http://www.mitsar-medical.com>). The EEG was recorded continuously, digitized at a sampling rate of 250 Hz, and stored on hard disk for off-line analyses. EEG data were filtered with a 0.5-60 Hz bandpass filter off-line (e.g., Mantini, et al., 2007). Artefact rejection methods consisted of the exclusion of epochs with large amplitudes (over $\pm 80\mu\text{V}$), eye-blinking, DC bias, physiologically unresolvable noise (Onton, et al., 2006), muscular activity of frontal muscles defined by fast activity over 20 Hz (Shackman, et al., 2009), and with slow eye movements coincident with the EOG (c.f., Viola, et al., 2009). It has been shown that ICA is capable of reliably separating eye activities, such as eye blinking and lateral eye movement (e.g., Jung, et al., 2000). Moreover, each 3 minute period of EEG was analyzed in 4-second epochs (50% overlapping with Hanning time window), resulting in 89 epochs. On average around 60-70 valid epochs without artefacts from the 27 subjects were analyzed. Then, spectral power analysis was applied to examine the dynamics of EEG-alpha power spectra change from EC to EO state. This evaluation allowed a more direct comparison of the present results with previous literature (for a review see Klimesch, 1999).

4.2.3.3 Source localization analysis

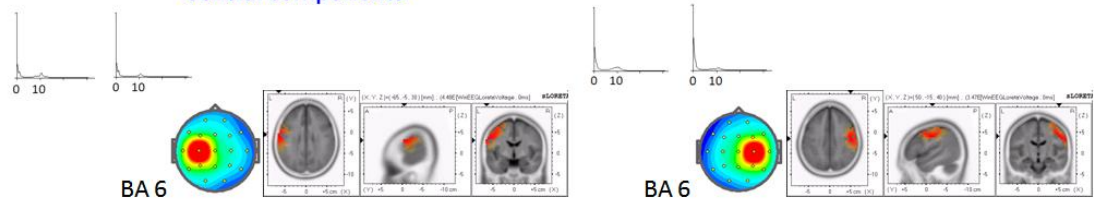
sLORETA analysis was performed on scalp maps with selected ICA components to find the maximal densities of their cortical sources (Pascual-Marqui, et al., 2002) (details in the section 1.3). sLORETA imaging provided source computations for the ICs using software provided from the Key Institute for Brain-Mind Research in Zurich, Switzerland (<http://www.uzh.ch/keyinst/loreta.htm>). sLORETA is an inverse

solution technique that estimates the distribution of the electrical neuronal activity in three-dimensional space. Specifically, sLORETA computes 3D linear solutions for the EEG inverse problem within a head model co-registered with the Talairach probability brain atlas (Talairach, 1988) and viewed within MNI (Montreal Neurological Institute) 152 coordinates at 5mm resolution. Valid ICA components were defined by their single dipole fitting having satisfactory relative residual energy below 10% (e.g., Grin-Yatsenko, et al., 2010), indicating each was clearly generated by a strong locally circumscribed cortical source (Figure 4-2).

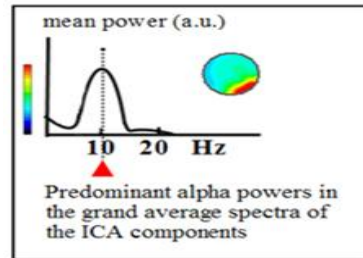
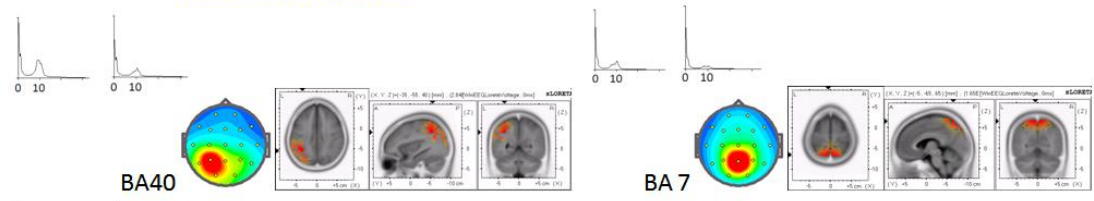
EC vs. EO Frontal components



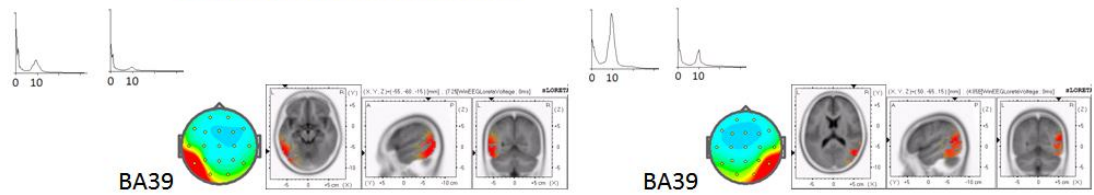
Central components



Parietal components



Occipito-temporal components



Occipital components

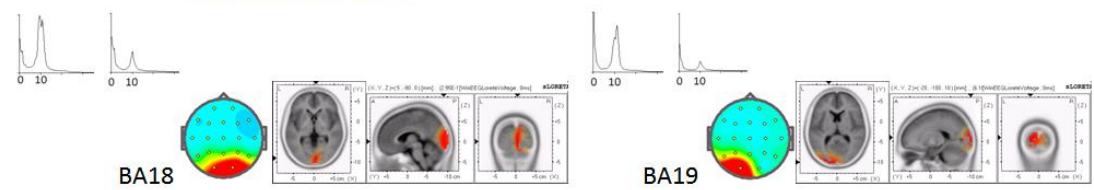


Figure 4-2. The topographies, power spectra, and source localization of 13 independent components (ICs) in the EO and EC states. For cortical localization of generators the sLORETA equivalent source current density (5mm resolution) for each extracted IC was estimated using component topographies as input data (Pascual-Marqui, 2002). For each IC, its spectral power (left panel, EC vs. EO state, same scale for all ICs), scalp topography (middle panel), and 3D spatial maps (right panel) are illustrated.

4.2.3.4 Computation of Mean Regional Correlation Matrix and Graph Analysis

According to graph theory, within any chosen frequency information exchange may be measured by the (non-random) cross-correlation coefficients in the band-power spectrum, reflecting functional connectivity. Graph theory defines a graph as a set of nodes (in this study, ICs) and edges (connections between nodes) (Bullmore and Sporns, 2009; Rubinov and Sporns, 2010). Independent components were cross-correlated region by region according to their alpha-power across epochs during the full length of two resting time series, thus creating two square correlation matrices in the EC and EO states. This present study then performed one-sample t-tests (two-tailed) on the Fisher's r to Z -transformed (normally distributed) correlation coefficients to test whether they were significantly different from zero (Salvador, et al., 2005). To account for multiple comparisons, Bonferroni's correction was applied to eliminate false positive errors ($p=0.01/78$ connections = 0.000128), and statistically significant results with p -values < 0.000128 were accepted as significant. All graph analysis calculations were performed in Matlab 7.04 (Mathworks, MA). This study computed only weighted undirected graphs (Figure 4-3).

Figure 4-3. Resting-state functional connections revealed by EEG-alpha power spectra, compared between EC and EO states. (A) Significantly enhanced connections of DAN between frontal and parietal regions (anterior to posterior) are demonstrated during the EO state, compared to the EC state. The significantly enhanced connections in the EO state (75%) are depicted, more than those connections in the EC state (50%). (B) Statistically significant connections of DMN, DAN and visual networks are depicted by top 15%, 10%, 8% pairs of z scores, compared EO to EC state (two-tailed t-tests, Bonferroni corrected). Visual networks are enhanced in the parietal, occipital and occipitotemporal regions in the EO state. Increased connection strength between medial prefrontal cortex and precuneus regions, strong DMN in the EO state, is still noted in line with Yan, et al. (2009). The significantly decreased functional connectivity among left precentral, right precentral and cuneus from EC to EO state ensures that the improvement of intrinsic networks' activity does not come from the general improved signal-to-noise ratio between states.

4.2.3.5 Clustering of ICA components

The goal of IC clustering is to group together highly similar activity from multiple subjects to express the relevant components and their characteristic activity. Alpha desynchronisation upon visual input from EC to EO is generally considered to reflect activation of the entire cortex (Schurmann and Basar, 1999). Therefore, in order to extend the ICA analysis from single- to multi-component dynamics, the estimated frequency-domain components were clustered according to their mutual similarities in EEG-alpha power correlation coefficients in the frequency domain. A similar framework has been generated to summarize relevant components at the group level in fMRI studies (Esposito, et al., 2005; Jann, et al., 2009; Mantini, et al., 2007).

Components with similar alpha power spectra were then grouped into alpha power-associated clusters to examine the consistency of brain networks involved in the dynamic change from the EC to the EO state. In order to circumscribe the alpha power-associated components, agglomerative hierarchical cluster analysis was performed on the components' alpha power correlation coefficients with the statistical software package, SPSS (SPSS Inc, Chicago, USA). Each component measure was normalized by z-transformation prior to cluster analysis. Then, to assess mutual similarity, all pairs of components were compared by calculating the Pearson correlation of their alpha power, and classified into a hierarchical cluster tree according to their proximity (dendrogram). A dendrogram consists of mirrored C-shape lines, where the length of the mirrored C indicates the distance between objects (components). To calculate the distance between clusters, the Average Linkage method (Pearson correlation) was used. Then the "distance" matrix was calculated, namely the Euclidean distances in the original space of the components using multidimensional scaling (MDS) in order to fit an optimal configuration of groups of components in a 2-D space by minimizing the mismatch of the distances between the components in the MDS plot (Esposito, et al., 2005; Torgerson, 1952). From these components five groups (alpha power-associated clusters) were qualitatively selected by the similarity matrix, the dendrogram, the MDS plot, and visual inspection, as anatomically relevant areas across subjects, potentially depicting functionally related groups in the EC and EO resting states.

4.3 Results of Experiment Two

4.3.1 Aim 1: The application of group ICA to extract independent components (ICs) from epoch-wise alpha-band power.

4.3.1.1 Extract independent components

As illustrated in Figure 4-1, the results in each resting state were calculated using 1581 epochs obtained from 27 subjects (about 60 epochs in each condition). Infomax ICA was applied to extract independent components (ICs) from the concatenated EEG data of the 27 participants in both EC and EO states. All EEG data were decomposed into 13 spatially fixed and maximally-independent components. Only 6 artifact ICs were excluded (horizontal and vertical eye-movements \times 2, temporal muscle artifacts \times 2, and ICs with unspecific muscle artifacts \times 2). The findings of components from the concatenated EEG data in rest states were consistent with the first aim.

4.3.1.2 Epoch-wise alpha-band power

The schema of the pipeline steps from raw EEG to epoched-EEG recordings, and then to the constructed mean power spectra of valid components is illustrated in Figure 4-1. The following procedure of depicting EEG RSNs is analogous to approaches that have been adopted to calculate functional connectivity from BOLD signal strength in fMRI data (e.g., Buckner, et al. 2009). After spectral power analysis and estimating the cross-correlation of (alpha-band) EEG power between different ICs within subjects, a functional relationship between such source “nodes” can be

established (see the next results). The finding of cross-correlation of alpha-band EEG power supported the major hypothesis (aim) with the EEG-alpha correlation-based results indicating the robust formation of functionally and consistently linked networks in the brain during resting conditions (see the next results).

4.3.2 Aim 2: The application of sLORETA for cortical source localization of the ICs.

4.3.2.1 sLORETA and cortical source localisation.

In line with supporting the aim that the cortical locations of these components would be resolved into spatially well-defined “sources” (Pascual-Marqui, et al., 2002) sLORETA analysis was performed on scalp maps with selected ICA components to find the maximal densities of their cortical sources.

The cortical location and Brodmann area number of source locations of each IC are illustrated in Figure 4-2. The Talairach coordinates are further listed in Table 4-1. Indeed, all components in EC/EO states (Figure 4-2) exhibited a high repeatability across subjects with strong cortical source locations. Moreover, it is suggested that the consistency in the cortical localization of components in healthy individuals in both EC and EO states is due to the absence of experimental stimuli (for a review see Onton, et al., 2006), although some unsuccessfully represented artefact components may always be caused by participant confounds such as drowsiness, muscle activity, or eye-movements.

Table 4-1.

Coordinates of the main ICs of the circumscribed groups in the resting state, as shown in Fig. 4-2, the stereotactic space of Talairach and Tournoux (1988).

Group	x	y	z	Brodmann area	Anatomical region
Group F	5	63	-7	BA10	Superior frontal gyrus
	-40	45	25	BA10	Middle frontal gyrus
	40	45	25	BA10	Middle frontal gyrus
	-5	51	39	BA8	Medial frontal gyrus
Group C	-59	-3	32	BA6	Precentral gyrus
	50	-8	37	BA6	Precentral gyrus
Group P	-40	-47	39	BA40	Inferior parietal lobule
	-5	-60	63	BA7	Precuneus, parietal lobe
	40	-51	49	BA40	Inferior parietal lobule
Group OT	54	-62	22	BA39	Superior temporal gyrus
	-54	-62	22	BA39	Superior temporal gyrus
Group O	5	-87	14	BA18	Cuneus, occipital lobe
	-20	-96	14	BA19	Middle occipital gyrus

Brain regions are identified by putative Brodmann area (BA). Group F, C, P, OT, O and mean the circumscribed frontal, central, parietal, occipitotemporal, and occipital components

Importantly, these findings are critical for the further aims to investigate the EEG power-associated correlation of spatially localized sources and their functional connectivity in resting states, and to demonstrate the feasibility and potential of using spectral analysis of ICA components to estimate EEG resting-state connectivity by representing the spatially-segregated, unmixed EEG sources as functional nodes in electro-cortical networks.

4.3.3 Aim 3: The application of graph theory for functional connectivity estimation.

4.3.3.1 Graph theory

To recapitulate, using the cross-correlation of EEG-alpha band power between different components within subjects, graph theory defines a graph as a set of nodes (components) and edges (connections between nodes according to their cross-correlated alpha-power) (Bullmore and Sporns, 2009; Rubinov and Sporns, 2009). In addition, two square correlation matrices in the EC and EO states were created. Here, it was hypothesized that graph analysis would reveal EEG functional networks with fronto-parietal connectivity: a more medial network with nodes in the mPFC/precuneus which overlaps with the “default-mode network” (DMN), which has been found in several fMRI studies.

In accordance with the traditional graph theoretic approach, the square correlation matrix was used, to create a weighted undirected binary graph such that nodes (ICs) were either connected or not connected. The distribution of r-values suggested significantly enhanced connections in the EO state (75%) compared to those in the EC state (50%, in Figure 4-3A, and please refer to the section 4.2.3.4). For the EO to EC state contrast (two-tailed t-tests, Bonferroni corrected) the top 8% of all possible connections, were defined by Fisher's $z > 6.24$, $P < 0.01$ (e.g., Dosenbach, et al., 2007).

By lowering the graph definition threshold more potential connection patterns to other parts of the brain were revealed, indicating that the findings were sensitive to small changes in the graph-definition threshold. Hence for visualization purposes, the z-score threshold was made to vary from the top 8% to 15% of all interregional correlations (top 15% of all possible compared connections, $z > 4.35$, $P < 0.01$). Figures 4-3A and 4-3B illustrate the top 15% pairs of z-scores for the functional connections between cortical nodes. Furthermore, comparing functional connectivity value pairs revealed a significant between-condition difference within the midline connectivity of the DMN, specifically between medial prefrontal cortex (mPFC) and precuneus (medial frontal BA 8-precuneus BA7, $z > 4.35$, $P < 0.01$, Figure 4-3B).

4.3.3.2 Functional connectivity

In line with supporting the hypothesis with the application of graph theory for functional connectivity estimation, a more lateralized network comprised of the middle frontal gyrus and the inferior parietal lobule coincided with the “dorsal

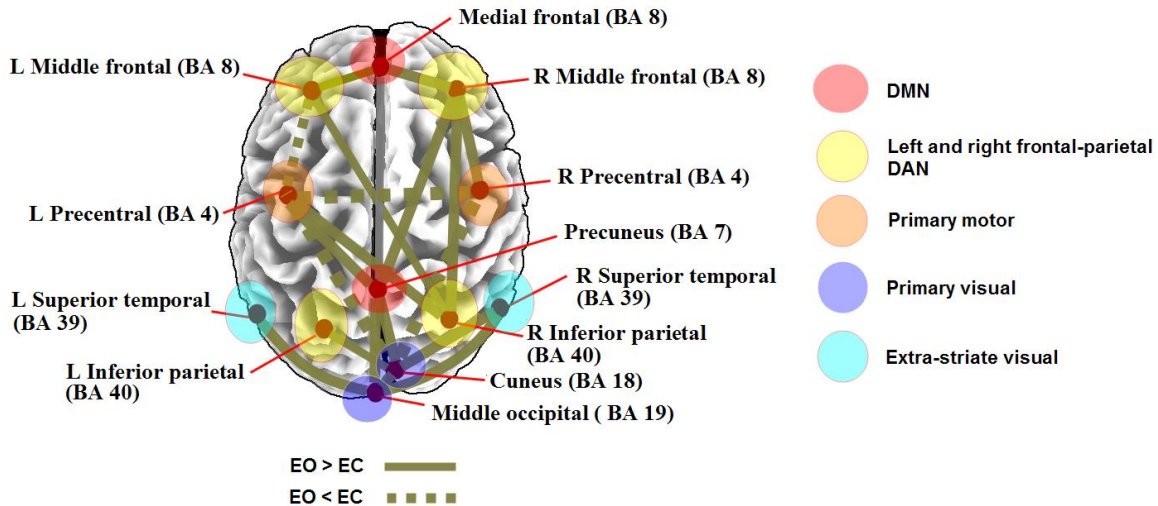
attention network” (DAN) during the EO compared to the EC state, which is hypothesized to result from engagement of the visual attention system in the EO state.

Significant correlations occurred (a) intra-hemispherically in the EO state superior to the EC state (right BA40-BA8, $z > 5.31$, $P < 0.01$; right BA4-BA8, $z > 6.24$, $P < 0.01$); (b) inter-hemispherically between homologous region pairs (precentral BA4, $z < -6.05$, $P < 0.01$, in the EO state inferior to the EC state); and (c) inter-hemispherically between nonhomologous regions (Left frontal BA8- right parietal BA40, $z > 4.35$, $P < 0.01$; left precentral BA4-right parietal BA40, $z > 5.31$, $P < 0.01$) in the EO state superior to the EC state. In other words, within-DAN correlations were generally greater than other cross-network correlations in the EO condition. Thus, DAN was always at least partially engaged and intra-hemispheric connectivities become as strong as inter-hemispheric ones when the eyes are open.

Figure 4-4 depicts the representation of these nodes within RSNs related in recent fMRI studies, including the primary sensorimotor network, the primary visual and extra-striate visual network, left and right lateralized networks consisting of superior parietal and superior frontal regions (DAN, reported as one single network) as well as the so-called default mode network (DMN) consisting of precuneus, medial frontal, and inferior parietal cortical regions.

Resting-state network nodes

Figure 4-4. Resting-state functional connections revealed by EEG-alpha power spectra, compared with



other fMRI-RSN reports. The illustrated cortical node locations and their membership(s) within previously identified resting-state networks with fMRI are presented together with the results of the current study (Beckmann, et al., 2005; Biswal, et al., 1995; Damoiseaux, et al., 2006; De Luca, et al., 2006; Salvador, et al., 2005; Van Den Heuvel and Hulshoff Pol, 2010).

4.3.4 Aim 4: circumscribing IC similarity measures via hierarchical cluster analysis.

4.3.4.1 Hierarchical cluster analysis

Hierarchical cluster analysis of cross-correlations between alpha power ICs identified a consistent set of five spatiotemporally distinct groups from 1581 epochs of 27 subjects in each resting condition, in line with resting state networks disclosed by fMRI studies (Toro, et al., 2008; Van Den Heuvel and Hulshoff Pol, 2010). Five

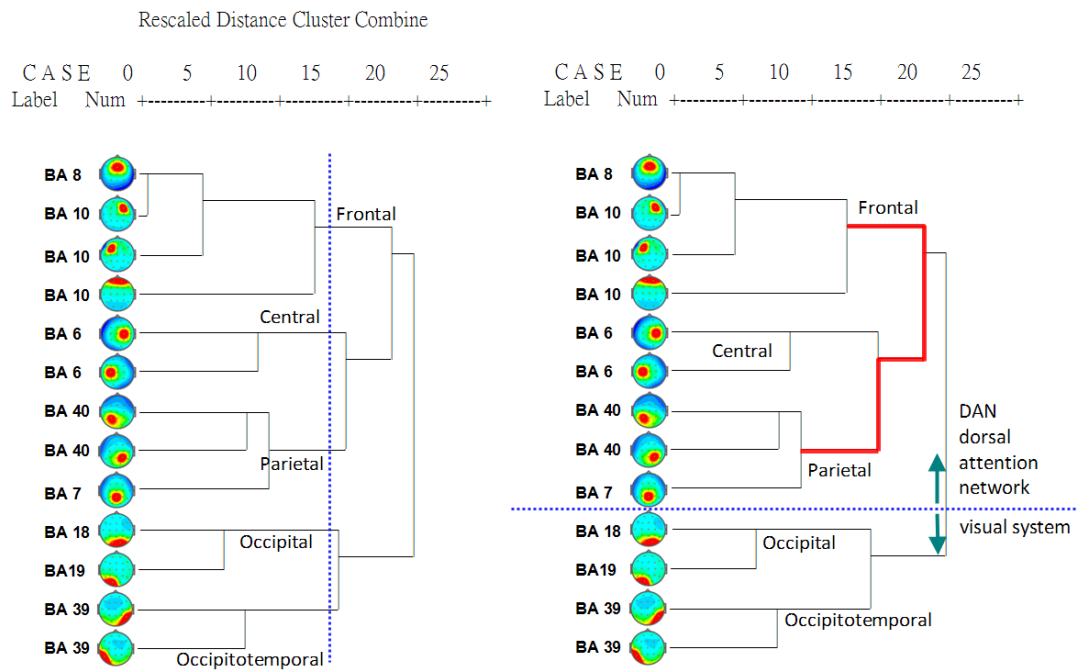
groups were then classified on the basis of coordinates in Talairach space and by regional anatomy (see also Figure 4-5 and Table 4-1):

1. Group F: a network involving predominantly lateral and middle prefrontal cortices, as well as an anterior pole of the prefrontal lobe.
2. Group C: a lateral network involving the precentral gyri.
3. Group P: a posterior-lateral and midline network involving primarily the parietal regions.
4. Group OT: a lateral network dominated by the bilateral middle temporal cortices in the occipitotemporal regions.
5. Group O: a posterior network characterized by involvement predominantly of the occipital cortex.

All of the spatial maps of groups mentioned above were found in both EC and EO states. As illustrated in Figure 4-4, the results are consistent with fMRI resting-state network (RSN) reports of regions showing functional connectivity patterns of the DMN across resting states (Fox, et al., 2005; Fransson, 2006; Yan, et al., 2009) and those with strong anatomical connectivities (Honey, et al., 2009; Honey, et al., 2007). In addition the DAN consisting of the frontal and parietal groups in the EO state, but not showing a strong connection between two groups in the EC state, is depicted by the dendrogram (Figure 4-5).

(A) EO resting state

Dendrogram using Average Linkage (Within Group)



(B) EC resting state

Dendrogram using Average Linkage (Within Group)

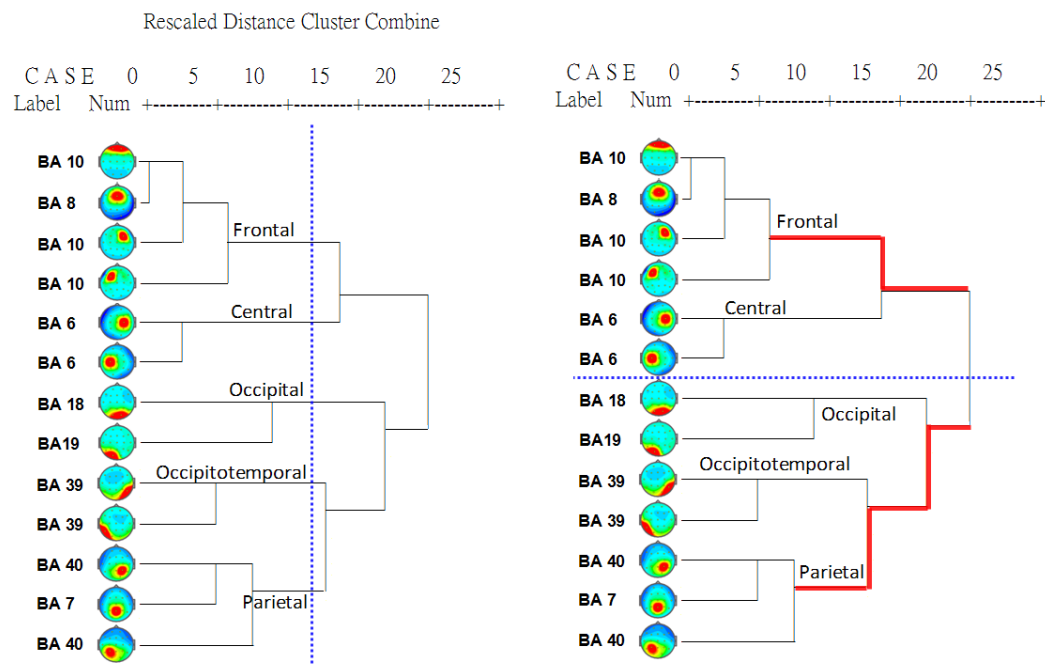


Figure 4-5. The Dendrogram was performed to illustrate the grouping of the 13 ICs, suggested by Pearson correlations (r values) of alpha power spectra (from 1581 epochs) among all ICs; (A) in the EO condition. (B) in the EC condition. (EC, eyes-closed; EO, eyes-open; BA, brain regions are identified by putative Brodmann area; vertical blue-dot lines, instruction lines to help illustrate 5 groups according to the dendrogram and similarity; horizontal blue-dot lines, lines to help differentiate the dorsal attention network from the visual system in both states; red lines, indicating the distance (relationship) between the frontal and parietal groups).

4.3.4.2 Circumscribing IC similarity.

It was hypothesised that several statistically clustered groups by the cross-correlation of (alpha-band) EEG power would be found and considered as a good signature of the resting EEG in both EC and EO states, indicating similarities between EC and EO resting states.

Importantly, the five grouped-ICs were explained by the correlation coefficient in each clustered group ($p < 0.01$, corrected) via the application of the hierarchical cluster analysis and the dendrogram plots, represented in Figure 4-5. This revealed distinct grouping patterns for components in both EC and EO states. Meanwhile, from the artefact-free resting EEG ICs pairwise alpha-power correlations (functional connection weights) were extracted to form a square correlation matrix in accordance with the traditional graph theoretical approach. Functional connectivity correlation matrix represents the cross-correlation of the groups, significant threshold (correlation coefficient r -value) and arranged by the similarity among components (Figure 4-6). The enhanced correlation of the Group F, C and P in the DAN is showed in the EO condition, but absent in the EC condition.

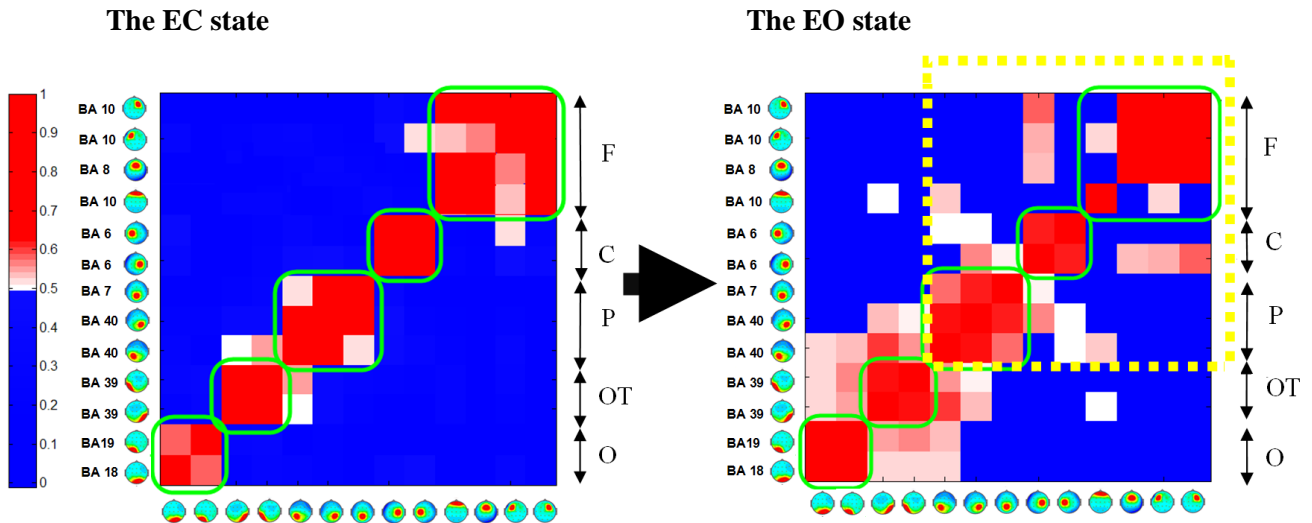


Figure 4-6. Illustrative functional connectivity correlation matrices from the EC to EO state. Functional connectivity correlation matrix (unweighted undirected network) represents the cross-correlation of the independent component (IC) pairs for alpha-band spectral power, significant threshold and arranged by the similarity among components. Green boxes depict circumscribed IC groups according to their significant functional connectivity ($r > 0.50$, $P < 0.01$ corrected), please refer to the dendrogram and MDS plots (Figures 5 and 7). The yellow box indicates enhanced correlation of the Group F, C and P in the dorsal attention network (DAN) during the EO condition. (F: frontal, C: central, P: parietal, OT: occipitotemporal, O: occipital; r: Pearson's correlation coefficient)

4.3.5 Aim 5: circumscribing IC similarity measures via multi-dimensional scaling (MDS).

4.3.5.1 Multi-dimensional scaling (MDS)

Again, the aim of applying the MDS analysis to demonstrate the feasibility of studying the emergence of increased proximity (mutual information) was supported, specifically the relationship between frontal and parietal clusters from EC to EO state.

The functional distances between IC groups within the two conditions were approximated by graphical distances in two-dimensional space, as depicted in Figure 4-7. MDS provides an interpretable map of the relations among all ICs whose similarity has been determined by Pearson correlations (r values) and whose IC group membership was revealed by dendrogram cluster analysis (Figure 4-5). Hence, co-representation of the clustered ICs group membership may aid in highlighting differences in functional association from EC to EO states on a network level. Here, functionally similar IC components, represented by topographical icons, were plotted in closer proximity within the MDS plot (Figure 4-7). This analysis confirms many of the organizational features already highlighted in Figure 4-5 with symmetrically paired regions in cortical space, reflecting anatomical relations and correlational similarity among the five principal IC groups (Table 4-1).

In accordance with some prior studies reporting stronger alpha-band similarities posteriorly rather than anteriorly in the EC condition (Barry, et al., 2007; Chorlian, et al., 2009), the components within Group F were more segregated than those in Group P and Group OT (Figure 4-7). Moreover, comparing the relationship between Groups

F and P in the EC vs. EO conditions, the closer distance between the two groups in the MDS plot in the EO state, also represents the tight coupling of the two groups within the DAN (e.g., Mantini, et al. 2007).

Euclidean distance model

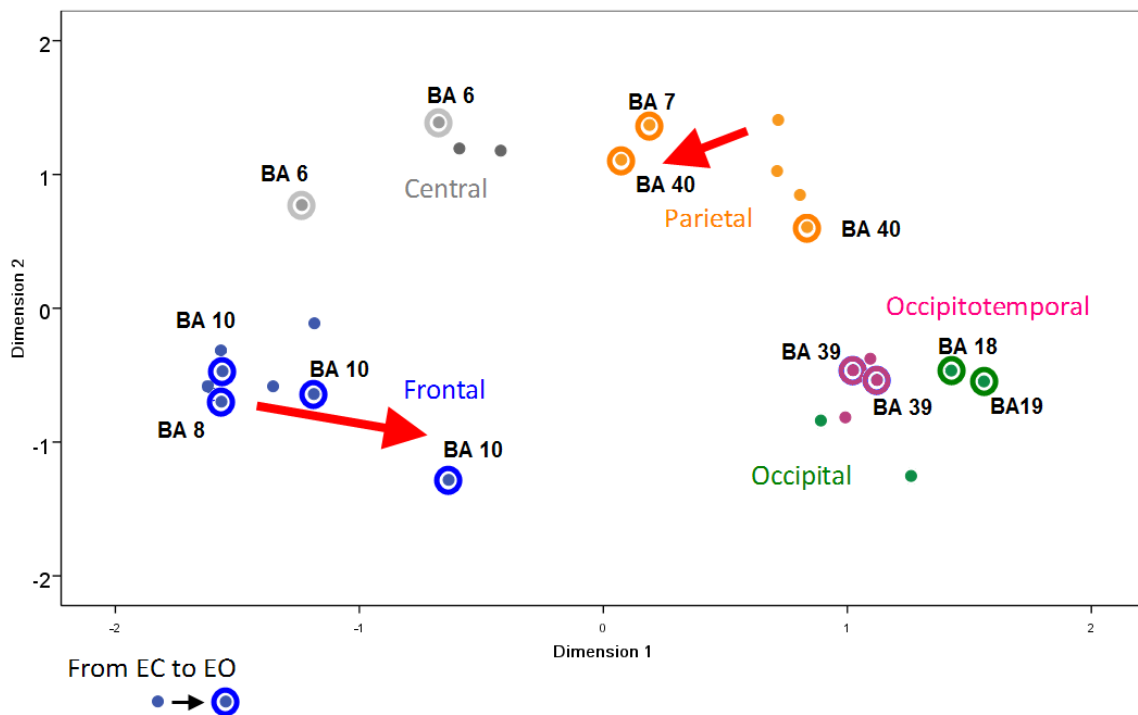


Figure 4-7. The Euclidean distances matrix of the 13 ICs in the resting state was visualized in a two-dimensional space using multidimensional scaling (MDS). Five groups (frontal, central, parietal, occipital and occipitotemporal groups) were presented by five different color according to the dendrogram and Pearson correlations of 13 ICs (please see also Figure 4-5). The distance between groups shows their relationship, and the connectivity of frontal and parietal groups is increased from EC to EO state, and the same as the visual system (occipital and occipitotemporal groups).

4.4 Discussion of Experiment Two

This is the first study to combine EEG-ICA and graph theory to investigate the EEG power-associated correlation of spatially localized sources and their functional connectivity from the eyes-closed to the eyes-open state. Although blind source separation (BSS) methods have been exploited to analyze resting-state EEG activity in healthy subjects (Chen, et al., 2008; Congedo, et al., 2009; Gomez-Herrero, et al., 2008; Scheeringa, et al., 2008) or those with clinical disorders (Chen, et al., 2009; De Vico Fallani, et al., 2007; Grin-Yatsenko, et al., 2010), the present study demonstrates the feasibility and potential of using spectral analysis of ICA components to estimate EEG resting-state connectivity by representing the spatially-segregated, unmixed EEG sources as functional nodes in electrocortical networks, in accordance with graph theory (Salvador, et al., 2005; Bullmore and Sporns, 2009; for a review, Stam and Reijneveld, 2007). EEG and MEG directly measure the electrophysiological activity of interest. Furthermore, with their high temporal resolution, these electrophysiological measures sample the rich temporal dynamics of neuronal population activity. These temporal dynamics entail neuronal oscillations that, with their specific frequencies, reflect the biophysical properties of different local and large-scale network interactions (Hipp, et al., 2012, and please refer to the section 4.1.1).

The first graph theoretical analysis of MEG data was reported by Stam (2004), who applied 126 MEG sensors on five healthy individuals and studied in a resting state with eyes closed. The resulting functional connectivity matrices were thresholded to create a set of undirected graphs depicting brain functional networks specific to each of the frequency bands, and they reported that graphs from the alpha

band (8–13 Hz) and beta band (13–30 Hz) had regular, lattice-like topology whereas graphs showed small-world properties (Stam, 2004; Bassett and Bullmore, 2006). An undirected graph simply summarizes symmetric relations (such as correlations) between nodes, whereas a directed graph additionally models the causal relationships between nodes (Bassett and Bullmore, 2006). Edges can also be categorized as weighted or unweighted, and in an unweighted graph, all the edges are assumed to indicate relations of equivalent strength between nodes, whereas a weighted graph can be used to differentiate stronger and weaker connections (Bassett and Bullmore, 2006). Most graph measures have only been defined for the simplest case of unweighted graphs. However in many cases weighted graphs may represent more accurate models of real networks (Stam and Reijneveld, 2007).

Stam and de Bruin (2004) also analyzed EEGs of 15 healthy subjects during eyes-closed and eyes-open no-task conditions. They applied detrended fluctuation analysis (DFA) of global synchronization time series showed that the scaling exponent as determined with DFA differed significantly for different frequency bands and conditions. Eye opening decreased the exponent, in particular in alpha and beta bands. In addition, the existence of scaling suggests that the underlying dynamics may display self-organized criticality, possibly representing a near-optimal state for information processing (Stam and de Bruin, 2004).

Compared with previous source-space attempts to provide a global pattern of electrocortical connectivity, the current experiment II with the multi-step approach effectively integrates information about functional interactions and provides a parsimonious procedure to describe the dynamic state-changes in EEG resting-state networks.

The principal findings indicate that there is an increase in functional connectivity from EC to EO states particularly between posterior and anterior regions, and that the electrophysiological network of the resting brain (without stimulation or task) is composed of 5 well-defined clusters of EEG activity: frontal, central, parietal, occipito-temporal, and occipital. Moreover, the alpha-band topographical maps and connectivity patterns are consistent with the estimated resting patterns from previous fMRI –RSN studies, such as the default-mode network (DMN) and dorsal attention network (DAN) (for a review see Van Den Heuvel and Hulshoff Pol, 2010; Toro, et al., 2008). In addition, the occipital group (O) and the occipitotemporal group (OT) are similar to the reported visual and extra-striate visual networks. Cortical localization of ICA components and connectivity maps showed that prefrontal and parietal areas are also functionally connected within and between hemispheres during the resting state (Van De Ven, et al., 2004). These connectivity maps showed an extremely high degree of consistency in spatial, temporal, and frequency parameters within and between subjects during rest. It may be beneficial to implement this EEG-ICA functional connectivity approach to clinical populations during resting-state baseline recordings.

Functional connectivity changes from EC to EO – compatible with hypotheses (aims) 1-3: the application of group ICA, sLORETA (for cortical source localisation), and graph theory (for functional connectivity) to investigate the difference between EC and EO resting states.

The salient electrophysiological clustered groups in the healthy EEG decomposed by the ICA method may disclose differences between EC and EO resting states. Inter-hemispheric connectivity varied both as a function of the resting state (from EC to EO) and cerebral areas. During the EC state, it is observed that alpha power-associated correlations of spatially localized sources conveyed a preferred inter-hemispheric direction (Figure 4-3A, the EC state). Alpha power-related association showed a more distinct posterior than anterior focus (e.g., Chorlian, et al., 2009). As the results of prior published fMRI-RSN studies revealed significant patterns of correlated spontaneous activity between homologous regions in opposite hemispheres (e.g., Fair, et al., 2008; Salvador, et al., 2005), the corpus callosum may be the major conduit for information transfer between the cerebral hemispheres (Innocenti, 1994; Rosas, et al., 2010). In addition, connectivity strength occurred more significantly between posterior regions of the left hemisphere (left temporo-parietal junction (TPJ), BAs 39/40) than between regions in the right hemisphere (Figure 4-3A). In line with traditional findings, increased communication within the left TPJ may be reflective of a lateralised language processing network (Hutsler and Galuske, 2003). The only other report of an intrinsically lateralized system is the left-lateralized language system, which includes Broca's and Wernike's areas (Hampson, et al., 2002). The presence of lateralization in resting activity is important because it suggests that hemispheric lateralization in function is not induced by task processing but is sculpted more fundamentally in the pattern of spontaneous activity (Fox, et al., 2006).

This feature of MEG power correlation occurs more frequently between regions of the same hemisphere than between regions in opposite hemispheres (de Pasquale et

al., 2010), indicating that spontaneous (not task-evoked) oscillations occur predominantly within one hemisphere and are only loosely coupled between hemispheres (MacDonald, et al., 1996).

While most cortical sources manifested inter-hemispheric connections in the EC state between bilateral homologous regions, in the EO state significant correlations occurred most frequently intra-hemispherically, demonstrated by the increased dynamic linkage between ipsilateral frontal and parietal regions (Figure 4-3A, the EO state). Here, the frontal sources (F) were localized to Brodmann areas (BA) 8 and 10 (medial, right and left middle frontal gyri), while the parietal sources (P) consisted of BA 7 and BA 40 (precuneus, right and left inferior parietal lobules).

Importantly, the dorsal attention network (DAN) and default-mode network (DMN) appeared to become more prominent in the EO state (Figure 4-3B, EO > EC). This observation is directly in line with reports of increased fMRI coupling between medial prefrontal cortex and precuneus (BA7) in the EO vs EC condition (Yan, et al., 2009), and multimodal associations between alpha-power fluctuations and DMN activity (Ben-Simon, et al., 2008; Jann, et al., 2009; Mantini, et al., 2007). Amongst others, these RSNs have been reported in the work by Biswal et al. (1995), Beckmann et al. (2005), De Luca et al. (2006), Damoiseaux et al. (2006), and Salvador et al. (2005) (Figure 4-4). Although these studies made use of different groups of subjects, methods (e.g., seed, ICA or clustering) and types of MR acquisition protocols, they coincide with the EEG-based results of the present study, indicating the robust formation of functionally and consistently linked networks in the brain during resting conditions.

Neurophysiological implications of the five functionally-clustered groups – compatible with hypothesis (aim) 4: the circumscribing IC similarity measures via hierarchical cluster analysis, from EC to EO state.

Although the RSN and DMN concepts have come from important fMRI BOLD evidence demonstrating consistent activation patterns across distinct brain regions (Greicius, et al., 2003; Raichle, et al., 2001), it is as yet unclear how these relate to the concurrent coupling and degree of neuronal activity (Debener, et al., 2006). In contrast, EEG has excellent temporal resolution and is a direct electrophysiological correlate of spontaneous and task-related neuronal activity. ICA has been extensively used for the analysis of electromagnetic brain signals (James and Hesse, 2005; Vigario and Oja, 2000), and provides a statistical approximation of maximally independent cortical sources. Several previous studies have also demonstrated the application of ICA to multi-channel EEG data for distinguishing artefacts and functional brain sources (e.g., Jung, et al., et al., 2000; Makeig, et al., 2004; Marco-Pallares, et al., 2005). Interestingly, about 20% of all grey matter neurons, non-pyramidal type, express metabolic activity well reflected in the BOLD signal, but not in the EEG (Broyd, et al., 2009). To solve the problem originating from a degree of incongruence between hemodynamic and electrophysiological signals, more recent research has tried combining different modalities, such as EEG-fMRI, to better understand which portions of BOLD activity are reflected in the EEG (Jann, et al., 2009; Mantini. et al., 2007). In addition regarding EEG-correlated fMRI and human alpha activity during eyes-closed rest, Lauf et al., (2003) concluded that the plausible functional interpretation of their result with demonstrating alpha power with maxima

over parietal and frontal cortices was that spontaneous fluctuations in attention, expressed in terms of both alpha power and frontoparietal activity.

Here the present study examined directly the spatial characteristics of the 5 hierarchically clustered groups based on the EEG alpha-band spectral power of each IC, with the aim of validating this approach in comparison with previous reports of EEG dynamics and fMRI default patterns.

An important question is whether these groups directly reflect anatomical connectivity. The alpha rhythm was selected, which is the most prominent EEG rhythm during the conscious resting state, as the basis of the ICA-based EEG RSNs cluster groups. In previous reports (Barry, et al., 2007; Barry, et al., 2005; Chen, et al., 2008) the distribution of scalp EEG power in relation to anatomical connectivity in the RSN was unresolved due to the masking of underlying source activity through volume conduction (Nunez and Srinivasan, 2006). Compared to blood-oxygenation level fMRI recordings, the combined ICA-based and components localised by sLORETA figures suggest an electrophysiological, and therefore neuronal, functional connectivity amongst cortical regions.

Visual versus parietal system.

The best example in this study is the separation of the dorsal parietal cluster (Group P, parietal clustered group in both EC and EO) from the rest of the visual system (Group O and Group OT, in Table 4-1 and Figure 4-5) (De Luca et al., 2006; Gusnard, et al., 2001; Mantini, et al., 2007). The visual system is organized into two parallel anatomical pathways—the dorsal (occipito-parietal) pathway related to spatial

vision and visually guided actions, and the ventral (occipito-temporal) pathway associated with identification of visual objects (Corbetta and Shulman, 2002; Sereno, et al., 2001). Interestingly here these three groups are shown to be separated by alpha power-associated clustered ICs, compared to similar results of correlations between EEG rhythms and fMRI RSNs reported by Mantini et al. in 2007, and a weak interaction between two EEG-alpha generators (precuneus and cuneus) found by Gomez-Herrero et al. (2008).

Frontal and parietal subdivisions.

Previous work had shown that the DMN can be divided into at least two sub-networks, with anterior and posterior (frontal and parietal) subdivisions (Damoiseaux, et al., 2006; Kiviniemi, et al., 2009). Compatible with this finding and based on cluster analyses of alpha power-associated ICs, the present study also demonstrated the divided parietal sub-network (Group P in Table 4-1 and Figure 4-5) and the frontal sub-network (Group F in Table 4-1 and Figure 4-5). Moreover, during EEG-fMRI coregistration, Mantini et al. (2007) observed that both the DMN and the dorsal attention network (DAN) were coupled in terms of EEG power. These two networks, DMN and DAN, are two of the most robust and well-studied RSNs that have been associated with task-negative and task-positive functions, respectively (Shulman, et al., 1997). Previous reports have suggested that default and attention networks show a very similar correlation with EEG-alpha band power (Laufs, et al. 2003a; Laufs, et al. 2003b). In particular, a study of the temporal dynamics of spontaneous MEG activity has also demonstrated strong correlations in the alpha-band in both the DAN and the DMN (de Pasquale, et al. 2010). The results of

the present study underline the prominence of the DMN and DAN particularly in the eyes open state, and the findings of relevant circumscribed regions are consistent with the idea that the DAN as well as the DMN appears to exhibit more functional coupling during the EO vs EC condition; the latter being characterised by increased connection strength between medial prefrontal cortex (MPFC) and precuneus (PCu) regions (Figure 4-3B and Figure 4-4), in line with Yan, et al. (2009).

Group interactions visualized with MDS – compatible with hypothesis (aim) 5: the circumscribing IC similarity measures via MDS, from EC to EO state.

The MDS method with a simple two-dimensional plot facilitates visualizing the similarity matrices of the alpha power-associated correlation coefficients and the proximity of the EEG components. During the shift from EC to EO, the frontal and parietal clusters appear to become closer in the EO state, suggesting more tightly coupled activities among the regions of both the DAN and DMN, potentially to increase contextual integration and evaluation of visual information (Hamzei, et al., 2002; Mason, et al., 2007; Yan, et al., 2009). Interestingly, the present study also discovered a number of symmetrical functional inter-hemispheric connections that were stronger than would be predicted by the anatomical distance between bilaterally homologous regions in both EC and EO states (Salvador, et al. 2005); for example the coupling between left and right occipito-temporal areas (BA 39; Figure 4-3A and Figure 4-5). Another example is the visual system in the MDS plot (Figure 4-7). The distance from the occipital group (Group O) to the parietal group (Group P) was

approximately similar to the distance from the occipital group to the occipitotemporal group (Group OT) in the EC state, suggesting a similar strength of coupling of the two parallel visual pathways in keeping with the relatively more inactivated visual cortex. In contrast, in EO with fixation (Figure 4-7), the components of occipital and occipitotemporal groups move together more closely, showing increased functional connectivity (Figure 4-3B), but not including the parietal group, suggesting a more pronounced coupling of the prevalent ventral pathway, activated during visual object detection (a cross presented in the EO fixation condition), rather than the dorsal pathway which is used during visually guided actions (e.g., Virji-Babul, et al., 2007). Together, this is consistent with reports that the oculomotor and attentional systems appear to be activated upon eyes opening, showing an “exteroceptive mental state”, as indicated by Marx et al (2003) in an fMRI study. On the other hand, it is evident that the sensorimotor group (Group C) remained closer to the occipital group in the EC state (Figure 4-5B and Figure 4-7), possibly reflecting stronger co-activation of the visual and somatosensory systems in the “interoceptive mental state” with eyes closed, and characterized by imagination and sensory activity (Marx, et al., 2003).

Methodological limitations

The principal drawback of the present study was the use of a limited number of electrodes. Although the results found with the ICA-sLORETA method seem encouraging, they could be refined with the use of a greater number of electrodes (given that the number of resolved ICs is numerically equal to the number of recording electrodes used). Notwithstanding, there is a limit to this reservation, since owing to volume conduction, high-density EEG channels close to each other tend to

be increasingly influenced by activity from similar brain regions. Nevertheless, volume conduction is a widely recognized problem that pervades almost all functional connectivity analyses of the EEG. In this case EEG signal changes occurring at one location may “spread” and be detected at another, and thus be (erroneously) interpreted as evidence of altered synchrony *between* locations (sensors). One proposed workaround has been to utilize strictly phase-lagged signals in connectivity analyses (given that volume conduction is instantaneous) (Stam, et al., 2007). However this may run the risk of “throwing the baby out with the bathwater”, as there is evidence that considerable cortico-cortical coupling occurs with zero phase-lag in the brain, independent of volume conduction (Gollo, et al., 2011; Roelfsema, et al., 1997). The present study has proposed an alternative approach in the frequency-domain which, although phase-insensitive, explicitly identifies the activity of independent “sources” (ICs) of EEG activity. Here, the time-course of each independent component is defined individually from the source-space matrix, thereby minimising the source “spread” which manifests itself in sensor-space. Moreover, since the ICA was performed before frequency-domain transformation, it would be comparatively easy to apply this processing pipeline to phase-sensitive measures (such as phase synchrony) by likewise taking advantage of maximal signal independence in ICA source-space. Importantly, ICA source-space is qualitatively different from the “source-space” of inverse-source localisation methods (minimum-norm or dipole-fitting methods). The latter may be envisaged as computing “virtually implanted electrodes”, which can detect distinct but potentially spatiotemporally overlapping activities within the same cortical location. ICA, in contrast, employs higher-order statistical methods to linearly unmixed the sources in the signal *a priori*, which may be followed by a subsequent step of cortical source

localisation (e.g., sLORETA). This may be additionally useful in view of the fact that volume conduction is expressed through linear summation of the signal.

Notwithstanding, the most obvious limitation may be in the EEG signal itself, which reflects widespread synchrony of pyramidal neurons in cortical grey matter, and is more problematic for resolving activity from deeper brain structures, as can be done with fMRI. Therefore more EEG-fMRI studies should be encouraged, with efforts also directed toward standardizing methods for ICA-based EEG networks and their differentiation between different behavioural states. For example, future studies could be carried out to determine the functional connectivity of theta or beta-power clustered ICs, compared with networks demonstrated by previous fMRI studies (e.g. Hipp, et al., 2012). Likewise, studies could be designed to reveal if connectivities within/between RSNs vary with pharmacological intake or relate to various brain-related pathologies, and to clarify whether observed clustered IC patterns are equivalent during altered brain states (e.g., for sleep, Tinguely, et al., 2006; for motion sickness, Chen, et al., 2009).

4.5 Summary

In conclusion, this work demonstrates the feasibility and addresses the potential of using a multi-step, data-driven approach for source-based EEG functional connectivity analysis, based on the combined advantages of ICA, source localization, graph theory, and multidimensional scaling in order to reveal the spatiotemporal dynamics of EEG changes from EC to EO states. These procedures suggest that cerebral processing underlying eyes-closed and eyes-open baseline consists of

statistically clustered groups within spatially and functionally-related cortical regions (frontal, central, parietal, occipitotemporal and occipital), clearly identified in 2D and 3D space. From EC to EO, and in line with previous fMRI studies, graph analyses and MDS plots indicated enhanced functional connectivity of frontal and parietal groups putatively subserved by the default-mode network (DMN) and dorsal attentional network (DAN), as well as the close correlation of occipitotemporal groups associated with processing in more ventral areas, in keeping with the dichotomy of the dorsal/ventral stream hypothesis of the visual information system (Hilgetag, et al., 2000; Salvador, et al., 2005). These results imply that two physiological mechanisms (ventral and dorsal attention networks) functionally co-exist during simple resting states such as eyes-open fixation.

Since resting-state connectivity has been shown to correlate with behavioural performance and cognitive measures in several published studies (for a review, see Greicius, 2008), EEG spectral-power based RSNs, resolved with ICA, may provide a useful measure with which to directly quantify neuronal functional connectivity during activational challenges and dysfunctional brain conditions. This approach could subsequently be applied to validate evidence of enhanced cognitive performance as shown in Exp I, for example, and the improved attention found after NF training with or without exogenous stimulation as will be outlined in Exp III.

The benefits of neurofeedback self-regulation combined with electroacupuncture stimulation in increasing perceptual sensitivity in attention performance and in enhancing the beta power of the attention network in the resting state.

5.1 Introduction

The third experiment investigates the behavioural and neurophysiological processes and the EEG dynamics that are commonly associated with the concept of ‘neuromodulation’, herein indicating the ability to appropriately adjust the nervous system for optimal function, within a given environmental context. The third experiment aims to provide a framework of converging evidence which logically supports the use of a variety of modern neuromodulation techniques – culminating in neurofeedback assisted by electroacustimulation – to promote or “optimize” the neurocognitive mechanisms responsible for the acquisition of improved levels of attention and enhanced perceptual sensitivity.

5.1.1 Neurofeedback

A special case of feedback modality, which differs from traditional peripheral measures, is used to tap directly into the self-regulation of brain activity, through biofeedback from the electroencephalogram (EEG); this is also called “neurofeedback”. Neurofeedback is a closed-loop design for a brain-computer

interface (BCI) that records, processes, and translates real-time information about a person's brain activity using a computer. A sensory description of the brain activity itself is fed-back to the user to enable learning and volitional control of the neural substrate(s) being represented (Fetz, 2007). Simply speaking, during neurofeedback, the signals from brain EEG recordings mirror neuronal activity that occurs within the brain, so a person can have effective control over this activity. Indeed, this process of self-regulation has been historically attributed to learning through “operant conditioning” (Barry, 2000; Fetz, 1969; Reynolds, 1975), while an alternative framework can be found in control theory (Marken, 2009). Interestingly, one report implicates the frontal lobe in the initial learning of neurofeedback control. According to the results, patients who have extended prefrontal lobe lesions but who intact intellectual function are unable to learn neurofeedback control (Lutzenberger, et al., 1980). Although the precise mechanisms of these learned control processes are still unclear, neurofeedback may be considered to operate within a fully closed loop, without the presence of external agents or forces, which indicates “endogenous” work, in and of itself, to produce changes in neuronal activity. Hence neurofeedback may differ functionally from pharmacological, electrical, or electromagnetic interventions, because the nervous system does not receive any extrinsic input or support. This provides evidence of an important feature of a biological brain – that of dynamic equilibrium and adaptation (Poulos and Cappell, 1991).

Crucially, current EEG, fMRI and even functional near-infrared spectroscopy (fNIRS) studies have investigated real-time information for the regulation of brain activity (e.g., deCharms, 2007; Delorme and Makeig, 2003; Holper, et al., 2010). These investigations have provided evidence of the successful regulation of select

cortical activities and oscillations, via neurofeedback and fMRI (Caria, et al., 2007; deCharms, 2007; Lee, et al., 2012; Ros, et al., 2012) and via neurofeedback and EEG (Birbaumer, et al., 2006; Delorme and Makeig, 2003), neurofeedback and fNIRS (Holper, et al., 2010) and there is even evidence of volitional control in neural signals, with particular emphasis on the activity of cortical neurons (Fetz, 2007).

The resultant neurofeedback results have helped to provide crucial evidence for the validation of the revised field of EEG-biofeedback and have provided a stimulus for a range of validation studies in the clinical domain, for performance enhancement and even educational fields. For example, neurofeedback training has been shown to enhance attention levels, memory, micro-surgical skills, intelligence and well-being in healthy participants (Egner and Gruzelier, 2001, 2004; Egner, et al., 2004; Hanslmayr, et al., 2005; Keizer, et al., 2010; Raymond, et al., 2005; Ros, et al., 2009; Vernon, et al., 2003). Some clinical controlled studies have even demonstrated efficacy for epilepsy (Kotchoubey, et al., 2001; Rockstroh, et al., 1993), attention deficit hyperactivity disorder (ADHD) (Arns, et al., 2009; Fuchs, et al., 2003) and autism (Kouijzer, et al., 2009). Studies of the underlying neural mechanisms have recently begun (Fetz, 2007; Ros, et al., 2010).

The close relationship between the basic modulation of the nervous system, the DA system and an associated improvement in attention, reward and learning has been extensively covered in the previous sections. In addition, the probable mechanism that describes the effect of NFT on the cerebral DA system is based on the premise that neurofeedback sessions which direct change in the EEG characteristics may cause up-regulation of dopaminergic tone, because of the observed augmentation of the spike activity of DA neurons (Kulichenko, et al. 2009). It is therefore pertinent to

review the literature pertaining to EEG oscillations, which is relevant to particular enhancement and inhibition of EEG rhythms due to neurofeedback that produces an improvement in attention levels (in the next sections). Most neurofeedback research to date has concentrated on the improvement of cognitive functions, such as attentional skills, and mood.

5.1.2 EEG-based neurofeedback

The idea of employing EEG frequency band activity as a feedback criterion in biofeedback training stems from the close association that has been observed between the speed of EEG frequencies and the arousal-state of the organism. For example, very slow brainwaves in the so-called “delta” range (0 – 4 Hz) are primarily found in the human EEG during deep sleep. Slightly faster “theta” waves (4 – 8 Hz), on the other hand, are often associated with drowsiness and early sleep stages, while the adjacent “alpha” frequency (8 – 12 Hz) is characteristic of a relaxed waking state. Faster frequencies in the “beta” (~ 12 – 30 Hz) and “gamma” ranges (> 30 Hz) are associated with the more aroused, active cortical processing that occurs during cognitive operations in the alert brain (Evans and Abarbanel, 1999). It is important to stress that this association between EEG rhythms and the arousal/activation state of the organism is but one of many functional correlates of EEG activity and, as such, constitutes only a convenient simplification. For instance, in different cognitive-behavioural contexts, any one particular rhythm may reflect many diverse functional states of neural communication and may be generated through different processes by various anatomical structures. One example is the use of EEG to study the dynamics of the decreased performance in an auditory vigilance task that is

associated with sleep deprivation, where there is a pattern of increased theta and decreased gamma for missed targets and an opposite pattern for accurate target detections (Makeig and Jung, 1996). Furthermore, many aspects of EEG generation and functional significance are very much the subject of active research and are not entirely understood, as yet. In some cases, learning to enhance particular EEG rhythms through neurofeedback may lead to unpredictable effects on the distributed cortical EEG spectrum. For example, training to raise theta (4-8 Hz) over alpha (8-12 Hz) amplitudes at parietal sites is associated with a post-training reduction of beta (14-18 Hz) activity in the prefrontal cortex, after repeated sessions (Egner, et al., 2004). It should therefore be borne in mind that EEG dynamics are complex and that the modulation of a self-organising system such as the brain cannot preclude the possibility of some unforeseen downstream effects. However, this phenomenon inevitably supports the theory that neurofeedback can shape the brain and its related networks.

Similarly to general learning processes, such as language acquisition, neurofeedback usually requires repeated individual ‘training’ sessions of about 30-60 minutes each, called neurofeedback training (NFT). NFT sessions can occur on separate days and over weeks or months, depending on the person’s response. There is a definite long-term effect after several NFT sessions. However the mechanism whereby a long-term effect on brain activity is induced by the apparent entrainment of the EEG is still unclear. Evidence derived from maintaining the cortex in a persistent oscillatory pattern shows that neurofeedback effectively “conditions” the neuronal circuits to produce this same pattern with a higher probability, sooner or later (Cho, et al., 2008; Gevensleben, et al., 2010; Gevensleben, et al., 2009a; Kouijzer, et al., 2009;

Sterman, et al., 1970). This may be theoretically explained by evidence from the enhanced magnitude of an EEG oscillation due to the increased number of neurons/synapses (Niedermeyer and Lopes da Silva, 1999). Furthermore, in Hebbian learning, ‘units that fire together, wire together’. Such long-term effects on brain activity may occur at the neural level, because of long-term potentiation (LTP) and long-term depression (LTD). Many features of Hebbian learning are relevant to a self-organizing nature, so Hebbian learning may be a biologically valid learning mechanism (Munakata and Pfaffly, 2004). Accordingly, during NFT with ‘synchronised’ oscillations, the population(s) of neurons which are coherently involved in generating an oscillatory pattern repeatedly strengthen these connections, making it easier for this population pattern to emerge once again in the future. By contrast, a prolonged desynchronised state weakens the correlated firing of their synapses and attenuates the connections for synchronisation, as verified, *in vivo*, by the desynchronising electrostimulation of hippocampal circuits (Tass, et al., 2009).

From the point of view of metabolic activity within the brain, the EEG neuronal patterns can be dynamically linked to the brain’s cortical metabolic activity, which have been measured using the association between EEG power and cerebral glucose metabolism, using 18-fluoro-deoxyglucose positron emission tomography (PET) (e.g., Oakes, et al., 2004). However, a limitation of the 18-fluoro-deoxyglucose tracer is that it requires a period of 20-30 min, so it is difficult to ensure that the subject remains in the same functional state. Therefore, the measurement of regional cerebral blood flow (rCBF) using $H_2^{15}O$ PET with shorter time frame (10–30 s) is widespread. The results of $H_2^{15}O$ PET examinations depend directly on the acuity of the cerebral state of activation during tracer injection (Schreckenberger, et al., 2004). The

quantitative evaluation of the correlation between rCBF changes and changes in EEG power induced by several motor tasks clarifies which brain regions are involved in the generation and suppression of the regional EEG rhythms (Oakes, et al., 2004). An EEG may therefore be considered to be a unique non-invasive indicator of coordinated synaptic activity across cortical networks (Niedermeyer and Da Silva, 2005).

The feasibility of modifying aspects of the EEG, by means of instrumental conditioning, has been demonstrated in animals by supplying a food reward for the production of a particular frequency component of the EEG. For example, it has been shown that cats (Sterman, et al., 1969; Wyrwicka, et al., 1962), as well as rhesus monkeys (Sterman, et al., 1978), can easily learn to enhance specific frequency components in their EEG. Sterman and colleagues also demonstrated for the first time that the natural entrainment of EEG rhythms via operant conditioning could alter the long-term susceptibility to drug-induced motor seizures (Sterman, et al., 1969). Around the same time, another important discovery was made: more than 40 years ago, Kamiya first demonstrated that control of human EEG rhythms can be successfully learned with the aid of a neurofeedback loop (Kamiya, 1968; Nowlis and Kamiya, 1970). In this case real-time information about alpha rhythm activity was provided to users via auditory feedback, to allow the enhancement of spontaneous alpha, reflecting relaxation and “letting go”.

Although research on neurofeedback has been protracted and mostly greeted with scepticism, these two historic discoveries still demonstrate the feasibility of human control of EEG rhythms, using neurofeedback and the long-term induction of brain plasticity by direct EEG entrainment, which indicates a new method of modulating

the brain function of both healthy and dysfunctional subjects. Moreover, the recent advent of larger controlled studies and meta-analyses promises to verify previous NFB research, especially in the treatment of epilepsy (Tan, et al., 2009), ADHD (Arns, et al., 2009) and autism (Coben, et al., 2010).

5.1.3 Neurofeedback and Attention

Most neurofeedback research to date has concentrated on improving cognitive functions, such as attentional and self-management capabilities (e.g., Arns, et al., 2009). A pioneering line of neurofeedback research was set in motion by Serman's operant conditioning experiments on cats (for a review, see Serman, 1996), mentioned in the previous section. In summary, in a series of studies by Serman and other associates (Roth, et al., 1967; Serman and Wyrwicka, 1967; Serman, et al., 1969; Wyrwicka and Serman, 1968), it was noted that during learned suppression of a previously conditioned response (via bar pressing for a food reward), a particular EEG rhythm emerged over the cats' sensorimotor cortex. This rhythm was characterized by a frequency of 12 – 20 Hz, with a spectral peak in the 12 – 14 Hz bin, and has been subsequently termed the "sensorimotor rhythm" (SMR) (Roth, et al., 1967). The researchers decided to study this distinct rhythm directly, attempting to instrumentally condition the cats to produce SMR by making the food reward contingent on increments in the SMR amplitude (Serman, et al., 1969; Wyrwicka and Serman, 1968). Cats learned EEG self-regulation with apparent ease; the behaviour associated with SMR production was again one of corporal immobility, with SMR bursts being regularly preceded by a drop in muscle tone.

Interestingly, this type of research was also successfully applied to cats and humans with epileptic motor seizure, wherein the incidence of seizures was lowered

significantly by SMR feedback training (for cat, see Serman and Friar, 1972); for the review, see (Serman and Egnor, 2006). A protocol for SMR-enhancement for the treatment of ADHD, based on the apparent calming effect of SMR training on the excitability of the sensorimotor system, was developed and applied by Lubar and co-workers (Lubar and Shouse, 1976; Lubar, et al., 1995). These researchers reported that the enhancement of SMR and the concurrent suppression of slow wave theta (4 – 8 Hz) activity resulted in improvements primarily facilitated by reduced motor hyperactivity (Lubar and Shouse, 1976; Shouse and Lubar, 1979). Subsequently, types of “beta” protocols that use the suppression of theta combined with increments in beta components have been conceptually developed to provide improvements in attentiveness (e.g., Lubar and Lubar, 1984).

The application of beta/SMR protocols to attention disorders has since evolved into probably the most widely employed application within the field of frequency band neurofeedback. Moreover recently, properly designed studies have identified a scientific basis for the training’s efficacy. Both Rossiter and LaVaque (Rossiter and LaVaque, 1995) and Fuchs and colleagues (Fuchs, et al., 2003) reported that beta/SMR neurofeedback leads to significant improvements in attention, in laboratory tests, as well as the observational ratings for children with ADHD, to levels comparable to those seen with stimulant medication. Monastra et al (2002) showed that an extensive course of beta band training, in addition to standard pharmacological treatment, leads to lasting benefits, even after medication has been suspended (Monastra, et al., 2002). Furthermore, in the only fMRI study to date which explored the after-effects of EEG neurofeedback, 15 children with ADHD received NFB for a total of 40 sessions, in three training sessions per-week (Levesque, et al., 2006).

Neuroimaging during the conflict condition on a Stroop task revealed a significant post-intervention upregulation of metabolic activity in the anterior cingulate cortex and in the basal ganglia (caudate nucleus and substantia nigra) compared to a control group. This is consistent with the NFB modulation of the regions that are anatomically responsible for attentional and motor processing.

These studies provide evidence for the potential of neurofeedback in enhancing attention function in clinical groups and offer the promise of possible applications for the improvement of attention abilities in healthy people. For example, Egner and Gruzelier investigated the potential long-term effect of NFB on the sustained attention of healthy subjects (Egner and Gruzelier, 2004), using an increased perceptual sensitivity index (which expresses a ratio of hit rate to false alarm rate, derived from signal detection theory), and reduced omission errors and variation in reaction times via a once-weekly NFB schedule with a total of 10 sessions of 15 min each. These findings validate a previous study which demonstrated EEG correlated improvements in attention variables and which constituted the first evidence of the enhancement of the cognitive performance of healthy volunteers through neurofeedback (Egner and Gruzelier, 2001). Of relevance to the current study, Egner and Gruzelier (2001) found that trained increments in SMR activity were related to a reduction in commission errors and improved perceptual sensitivity in the visual attention task, “Test Of Variables of Attention” (TOVA), which indicates that SMR training can enhance attentional processing and advance perceptual sensitivity in healthy participants (details in the following sections). In a subsequent study by Vernon et al. the same ‘SMR-Theta’ protocol was used for a total of eight sessions and was demonstrated to lead to a significant improvement in cued recall performance on a computerised

working memory task. The accuracy of focused attention processing was improved, to some extent, using a 2-sequence continuous performance task (Vernon, et al., 2003). In addition, an increase in theta amplitude was found in the control group whose EEG feedback was contingent on an increase in theta amplitude. No enhancement in attention was noted.

The direct link between SMR (or called low beta) rhythms and their impact on cognitive performance is still unclear. Invasive recordings of these rhythms in animals have identified a neurophysiological substrate that is responsible for their emergence; they seem to occur during the wakeful but immobile behaviour that is associated with the bursting of thalamic ventrobasal neurons, the hyper-polarization of relay cells and attenuation of the conduction of somatosensory information to the cortex (Serman, 1996). These findings support the notion that learned SMR enhancement is associated with increased excitability thresholds in sensorimotor cortical neurons. More recently, human studies have shown that low beta rhythms occur during the inhibition of a prepared movement in the Go-NoGo task, focused in the motor cortex around 300 ms after the presentation of the NoGo stimulus (Zhang, et al., 2008).

The suppression of the theta component is also an undeniably important issue for attention. The first study of NFB regulation that showed a decreased theta rhythm and its impact on the execution of a simulated radar monitoring task was published in the journal, *Science* (Beatty, et al., 1974). Based on previous observations that drowsiness and decreased arousal commonly result in elevations in theta power, the main findings of this research demonstrated that the theta suppression group had the highest rate of detection, which was furthermore associated with a decrease in the NFB theta ratio, during performance of a task. In other words, decreased vigilance was associated with

increased theta band activity in the EEG, but a suppression of theta activity, via operant methods, enhances monitoring efficiency and task performance. These results demonstrate a valid relationship between operant-regulated cortical activity and behaviour, in man (Beatty, et al., 1974).

A further application of NFT involved musicians, for whom a great amount of control over the brain processes that underlie shifts of attentional, and activational processes is very important. A few years ago, Professor Gruzelier's team embarked upon a program of experiments that applied clinical neurofeedback paradigms to performing musicians (Egner and Gruzelier, 2003; Gruzelier, 2009, 2012; Gruzelier, et al., 2006). The research group intended to establish the impact of these training paradigms for laboratory behavioural and neurophysiological measures of attention on the spectral topography of the EEG and, more importantly, on the quality of musical performance. Aside from producing professionally significant and replicable improvements in music performance, especially creativity in performance, it was specifically noted that beta band neurofeedback training is associated with increments in the P300 event-related brain potential (Egner and Gruzelier, 2001), which is thought to be a response to activity in the neuronal sources that are responsible for up-dating relevant information from environmental stimuli in the working memory (Donchin and Coles, 1988). This demonstrates the general feasibility of using neurofeedback to improve cognitive performance in healthy subjects. The greatest performance-enhancing effect of NFT has been noted for artists. For example, using dancers, Raymond and colleagues discovered positive effects for NFT on the "Timing" subscale of a dance performance (Raymond, et al., 2005). In one more example that used actors as subjects, Gruzelier and his team demonstrated

improvements after SMR training, including higher overall ratings for acting performance, a more rounded performance and, especially, an improvement in the creativity subscales of imaginative expression, conviction and characterisation (Gruzelier, et al., 2010).

5.1.4 The effect of neurofeedback and electrostimulation on attention and the EEG

The third experiment set out to replicate the results of the first experiment with the two acustimulation protocols for the effects found on attention with the addition of neurofeedback training. While alternating frequency stimulation was on average more successful than low frequency stimulation due to sustained effects post-stimulation, both protocols facilitated d-prime during stimulation. It was therefore of interest to replicate this differential effect and to determine whether it held when neurofeedback training was combined with stimulation or whether neurofeedback would assist in prolonging the effects of low frequency stimulation. Comparisons were made as before between alternating and low frequency stimulation, both with the addition of SMR/theta neurofeedback training. In addition there was a neurofeedback alone group and a mock neurofeedback group, four groups in all. While a fifth stimulation alone group would also have been of interest, for practical reasons of the testing load involved – over 340 lab sessions, and of recruitment, here 36 subjects with 9 in each group, the decision was made to prioritise the interest in replication, before excluding a low frequency group from further consideration.

5.1.5 Assessment of Neurofeedback Learning

In order to study the effect of NFT learning the following procedures were adopted for the EEG measures and the SMR/theta ratio in both baseline and feedback periods (e.g., Hoedlmoser, et al., 2008). Improvements in the parameters for late-conditioning (vs. early) are assessed as follows:

(a) an increase in SMR activity for the baseline (resting EEG recording period before NFT) and feedback periods (EEG recording period during NFT);

(b) a decrease in theta activity for the baseline and feedback periods;

(c) an increase in the SMR/theta ratio for the baseline and feedback periods due to (a) and (b), or due to either;

(d) an increase in relative SMR activity (mean SMR amplitude values during the feedback period divided by mean SMR amplitude values during the baseline period in each session);

(e) a decrease in the relative theta activity (mean theta amplitude values during the feedback period divided by the mean theta amplitude values during the baseline period in each session).

The relative SMR and relative theta values are provided to reduce the very significant and nonspecific effects of inter-subject variation in values for absolute amplitude during NFT, in order to evaluate the efficacy of SMR conditioning in manipulating EEG oscillations (SMR and theta rhythms) during NFT sessions. In addition, in order to compare the EEG during early vs. late instrumental conditioning, EEG data for each subject were averaged across sessions 2 to 4 (early conditioning)

and sessions 8 to 10 (late conditioning). The first instrumental conditioning session served as a familiarisation session and was excluded from the analyses.

As neurofeedback learning is progressive across sessions, then it will be manifested in each session's baseline tonic EEG recording following session 1, as well as during the training period of each session. (Hoedlmoser et al, 2008). Accordingly both baseline and feedback periods will be examined for evidence of learning. This will be done by comparing the average of sessions 8-10 with sessions 2-4.

Combining ICA with spectral power and cross-correlation analyses of the selected ICs, at the group-level, has shown the EEG to yield a rich source of information about the mechanisms of neural synchronization (Chen, et al., 2010; Grin-Yatsenko, et al., 2010). In an attempt at replication of Experiment II, the methods and results of Experiment III are used to explore ICA-derived EEG functional connectivity. It is anticipated that in all groups the same five statistically clustered regions will be shown with frontal, central, parietal occipitotemporal and occipital cortical loci and networks involving those loci.

In addition, it is anticipated that following learning/stimulation there will be enhanced relevant spectral power, but no increase in the number of cortical sources, an increase in power which will not be seen in the control group. This new approach enriches and complements previous electrophysiological studies of the spectral topography of NFT in the resting state. In line with the results of Egner et al (2004) it is anticipated that the effect of SMR training on attention networks will result in increased attention-related beta power in the frontal regions of the dorsal attention network. However, here this will be coupled with decreased theta power in the central

regions (pre- vs. post-training), and provide a further demonstration of the long-term effect of NFT on attention and vigilance.

5.1.6 Aims and hypotheses for Experiment Three

This study develops a plausible method to efficiently combine endogenous feedback with exogenous stimulation, to produce better changes than with NF alone. To the best of the authors' knowledge, the specific changes in EEG dynamics and enhanced attention performance that are produced by combining NFT with EA stimulation have not been studied.

Exp I shows that there is a greater enhancement of attention with alternating frequency electro-stimulation (AE) with low frequency electro-stimulation (LE), but both yield an improvement in attention (e.g., Chen, et al., 2006; Chen, et al., 2011). As this was a single demonstration in Experiment I, one aim was to replicate the possible differential effects on attention of the two stimulation protocols. Thus Exp III tests the hypotheses that SMR training in conjunction by EA has superior benefits for attention (enhanced perceptual sensitivity), as well as on the EEG measurements, than SMR training alone, but that alternating frequency electro-stimulation (AESMR group) results in a greater improvement than low frequency electro-stimulation (LES MR group). In addition, the group receiving the mock control, non-contingent SMR feedback (control group) is expected to demonstrate no change in perceptual sensitivity and EEG measurements and ratios, in the later conditioning sessions after mock NFT.

In line with these aims and the six hypotheses outlined below, the attention performance of each subject was estimated by analyzing the parameters of the TOVA task (pre- vs. post-training), in particular by using the errors of commission and omission to represent each subject's perceptual sensitivity (d'). Furthermore, the cognitive benefits from the change in the resting EEG dynamics after NFT are validated by the increased regional, attention-related spectral beta power of the frontal attention network.

Hypothesis 1: That there will be an improvement in perceptual sensitivity (d' -prime) post SMR training assisted by EA stimulation:

- a) Performance in replication of Experiment I this will be greater with alternating than lower frequency stimulation.
- b) This will be largely due to a reduction in errors of commission.
- c) Any improvement in attention assisted by EA will be greater with alternating than with lower frequency stimulation.
- d) The non-contingent SMR feedback (control group) will demonstrate less improvement in perceptual sensitivity after mock NFT.

In other words, SMR training assisted by AE (AESMR group) will result in an improved attention performance, with enhanced perceptual sensitivity that is superior to SMR training assisted by LE (LES MR group) and superior to the attentional results for SMR training alone (SMR group), which will be superior to the mock NFT group.

Hypothesis 2: As a demonstration of the long-term effect of NFT on EEG dynamics, SMR training assisted by EA stimulation will result in improved SMR and/or decreased theta activity in the *baseline* period of late compared with early conditioning sessions.

More specifically, compared to early-conditioning (2-4 sessions), there will be an improvement in EEG measurements for the baseline period of the late-conditioning (8-10 sessions), as follows: an increase in SMR amplitude, a decrease in theta amplitude and an increase in the SMR/theta ratio in the three experimental groups receiving actual NFT, relative to those for the mock control group that is not subject to NFT.

Regarding the magnitude of the effect, the groups will be ordered as for Hypothesis 1: AESMR > LESMR > SMR > controls.

Hypothesis 3: As for Hypothesis 2 but regarding the feedback period.

Hypothesis 4: As for hypotheses 2 and 3, but instead of examining absolute amplitudes of SMR and theta, relative amplitudes were examined.

Hypothesis 5: In replication of Experiment II, group ICA is used to extract ICs from the resting state EEG (pre- vs. post-training) with the prediction that NFT/EA will result in enhanced relevant spectral power but no increase in the number of cortical loci.

Hypothesis 6: the effect of SMR training on attention networks will result in increased attention-related beta power in the frontal regions of the dorsal attention network and decreased theta power in the central regions (pre- vs. post-training), demonstrating a long-term effect of NFT on attention and vigilance.

5.2 Methods of Experiment Three

5.2.1 Subjects

Subjects were excluded if they had any history of drug abuse, head injury, epilepsy, or psychopathology. Those participants who had any pain, cut, sore, or who were receiving psychoactive medication or who had skin problems on the hands, around the electroacustimulation sites, were omitted from the study. All participants had normal hearing and corrected-to-normal eyesight. Data were recorded for forty individuals, but four data sets were excluded from further analysis, because of excessive artefacts. Thirty-six healthy volunteers (20 women and 16 men aged from 18-30 years, 21.5 ± 2.5 years, all right-handed) from Goldsmiths, University of London, participated in the study. All participants had no prior experience of the neurofeedback training and electroacupuncture stimulation used in this study. Written consent was obtained from each subject, prior to the start of the experiment, in accordance with the Helsinki Declaration, and the study received approval from the College Research Ethics Committee.

5.2.2 Design

Participants (total 36 cases) were randomly allocated to one of four experimental groups. The four groups were of equal size (N=9), in order to optimize the statistical comparison of power. The method of randomly permuted blocks was used to ensure randomization, whilst also ensuring equal cell sizes: <http://www.randomization.com>. Group-AESMR consisted of 9 subjects, who each received 15-mins electroacupuncture stimulation (EA) with alternating low (5 Hz) and high (100 Hz) frequencies, before each SMR training session; Group-LES MR consisted of 9 subjects, who each received 15-mins EA with low frequency (5 Hz) stimulation before each SMR training session. The subjects in these two groups received EA on two acupoints on both hands (details in the chapter for Exp I, section 3.2.2). Group-SMR consisted of 9 subjects, who only received SMR training; Group-CONTROL consisted of 9 subjects, who received non-contingent SMR training and who acted as the control group for the study (details in the next paragraph).

In general, all subjects were required to attend the laboratory 12 times, for pre- and post-treatment and 10 SMR training sessions. Each subject completed all 10 sessions within 3-4 weeks (two or three times per week). Pre- and post-treatment sessions included measurement of resting EEG and the TOVA task (details in the next paragraph). The scheme for the experimental sessions is shown in Figure 5-1.

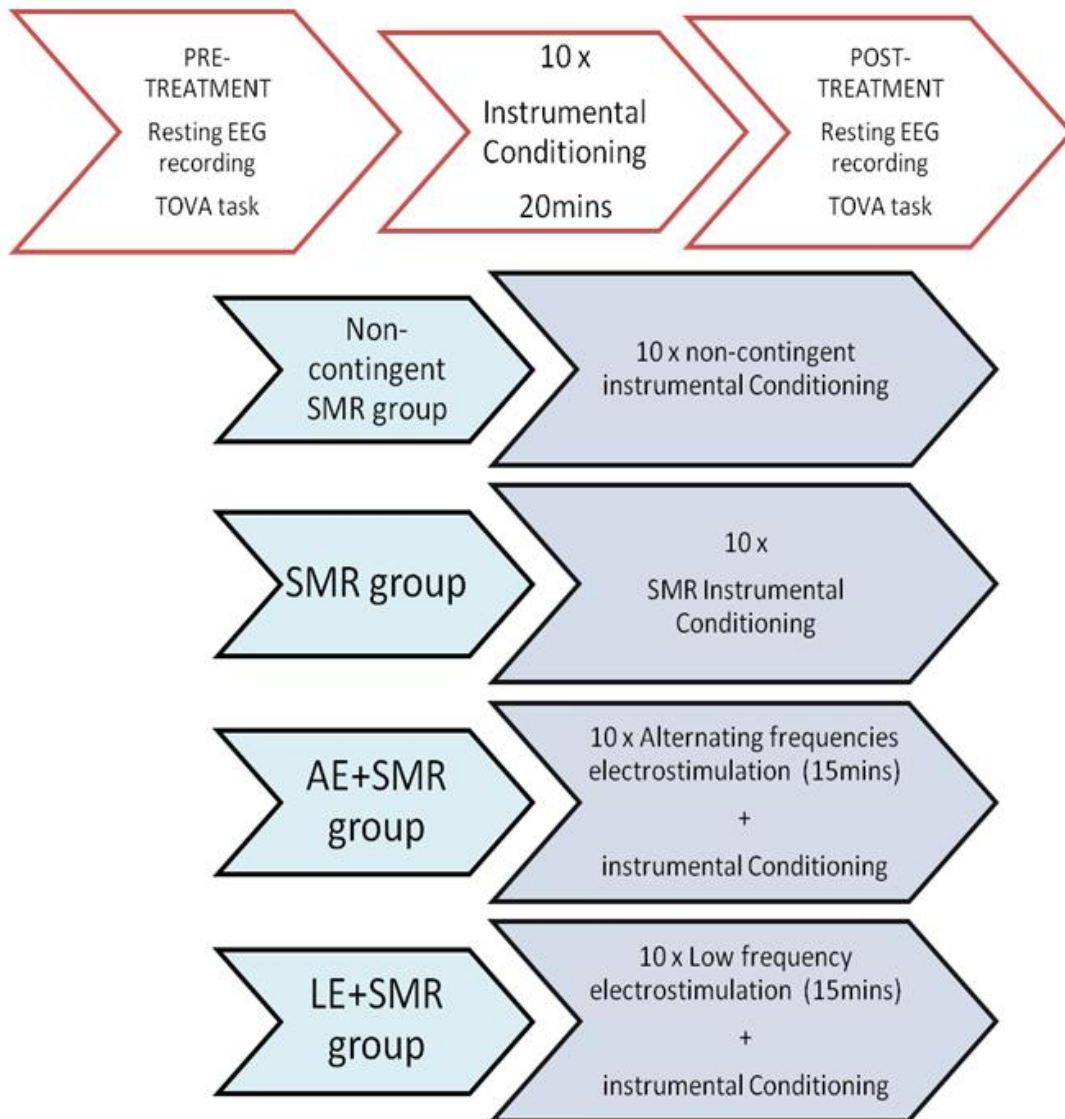


Figure 5-1. Subjects were required to attend the laboratory 12 times. The first visit (prior to pre-treatment) was used to measure resting EEG for EEG networks and to complete an entrance examination that contained a TOVA task, to assess attention performance. There then followed 10 instrumental conditioning sessions, within 3-4 weeks (two or three times per week). Post-treatment (the same procedure like pre-treatment) was conducted in one day, after the last conditioning session, in order to complete the study protocol.

5.2.3 Procedure

5.2.3.1 Instrumental Conditioning Procedure (SMR training) and associated apparatus

EEG signals were recorded using the BrainMaster System Type Atlantic I 4 × 4 Module with BrainMaster 3.0 software (BrainMaster Technologies, Oakwood Village, OH. <http://www.brainmaster.com>), which is capable of single channel EEG recording for SMR training. The EEG used for both recording and feedback was sampled at 256 Hz (by the A/D converter), using an Ag/Cl scalp electrode placed at Cz (the 10-20 international system) with a reference electrode on the right earlobe and the ground electrode placed on the left earlobe; impedance was maintained below 5k Ω with a common mode rejection of 120 μ V for eye or muscle artefacts. The ongoing EEG at site, Cz, was Fast Fourier Transformed (FFT), band-pass filtered (from 0.1 to 70 Hz) and notch filtered (50 Hz), in order to continuously measure the amplitude values for three bands (high beta (22–30 Hz), SMR (12–15 Hz) and theta (4–7 Hz) amplitudes, in microvolts, μ V, peak-to-peak), in accordance with the recommendations made in reports pertaining to SMR training (Gruzelier, et al., 2006; Ros, et al., 2009).

Each session used a standardized procedure and lasted for 26 minutes. After suitable adjustment of the electrodes, the subjects were instructed to relax, with their eyes open, for three minutes, while the EEG at rest was recorded, represented by a cross on the table. The baseline EEG measurement was conducted just before the start of feedback and after the end of training. The initial baseline was then used as the first criterion for the contingent feedback that followed. Subjects were subjected to ten 2-min blocks of the instrumental conditioning. The Brainmaster software filtered the EEG data stream into its component bandwidths, using third order Butterworth filters,

and immediately displayed both raw and filtered waveforms on the screen. In addition, the value of the band amplitude was transformed online into audiovisual feedback, displayed on a 15" computer monitor. All subjects were seated in a comfortable chair, about 1.5 m from the monitor. Operant contingencies were such that rewards ("points" in a game) were gained whenever the subject increased the SMR band amplitude without causing increases in the theta and high beta band amplitudes. Feedback thresholds were automatically reset, from block to block, to maintain a constant level of reinforcement. The reward SMR band threshold for the successive block was set at 0.6 times the mean amplitude for the previous 2 minutes, while the theta and high beta thresholds were respectively automatically set at 0.2 times and 0.1 times their average amplitude in the previous block.

In the "thermometer" game, for example, subjects were instructed to simply let the feedback process guide them into learning how to maximize their score. The height of three, differently coloured parallel bar graphs (blue, green, and yellow) was proportional and fluctuated according to the instant amplitude of the relevant scalp EEG rhythm (theta, SMR and high beta, respectively) in Figure 5-2. Participants were told to try to learn how to maintain the level of the green bar graph above a set threshold (a white line), for as long as possible and also to maintain the level of the blue bar graph below a threshold. Instantaneous audio feedback was provided by a sound which indicated that all designated thresholds were being met. The motion of the bars in this game could, therefore, be driven by each subject, depending on the degree of volitional control of the EEG amplitude and whether the reward threshold condition was met, for the award of points.

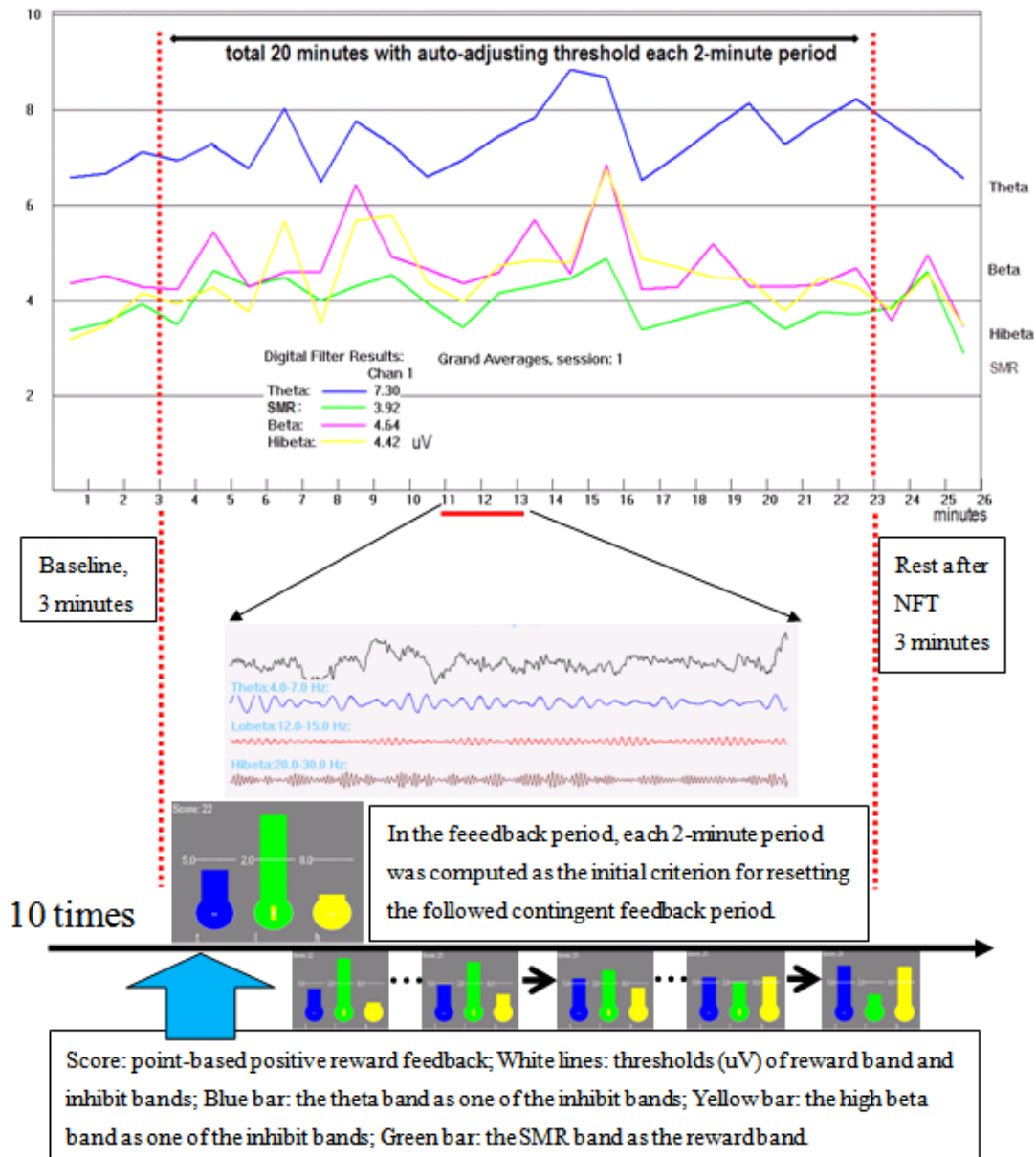


Figure 5-2. Schematic representation of one (2-minute) period within an instrumental conditioning session. A 3-minute “Baseline” value, measured before the visual feedback training session, was used to calculate the mean amplitude, which became the reference for the “Feedback period.” The audiovisual feedback in a point-based game was triggered by the EEG signals, when the appropriate criteria for three bands were met: the amplitude of the reward band exceeds its threshold when the amplitudes are below their thresholds in the inhibit bands. The reward band (SMR) “autothreshold” was set at 60 percent of time (during 2 minutes) over the threshold, while the theta and high beta inhibit autothresholds were set at 20 percent and 10 percent of time over the threshold, respectively.

5.2.3.2 The setting of non-contingent SMR training in the control group

The instrumental conditioning design for the control group (non-contingent SMR) consisted of a video film of pseudo-visual feedback. The three fluctuating bars simulated noise from the software and did not represent the subject's scalp EEG rhythm. In each of the 10 sessions, the subjects in the control group had to try to focus on the bars that represented simulated frequencies on the monitor, as the guidance of how to maximize their score in the experimental groups. All subjects remained blind to their group assignment and were not informed until the end of the study.

5.2.3.3 Visual Attention Task -- the Test of Variables of Attention (T.O.V.A)

A continuous performance test, the Test of Variables of Attention (T.O.V.A., Version 7.3, Universal Attention disorders Inc.), was used as the visual attention task for the pre-treatment assessment and, again, for the post-treatment assessment of an individual's performance, after 10 SMR sessions. The TOVA task was selected, because it was used as one of the outcome measures in previous EEG-biofeedback studies (e.g., Lubar, et al., 1995; Rossiter and LaVaque, 1995; Thompson and Thompson, 1998) and attention deficit disorder (ADD) studies (Forbes, 1998; Monastra et al., 2001; Monastra, et al., 2002).

The TOVA is a computerized, sustained visual attention performance test that requires the tracking of visual stimuli with a different response/non-response to target/non-target stimuli. The subject was instructed to press a button on a hand-held microswitch, as quickly as possible, each time they saw a simple visual stimulus (the target - a white square with a black square in its top half) presented on the computer

screen, but not to respond when they saw the non-target (the same white square with a black square in its bottom half), depicted in Figure 5-3. The stimuli were presented for 100 ms, every 2-sec, during a 3-min practice test, and during the 22.5 minutes of the full test. Four scores were recorded for (a) omission errors (inattention, the number of failures to respond to target stimuli), (b) commission errors (impulsiveness, the number of responses to non-target stimuli), (c) reaction time (mean response latency, in milliseconds) and (d) variability of reaction time (the consistency of response rate). The signal detection theory and details of the parameter “d-prime” (d') have been introduced in the section 3.2.3.4. Greenburg (1987) demonstrated that there is no practice effect and that subjects generally do worse, when tested again after a short period of rest, perhaps due to boredom (Greenberg, 1987; Thompson and Thompson, 1998).

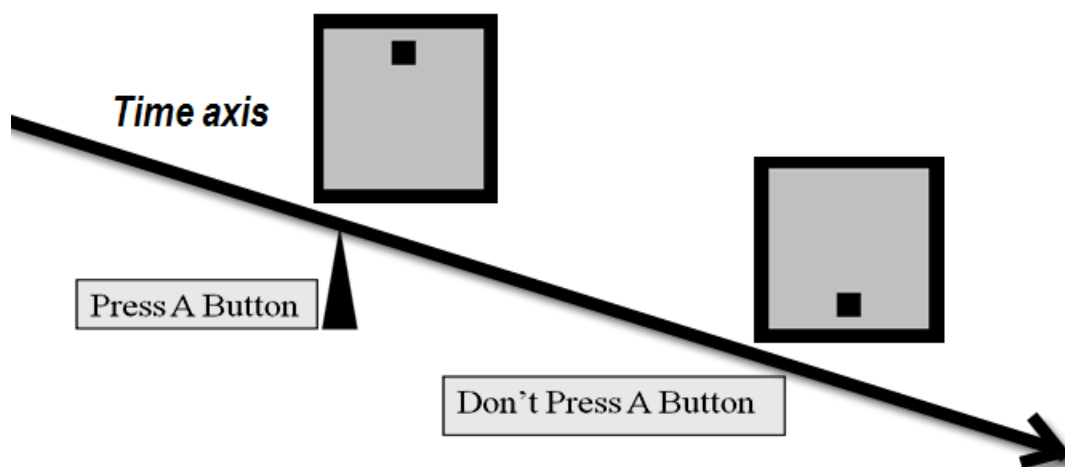


Figure 5-3. The scheme for the presentation of stimuli in the visual attention task, a TOVA task. The arrow and line represent the continuous time axis, during the task, in which two pictures are randomly shown on the screen. The first picture represents a “go” cue and the subject must press a button. The second picture represents a “nogo” cue and the subject must not respond.

5.2.4 Resting EEG recordings, pre-processing of EEG, Independent component (ICA) and spectral power analysis

Scalp resting EEG recordings and pre-processing of EEG have been presented in details, and please refer to the section 4.2.3.2.

The general scheme of this approach is illustrated in Figure 5-4. Artefact-free EEG epochs were concatenated into one file, which was then decomposed into independent brain sources using a group ICA procedure (details in the section 4.2.3.1).

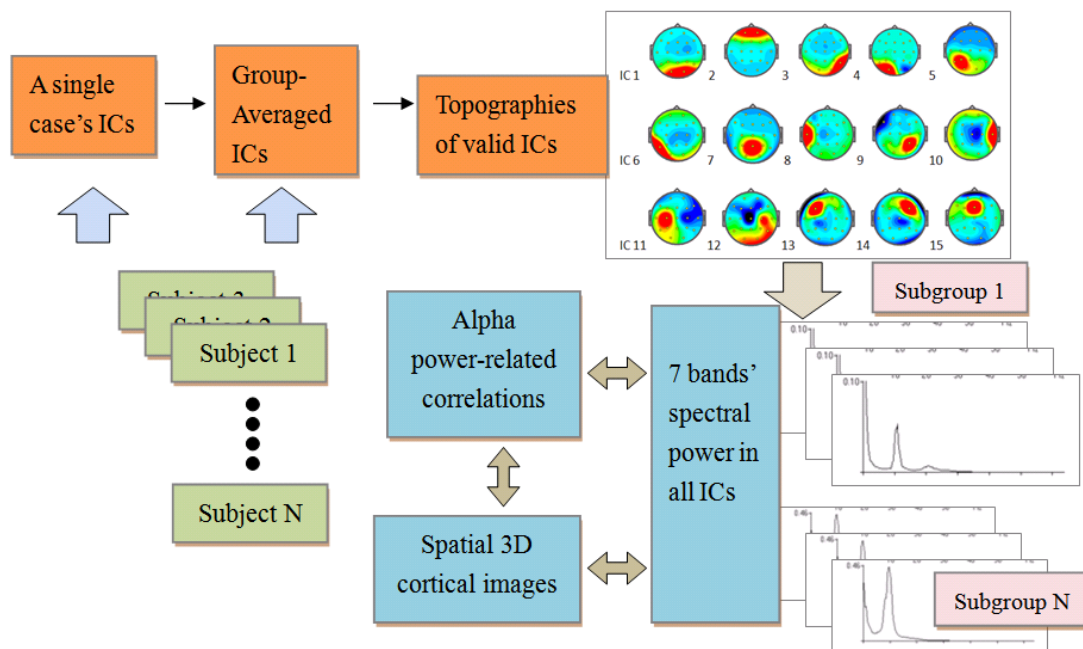
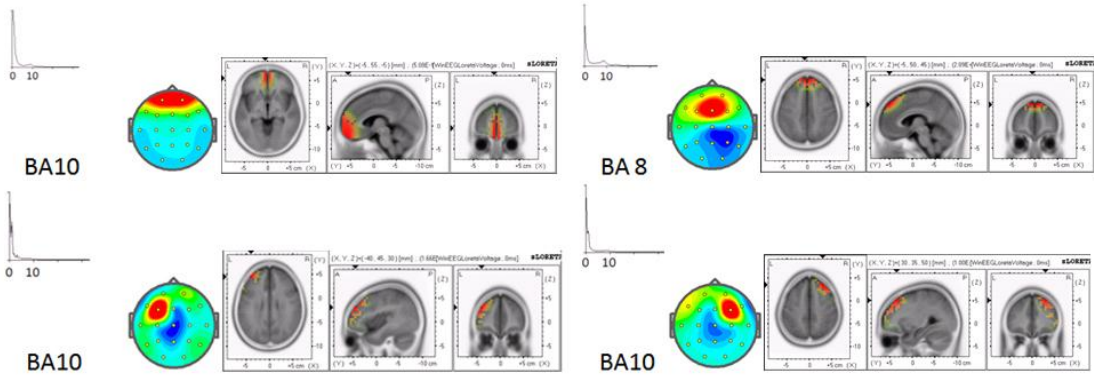


Figure 5-4. General schema for the approach used for the group-averaged ICs, alpha power-related correlations, spatial 3D cortical images and spectral powers in all independent components (ICs). The spectral power of seven bands in each IC is prepared for further spectral power analysis and cross-correlation matrices of alpha power. Then, alpha power-related correlations are performed on all ICs, to cluster all ICs into subgroups in their resting-states. The 3D cortical images are to help the reader visualize the related ICs within subgroups.

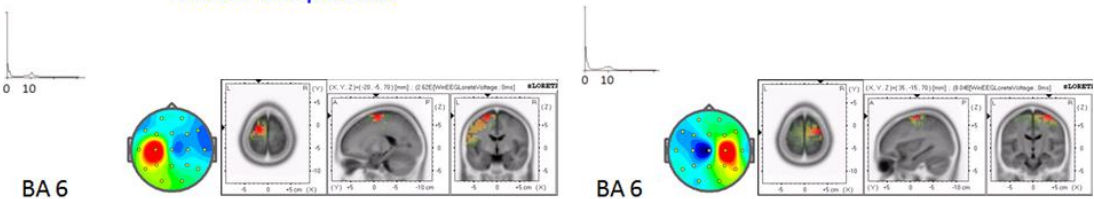
The time courses of the sources are assumed to be statistically independent. The alpha-band (8-12 Hz) power spectra of the back-reconstructed ICs for each subject were computed by short-time Fourier Transform (STFT), for each selected time interval (4-second epochs with a 50% overlapping Hanning time window). The predominant frequency of ICs is alpha (8-12 Hz) in almost 70%, or 9 out of 13 ICs. Finally, for the EC condition, this study cross-correlates the 13 IC alpha-band powers across all epochs and within subjects. The individual within-subject connectivity matrix r^2 values are then averaged across subjects to produce a group-wise matrix for each condition. Using this time-frequency analysis, this study demonstrates that several grouped components oscillate synchronously, with alpha-frequency dynamics, in the resting state (Figure 5-5).

EC

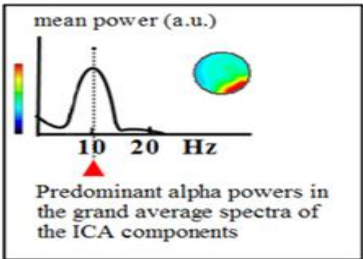
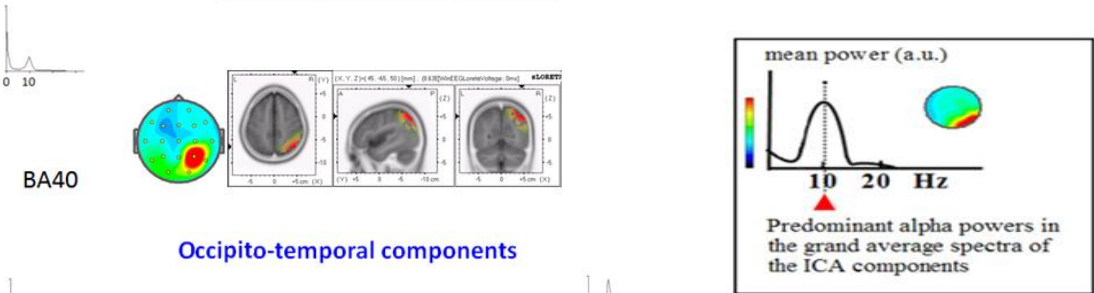
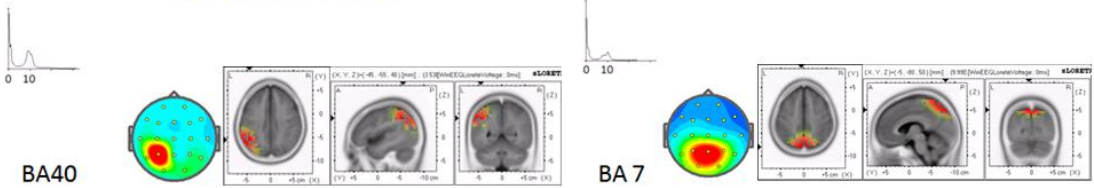
Frontal components



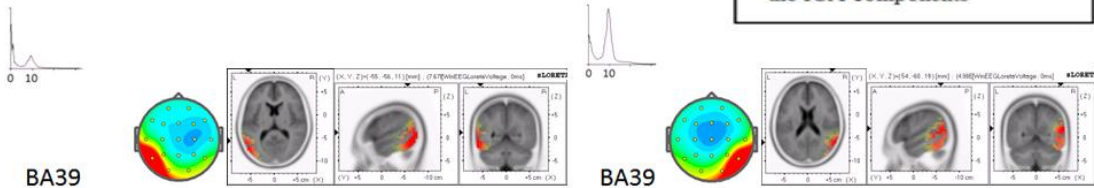
Central components



Parietal components



Occipito-temporal components



Occipital components

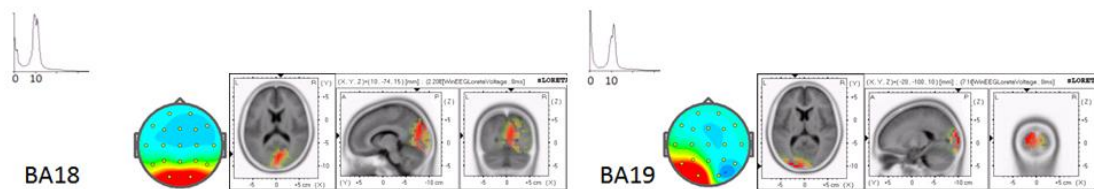


Figure 5-5. The topographies, power spectra and source localization for 13 independent components (ICs) in the EC state. For the cortical localization of generators, the component trajectories were used as input data to estimate the sLORETA equivalent source current density (5mm resolution) for each extracted IC (Pascual-Marqui, 2002). The spectral power (left panel, same scale for all ICs), scalp topography (middle panel) and 3D spatial maps (right panel) are illustrated for each IC.

5.2.5 Source localization analysis, Graph Analysis and Clustering of ICA components

sLORETA analysis was performed on the scalp maps with selected ICA components, to determine the maximal density of their cortical sources (Pascual-Marqui et al., 2002). sLORETA imaging provided source computations for the ICs, using software from the Key Institute for Brain-Mind Research, in Zurich, Switzerland (<http://www.uzh.ch/keyinst/loreta.htm>). sLORETA is an inverse solution technique that estimates the distribution of the electrical neuronal activity in three-dimensional space (Figure 5-5, more details in the chapter for Exp II, section 4.2.3.3). Independent components were cross-correlated, region-by-region, according to their alpha-power across epochs during the full length of two resting time series, thus creating two square correlation matrices in the EC and EO states (details in the chapter for Exp II, section 4.2.3.4). In order to circumscribe the components with similar alpha power, the components' alpha power correlation coefficients were subjected to agglomerative hierarchical cluster analysis, using the statistical software package, SPSS (SPSS Inc, Chicago, USA). Each component measure was normalized by z-transformation, prior to cluster analysis. To assess mutual similarity, all pairs of

components were compared by calculating the Pearson correlation of their alpha power. They were then classified into a hierarchical cluster tree, according to their proximity (details in the chapter for Exp II, section 4.2.3.5).

5.2.6 Statistical analysis

In general, statistical analyses were performed using SPSS 16.0 software (SPSS INC., Chicago, Illinois). Kolmogorov-Smirnov tests revealed that all of the data was normally distributed. Protocol group differences were examined for EEG outcome and behavioural measures and between-group differences in change scores, using repeated-measured ANOVAs (One-way ANOVA with post hoc comparisons), in order to identify any significant changes between pre- and post- NFT behavioural measurements, or between EEG outcome measurements, for early and late conditioning. The adjusted alpha was calculated using a Bonferroni adjustment, based on the number of planned multiple comparisons (i.e. $0.05/3 = 0.0167$).

5.2.6.1 Behavioural measurements of attention performance in 4 groups (hypothesis 1)

Behavioural measurements for the visual sustained attention TOVA task were d', commission errors, omission errors, response time and variation in response time (more details in the chapter for Exp I, section 3.2.3.4), which were also examined pre- and post-treatment, using a 2-way repeated measures ANOVA of the between-subject factor, GROUP, and the within-subject factor, PREPOST (GROUP \times PREPOST, 4 \times 2). A one-way ANOVA with post hoc comparisons was performed on the

between-group significant differences in change scores (pre- vs. post- NFT), compared to the control group. In addition, group differences in the initial scores of all TOVA measurements for the four groups in Exp III were subjected to a one-way ANOVA with post-hoc Tukey tests (for multiple comparisons), in order to identify significant differences in pre- NFT measurements.

5.2.6.2 EEG outcome measurements of SMR training in 4 groups (hypotheses 2-4)

The first SMR session was considered to be a practice session. IN order to compare the EEG outcome measurements for early and late SMR training, the recorded EEG-biofeedback data were averaged across sessions 2 to 4 to represent early conditioning and sessions 8 to 10 to represent late conditioning, for each subject. The four basic parameters included the mean SMR and theta amplitudes for the baseline period and the mean SMR and theta amplitudes for the feedback period. In addition, in order to reduce the effect of nonspecific effects on the absolute amplitude values for subjects during training sessions, the relative SMR and theta activity (feedback during each session divided by baseline before each session, $SMR_{Relative}$ and $theta_{Relative}$) were calculated. Two additional indices for SMR learning were then calculated for the baseline and feedback SMR/theta ratios (SMR divided by theta amplitude during the SMR baseline and the feedback intervals in each session). Eight dependent outcome measurements were designed to identify the significant changes after SMR training. In order to verify the hypothesis relating to an improvement in EEG measurements in the baseline period (hypothesis 2), the mean SMR and theta amplitudes in the baseline period and the baseline SMR/theta ratio were evaluated. In

order to verify the hypothesis relating to an improvement in EEG measurements in the feedback period (hypothesis 3), the mean SMR and theta amplitudes in the feedback period and the feedback SMR/theta ratio were evaluated. In order to verify the hypothesis relating to an improvement in the relative SMR and theta activity (hypothesis 4), the mean $SMR_{Relative}$ and $theta_{Relative}$ values were calculated.

In order to estimate the changes in these measurements for SMR training, from early to late conditioning, a 2-way repeated measures ANOVA was applied to the between-subject factor, GROUP, and the within-subject factor, CONDITION (early conditioning (sessions 2-4) vs. late conditioning (sessions 8-10), (GROUP \times CONDITION, 4 \times 2). A one-way ANOVA with post hoc comparisons was then performed on the significant differences in change scores between groups (early vs. late conditioning), compared to the control group. In addition, group differences in the initial scores of all of the EEG measurements for the four groups in Exp III were examined using a one-way ANOVA with post-hoc Tukey tests (for multiple comparisons), in order to identify significant differences in EEG measurements for early conditioning sessions.

5.3 Results of Experiment Three

5.3.1 Hypothesis 1: That there will be an improvement in perceptual sensitivity (d-prime) post SMR training assisted by EA stimulation.

5.3.1.1 Perceptual sensitivity

It was hypothesised that young adults would experience an improvement in perceptual sensitivity in the sustained attention task, due to SMR training alone, or SMR training assisted by EA stimulation, as indicated by an increase in d-prime. Correspondingly, with a significant reduction in commission and omission errors, the improvement in attention would be greater with SMR training assisted by EA stimulation (the AESMR and LESMR groups) than with SMR training alone (the SMR group) and there would be a greater improvement following SMR training alone than with non-contingent SMR feedback (control group), after stimulation.

The descriptive statistics for all pre- and post-treatment TOVA measurements for the four groups are presented in Table 5-1. The group differences in the initial scores for all TOVA variables (d', commission errors, omission errors, RT and RTV scores) were examined by one-way ANOVA with post-hoc Tukey tests (for multiple comparisons). This indicated no differences between groups, prior to treatment (Table 5-2). An ANOVA with repeated measures was used to determine the differential effects of the designed protocols on the variables (see Table 5-3). A one-way ANOVA with post hoc comparisons was used to assess differences in change scores between groups. This indicated significant changes in the variables, from pre- to post-treatment.

Table 5-1

Scores (mean \pm standard deviations) for the TOVA attention task measurements, pre- and post-treatment, of the four groups (AESMR, LESMR, SMR and control groups)

Groups	TOVA Measurements	Pre-treatment	Post-treatment
AESMR	Omission errors	0.44 \pm 0.73	0.11 \pm 0.33
	Commission errors	8.33 \pm 2.69	6.11 \pm 3.22
	d'	5.70 \pm 0.87	6.41 \pm 0.29
	RT (ms)	302.33 \pm 31.68	299.33 \pm 36.67
	RTV (ms)	70.11 \pm 16.51	67.78 \pm 21.18
LESMR	Omission errors	0.44 \pm 0.88	0.00 \pm 0.00
	Commission errors	6.11 \pm 5.35	5.56 \pm 3.88
	d'	6.04 \pm 0.88	6.65 \pm 0.77
	RT (ms)	316.44 \pm 41.80	324.78 \pm 52.91
	RTV (ms)	69.44 \pm 12.88	73.11 \pm 23.70
SMR	Omission errors	0.78 \pm 0.83	0.33 \pm 0.50
	Commission errors	7.44 \pm 4.07	4.78 \pm 3.38
	d'	5.43 \pm 0.77	6.35 \pm 0.52
	RT (ms)	324.78 \pm 47.19	307.89 \pm 48.98
	RTV (ms)	76.11 \pm 17.53	76.11 \pm 22.49
Control	Omission errors	0.78 \pm 1.30	0.56 \pm 0.53
	Commission errors	8.56 \pm 5.03	9.89 \pm 6.17
	d'	5.52 \pm 0.78	5.38 \pm 0.78
	RT (ms)	341.78 \pm 60.12	333.00 \pm 45.33
	RTV (ms)	86.33 \pm 29.39	84.89 \pm 23.14

AESMR - SMR training assisted by alternating frequency electro-stimulation; LESMR - SMR training assisted by low frequency electro-stimulation; SMR - sensorimotor rhythm training alone; control - the non-contingent SMR feedback; RT - response time; RTV - response time variability.

Table 5-2

Group differences in the initial scores of all TOVA variables, prior to treatment, examined by one-way ANOVA.

Measurements	Mean \pm SD				<i>F</i>	<i>p</i>
	AESMR	LES MR	SMR	Control		
Omission errors	0.44 \pm 0.73	0.44 \pm 0.88	0.78 \pm 0.83	0.78 \pm 1.30	0.36	0.78
Commission errors	8.33 \pm 2.69	6.11 \pm 5.35	7.44 \pm 4.07	8.56 \pm 5.03	0.57	0.64
<i>d'</i>	5.70 \pm 0.87	6.04 \pm 0.88	5.43 \pm 0.77	5.52 \pm 0.78	0.97	0.42
RT (ms)	302.33 \pm 31.68	316.44 \pm 41.80	324.78 \pm 47.19	341.78 \pm 60.12	1.14	0.35
RTV (ms)	70.11 \pm 16.51	69.44 \pm 12.88	76.11 \pm 17.53	86.33 \pm 29.39	1.37	0.27

Table 5-3

The effects of the factors, Group (AESMR, LESMR, SMR, and NON) and PrePost (pre- vs. post-) on the TOVA attention test measurements, examined using a two-way repeated measures ANOVA.

Measurements	Source	<i>df</i>	<i>F</i>	<i>P</i>
Omission errors	Group	3	1.33	0.28
	PrePost	1	7.80	0.01**
	Group × PrePost	3	0.16	0.92
Commission errors	Group	3	2.01	0.13
	PrePost	1	1.45	0.24
	Group × PrePost	3	3.08	0.041*
d' (d-prime)	Group	3	3.75	0.020*
	PrePost	1	14.59	0.0001**
	Group × PrePost	3	3.53	0.026*
RT (ms)	Group	3	1.10	0.36
	PrePost	1	0.77	0.39
	Group × PrePost	3	0.83	0.49
RTV (ms)	Group	3	1.19	0.33
	PrePost	1	0.00	0.99
	Group × PrePost	3	0.34	0.80

Group × PrePost indicates the interaction between group and PrePost (pre- and post-treatment); * indicates a significance level, $P < 0.05$ and ** indicates a significance level, $P < 0.01$, in accordance with the Bonferroni correction ($0.05/5=0.01$).

The results for post-treatment changes in the mean d' scores are shown in Figure 5-6. There was a significant effect for PrePost ($F(1,32) = 14.59, P = 0.0001$) and a Group \times PrePost interaction in d' ($F(3,32) = 3.53, P = 0.026$, see Table 5-3). As can be seen in Figure 5-6, there was a higher d' score, post treatment, in the experimental groups, compared to the control group. Post-hoc analysis with Bonferroni correction shows only a significant change in the d' score in the SMR ($p = 0.005$) group, compared to the control group (approaching significance in the AESMR group, $p = 0.019$; non-significance in the LESMR group, $p = 0.036$). Evidently, the control group with non-contingent SMR feedback experienced almost no improvement in perceptual sensitivity, after mock NFT. However, EA did not add significantly to the benefits of SMR training, based on the post-hoc analysis of the change in d' scores, post treatment (Figure 5-6), in fact there was a larger and more reliable improvement without it.

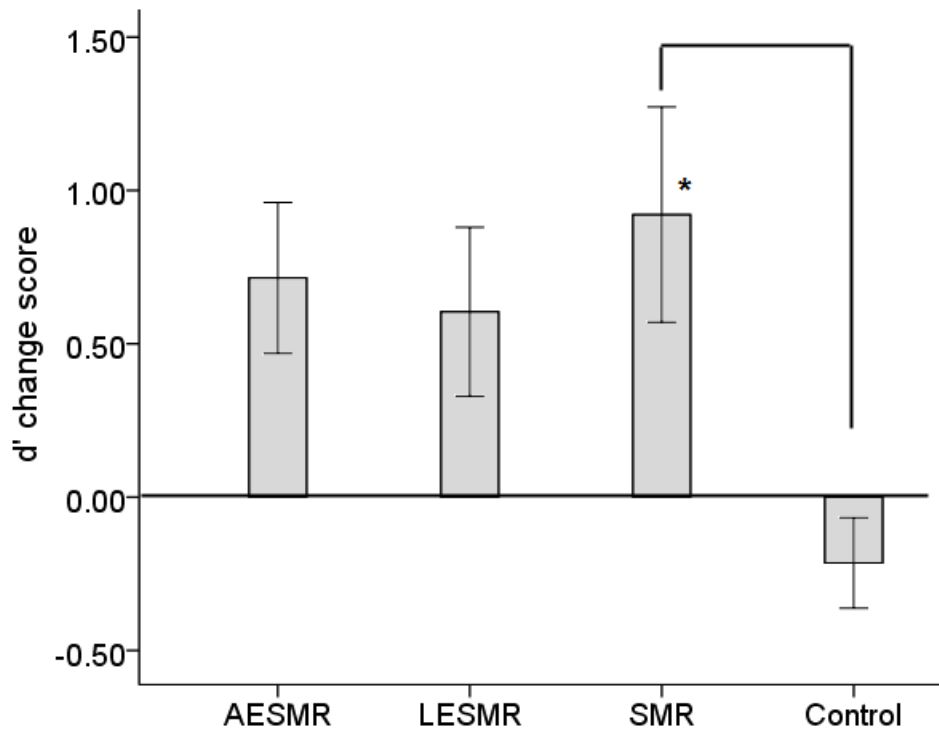


Figure 5-6. Post-treatment changes in the mean d' scores (\pm SE) of the TOVA task, for the AESMR, LESMR, SMR and control groups. * indicates a significance level, $P < 0.0167$ (Bonferroni corrected).

For the omission errors, shown in Table 5-1, there was only a significant PrePost effect ($F(1,32) = 7.84, P = 0.009$) and no significant Group \times PrePost interaction, which indicates a significant decrease in the level of omission errors, post treatment, for all groups (Tables 5-3). Post-hoc analysis showed no significant differences in the change in score for omission errors for the AESMR ($p = 0.58$), LESMR ($p = 0.58$) and SMR ($p = 0.58$) groups, compared to the control group.

However, for commission errors there was a significant Group \times PrePost interaction ($F(3,32) = 3.08$, $P = 0.041$, see Table 5-3). Post-hoc comparisons with Bonferroni correction revealed a significant change in the number of commission errors for the SMR ($p = 0.010$) group only, compared to the control group (approaching significance in the AESMR, $p = 0.018$; in the LESMR, $p = 0.12$, Figure 5-7). Thus, the significant effect of SMR training and the approaching significance of SMR training assisted by alternating frequency electro-stimulation on d' were found to be largely attributable to the reduction in the number of commission errors. The increased perceptual sensitivity, which was largely due to a reduction in the number of commission errors for both SMR and AESMR groups, is partially consistent with the hypothesis, but there was no advantage following EA. EA did not add to the benefits of SMR training significantly as based on examining post-hoc analysis with Bonferroni correction of d' change scores post treatment.

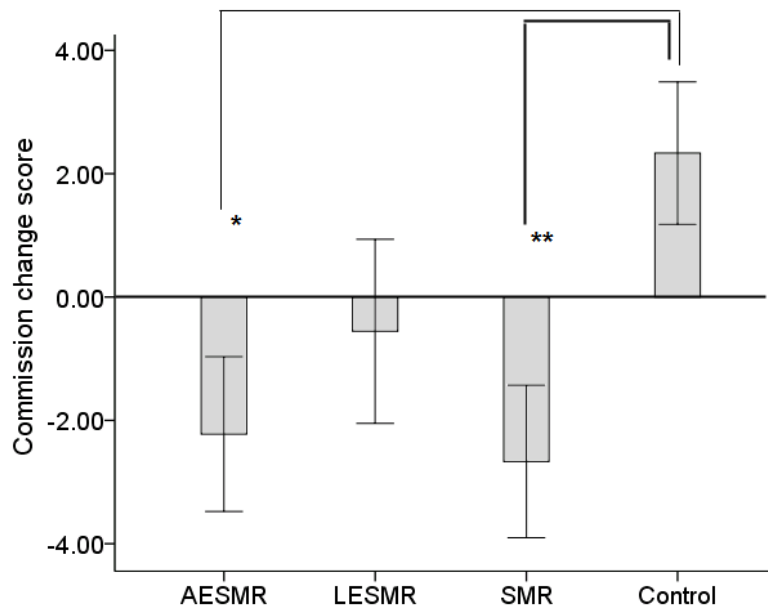


Figure 5-7. Post-treatment changes in the mean number of commission errors (\pm SE) for the TOVA task, for the AESMR, LESMR, SMR and control groups. * indicates a approaching significance level; ** indicates a significance level, $P < 0.0167$ (Bonferroni corrected).

Interestingly, the absence of a significant reduction in commission and omission errors for the LESMR group, post treatment, was unexpected. In contrast to the hypothesis, there was no significant reduction in the number of commission errors, but there was a significant improvement in the d' score for the LESMR group, compared to the mock group (Post-hoc comparisons in Figure 5-6). This indicates that a decrease in both the number of commission and omission errors contributes to an improvement in perceptual sensitivity (d'). Whether this special effect may be caused by the sustained stimulation effect found in Experiment I will be considered in the discussion section (see also section 3.3.1.2).

In regard to the response time (RT) measurements, there was no significant effect for Group (Table 5-3. $F(3,32) = 1.102$, $p = 0.363$) and PrePost ($F(1,32) = 0.766$, $p = 0.388$), nor was there a Group \times PrePost interaction ($F(3,32) = 0.833$, $p = 0.486$). In regard to the variation in response time, (RTV), there was no significant effect for Group ($F(3,32) = 1.192$, $p = 0.328$) and PrePost ($F(1,32) = 0.001$, $p = 0.990$), nor was there a Group \times PrePost interaction ($F(3,32) = 0.339$, $p = 0.797$).

In summary, the improvement in the changes in d' scores for the three non-control groups, post-treatment, are a consequence of the effect of SMR training and the increase in the number of commission errors, post-treatment, for the SMR group, support a plausible improvement in perceptual sensitivity in the sustained attention task, due to the significant increase in the change in d' scores and the number of commission errors (pre- vs. post- treatment), compared to the control group.

5.3.2 Hypothesis 2: As a demonstration of the long-term effect of NFT on EEG dynamics SMR training assisted by EA stimulation will result in improved SMR and/or decreased theta activity in the *baseline* period of late compared with early conditioning sessions.

5.3.2.1 EEG measurements in the baseline period

It was hypothesised that there would be improvement in the EEG measurements for the baseline period in late-conditioning (sessions 8-10), for the three experimental groups receiving actual SMR training, compared to the mock control group. With the increase in the SMR amplitude, the decrease in theta amplitude and the consequent

increase in the SMR/theta ratio, subjects in the AESMR and LESMR groups would experience the greatest improvement in these EEG measurements for the baseline period in late-conditioning sessions and the SMR group would demonstrate a greater improvement than the control group.

Hypothesis 2 mainly evaluates improved SMR and/or decreased theta activity in the baseline period for late-conditioning sessions, compared to that for early-conditioning sessions. Therefore, to ensure a clear presentation of EEG data, only the descriptive statistics for EEG measurements in the baseline period for early and late conditioning sessions are presented in Table 5-4, showing the means and standard deviations of average SMR amplitudes, theta amplitude and SMR/theta ratio for the four groups (S/T), in the baseline period for early SMR training sessions (2-4) and late SMR training sessions (8-10). Group differences in the initial scores for all EEG measurements for the four groups for SMR training early conditioning were examined using a one-way ANOVA with post-hoc Tukey tests (for multiple comparisons). No significant differences between groups in the early conditioning sessions (session 2-4) are indicated (Table 5-5).

However, marginally significant differences between groups in the initial baseline SMR and theta amplitudes must be explained (Baseline SMR, $F = 2.82$, $p = 0.06$; baseline theta, $F = 2.58$, $p = 0.07$, see Table 5-5). Post-hoc analysis with Bonferroni correction of the initial baseline SMR amplitudes showed non-significantly reduced SMR amplitudes in the AESMR group ($p = 0.041$), compared to the control group (in the LESMR group, $p = 0.37$; in the SMR group, $p = 0.82$). One possible reason for the decreased SMR amplitude in the AESMR group

is the effect of EA stimulation (before each NFT session) on the EEG, as elaborated in the Discussion.

Post-hoc analysis of the initial baseline theta amplitudes showed no significant reduction in theta amplitudes for the AESMR ($p = 0.29$), LESMR ($p = 0.45$) and SMR ($p = 0.95$) groups, compared to the control group (Table 5-5). Neither was there any significant difference in the theta amplitudes of the AESMR and SMR groups (post-hoc analysis, $p = 0.11$). The initial decrease in baseline theta amplitudes for the AESMR group may be caused by the effect of stimulation on the EEG. The decrease in theta power noted for the Fz and Cz areas, due to EA stimulation, was also noted by Andrew Chen et al. (Chen, et al., 2006). Further discussion will be presented in the discussion section.

Table 5-4

Averaged EEG measurements (mean amplitudes \pm standard deviations) of SMR training in the baseline period of early (training sessions 2-4) and late (training sessions 8-10) conditioning, in the four groups (AESMR, LESMR, SMR and control)

Groups	EEG Measurements	Early	Late
		Conditioning	Conditioning
AESMR	Baseline SMR	3.04 ± 0.37	3.05 ± 0.32
	Baseline theta	7.13 ± 1.92	6.26 ± 1.01
	Baseline S/T	0.45 ± 0.11	0.50 ± 0.09
.....			
LESMR	Baseline SMR	3.50 ± 0.76	3.55 ± 0.63
	Baseline theta	7.38 ± 1.49	7.10 ± 1.55
	Baseline S/T	0.48 ± 0.05	0.51 ± 0.06
.....			
SMR	Baseline SMR	3.80 ± 0.99	3.66 ± 0.92
	Baseline theta	9.00 ± 1.57	8.08 ± 1.42
	Baseline S/T	0.43 ± 0.13	0.46 ± 0.13
.....			
Control	Baseline SMR	4.54 ± 1.02	4.14 ± 1.08
	Baseline theta	8.58 ± 1.76	8.65 ± 1.68
	Baseline S/T	0.48 ± 0.07	0.48 ± 0.07

S/T is the ratio of SMR and theta amplitudes

Table 5-5

Group differences in the initial scores of all EEG measurements during SMR training for early conditioning in the four groups, examined by one-way ANOVA.

Measurements	Mean \pm SD				<i>F</i>	<i>p</i>
	AESMR	LES MR	SMR	Control		
Baseline SMR	3.04 \pm 0.37	3.50 \pm 0.76	3.80 \pm 0.99	4.14 \pm 1.02	2.82	0.06
Baseline theta	7.13 \pm 1.92	7.38 \pm 1.49	9.00 \pm 1.57	8.58 \pm 1.76	2.58	0.07
Baseline S/T	0.45 \pm 0.11	0.48 \pm 0.05	0.43 \pm 0.13	0.48 \pm 0.07	0.59	0.63
Feedback SMR	3.16 \pm 0.39	3.55 \pm 0.85	3.63 \pm 0.92	4.09 \pm 1.02	1.93	0.15
Feedback theta	7.50 \pm 1.30	8.27 \pm 1.85	8.96 \pm 1.41	9.51 \pm 2.32	2.17	0.11
Feedback S/T	0.43 \pm 0.08	0.43 \pm 0.05	0.41 \pm 0.09	0.44 \pm 0.07	0.31	0.82
SMR _{Relative}	1.04 \pm 0.10	1.01 \pm 0.06	0.96 \pm 0.06	0.99 \pm 0.08	1.83	0.16
Theta _{Relative}	1.08 \pm 0.14	1.12 \pm 0.06	1.00 \pm 0.12	1.10 \pm 0.08	2.01	0.13

There was a significant effect for Condition ($F(1,32) = 7.36, P = 0.011$), but no Group \times Condition interaction ($F(3,32) = 1.49, P = 0.24$), on the baseline S/T ratio (Table 5-6). Mean results indicate an increase in S/T ratios for all groups. While no omnibus Group \times Condition effects were detected, the predicted increase in the ratio of the baseline S/T measurement in the AESMR group was only exploratory, due to marginal increase in the baseline S/T ratio for the AESMR group only (uncorrected), compared to the control group (post-hoc and contrast analysis for the AESMR, $t_{32} = 2.04, p = 0.05$; LESMR, $t_{32} = 1.45, p = 0.16$; SMR, $t_{32} = 1.37, p = 0.18$), as shown in Figure 5-8.

There was no evidence of a tonic increase in session baselines in the S/T ratio when comparing early with late conditioning sessions, in line with a possible successive carryover of learning manifested in the resting session-baseline EEG.

Table 5-6

The effects of Group (AESMR, LESMR, SMR and control) and Conditioning (early vs. late) on EEG measurements related to SMR training in the baseline period, ANOVA with repeated measures.

Period	Rhythms	Source	<i>df</i>	<i>F</i>	<i>P</i>
Baseline	S/T ratio	Group	3	0.43	0.73
		Condition	1	7.36	0.011*
		Group × Condition	3	1.49	0.24
	SMR	Group	3	2.83	0.06
		Condition	1	0.17	0.68
		Group × Condition	3	0.97	0.42
	Theta	Group	3	3.74	0.021*
		Condition	1	8.52	0.006**
		Group × Condition	3	1.99	0.14

Group × Condition indicates the interaction between group and conditioning (early and late); * indicates a significance level, $P < 0.05$ and ** indicates a significance level, $P < 0.01$, in accordance with the Bonferroni correction.

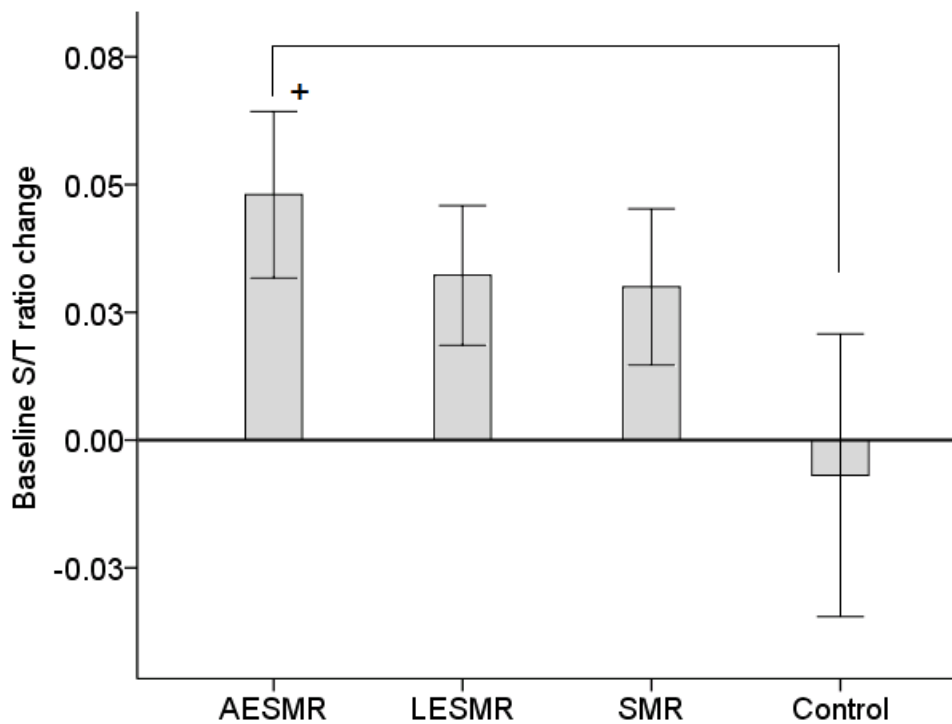


Figure 5-8 Changes in the mean baseline S/T ratios (\pm SE) of EEG measurements during SMR training for the AESMR, LESMR, SMR groups, between early and late conditioning, compared to the control group. + indicates an exploratory and uncorrected significance level, $P \leq 0.05$.

For SMR amplitude per se, in the baseline period for early and late conditioning sessions, only the effect of Group approached statistical significance ($F(3,32) = 2.83$, $P = 0.06$). Post-hoc comparisons of baseline SMR amplitudes for the four groups, between early and late conditioning, showed significantly different means for the SMR amplitudes of the AESMR group ($p = 0.033$; the LESMR group, $p = 0.37$; the SMR group, $p = 0.70$), compared to the control group. There was no significant

difference in the initial baseline SMR amplitude, between groups, in the early sessions (in Table 5-4, $F = 2.82$, $P = 0.06$), however post-hoc analysis of the initial baseline SMR amplitudes showed significantly reduced SMR amplitudes for the AESMR group ($p = 0.041$), compared to the control group. In addition, in the absence of a significant Group \times Condition interaction ($F(3,32) = 0.97$, $P = 0.42$, Tables 5-5 and 5-6), the results indicate a minor difference between the initial and final levels of the SMR amplitudes for the four groups, in the baseline period (Table 5-5).

A reduction in baseline theta activity, from early to late conditioning sessions, may play an important role in increasing the baseline S/T ratio for the experimental groups. The results for the theta amplitudes in the baseline period (early vs. late sessions) are shown in Table 5-5. There were significant effects for Group ($F(3,32) = 3.74$, $P = 0.021$) and Condition ($F(1,32) = 8.52$, $P = 0.006$), but no Group \times Condition interaction ($F(3,32) = 1.99$, $P = 0.14$), which demonstrates a trend for a decrease in theta, from early to late sessions, for the three experimental groups (Tables 5-5 and 5-6). In addition, there was no significant difference in the initial baseline theta amplitude between groups, for the early sessions (in Table 5-4, $F = 2.58$, $P = 0.07$). Again, post-hoc analysis of the initial baseline theta amplitudes showed no significant decrease in the theta amplitudes for the AESMR ($p = 0.29$), LESMR ($p = 0.45$) and SMR ($p = 0.95$) groups, compared to the control group (Table 5-5).

Importantly, post-hoc and contrast analysis with Bonferroni correction showed no significant changes in the baseline theta amplitude for the AESMR ($t_{32} = -2.03$, $p = 0.05$) and SMR ($t_{32} = -2.06$, $p = 0.047$) groups, compared to the control group (in the LESMR, $t_{32} = -0.74$, $p = 0.46$, Figure 5-9). The absence of a significant difference in

the baseline theta amplitude for the AESMR and SMR groups, who experienced actual SMR training, does not support the hypothesis.

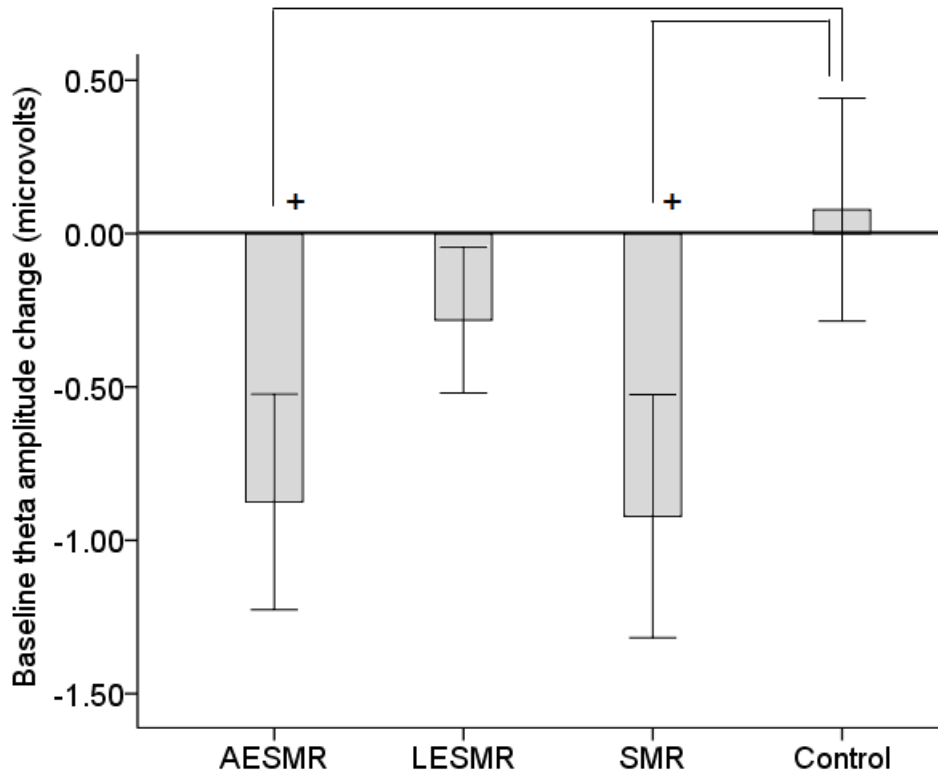


Figure 5-9. Changes in mean baseline theta amplitude (\pm SE) of EEG measurements, during SMR training, for the AESMR, LESMR and SMR groups, between early and late conditioning, compared to the control group. + indicates an exploratory and uncorrected significance level, $P \leq 0.05$.

In summary, the changes of baseline S/T ratio and baseline theta activity, from early to late SMR conditioning, even for the AESMR and SMR groups, do not significantly support hypothesis 2, because of the exploratory and uncorrected significant increase in the baseline S/T ratio and decrease in the baseline theta amplitude, from early to late conditioning, compared to the control group. These

results do not support the hypothesis, possibly due to the error from randomized samples because of an insufficient number of cases in each group. Further discussion is presented in the following discussion section.

5.3.3 Hypothesis 3: As for Hypothesis 2 but regarding the feedback period.

5.3.3.1 EEG measurements in the feedback period

It is hypothesised that there would be an improvement in EEG measurements in the feedback period, during late-conditioning (sessions 8-10), for the three experimental groups who receive actual SMR training, compared to the mock control group. Because of an increase in the SMR amplitude, a decrease in theta amplitude and the consequent increase in the SMR/theta ratio, subjects would demonstrate a greater improvement in EEG measurements, in the order; AE > LE > SMR alone, than the control group, for the feedback period in late-conditioning sessions, compared with the mock control group, who did not receive actual NFT.

Hypothesis 3 mainly evaluates enhanced SMR and/or decreased theta activity, for the feedback period of the late-conditioning sessions, compared to the early-conditioning sessions. To ensure clear presentation of the EEG data, the descriptive statistics of the EEG measurements for the feedback period of the early and late conditioning sessions are presented in Table 5-7. This figure shows the means and standard deviations of the averaged SMR amplitudes, theta amplitude and SMR/theta ratio (S/T) for the feedback period of early SMR training sessions (2-4) and late SMR training sessions (8-10), for the four groups. Group differences,

analysed by a one-way ANOVA with post-hoc Tukey tests (for multiple comparisons) showed no significant differences between groups for the feedback periods of the early second, third and fourth sessions (feedback SMR, $F = 1.93$, $p = 0.15$; feedback theta, $F = 2.17$, $p = 0.11$; feedback S/T ratio, $F = 0.31$, $p = 0.82$, see Table 5-5).

Table 5-7

Averaged EEG measurements (mean amplitudes \pm standard deviations) of SMR training in the feedback period of early (training sessions 2-4) and late (training sessions 8-10) conditioning, in the four groups (AESMR, LESMR, SMR and control groups).

Groups	SMR	Early	Late
	EEG Measurements	Conditioning	Conditioning
AESMR	Feedback SMR	3.16 ± 0.39	3.37 ± 0.52
	Feedback theta	7.50 ± 1.30	6.94 ± 1.16
	Feedback S/T	0.43 ± 0.08	0.51 ± 0.11
LESMR	Feedback SMR	3.55 ± 0.85	3.75 ± 0.78
	Feedback theta	8.27 ± 1.85	8.19 ± 1.74
	Feedback S/T	0.43 ± 0.05	0.46 ± 0.05
SMR	Feedback SMR	3.63 ± 0.92	3.67 ± 0.91
	Feedback theta	8.96 ± 1.41	8.52 ± 1.57
	Feedback S/T	0.41 ± 0.09	0.44 ± 0.11
Control	Feedback SMR	4.09 ± 1.02	4.18 ± 1.40
	Feedback theta	9.51 ± 2.32	9.09 ± 1.93
	Feedback S/T	0.44 ± 0.07	0.44 ± 0.07

There was a significant effect for Condition ($F(1,32) = 20.82, P < 0.001$) and a Group \times Condition interaction ($F(3,32) = 4.63, P = 0.008$) on the feedback S/T ratio (Table 5-8). Mean results indicate increased S/T ratios for the three non-control groups. The predicted increase in the feedback S/T ratio for the AESMR group was confirmed, only in comparison with the control group (post-hoc and contrast analysis in the AESMR, $t_{32} = 3.69, p = 0.001$; LESMR, $t_{32} = 1.48, p = 0.15$; SMR, $t_{32} = 1.46, p = 0.15$), as is depicted in Figure 5-10. In summary, compared to the control group, only one significant increase in the feedback S/T ratio (from early to late conditioning sessions) in the AESMR group supports the hypothesis. However, the increase in the feedback S/T ratio for the other two non-control groups, the LESMR and SMR groups, showed a trend for an increase in the feedback S/T ratio, compared to the control group, that was not statistically significant. These results for the LESMR and SMR groups do not, therefore, support the hypothesis, possibly due to the error from randomized samples that have an insufficient number of cases in each group. Further discussion is presented in the discussion section.

Table 5-8

The effects of Group (AESMR, LESMR, SMR and control) and Conditioning (early vs. late) on EEG measurements related to SMR training in the feedback period, analysed using ANOVA with repeated measures.

Period	Rhythms	Source	<i>df</i>	<i>F</i>	<i>P</i>
Feedback	S/T ratio	Group	3	0.60	0.62
		Condition	1	20.82	0.00007**
		Group × Condition	3	4.63	0.008**
	SMR	Group	3	1.48	0.24
		Condition	1	6.32	0.017*
		Group × Condition	3	0.63	0.60
	Theta	Group	3	2.51	0.08
		Condition	1	17.62	0.0002**
		Group × Condition	3	1.29	0.29

Group × Condition indicates the interaction between group and conditioning (early and late); * indicates a significance level, $P < 0.05$ and ** indicates a significance level, $P < 0.01$, in accordance with the Bonferroni correction.

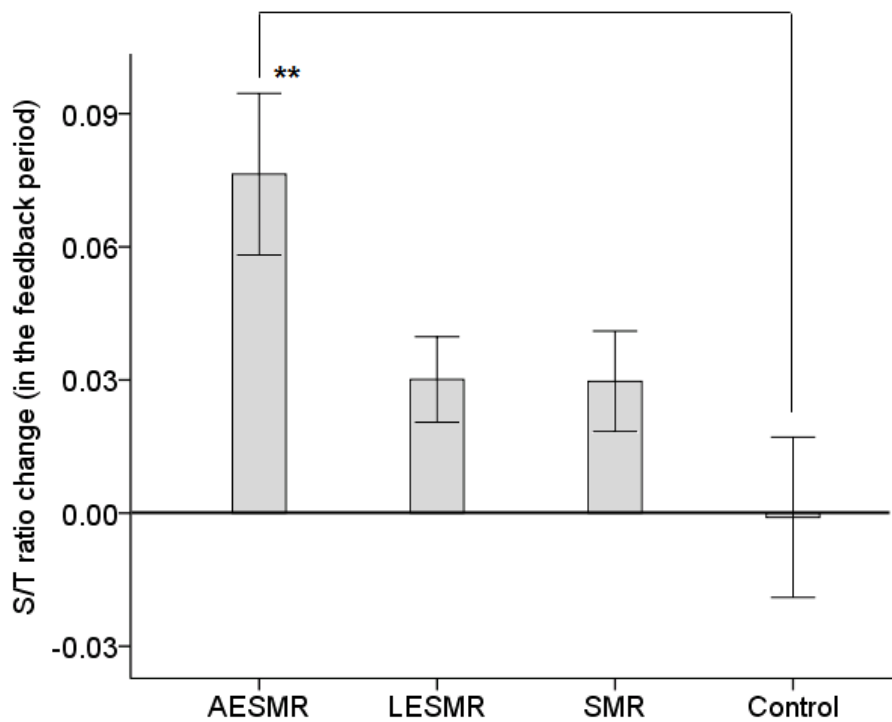


Figure 5-10. Changes in mean S/T ratios (\pm SE) from early to late conditioning, for the EEG measurements during the feedback period for SMR training, for the AESMR, LESMR and SMR groups, compared to the control group. ** indicates a significance level, $P < 0.0167$ (Bonferroni corrected).

Evidently, in agreement with hypothesis 3, subjects in the AESMR group show a significant improvement in S/T ratios during the feedback period, between early and late conditioning sessions, compared to subjects in the control group.

There was no main Group effect ($F(3,32) = 1.48, P = 0.24$) or a Group \times Condition interaction ($F(3,32) = 0.63, P = 0.60$) for the change in SMR amplitude in the feedback period, from early to late conditioning sessions, but there was a significant effect for Condition ($F(1,32) = 6.32, P = 0.017$, Table 5-8), which

indicated a minor increase in SMR amplitudes in the feedback period for late SMR training sessions, compared to early sessions, for all four groups, (Table 5-7). In addition, the predicted increased change in SMR amplitudes for the three non-control groups for the feedback period was not significant, compared to the control group (post-hoc and contrast analysis in the AESMR, $t_{32} = 0.83$, $p = 0.42$; LESMR, $t_{32} = 0.79$, $p = 0.45$; SMR, $t_{32} = -0.28$, $p = 0.78$). The small increase in SMR amplitudes for the feedback period, for the experimental groups that received actual SMR training, does not support the hypothesis.

It is seen that a reduction in feedback theta activity, from early to late conditioning sessions, may also play an important role in increasing the feedback S/T ratios for the experimental groups. The results for theta amplitudes in the feedback period (early vs. late sessions) are shown in Table 5-7. There was a significant effect for Condition ($F(1,32) = 17.62$, $P = 0.0002$) and an effect for Group that approaches significance ($F(3,32) = 2.51$, $P = 0.08$), but no Group \times Condition interaction ($F(3,32) = 1.29$, $P = 0.29$, Table 5-8), which is indicative of a decrease in the theta amplitude, from early to late sessions, for all four groups (Table 5-7). The post-hoc comparisons of the theta amplitudes in the feedback period, for the four groups, between early and late conditioning, show an effect that approaches significance only for the AESMR group ($p = 0.059$; the LESMR group, $p = 0.54$; the SMR group, $p = 0.89$), compared to the control group. This may have contributed to the marginal main Group effect ($P = 0.08$). However, there were no significant group differences between groups in the initial theta amplitudes for feedback periods in the early sessions (in Table 5-4, $F = 2.17$, $P = 0.11$).

Post-hoc and contrast analysis shows no significant change in the feedback theta amplitudes, for the AESMR ($t_{32} = -0.56$, $p = 0.58$), LESMR ($t_{32} = 1.31$, $p = 0.20$) and SMR ($t_{32} = -0.08$, $p = 0.94$) groups, compared to the control group. The theta amplitudes in the feedback period for the experimental groups that experience actual SMR training do not support the hypothesis.

The SMR training assisted by alternating frequency electro-stimulation had a significant increasing effect on the feedback S/T ratio and reflected contributions from both increased SMR and a decrease in theta, because neither was individually significant. The main aim of SMR/theta training is to simultaneously enhance SMR and decrease theta activity. This ratio training of NFT may imply that real-time NFT conditioning to increase learning ability or neuroplasticity is specific to the actual NFT protocol to which the subjects are subjected, for example ratio training for brain cortical activity that results in an increased or decreased ratio of EEG measurements, based on the NFT protocol, in the late training sessions.

In summary, the increase in the feedback S/T ratio in the AESMR group, as a result of SMR training and electro-stimulation, may partially support hypothesis 3. The idea of plausible real-time EEG operant conditioning and the subjects' ability to learn how to manipulate their brain cortical activity, because of the significant increase in the change in the feedback S/T ratio, from early to late conditioning, compared to the control group. However, these results for the other two experimental groups do not totally support the hypothesis 3, possibly due to the error from randomized samples that have an insufficient number of cases in each group. Further discussion is presented in the discussion section

5.3.4 Hypothesis 4: As for hypotheses 2 and 3, but instead of examining absolute amplitudes of SMR and theta, relative amplitudes were examined.

5.3.4.1 Relative SMR and theta activity

It was hypothesised that there would be an improvement in baseline-to-feedback SMR ($SMR_{Relative}$) and a decrease in the baseline-to-feedback theta ($theta_{Relative}$) values, between early and late SMR conditioning, for the three experimental groups that were subject to actual SMR training, compared to the control group. Thus, subjects in the AESMR and LESMR groups would register the greatest values for these baseline-to-feedback measurements, in late-conditioning sessions (vs. early), and the SMR group would register greater robust values than the control group. The increased relative SMR and the decrease in relative theta values imply the efficacy of SMR conditioning, in order to manipulate SMR and theta rhythms (from baseline to feedback period) and improve brain cortical activity, after at least ten SMR sessions, which would be only noted for the three experimental groups that were subject to actual NFT, but not for the control group, which was not subject to actual NFT.

The descriptive statistics for the EEG measurements of averaged relative SMR $Relative$ and theta $Relative$ activity from early to late conditioning sessions are presented in Table 5-9, which shows the mean and standard deviation of averaged $SMR_{Relative}$ and $theta_{Relative}$ values for the four groups, for early training sessions (2-4) and late training sessions (8-10). Group differences in the initial scores for $SMR_{Relative}$ and $theta_{Relative}$ values for early conditioning for the four groups were analysed using a one-way ANOVA with post-hoc Tukey tests (for multiple comparisons). There were

no significant differences between groups in the early second, third and fourth conditioning sessions ($SMR_{Relative}$, $F = 1.83$, $p = 0.16$; $\theta_{Relative}$, $F = 2.01$, $p = 0.13$, see Table 5-5).

There were significant main effects for Group ($F(3,32) = 2.97$, $P = 0.047$) and Condition ($F(1,32) = 8.65$, $P = 0.006$) in $SMR_{Relative}$ values, from the baseline to the feedback state, but no Group \times Condition interaction ($F(3,32) = 0.97$, $P = 0.42$, Table 5-10). The Mean results indicate an increase in $SMR_{Relative}$ for the three non-control groups (Table 5-9). However, the predicted increase in the change in $SMR_{Relative}$ for the AESMR group was not confirmed by a significant increase (by Bonferroni correction) in $SMR_{Relative}$ for the AESMR group, compared to the control group (post-hoc and contrast analysis of $SMR_{Relative}$ change score in the AESMR, $t_{32} = 2.04$, $p = 0.05$; LESMR, $t_{32} = 1.53$, $p = 0.14$; SMR, $t_{32} = 1.61$, $p = 0.12$), as shown in Figure 5-11.

Table 5-9

Averaged baseline-to-feedback $SMR_{Relative}$ and $\theta_{Relative}$ activity (mean \pm standard deviation) of early (training sessions 2-4) and late (training sessions 8-10) conditioning, in the four groups (AESMR, LESMR, SMR and control).

Groups	SMR	Early	Late
	EEG Measurements	Conditioning	Conditioning
AESMR	$SMR_{Relative}$	1.04 ± 0.10	1.10 ± 0.11
	$\theta_{Relative}$	1.08 ± 0.14	1.11 ± 0.07
LESMR	$SMR_{Relative}$	1.01 ± 0.06	1.06 ± 0.09
	$\theta_{Relative}$	1.12 ± 0.06	1.16 ± 0.12
SMR	$SMR_{Relative}$	0.96 ± 0.06	1.01 ± 0.05
	$\theta_{Relative}$	1.00 ± 0.12	1.05 ± 0.09
Control	$SMR_{Relative}$	0.99 ± 0.08	0.99 ± 0.09
	$\theta_{Relative}$	1.10 ± 0.08	1.05 ± 0.14

baseline-to-feedback means from the baseline to the feedback state; $SMR_{Relative}$ is the mean SMR amplitude value during the feedback period divided by mean SMR amplitude value during the baseline period for each session; $\theta_{Relative}$ is the mean theta amplitude value during the feedback period divided by mean theta amplitude value during the baseline period, for each session.

Table 5-10

The effects of Group (AESMR, LESMR, SMR and control) and Conditioning (early vs. late) on EEG measurements ($SMR_{Relative}$ and $\theta_{Relative}$), in relation to SMR training from the baseline to the feedback state, analysed using ANOVA with repeated measurements.

Period	Value	Source	<i>df</i>	<i>F</i>	<i>P</i>
Baseline-to- Feedback	$SMR_{Relative}$	Group	3	2.97	0.047*
		Condition	1	8.65	0.006**
		Group × Condition	3	0.97	0.42
	$\theta_{Relative}$	Group	3	2.16	0.11
		Condition	1	1.08	0.31
		Group × Condition	3	1.45	0.25

Group × Condition indicates the interaction between group and conditioning (early and late); * indicates a significance level, $P < 0.05$, and ** indicates a significance level, $P < 0.01$, in accordance with the Bonferroni correction.

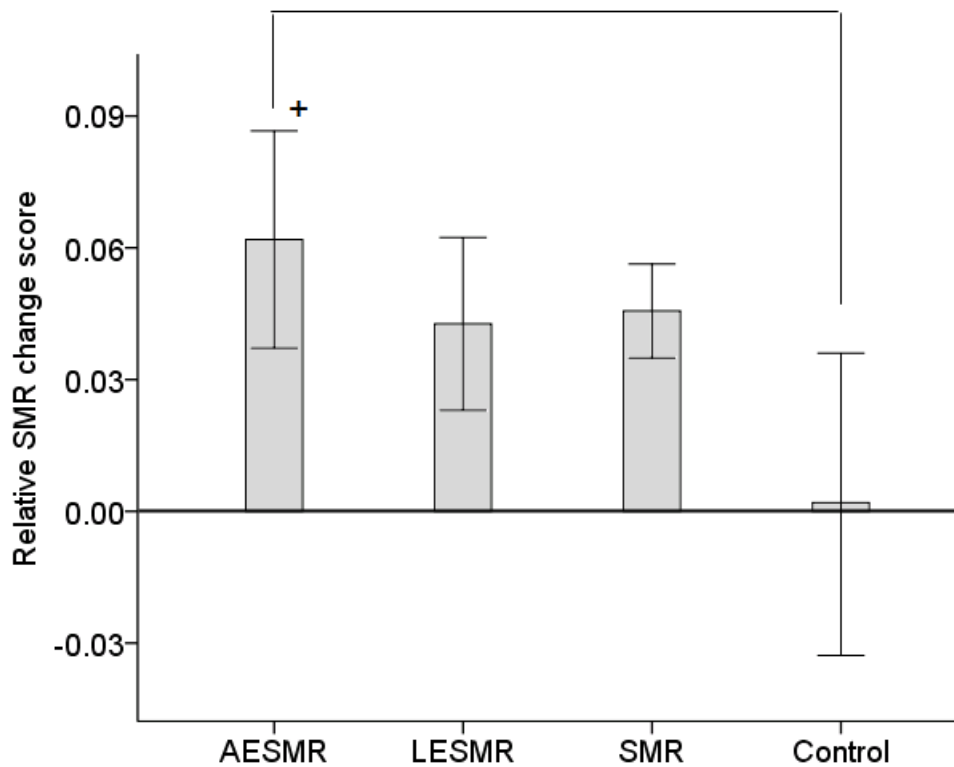


Figure 5-11. Changes in mean SMR_{Relative} (\pm SE) of EEG measurements in the AESMR, LESMR and SMR groups, from early to late conditioning, compared to the control group. ⁺ indicates an exploratory and uncorrected significance level, $P \leq 0.05$.

In addition, the theta_{Relative} from early to late conditioning sessions showed neither a main Group effect ($F(3,32) = 2.16, P = 0.11$), nor a main effect for Condition ($F(1,32) = 1.08, P = 0.31$, Table 5-10), nor a Group \times Condition interaction ($F(3,32) = 1.45, P = 0.25$, Table 5-10). There were no between-group differences between the three non-control groups and the control for theta_{Relative} (post-hoc comparisons to the control group, in the AESMR, $p = 0.45$; LESMR, $p = 0.34$; SMR, $p = 0.28$)

In summary, the results of the change in $SMR_{Relative}$ and $\theta_{Relative}$ for the three experimental groups, from early to late conditioning sessions, only showed a trend for an increase in the change in $SMR_{Relative}$ that was not statistically significant after Bonferroni correction, compared to the control group. These results do not support the hypothesis 4, the idea of the subjects' ability to learn how to significantly manipulate their brain cortical activity, possibly due to the error from randomized samples that have an insufficient number of cases in each group. Further discussion is presented in the discussion section that follows.

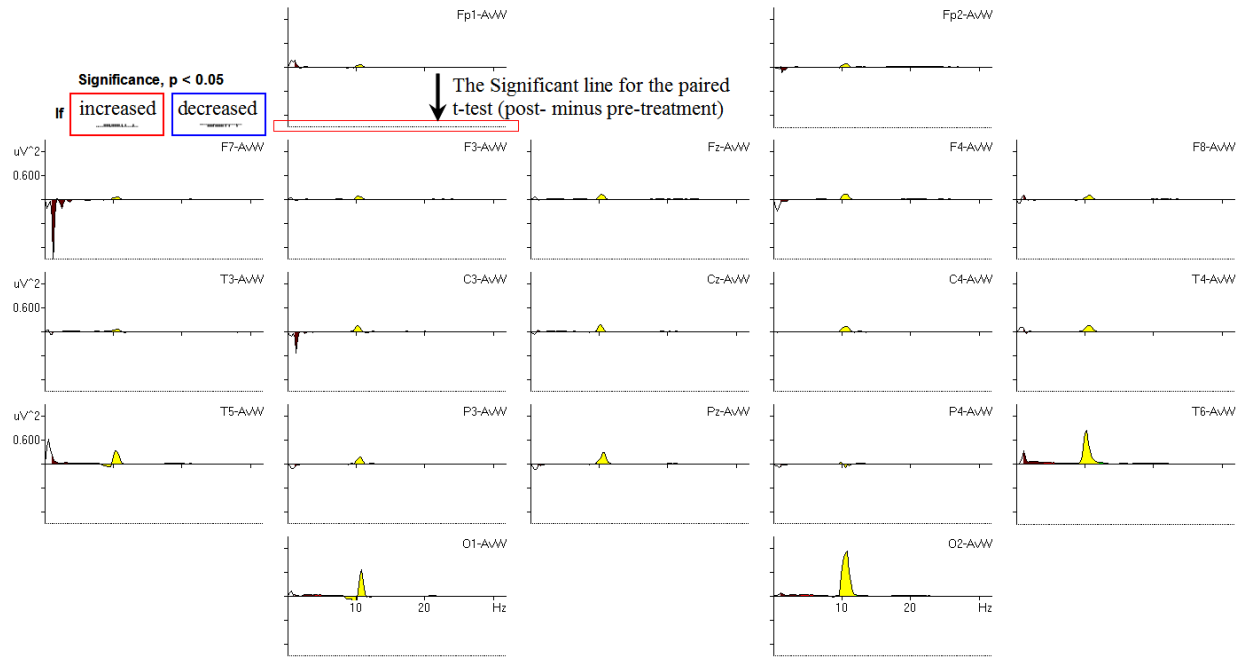
5.3.5 Hypothesis 5: In replication of Experiment II, group ICA is used to extract ICs from the resting state EEG (pre- vs. post-training) with the prediction that NFT/EA will result in enhanced relevant spectral power but no increase in the number of cortical loci.

5.3.5.1 Conventional EEG comparisons for 19 channels, pre- vs. post- SMR training

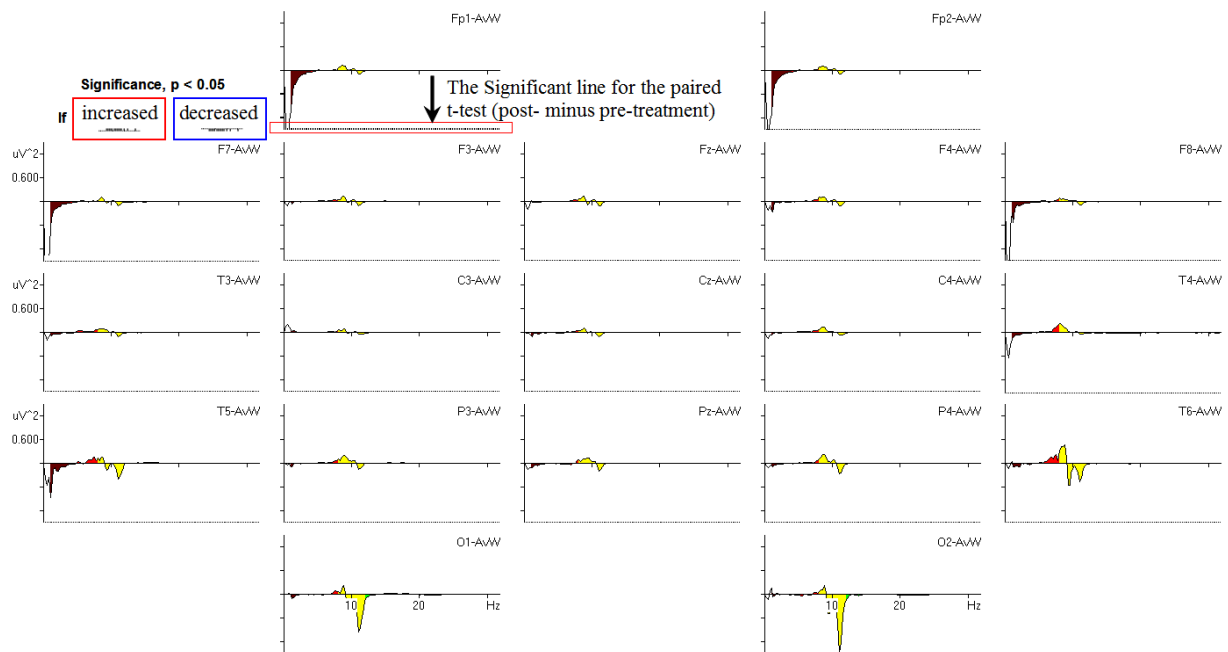
The results of this study are shown in Figure 5-12, which presents the changes in relative EEG band activity for the four groups. The lines with non-significant t-values, for pre- vs. post- SMR training, are shown at each electrode site. With regard to relative EEG values, the initially hypothesized changes in associated EEG oscillations

and cortical activity in the 19 channels for the four groups were not detected, as they were in Egner et al's 2004 study of spectral topography after SMR training (Egner, et al., 2004). Accordingly, in connection with the hypothesis, there was no significant improvement in the relevant EEG spectral power in related cortical regions, after SMR training, perhaps due to a mixture of underlying source activity and volume conduction (Congedo, et al., 2009). Thus, based on the methods and outcome of Exp II, which examined ICA-derived EEG functional connectivity, group ICA was used to extract ICs from the resting state EEG (pre- vs. post-training). This revealed five statistically clustered regions, so it was hypothesised that resting EEG networks enhances relevant spectral power, but there are no additional cortical sources, after NFT and EA stimulation.

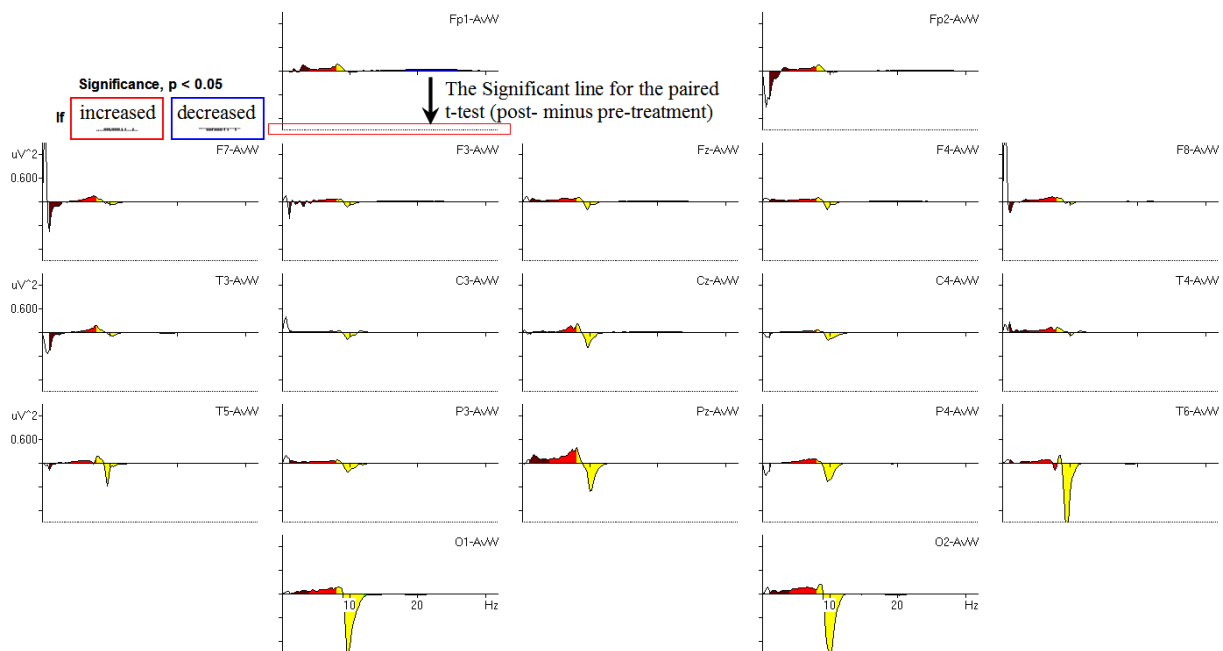
(A) AESMR



(B) LESMR



(C) SMR



(D) Control

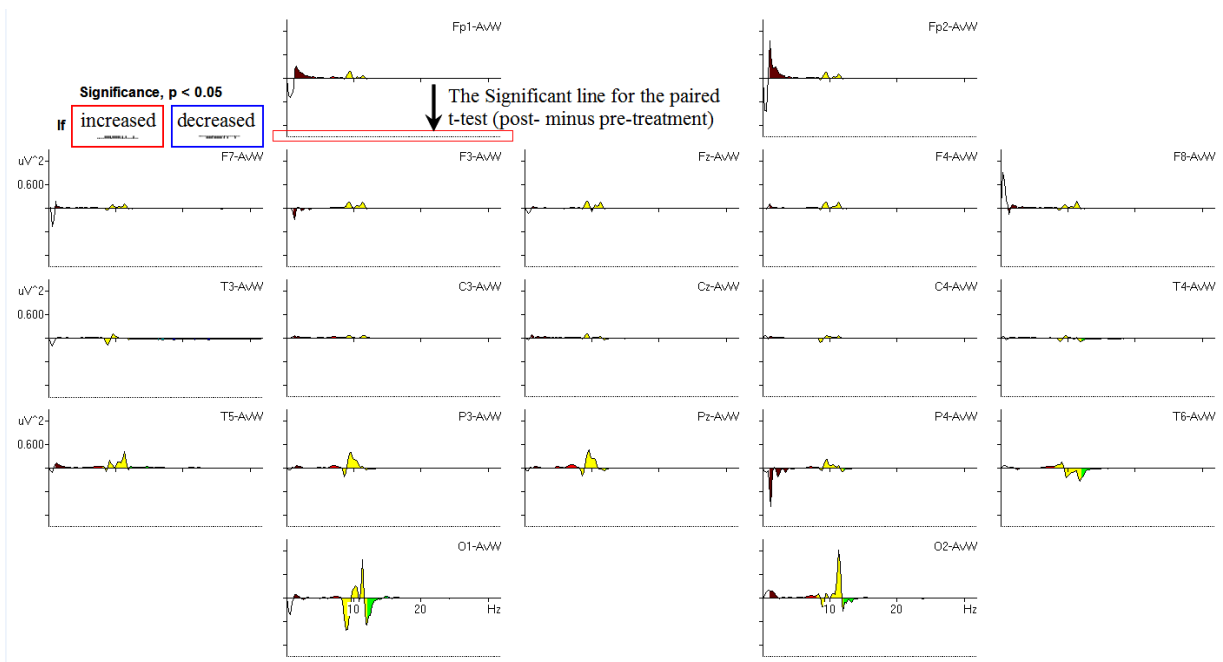


Figure 5-12. Traditional EEG spectral analyses present the changes in relative EEG band activity for the four groups. The lines with non-significant t-values, for pre- vs. post- SMR training, are shown at each electrode site. ((A) the AESMR group; (B) the LESMR group; (C) the SMR group and (D) the control group, in the resting eyes-closed state).

5.3.5.2 Group ICA as a valid method for extracting ICs in the resting state EEG

The schema for the progression from raw EEG to epoched-EEG recordings and then to the construction of the mean power spectra of valid components is illustrated in Figure 5-4. There were no extra cortical sources after NFT and EA stimulation, according to the inverse localization tool, sLORETA (also see the next paragraph, Table 5-11 and Figure 5-13). This result supports the hypothesis that functional and consistent sources are present in the brain, during the resting states for pre- and post-SMR training.

As illustrated in Fig. 5-13, the results were calculated using the 3-minute resting state EEG, in each case. Sixty averaged valid epochs (without artefacts) from the 36 subjects were analyzed (a total of 2160 epochs). Infomax ICA was used to extract ICs from the concatenated EEG data of the 36 participants, for both the pre- and post-NFT eyes-closed EEG resting states. All EEG data were decomposed into 13 spatially fixed and maximally independent components. Only 6 artefact ICs were excluded (horizontal and vertical eye-movements \times 2, temporal muscle artefacts \times 2 and ICs with unspecific muscle artefacts \times 2, Fig. 5-14). The components from the concatenated EEG data in the resting EEG support hypothesis 5. Spectral power analysis was then used to examine the dynamics of the EEG-alpha power spectra in the EC resting state (details in the next paragraph).

Table 5-11.

Coordinates of the 13 ICs in the five circumscribed regions, in the EC resting state, as shown in Figure 5-14, pre- vs post-SMR training, presented with the same stereotactic space as that of Talairach and Tournoux (1988).

Region	ICs (number)	x	y	z	Anatomical localization	
Frontal	1	-5	58	-7	BA10	Superior frontal gyrus
	13	-40	45	25	BA10	Middle frontal gyrus
	11	31	36	42	BA8	Middle frontal gyrus
	7	-5	51	39	BA8	Medial frontal gyrus
Central	8	-25	-11	65	BA6	Precentral gyrus
	12	34	-12	63	BA6	Precentral gyrus
Parietal	9	-45	-51	39	BA40	Inferior parietal lobule
	5	-5	-75	50	BA7	Precuneus, parietal lobe
	10	45	-61	49	BA40	Inferior parietal lobule
Occipitotemporal	3	53	-57	20	BA39	Superior temporal gyrus
	6	-54	-54	13	BA39	Superior temporal gyrus
Occipital	2	10	-71	17	BA18	Cuneus, occipital lobe
	4	-20	-96	14	BA19	Middle occipital gyrus

Brain regions are identified by the putative Brodmann area (BA) and similar localization imaging (pre- vs. post-) of the spontaneous EEG activity.

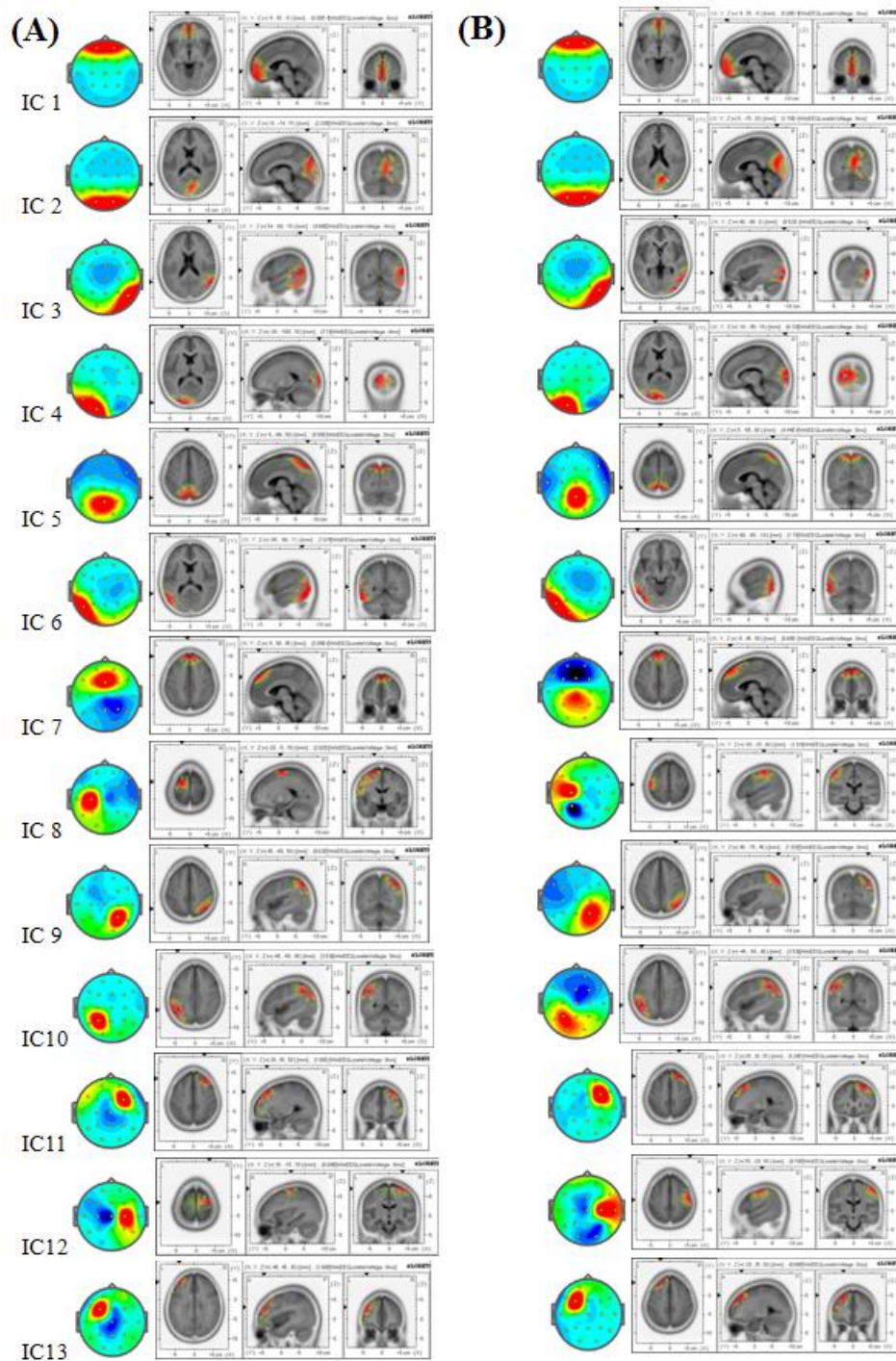
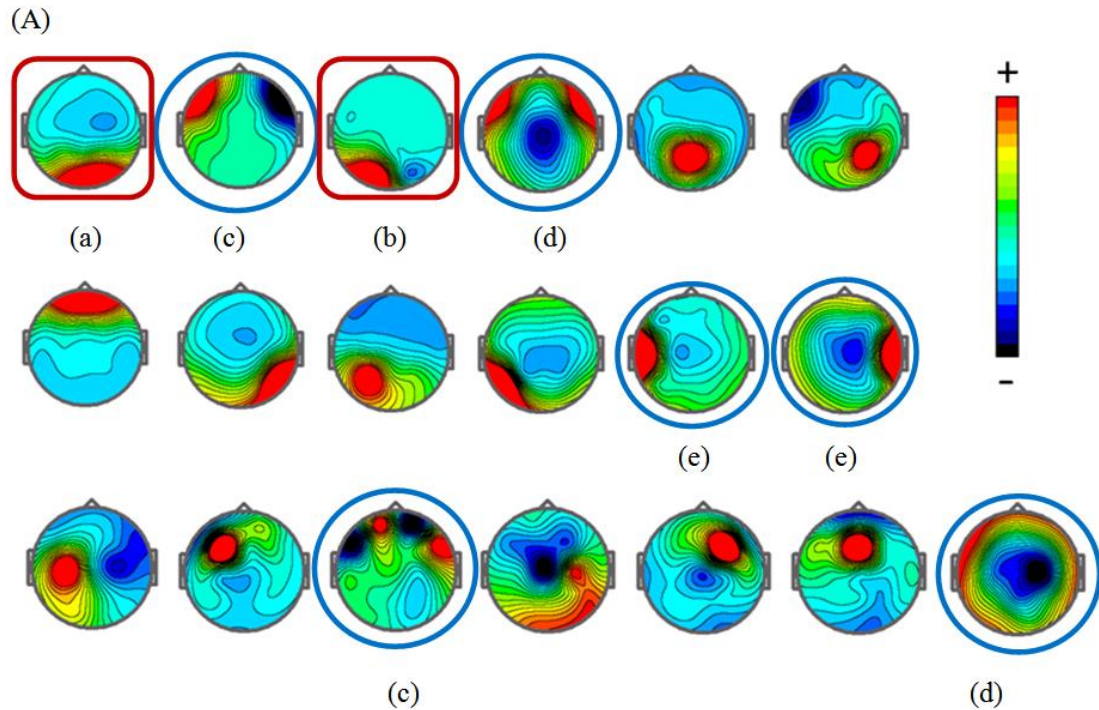
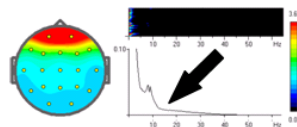


Figure 5-13 (A) The 2D topographies of the selected 13 ICs and their sLORETA images for source localization of cortical generators, pre- SMR conditioning, in the EC state. (B) The selected 13 ICs post- SMR conditioning in the EC state. Both of the localization images (pre- vs. post-) show stable and consistent features in the spontaneous EEG activity (see also Table 5-11).

Upon completion of the spectral power analysis and the estimation of the cross-correlation of (alpha-band) EEG power between different ICs within subjects, a functional relationship between such source “nodes” can be established (see the next results). As illustrated in Figure 5-13, the results were calculated using the 3-minute resting state EEG, in each case. Sixty averaged valid epochs (without artefacts) from the 36 subjects were analyzed (a total of 2160 epochs). Infomax ICA was used to extract ICs from the concatenated EEG data of the 36 participants, for both the pre- and post-NFT eyes-closed EEG resting states. All EEG data were decomposed into 13 spatially fixed and maximally independent components. Only 6 artefact ICs were excluded (horizontal and vertical eye-movements \times 2, temporal muscle artefacts \times 2 and ICs with unspecific muscle artefacts \times 2, Figure 5-14). The components from the concatenated EEG data in the resting EEG support hypothesis 5. Spectral power analysis was then used to examine the dynamics of the EEG-alpha power spectra in the EC resting state.



(B) Signals come from brain activity, but not predominantly from muscle activity.



(C) Predominant muscle activity near bilateral temporal areas.

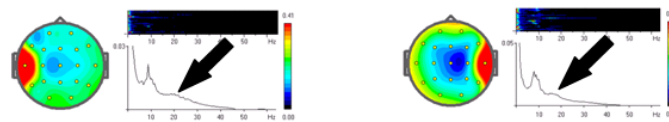


Figure 5-14 (A) All of the 19 ICs from 19 channels of scalp EEG recordings. The maps are individually scaled to their maximum absolute value (green is zero in the scale bar). For example, red boxed ICs represent an occipital alpha rhythm, (a) and (b); and blue circled ICs represent eye movement, (c), or any possible physiologically unresolvable noise with more than a single dipole, (d), or a bilateral, temporal muscle artefact, (e). The artefact and noise ICs (c, d and e) were excluded, to acquire 13 artefact-free ICs. (B) This component is located in the frontal area, but is without predominant muscular artefact. (C) These two ICs predominantly result from bilateral, temporal muscle activity (Arrows).

All components for both pre- and post-NFT in the resting EEG recordings exhibited a high repeatability across subjects with strong cortical source locations (Figure 5-13). Importantly, these findings are critical to further study of the EEG power-associated spectral analysis of ICA components, which is based on the estimated EEG resting-state connectivity and represents the spatially-segregated, unmixed EEG sources as functional nodes in electro-cortical networks.

5.3.6 Hypothesis 6: the effect of SMR training on attention networks will result in increased attention-related beta power in the frontal regions of the dorsal attention network and decreased theta power in the central regions (pre- vs. post-training), demonstrating a long-term effect of NFT on attention and vigilance.

5.3.6.1 The five circumscribed functional regions, across subjects

Hierarchical cluster analysis of cross-correlations between alpha power ICs of the 36 subjects identified a consistent set of five spatiotemporally distinct groups from 2160 epochs in each resting condition, which is in line with the idea of resting state networks that arises from fMRI studies (Toro, et al., 2008; Van Den Heuvel and Hulshoff Pol, 2010), and the results of Exp II in this thesis (Chen et al., 2012). The five groups were classified on the basis of their coordinates in Talairach space and by regional anatomy (Table 5-11):

1. Group F: a network of predominantly lateral and middle prefrontal cortices, as well as an anterior pole of the prefrontal lobe.
2. Group C: a lateral network involving the precentral gyri.
3. Group P: a posterior-lateral and midline network primarily involving the parietal regions.
4. Group OT: a lateral network dominated by the bilateral middle temporal cortices in the occipitotemporal regions.
5. Group O: a posterior network characterized by the predominant involvement of the occipital cortex.

All of the spatial maps of these groups were found in both pre- and post-NFT EC states. As illustrated in Figure 5-13, the results are consistent with fMRI resting-state network (RSN) reports for regions showing functional connectivity patterns in the DMN across resting states (Fox, et al., 2005; Fransson, 2006; Yan, et al., 2009) and those with strong anatomical connectivity (Honey, et al., 2009; Honey, et al., 2007) (see also section 4.3.4.1).

Importantly, as the successful application of the hierarchical cluster analysis for the five grouped-ICs explained in Exp II, the correlation coefficient in each clustered group ($p < 0.01$, corrected) was also used in Exp III, in order to reveal distinct grouping patterns for components in both the pre- and post-NFT eyes-closed resting states. Functional connectivity, based on a significant threshold (correlation coefficient r -value), was evaluated according to the similarity between components (see the details in the chapter 4, sections 4.3.3 and 4.3.4).

5.3.6.2 A comparison of the changes in spectral power in the relevant regions of the resting EEG state, pre- and post- SMR training

It was hypothesised that there would be an increase in attention-related beta power in the frontal region of the dorsal attention network (DAN), because of the effect of SMR training on attention, in the three experimental groups that received actual NFT. However, no such beta power enhancement should occur in the same frontal region, in the control group that was not subject to actual NFT. Correspondingly, subjects in the AESMR and LESMR groups should also demonstrate the greatest increase in beta power in the frontal region and the greatest decrease in theta power in the central region. The SMR group should also have greater values than the control group. In addition, the change in beta and theta power in the resting EEG dynamics may also imply a long-term effect for SMR training on attention and vigilance (with at least 10 sessions of SMR training).

5.3.6.3 Beta power in the frontal region

Table 5-12 shows the mean and standard deviation for the averaged regional SMR, Theta, beta1 and beta2 power of the clustered components, for the four groups (pre- vs. post-). Table 5-13 shows the results of a three way ANOVA with repeated measurements. The mean results for the group give evidence of the increase in beta power, related to increased attention, and the decrease in theta power, related to improved vigilance, that is caused by SMR learning and EA stimulation. Evidently, based on the statistical results, the hypothesized increase in frontal beta activity (beta 1 and beta 2) in the three experimental groups was confirmed. The 3-way Group ×

PrePost \times Region ANOVA was significant for beta 1 band activity ($F(12,128)=1.87$, $P=0.044$, uncorrected). This interaction was due to the fact that there was a significant PrePost \times Region interaction ($F(4,128)=33.09$, $P < 0.0001$), and the effect of the interaction in the three non-control groups may be attributable to a significant increase in beta 1 activity in the frontal region (paired t -tests for AESMR, $t_8=3.26$, $p=0.011$; LESMR, $t_8=3.63$, $p=0.007$; SMR, $t_8=2.63$, $p=0.030$; Control, $t_8=0.30$, $p=0.77$, details in Tables 5-12 and 5-13 and in Figure 5-15). There was a marginally significant Group \times PrePost \times Region interaction in the beta 2 band activity ($F(12,128)=1.79$, $P=0.056$, uncorrected). There was also a significant PrePost \times Region interaction in beta 2 activity ($F(4,128)=29.74$, $P < 0.0001$), caused by a significant increase in beta 2 activity in the frontal region (paired t -tests in AESMR, $t_8=2.56$, $p=0.034$; LESMR, $t_8=2.61$, $p=0.031$; SMR, $t_8=2.32$, $p=0.049$; Control, $t_8=0.83$, $p=0.43$, details in Tables 5-12 and 5-13 and in Figure 5-15).

Table 5-12

Regional spectra power (mean \pm standard deviation; arbitrary unit, a. u.) of clustered components, pre- and post-SMR training, in the eyes-closed resting state, for the four groups (AESMR, LESMR, SMR and control)

pre- vs. post-treatment		Theta	SMR	Beta1	Beta2
Group					
Frontal region	AESMR	0.83 \pm 0.39 vs. 0.89 \pm 0.25	0.19 \pm 0.08 vs. 0.20 \pm 0.08	0.14 \pm 0.06 vs. 0.21 \pm 0.10 (t8=3.26, p = 0.011)*	1.09 \pm 1.20 vs. 1.58 \pm 1.71 (t8=2.56, p = 0.034)*
	LESMR	1.01 \pm 0.60 vs. 1.15 \pm 0.74	0.18 \pm 0.04 vs. 0.25 \pm 0.22	0.08 \pm 0.04 vs. 0.11 \pm 0.06 (t8=3.63, p = 0.007)**	0.22 \pm 0.08 vs. 0.29 \pm 0.14 (t8=2.61, p = 0.031)*
	SMR	1.11 \pm 0.41 vs. 1.67 \pm 1.11	0.18 \pm 0.06 vs. 0.29 \pm 0.16	0.14 \pm 0.05 vs. 0.32 \pm 0.27 (t8=2.63, p = 0.030)*	0.58 \pm 0.45 vs. 1.54 \pm 1.86 (t8=2.32, p = 0.049)*
	Control	1.05 \pm 0.31 vs. 1.26 \pm 0.41 (t8=4.20, p = 0.003)**	0.26 \pm 0.12 vs. 0.29 \pm 0.13	0.22 \pm 0.13 vs. 0.23 \pm 0.14	0.60 \pm 0.26 vs. 0.66 \pm 0.24
Central region	AESMR	0.19 \pm 0.08 vs. 0.12 \pm 0.04 (t8=3.11, p = 0.015)*	0.14 \pm 0.08 vs. 0.06 \pm 0.02 (t8=2.71, p = 0.027)*	0.06 \pm 0.02 vs. 0.05 \pm 0.03 (t8=2.82, p = 0.022)*	0.40 \pm 0.38 vs. 0.24 \pm 0.18 (t8=2.32, p = 0.049)*
	LESMR	0.43 \pm 0.56 vs. 0.30 \pm 0.41 (t8=2.61, p = 0.031)*	0.12 \pm 0.06 vs. 0.08 \pm 0.07 (t8=2.39, p = 0.044)*	0.09 \pm 0.06 vs. 0.07 \pm 0.07 (t8=2.41, p = 0.042)*	0.2 \pm 0.09 vs. 0.14 \pm 0.07 (t8=4.14, p = 0.003)**
	SMR	0.33 \pm 0.21 vs. 0.26 \pm 0.17 (t8=2.34, p = 0.048)*	0.14 \pm 0.10 vs. 0.08 \pm 0.05 (t8=2.47, p = 0.039)*	0.06 \pm 0.02 vs. 0.06 \pm 0.03	0.24 \pm 0.18 vs. 0.18 \pm 0.13 (t8=3.55, p = 0.008)*
	Control	0.29 \pm 0.14 vs. 0.22 \pm 0.05	0.17 \pm 0.12 vs. 0.10 \pm 0.06	0.11 \pm 0.07 vs. 0.07 \pm 0.03 (t8=3.00, p = 0.017)*	0.30 \pm 0.19 vs. 0.20 \pm 0.13 (t8=2.49, p = 0.038)*

* indicates a significance level, $P < 0.05$, and ** indicates a significance level, $P < 0.01$, in accordance with the Bonferroni correction.

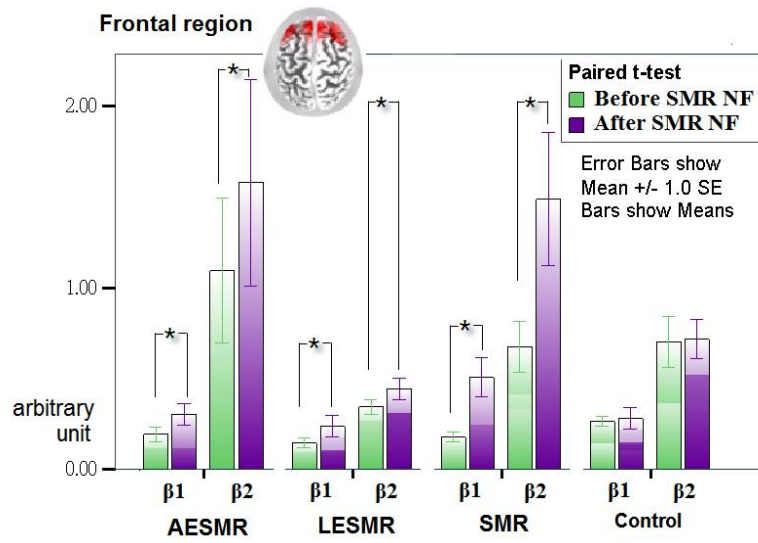


Figure 5-15. Beta 1 and Beta 2 power in the frontal region, pre- to post- training, showing significant improvement only in the three SMR experimental groups (see also Tables 5-12).

Table 5-13

The effects of Group (AESMR, LESMR, SMR and control) and PrePost (pre- vs. post-) on the ICA-derived beta power of the EEG components, using a 3-way (Group \times PrePost \times Region) repeated measurements ANOVA.

EEG	Source	<i>df</i>	<i>F</i>	<i>P</i>
spectral Power				
Beta 1	Group	3	1.57	0.22
	PrePost	1	15.44	P = 0.0004**
	Region	4	12.17	P = 0.0002**
	Group \times PrePost	3	0.39	0.76
	Group \times Region	12	1.80	0.054
	PrePost \times Region	4	33.09	P < 0.0001**
	Group \times PrePost \times Region	12	1.87	0.044*
Beta 2	Group	3	0.63	0.60
	PrePost	1	8.62	P = 0.006**
	Region	4	10.99	P < 0.0001**
	Group \times PrePost	3	2.87	0.052
	Group \times Region	12	3.01	P = 0.001**
	PrePost \times Region	4	29.74	P < 0.0001**
	Group \times PrePost \times Region	12	1.79	0.056

Group \times PrePost indicates the interaction between group and PrePost (pre- and post-treatment); Group \times Region indicates the interaction between group and Region (5 regions; frontal, central, parietal, occipital and occipitotemporal); PrePost \times Region indicates the interaction between PrePost and region; Group \times PrePost \times Region indicates the interaction between group, PrePost and region; * indicates a significance level, $P < 0.05$, and ** indicates a significance level, $P < 0.01$, in accordance with the Bonferroni correction.

The increased frontal beta power noted in the experimental groups with actual SMR training supports the hypothesis. In addition, the improvement that is evident in the attention-related beta power in the frontal region, which is shown to belong to the dorsal attention network (DAN) in the EEG resting state, is interpreted as being due to the effect of NFT on attention, in the three experimental groups that received actual NFT, because it was not noted for the control group, who were not subject to actual NFT. These results are also in agreement with those in the report of Mantini et al. (2007), which showed that DAN has a stronger relationship with alpha and beta rhythms (Mantini, et al., 2007), and those of another NFT study that used LORETA, which also reported increased beta power in the frontal area (ACC), after training (Cannon, et al., 2009; Cannon, et al., 2007; Congedo, et al., 2004).

It is seen that the control group, with non-contingent SMR feedback, shows almost no improvement in beta power after mock NFT. The aforementioned ICA-derived regional EEG components and the increase in power spectra in the AESMR and LESMR groups, which is caused by the SMR training and stimulation, supports the use of EA with alternating and low frequencies in conjunction with SMR training, in order to improve attention.

5.3.6.4 Theta and SMR power in the central region

As described in the previous paragraph, Table 5-12 shows the mean and standard deviation for the averaged regional SMR and Theta power of the clustered components, for the four groups (pre- vs. post-). Table 5-14 shows the results of a

three-way ANOVA with repeated measurements. Based on the statistical results, it is seen that the hypothesized decrease in central theta activity in the three non-control groups is confirmed. Although the 3-way Group \times PrePost \times Region ANOVA showed no significance for theta band activity ($F(12,128)=0.53$, $P=0.9$), a significant PrePost \times Region interaction ($F(4,128)=6.70$, $P < 0.0001$), due to a significant Region effect ($F(4,128)=11.40$, $P < 0.0001$), implies a strong regional effect for theta activity, in all groups. Theta activity showed a strong inclination to decrease activity in the central region in the three non-control groups (paired t -tests in AESMR, $t_8 = -3.11$, $p = 0.015$; in LESMR, $t_8 = -2.61$, $p = 0.031$; in SMR, $t_8 = -2.34$, $p = 0.048$; Control, $t_8 = -1.51$, $p=0.17$, Table 5-12).

Table 5-14

The effects of Group (AESMR, LESMR, SMR and control) and PrePost (pre- vs. post-) on the theta and SMR power of the ICA-derived EEG components, using a 3-way (Group \times PrePost \times Region) repeated measurements ANOVA.

EEG	Source	<i>df</i>	<i>F</i>	<i>P</i>
Spectral Power				
Theta	Group	3	1.37	0.27
	PrePost	1	2.94	0.10
	Region	4	11.40	P < 0.0001**
	Group \times PrePost	3	0.57	0.64
	Group \times Region	12	1.30	0.23
	PrePost \times Region	4	6.70	P < 0.0001**
	Group \times PrePost \times Region	12	0.53	0.90
SMR	Group	3	1.76	0.18
	PrePost	1	0.86	0.36
	Region	4	32.79	P < 0.0001**
	Group \times PrePost	3	1.54	0.22
	Group \times Region	12	2.21	0.015*
	PrePost \times Region	4	28.48	P < 0.0001**
	Group \times PrePost \times Region	12	1.41	0.17

Group \times PrePost indicates the interaction between group and PrePost (pre- and post-treatment); Group \times Region indicates the interaction between group and Region (5 regions; frontal, central, parietal, occipital and occipitotemporal); PrePost \times Region indicates the interaction between PrePost and region; Group \times PrePost \times Region indicates the interaction between group, PrePost and region; * indicates a significance level, $P < 0.05$, and ** indicates a significance level, $P < 0.01$, in accordance with the Bonferroni correction.

Again, the lack of a significant Group \times PrePost \times Region interaction for SMR band activity ($F(12,128)=1.41$, $P=0.17$), a significant PrePost \times Region interaction ($F(4,128)=28.48$, $P < 0.0001$), and a significant Group \times Region interaction ($F(12,128)=2.21$, $P = 0.015$) with a significant Region effect ($F(4,128)=32.79$, $P < 0.0001$) also implies a strong regional effect for SMR activity, in all groups the frontal and parietal regions. SMR activity also showed a strong inclination to decrease activity in the central region, in the three non-control groups for (paired t -tests in AESMR, $t_8 = -2.71$, $p = 0.027$; in LESMR, $t_8 = -2.39$, $p = 0.044$; in SMR, $t_8 = -2.47$, $p = 0.039$; Control, $t_8 = -1.95$, $p = 0.11$, Table 5-12).

The decreased central theta power that is noted in the three non-control groups that were subject to actual SMR training supports the hypothesis. In addition, the decrease in theta power that is seen in the central region, which may belong to the disclosed somato-motor network (SMN; including pre- and post-central gyrus) of EEG resting state, with no change being noted for the control group that was not subject to actual NFT. The control group with non-contingent SMR feedback also showed a small, but statistically insignificant decrease in theta power, after mock NFT. Further discussion is presented in the following discussion section.

Furthermore, these results may be in line with the research of Ding et al (2011) in demonstrating a topological fractionation between perceptual and higher cognitive networks (Ding, et al., 2011), with the six RSNs partitioned into two groups: higher cognitive networks (the dorsal attention network and the default mode network, associated in the thesis with the frontal and parietal regions) and perceptual networks (the somato-motor network, the auditory network and the visual network, associated in the thesis with the central, occipitotemporal and occipital regions). The higher

cognitive networks of RSNs can be only enhanced by actual SMR training, as shown by the enhanced spectral power of the frontal and parietal regions. Figure 5-16 summarises the outcome pictorially. In the topographical map the frontal and parietal regions may be contrasted with the other three of the five regions. Alongside the map and connected to each of the five regions with their EEG derivations are five spectral graphs, one for each region. These graphs depict the statistical differences within the EEG spectra, delta to gamma, comparing the spectra before and following SMR training with the differences colour coded as indicated in the figure caption. Further discussion is presented in the following discussion section.

One channel SMR training with repetition of audiovisual feedback within 10 sessions, may decrease the perceptual networks of RSNs due to habituation (in both actual SMR and mock control groups, in line with the results of Ding's research), but the higher cognitive networks of RSNs can be only enhanced by actual SMR training. Even one channel SMR training can have an effect on the entire brain, because the RSNs can be altered to improve attention or higher cognitive function, after actual SMR training.

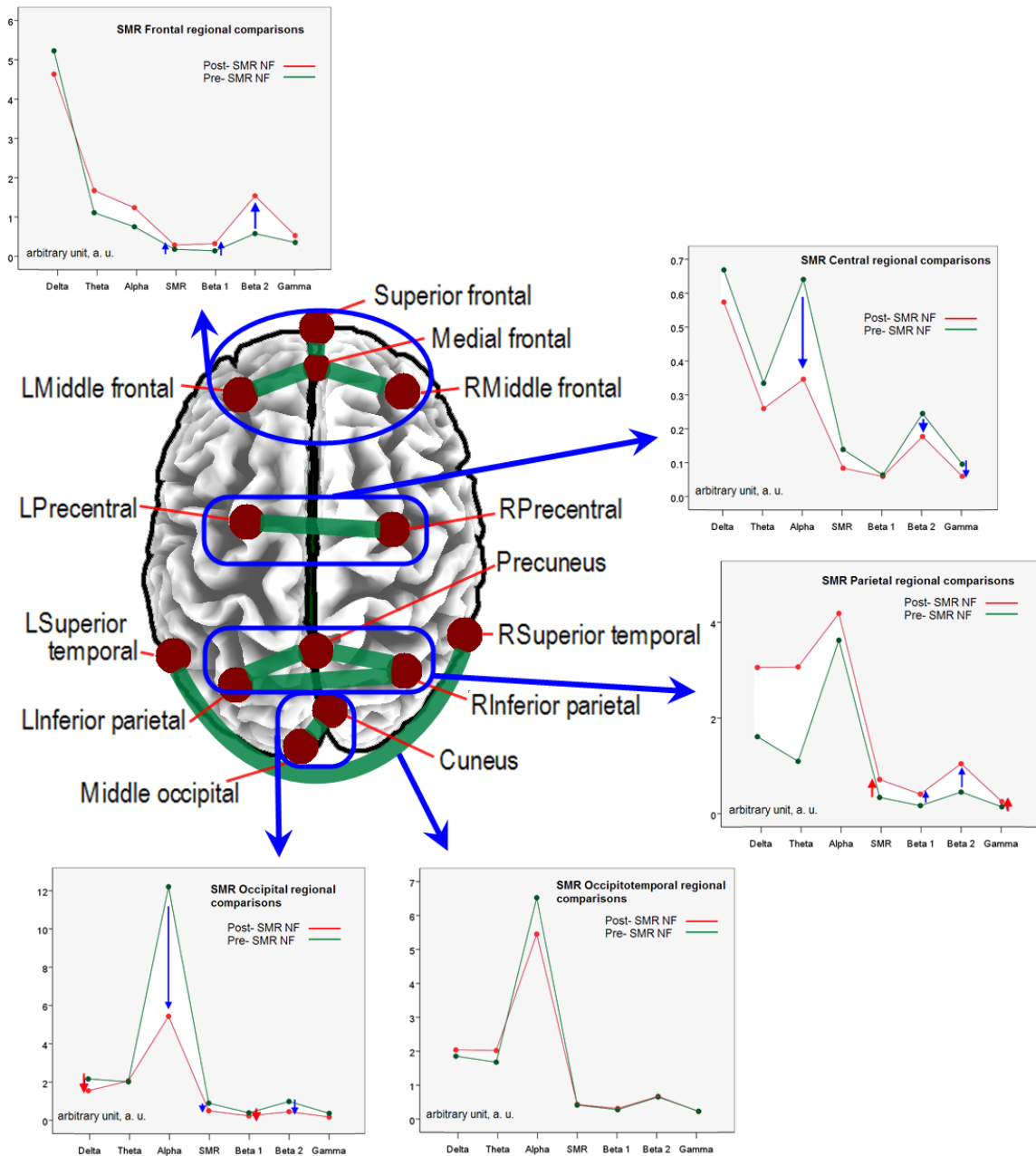


Figure 5-16. The total averaged power spectra within the 5 regions, pre- vs. post-SMR training, in the SMR group. The increase in the power spectra is shown in the frontal and parietal regions, post-treatment, with a reduction in the power spectra in the central, occipitotemporal and occipital regions. Blue arrows indicate $p < 0.05$; red arrows indicate $p < 0.005$ (Bonferroni corrected).

5.4 Discussion of Experiment Three

The primary purpose of Exp III was to investigate the effect of electroacupuncture stimulation combined with NFT. With a satisfactory outcome the combined protocol could form a plausible method for efficiently combining endogenous feedback with the application of exogenous stimulation to produce better behavioural performance or EEG outcome measurements than with NF alone. To the best of the authors' knowledge, the changes in specific EEG dynamics and enhanced attention performance resulting from combining NFT with EA stimulation have not yet been investigated. The relevant hypotheses are listed and discussed in the following subsections.

Hypothesis 1: Improved perceptual sensitivity post SMR training in conjunction with EA stimulation (pre- vs. post-training)

The results of this study, which show an upward trend in the d' scores in the three non-control groups post- SMR training, attributable largely to a reduction in commission errors, are in agreement with those of previous research on SMR-Theta training as a feasible method for enhancing executive attention (Egner and Gruzelier, 2001, 2004; Ros, et al., 2009). Learning to enhance SMR and reduce impulsiveness (commission errors) is in agreement with previous research on the treatment of hyperactivity (e.g., Arns et al., 2009; Vernon, 2005). However, the significant increase in the d' scores and the reduction in the number of commission errors, post-treatment, were only found in the SMR group after Bonferroni correction, compared to the control group.

In Exp III, EA stimulation was performed (15 minutes) before each SMR training session, followed by a three minute resting baseline period and then 20-mins of SMR/theta training, for the feedback period. The reduction in the number of commission errors made by the two groups with stimulation may be due to the short-term effect of EA stimulation in improving perceptual sensitivity and reducing the number of commission errors. The sustained stimulation effects from EA may not be reproducible in the Exp III without repetition of the visual attention task, as in Exp I, in each NFT session.

Another reason may be the error from randomized samples with an insufficient number of cases in each group (N=9, the total case number is 36).

Hypothesis 2: the use of SMR training in conjunction with EA stimulation to decrease theta activity in the baseline period in late-conditioning sessions vs. early sessions.

The participants in the AESMR group merely showed a trend toward an improved change in the baseline SMR/theta ratio (early vs. late conditioning), compared to the control group (analysed with Bonferroni correction). The AESMR and SMR groups also showed a trend toward a reduction in baseline theta amplitudes (early vs. late conditioning), compared to the control group (analysed with Bonferroni correction). The increased baseline SMR/theta ratio seemed to be mainly due to the decrease in the baseline theta amplitude. For healthy subjects the baseline SMR/theta ratio in SMR training may be considered as an index of cortical arousal level based on the description of vigilance stages (Sander, et al., 2010). The significant decrease in

theta activity in the resting EEG is considered to be associated with wakefulness (Bertini, et al., 2007; Strijkstra, et al., 2003). The vigilance stages refer to distinct states of global brain activation (Olbrich, et al., 2009), observable on a continuum, ranging from full wakefulness to sleep onset (e.g., Sander, et al., 2010).

Although a decrease in cortical theta power has been reported during activation of the attentional alerting network (Fan, et al., 2007), several studies of patients with ADHD have shown that less stable vigilance and an inferior continuous performance were associated with an elevation of theta activity and a decrease in fast (i.e. beta) frequency power (e.g., Arns, et al., 2009; Barry, et al., 2003; Sander, et al., 2010). Accordingly, this study supports the theory that SMR training reverses the theta/beta ratio and decreases low frequency activity. This concept is considered to be an elementary rule for the use of SMR training to treat subjects with ADHD. Based on the hypothesis of insufficient cortical arousal in ADHD patients, the use of NFT as a generic tool to stimulate cerebral arousal regulation for ADHD is considered to be "Efficacious and Specific" (Level 5), as noted in a meta-analysis (Arns, et al., 2009).

Given that SMR/theta training can influence the attentional performance of both healthy individuals (e.g., Egnér and Gruzeliér, 2001; 2004) and clinical populations (for example, ADHD; Fuchs, et al., 2003; Kropotov, et al., 2005; Monastra, et al., 2002), the exploratory and uncorrected results of this study's baseline EEG measurements support the idea that ten SMR/theta sessions of operant SMR training are adequate to improve healthy individuals' vigilance states of global brain activation following the significant reduction in the theta amplitude in the baseline period. This indicates that a plausible long-term effect is derived from SMR training using baseline EEG dynamics.

In contrast it may be relatively difficult to demonstrate a change in the baseline SMR amplitudes because SMR activity is easily induced during the feedback period, and this can result in a return to near baseline levels after the feedback period. For tiny changes in the baseline SMR amplitude (early vs. late conditioning in this study, table 5-4), the results for the change in the SMR amplitudes from the baseline to the feedback period imply that a notable change in the SMR amplitude was possible when SMR training was combined with AE stimulation (see also the discussion in the next section).

There was evidence of operant conditioning through a) the increase in the SMR/theta amplitude ratio, and b) the increase in the SMR relative amplitude, from early (sessions 2-4) to late (sessions 8 – 10) neurofeedback sessions. Healthy participants in the AESMR group were able to produce a more significant increase in the SMR/theta ratio (Bonferroni corrected) in the feedback period, while the LESMR and SMR groups merely showed a trend toward an increase in the SMR/theta ratio in the feedback period (early vs. late conditioning) compared to the control group. The AESMR group also showed a trend toward an increase in SMR_{relative} activity (uncorrected, early vs. late conditioning), compared to the control group.

The change in the SMR/theta ratios in the feedback period in the late sessions showed a significant increase in the SMR/theta ratio in the feedback period, which appeared to be due only to the effect of SMR training in conjunction with AE stimulation. There was a significant increase in the feedback SMR/theta ratio, but no increase in SMR or decrease in theta amplitudes by themselves. Whereas the increase in the baseline-to-feedback SMR_{relative} activity in the late sessions appeared to be mainly due to the ease of manipulation of the SMR amplitude.

The increased baseline-to-feedback SMR_{relative} activity for the three non-control groups when compared with the control group means that it was relatively easy to induce SMR up-training during the actual feedback period. However, it was also shown that the induced SMR returned to near baseline levels after SMR training, as evidenced by the small changes in the baseline SMR amplitude (early vs. late conditioning, Table 5-4). There was also a highly variable SMR amplitude over time in agreement with a report of the impossibility of maintaining a high amplitude in the SMR (μ) rhythm (Niedermeyer, et al., 2004).

Interestingly, the small change in baseline-to-feedback theta_{relative} activity means that both baseline and feedback theta amplitudes declined in the late sessions (vs. early, Tables 5-4 and 5-7). A plausible long-term mechanism for the effect of SMR/theta training effect may be explained via the successes of SMR/theta training in improving wakefulness and vigilance, due to a decrease in the theta amplitudes in the baseline resting EEG and in enabling further cognitive processing and attention (see also the discussion in the next section).

The effect of protocol-specific EA stimulation on the EEG outcome measurements

The results for the AESMR group are in line with the decrease in theta during high frequency EA stimulation that is mentioned in the 2006 study by Andrew Chen et al. and the improvement in sustained attention and longer lasting effect of stimulation, after AE stimulation, in the 2001 study by J-L Chen, et al. (Exp I in this thesis). In addition, a prolonged effect for activated CNS neurotransmitters, post acupuncture stimulation, has also been reported (e.g., Dhond, et al., 2008; Han, 2004,

which provides an impetus for the study of SMR training in conjunction with EA stimulation.

However, Exp III shows that EA with alternating frequencies is not significantly beneficial to SMR training to achieve an impact on attention after ten training sessions. In addition, the use of EA with low frequency stimulation seems to have no effect on either behavioural results or SMR/theta EEG measurements. While low frequency EA may not be beneficial to SMR training, it may be a better choice for assisting alpha up-training, because it increases alpha activity (Chen et al., 2006). To validate this hypothesis that alpha NFT is assisted by low frequency EA stimulation in enhancing EEG alpha activity a further combined study would be required.

In the protocol for this study, the control group with non-contingent SMR training was subjected to mimicked EEG signals derived from real SMR training. While this may induce an inattention state in subjects there was no evidence of any training effect for mock SMR feedback in changing brain activity, which is compatible with this study's hypothesis in relation to mock training.

The increase in beta power in the attention network in the frontal region and the decrease in theta power in the somato-motor network in the central region (pre- vs. post- SMR training) supported hypotheses 5 and 6, and a long-term effect on attention and vigilance, due to SMR training.

The conventional EEG (pre- vs. post-training) did not reveal any significant improvement in the relevant EEG spectral power in related cortical regions, for each group, possibly due to a combination of underlying source activity and volume conduction (Congedo, et al., 2009). Thus, based on the methods and outcome of Exp

II, which investigated ICA-derived EEG functional connectivity, group ICA revealed five statistically clustered regions.

As in Exp II, Exp III demonstrated the previously reported cortical location of these ICs to be spatially well-defined “sources” (Pascual-Marqui, et al., 2002), in the eyes-closed resting EEG networks, pre- and post-NFT.

All of the components of both pre- and post-NFT in the resting EEG recordings demonstrated high repeatability across subjects with strong cortical source locations (Figure 5-13), in support of hypothesis 5. The consistency in the cortical localization of components in healthy individuals, in the resting EEG may be due to the absence of experimental stimuli (for a review see Onton, et al., 2006). Importantly, these findings are critical to future investigations of the EEG power-associated spectral analysis of ICA components, based on the estimated EEG resting-state connectivity, because they represent the spatially segregated, unmixed EEG sources as functional nodes in electro-cortical networks. Extracting source-level information from EEG data by ICA decomposition allows the use of EEG imaging as a truly functional 3-D cortical imaging modality, with high temporal resolution and adequate spatial resolution for the study of distributed macroscopic cortical brain processes that support both normal and abnormal behaviour and experience (e.g., Chen, et al., 2012; Delorme, et al., 2012).

In line with the resting state networks disclosed by fMRI studies (Toro, et al., 2008; Van Den Heuvel and Hulshoff Pol, 2010) and the results of Exp II (Chen, et al., 2012), the results were consistent with fMRI resting-state network (RSN) reports of regions that show the functional connectivity patterns for the DMN across resting states (Fox, et al., 2005; Fransson, 2006; Yan, et al., 2009), and those with strong

anatomical connectivity (Honey, et al., 2009; Honey, et al., 2007). Importantly, the increase in frontal beta power noted in the groups who were subject to SMR training supports hypothesis 6. The attention-related beta power in the frontal region, which belongs to the revealed dorsal attention network (DAN), in the EEG resting state is related to the effect of NFT on attention, for the three non-control groups who were subject to actual NFT, but there was no change in the control group that was not subject to actual NFT. These results are also in agreement with the report of Mantini et al. (2007), which showed that DAN has a stronger relationship with alpha and beta rhythms (Mantini, et al., 2007). Another type of NFT that uses low-resolution brain electromagnetic tomography (LORETA) also produces an increase in beta power in the area of the anterior cingulate cortex (ACC), after training (Cannon, et al., 2009; Cannon, et al., 2007; Congedo, et al., 2004). Subjects were able to increase beta power in the ACC and adjacent areas, but no increase was detected in more distant locations (Cannon, et al., 2009). It is seen that the control group with non-contingent mock SMR feedback shows no improvement in beta power, post- mock NFT.

Recent studies of the EEG spectrum support a re-assessment of ADHD and beta activity in the frontal region. For instance, an ADHD patient's distinct EEG clusters are characterized by increased high amplitude theta and a decrease in beta activity (Chabot, et al., 2005; Clarke, et al., 2001). Therefore the hypothesis that an improvement in beta activity in the frontal region, caused by SMR training, is theoretically confirmed and is already being used to treat ADHD in clinics, without much controversy.

With regard to the role of theta in the resting EEG, the decrease in central theta power that was noted in the three groups that were subject to actual SMR training

supports hypothesis 6. This was, in the central region which may belong to the disclosed somato-motor network (SMN, including pre- and post-central gyrus). These resting results are in agreement with the research on vigilance or wakefulness, which notes that high theta power may indicate a disposition for falling asleep (Bertini, et al., 2007; Strijkstra, et al., 2003; Tanaka, et al., 1997).

Interestingly, some previously published reports have also illustrated a significant increase in SMR activity during the actual training period, but showed a decrease in SMR, post-training in the eyes-closed resting EEG state, in healthy humans (Doppelmayr, et al., 2009; Egner, et al., 2004), and even in patients (e.g., Gevensleben, et al., 2009b; Kropotov, et al., 2007; Pineda, et al., 2008). The surprising effect of SMR training on central SMR activity is also evident in the results for the three non-control groups (Table 5-12). However, an opposite tendency towards an increase in SMR was evident for the eyes open condition, after NF training, indicating high variability in SMR amplitude, over time, regardless of the protocol used for training (e.g., Cho, et al., 2008; Doppelmayr, et al., 2009). Furthermore, a reduction in SMR and theta power may imply networks specific to the central and occipital regions, different from the increases noted for other spectral power bands in the frontal and parietal regions in RSNs. These results may be in line with the research of Ding et al (2011) in demonstrating a topological fractionation between perceptual and higher cognitive networks (Ding, et al., 2011), with the six RSNs partitioned into two groups: higher cognitive networks and perceptual networks.

According to Ding's research, single channel SMR training with repetition of audiovisual feedback, for ten SMR training sessions, as in this study, may decrease the perceptual networks of RSNs, due to habituation, which is demonstrated by a

decrease in the spectral power of the central, occipitotemporal and occipital regions of both actual SMR and control groups. However, the higher cognitive networks of RSNs can be only enhanced by actual SMR training, as shown by the enhanced spectral power of the frontal and parietal regions (Figure 5-16).

Just single channel SMR training can enhance the higher cognitive networks of RSNs, via actual SMR training. In other words, even single channel SMR training can affect the entire brain, in view of the alteration to RSNs caused by enhanced frontal beta power and the resulting improvement in attention or higher cognitive functions, after actual SMR training.

The effect of protocol-specific EA stimulation on the EEG resting networks

Reduced theta activity has been reported during high frequency electrostimulation on the hands due to exogenous stimulation (Chen et al., 2006). In addition, besides the instant effect, a prolonged effect has also been reported (e.g., Dhond, et al., 2008; Han, 2004), and which demonstrated the effect of acupuncture on the RSN or DMN (e.g., Dhond, et al., 2008) and provided the stimulus for SMR training in conjunction with EA stimulation. The results for the combined groups (AESMR and LESMR) demonstrated that the different stimulation protocols produced changes in EEG RSNs similar to the protocol that used only SMR training. It is also important to emphasize that all of these three protocols produced probable long-term effects on the attention network and an increase in frontal beta power in the attention network in the resting EEG.

In agreement with previously published reports of the changes in spectral EEG topography after SMR training (e.g., Egner, et al., 2004), this study's initial traditional resting EEG analysis of all protocols still demonstrated a non-significant change in EEG, after NFT. However recently, there have been successes in using frequency-domain ICA or ICA power spectra to decompose the spontaneous EEG data, which have yielded appropriate methods for the decoding of the resting EEG, with good resolution of cortical activity and localization (e.g., Chen, et al., 2012; Hyvarinen, et al., 2010). Using the 13 components decomposed and their power spectra in the five circumscribed (alpha-synchronized) functional regions beta power (beta 1 and beta 2) was significantly increased in the parietal and frontal regions of the three SMR groups. These involved the frontal and parietal regions of the RSNs which are related to the dorsal attention networks, and evidence a change in the baseline EEG, compared to the non-contingent mock SMR training (control) group, which demonstrated no increase in frontal beta power.

Interestingly, beta 1 and beta 2 activities were enhanced in both SMR alone and EA stimulation groups without extra benefit from EA. In addition, the significant improvement in attention only in the SMR group did not match the increased beta 1 and beta 2 activities of frontal regions in the resting EEG for the latter occurred in all three experimental groups. An increase in beta activity subsequent to SMR training has been also reported in clinical studies. These studies involved subjects with abnormally low levels of beta band activity prior to training (Lubar and Lubar, 1984; Monastra, et al., 2002). Therefore, the mismatched behavioural and electrophysiological results in this thesis may be due to the insufficient number of participants for the separated groups, and for importantly due to the difference

between healthy subjects and patients. The previous study, which used only EEG spectral methods with resting EEG, may not have been sensitive enough to fully capture the effect of an increase beta activity caused by SMR in healthy subjects (e.g., Egner et al., 2004).

5.4.1 Limitations and future studies

This study has potential limitations, or at least issues that warrant further examination. Firstly, the optimal period for stimulation that putatively generates neuromodulation effects to assist NFT is still unknown. The predicted post stimulation period was around a minimum of 30 minutes, for this study, which was the duration of a training session. This duration is similar to that used for the study by Claydon et al. (2008), which used pressure pain threshold (Claydon, et al. 2008). However, the optimal period for the use of EA stimulation with NFT and its effect during EA stimulation was not evaluated. The design used in this study, with EA and then immediate SMR training for subjects, may be a feasible method according to the exploratory and uncorrected approach, but it still needs further studies with a sufficient number of cases to achieve the statistical significance via Bonferroni correction. Stimulation within the feedback period is not recommended, because stimulation directly interferes with EEG measurements. For example, the mu rhythm (8-15 Hz) can be inhibited by stimulation of the human hand (Cheyne, et al., 2003).

The optimal sites for influencing cognition have not been systematically examined. HeGu (Li4) and NeiGuan (P6) on the hands are well studied acupoints but

other acupoints such as Zusanli (St36) and Taichong (Liv3) on the legs, might be helpful in improving cognitive function. Thirdly, several neurotransmitters are also believed to contribute to the attention and memory systems (Boulougouris and Tsaltas, 2008; McNab, et al., 2009; Muller and Carew, 1998). It is not clear, however, to what extent these neurotransmitters are involved and how they are coordinated with each other during and after electrical stimulation and with NFT. Further research will be required to investigate the relationship between the behavioural and EEG measures and functional networks and neurotransmitters for the application of EA to assist NFT which might prove fruitful in healthy participants and patients.

There was an absence of parallel effects of the training protocols on d-prime and the EEG which requires further investigation with larger groups of subjects.

Although Ding's model wherein six RSNs are partitioned into two groups, higher cognitive networks and perceptual networks, was suitable for interpreting the effect of actual SMR training versus the mock SMR training in healthy subjects, studies on patients would be worthwhile for treatment implications of NFT. Additionally, the claimed long-term effect of NFT requires further study to prove the assumption that post-NF EEG activity demonstrates a possible long-term effect in both healthy subjects and patients.

5.5 Summary

In conclusion, this study provides some new evidence of a significant improvement in perceptual sensitivity, and changes in EEG measures and attention networks in the RSNs of healthy subjects through the use of SMR training in conjunction with electrostimulation, when compared with the effect of non-contingent mock SMR training. The attention performance benefits that were caused by actual SMR training are compatible with the results of previous published research, showing the efficacy of SMR in the reduction of both impulsive commission errors and perceptual sensitivity (d'). There was a significant increase in the SMR/theta ratio in the feedback period from early to late conditioning sessions, which implied the success of the SMR training in conjunction with alternating frequency electro-stimulation. Referring to the EEG measures and the behavioural results, the latter were stronger with SMR training alone compared with the combined protocols. However, the EEG results also demonstrated the possible advantages of SMR training in conjunction with electrostimulation.

Finally, with repetition of audiovisual feedback within 10 sessions, SMR training using single channel Cz EEG data may decrease power in the perceptual networks of RSNs, due to habituation in both the actual SMR and control groups, whereas the higher cognitive networks of RSNs that disclosed increased frontal beta power were only enhanced by actual SMR training. Even single channel SMR training can affect the entire brain and the attention network of RSNs in enhancing attention or higher cognitive function.

6.1 Evaluation of Results in Relation to the Aims of the Thesis

The ultimate aim of the experimental work for this thesis, as described in chapter 2, was to investigate the feasibility of neurofeedback protocols assisted by EA stimulation, in healthy populations. SMR training and SMR combined with EA protocols may produce significant effects on attentional performance, along with electrophysiological mediation. The results pertaining to these issues were evaluated by considering the different EA modes of alternating and low frequency stimulation, which had been shown to produce clinical benefits by others, NFT effects and EA frequency-specific effects from the combined strategies (NF + EA). The proposed ICA-derived EEG dynamics for evaluating the effect of the resting states and attention networks of EEG and NFT on EEG dynamics are discussed and summarised within this chapter.

6.1.1 Transcutaneous electrical acustimulation and frequency modulation

One aim of this thesis was to examine whether electroacupuncture stimulation, using alternating frequencies on pairs of acupoints on both hands, resulted in significantly better sustained behavioural performance and sustained cortical activation in a repeated visual continuous attentional performance task than low frequency stimulation, which in turn was superior to placebo. The use of any EA protocol to improve attentional performance in healthy participants had not previously

been addressed in the research literature. Exp I, with the single-blind randomized placebo-controlled design, provided convincing evidence of sustained attentional performance and sustained cortical activation in a repetitive visual attentional performance task. The results of Exp I, which showed improved d' scores because of a decrease in the mean number of commission errors, was compatible with a significant decrease in the motor inhibition component both during stimulation and post stimulation in the AE group, the one that received electroacupuncture stimulation with alternating frequencies. Theoretically, this ERP component reflects motor impulsiveness (Bokura, et al., 2001b; Kropotov, 2009a; Smith, et al., 2008). However, low frequency stimulation at 5 Hz showed only short-lived benefits during stimulation.

Therefore, EA with alternating frequencies may be an adjunct that helps healthy adults to successfully enhance their sustained attention and inhibit competing motor responses; this indicates a potential therapeutic benefit for psychiatric disorders that result in compromised attention and cognition. For other clinical practices, EA may also be an important adjuvant for treatments in the fields of pain control (Tong, et al., 2007) and in neurotherapy (Hirshberg, et al., 2005).

Furthermore, the real EA stimulation and control groups showed significant differences in the decomposed ERP processes relevant to a range of behavioural functions (visual comparison, P400 monitoring, working memory and passive auditory P300). Firstly, a decrease in activity attributed to habituation was observed in the control group with the placebo stimulation, when comparing the baseline with the pre-stimulation and post-stimulation periods. Interestingly, the absence of habituation in the experimental groups suggests a potentially successful activation that prevents

habituation after EA stimulation. Secondly, the different effects of stimulation for the real and placebo stimulation on the same sites (acupoints on the hands), without changing the topography of the regional loci disclosed by ICA, showed that the placebo stimulation was a useful control for the study of brain function and associated acupuncture effects, which is in agreement with prior research on EA that used placebo groups (Chao, et al., 2007; White, et al., 2004).

Thus the results of Exp I demonstrate the success of the design with two real EA stimulation modes (AE vs. LE) and one control placebo stimulation (SE), because of both the sustained change in the motor inhibition component, and decreased impulsivity (commission errors) contributing to increased perceptual sensitivity (d') in healthy subjects. All of these associations, shown details in the chapter for Exp I, section 3.4, are new findings and appear to be compatible with the nature of EA stimulation protocols (Han, 2004). These findings have been published (Chen et al, 2009).

While in Exp III the corresponding learning indices (TOVA measurements, omission errors, commission errors and d') and the measurements of SMR EEG-biofeedback (SMR/theta ratio in baseline and training period, relative and baseline power of SMR and theta waves) showed no disruption of the NFT effect from EA stimulation, the results in Exp III showed that there was no advantage following EA and no added value in adding EA to NF. These results for the groups with SMR assisted by EA do not support the hypotheses, possibly due to the error from randomized samples because of an insufficient number of cases in each group. The results of Exp I and III generally share the assumption that EA will only have a short-term effect.

In summary, this thesis demonstrates the general feasibility of combining EA stimulation with an NFT protocol, in order to capitalise on both endogenous neurophysiological responses and exogenous stimulation. However, some evidence suggests that, at least in healthy participants, following NFT resting EEG and attention ERP components may be modulated within and after sessions (Egner and Gruzelier, 2001; 2004; Doppelmayr, et al., 2009; Kropotov, 2009a; Kropotov, et al., 2007). The refinement of such exogenous EA stimulation for learning indices requires future replication of these documented relationships with a higher number of cases than used here and maybe with high density EEG recording instrumentation than that supplied by the hardware and software used in this thesis.

6.1.2 ICA-based EEG functional connectivity in the resting state

Although recent independent component analysis (ICA) of EEG-fMRI studies has explained spatiotemporal synchronous patterns and neuronal sources at rest (Laufs, et al., 2008; Mantini, et al., 2007), little is known about the changes in EEG dynamics that occur within the attention network post NFT.

Based on a significant change of occipital alpha activity in the EEG, from EC to EO, significant differences were noted in ICA-based EEG power spectral distributions, between EC and EO states. The methods used in Exp II effectively integrated information to construct functional networks and demonstrated changes in EEG dynamics, from EC to EO. Prior studies have shown patterns of functional connectivity across subjects (e.g., Congedo, et al., 2009; Dosenbach, et al., 2007), or used formulae that were too complicated to allow analysis or to apply in clinics (e.g.,

Gomez-Herrero, et al., 2008). In addition, some previous reports illustrating the distribution of scalp EEG power in relation to anatomical or functional connectivity in the RSN (e.g., Chen, et al., 2008) did not address the bias from the volume conduction which masks the underlying source activity (Nunez and Srinivasan, 2006). Therefore, Exp II was designed to minimize the bias from volume conduction and to find sources that were correlated with rhythmic activity, in order to outline the ICA-based EEG power spectra and functional networks.

Exp II provided a series of steps to describe five groups of functional networks, which were constructed from 12 independent components (ICs) of the ICA-based EEG activity in both EC and EO resting states. These network groups demonstrated not only anatomical connectivity, but also electrophysiological mechanisms. Unsurprisingly, the alpha rhythm was the most prominent EEG rhythm during the conscious resting state and it formed the basis for the analysis of the ICA-based EEG RSNs cluster groups. The merged sLORETA figures suggested both anatomical connectivity and electrophysiological associations between the clustered groups in Exp II. Among other implications of this research were that, firstly, the procedures may be easily applicable to patients without clear consciousness, for task-oriented ERP examination. Secondly, it is possible to compare the DMN, RSN, or functional networks in the EEG with fMRI. Thirdly, because of the high correlation between the task-negative network (DMN) and the task-positive network (dorsal attention network) found in fMRI (Uddin, et al., 2009), the effect of SMR training on the resting EEG (Egner, et al., 2004; Ros, et al., 2010) and its spectra in the different cortical regions related to the attention network demonstrates that it is an effective new method of

investigating electrophysiological outcome following SMR training (more details in the next section on neurofeedback training effects).

In summary, although this study did not undertake an examination of EEG recordings in resting state, or with stimulation, along with corresponding fMRI analyses, the method proposed in Exp II provides an important practical method for the study of synchronised rhythmic activity in cortical regions. Theoretically, evidence of resting EEG dynamics, pre- vs. post- NFT can be interpreted using this ICA-based EEG power spectra analysis, more effectively than through the use of traditional EEG topography. These results have been published (Chen et al, 2012).

6.1.3 The effect of Neurofeedback training and electrocortical findings refined by the ICA-based approach

One of the major goals of this thesis was to establish measurable variables that are compatible with healthy subjects' behavioural performance and electrocortical activation, compared to those for mock NFT (a pseudo-NFT). In order to identify the general effect of training, the electrocortical and behavioural dependent variables of the experimental groups were evaluated, pre- and post-training. The changes in the variables were then compared with the findings for the non-contingent NF group, using the methods of Exps II and III. Exp III demonstrated the significant effect of SMR training in healthy subjects, as noted in previously published articles (e.g., Egner, et al., 2004; Ros, et al., 2010).

In establishing the ICA-based approach, Exps II and III showed the possibility of combining ICA, time-frequency analysis, sLORETA, MDS and graph theory to

investigate the resting state EEG. Thirteen ICs represented five groups of functionally connected cortical regions, based on the high correlation coefficients for alpha power, in the eyes-closed (EC) state. Therefore, the decomposition of the EEG into ICs produces valid ICs for cortical functional connectivity, in Exps II and III. Moreover, the consistency of these ICs demonstrated simple and concise procedures for analysing the cortical localization of components in healthy individuals not subject to experimental stimuli (for review see Onton and Makeig, 2006; Onton, et al., 2006). Therefore, any significant effect of SMR training on attention, which was predicted but not found in the resting EEG topography, might be shown in the ICA-based resting EEG networks, as was the case. These results disclosed enhanced beta power, from parietal to frontal regions, in support of an improvement in the dorsal attention network.

The major reason why the effect of training was not present in previous EEG studies (e.g., Egner, et al., 2004) is possibly because of volume conduction and underlying source activity. Thus this new ICA method, using the blind source separation, may significantly reduce ambiguity in depicting an effect.

Furthermore, Exp III also provided additional evidence for the significant effect of SMR training on electrocortical and behavioural outcome variables in healthy subjects. Firstly, Exp III showed that a course of SMR produced significantly improved dorsal attention networks in the EEG (electrocortical variables), which were compatible with positive perceptual sensitivity (behavioural variables of sustained attention) and the increased SMR/theta ratio during the training sessions carrying over to subsequent session baselines. Evidently, no such results were noted for the group with pseudo-NFT. Crucially, these training effects are not attributable to practice or

motivational factors for the control group with pseudo-NFT were subject to similar audiovisual feedback training. The results for the pseudo-NFT group showed no significant changes in any of the variables that were assessed in the attention task.

From these results it is concluded that this thesis provides strong evidence of the significant effect of SMR training on electrocortical activation and attentional performance in healthy subjects compared to the use of pseudo NFT.

6.1.4 Does EA stimulation have a measurable effect in assisting SMR training?

This thesis also aimed to investigate whether EA stimulation had a significant effect on NFT and to identify any EA frequency-specificity in healthy subjects. In Exp I, by means of mixed-design ANOVA, used to examine the effects of Group (AE, LE, SE) and Time (before, during and after acustimulation) on behavioural measures, the findings overall had indicated that stimulation with alternating frequencies was superior to low frequency stimulation, in producing a sustained effect during the task, a benefit, which continued post-stimulation. In contrast, low frequency stimulation, while effective during stimulation, did not produce sustained benefits.

In Exp III the method for analysing the resting EEG used in Exp II was applied in order to properly validate any change in cortical activity after SMR training, compared to the prior reports of the traditional EEG after SMR training (Egner, et al., 2004). The use of ICA to decompose the ERP data in Exp I appeared a promising method to decode the resting EEG and to provide good resolution of the cortical activity and localization. The cortical changes resulting from three NFT protocols in

Exp III were also investigated with respect to electrophysiology, compared to the control group.

However, the data from Exps I, II and III did not clearly show the frequency-dependent effect of EA on the two SMR training-assisted-by-EA protocols (AE+SMR and LE+SMR). Exp III did not provide further significant evidence for the different effects of the AE+SMR and LE+SMR protocols on measurements of attention, compared to SMR-alone training. Whereas the SMR-alone training resulted in an increase in d' and a significant reduction in commission errors, SMR training followed by AE stimulation did not show additional benefits on the same attention task.

On the other hand, in terms of the potentially reliable effect of SMR training on spectral EEG topography, the initial analysis of traditional spectral electrocortical measures, which compared the different effects of different NF protocols on resting EEG, provided no significant evidence for EA frequency-specific effects on EEG measures. In Exps II and III, in the three groups that were subject to actual SMR training, in the resting ICA-based EEG power spectra during the eyes-closed resting condition beta power (beta 1 and beta 2) showed significant increases, from parietal to frontal regions. The frontal and parietal regions of the RSNs involved in the EEG were found to be closely related to the dorsal attention networks, providing evidence of a relation between resting EEG activation and increased attentional performance. Whereas SMR training resulted in significantly enhanced frontal beta power (beta 1 and 2), pseudo-SMR training was not related to a change in the power of frontal beta.

Increments in beta activity, subsequent to SMR training, have been reported in clinical studies. These investigations involved subjects with demonstrably abnormally

low levels of beta band activity, prior to training (Lubar and Lubar, 1984; Monastra, et al., 2002). The probable reason for the ease with which a change in beta was detected in clinical cases with low levels of beta power after NFT is the relatively larger change in the amplitude of the beta band activity, in these patients, compared to healthy subjects. Therefore, previous studies, which used only EEG spectral methods in resting EEG, may not have been sensitive enough to fully identify the effect of SMR on increasing beta activity, in healthy subjects (Egner, et al., 2004). Using the same conjecture, the use of behavioural dependent variables in reports on NFT may be sufficient to determine the potential effect of NF on such measures, but insufficient for the situation of combining EA stimulation and NF in healthy subjects. This theoretical treatment of the important issue of the mediating effect of combining endogenous and exogenous factors on behavioural change has not been presented in previous research.

In summary, this thesis significantly provides evidence for SMR training effects on electrophysiology and on behavioural change, compared to the control group with the pseudo-NFT. The electrophysiological effects on attentional networks with enhanced beta power mainly appear to be underpinned by NFT-specific electrophysiological effects mediating behaviour, and apparently attributable to factors inherent in SMR contingencies training, rather than practising and concentrating on a computer screen.

6.2 Implications of this Thesis

Although the results of the studies that constitute this thesis are discussed and presented without strong supportive evidence for a significant, EA frequency-specific effect on SMR training in healthy subjects, the demonstration of SMR training satisfied, in part, the goal to explore the mechanism of SMR training. Further research on the EA effects on SMR are required to prove this assumption, in accordance with the underpinning mechanism and the theoretical framework in both healthy subjects and patients.

The impact of the results on the theoretical conceptualisation of the EA stimulation and SMR neurofeedback paradigms, on the evolutionary method of studying ICA-based resting EEG networks, and on the combination of NF assisted by EA, is discussed separately in the following subsections, followed by some comments on methodological limitations and future research possibilities.

6.2.1 Transcutaneous Electrical Acustimulation and its application

The results of Exp I encourage the future use of EA with different frequencies in order to study brain function and associated effects on attention. In clinical practice it is important to obey the guidelines for safety. The acupoints around hands and wrists and the distal acupoints located on upper limbs require proper settings to avoid adverse effects in clinical application, as recommended by the British Medical Acupuncture Society (BMAS). In addition, the safety of the design, using a pair of acupoints on each hand in Exps I and III, has been reported in a recent study which claimed that electrical fields generated by pairs of needles below the knee or elbow do

not create a detectable spread of current along the limb or into the chest (Thompson and Cummings, 2008). In particular, electroacupuncture should not be applied such that the current is likely to traverse the heart, for example, from one shoulder to the other shoulder. Therefore the paired HeGu and NeiGuan (LI-4 and P-6) acupoints used in the thesis were not only effective, but also a safe method of studying attention, compared with methods used in previous published research or clinical trials which used the proximal location of the limbs, paraspinal muscles and neck or head regions (e.g., Luijpen, et al., 2005; van Dijk, et al., 2002).

Notwithstanding the beneficial outcome on sustained attention for safe peripheral stimulation that was demonstrated, this section must address some issues that will be relevant to future research, especially for the combined stimulation and feedback methods. Firstly, the prolonged period of the neurobiological effects on attention generated by stimulation remains unknown. Empirically the most effective post stimulation period was a minimum of 30 minutes in this study, which is similar to the report of Claydon et al. (2008) which used a pressure pain threshold. However, for post stimulation to assist NFT, the optimal period post stimulation is still worthy of study. Secondly, the optimal sites for influencing cognition have not been systematically examined. Although HeGu (Li4), NeiGuan (P6), Zusanli (St36) and Taichong (Liv3) have been reported to be possible sites for improving cognitive function (e.g., Hui, et al., 2005; Yan, et al., 2005), the optimal sites both for influencing cognitive function and for aiding NFT still require further research. Thirdly, the associated mechanism at the neuropeptides level is still not well understood, although several neurotransmitters, such as endorphins, serotonin, and dopamine are believed to influence attention and memory systems (e.g., Boulougouris

and Tsaltas, 2008; McNab, et al., 2009; Weizman, et al., 1987). Further research should be conducted to combine the behavioural, electrophysiological and neurochemical modulation measurements, in order to study these methods with combined NFT and EA stimulation.

In summary, not only do the EA studies in this thesis provide sufficient evidence for an immediate effect on healthy subjects' attention, as characterised by significant changes in behavioural attention performance in the repetitive visual attention tasks of Exp I, but also the results for behavioural attention performance are in agreement with the idea that EA aiding SMR training is a viable model of cognitive training or therapy for clinical populations with attention disorders.

6.2.2 SMR training

In the review section regarding NF protocols studied in clinics, SMR training has developed from the most elaborate empirical and theoretical studies (see the Introduction section, 5.1). The role of SMR operant conditioning in controlling seizures and in studying the physiological basis of the rhythm, in both animals and humans, has been the subject of extensive research (Serman, 1996; Serman and Egner, 2006). However, the impact of SMR training on healthy subjects remains equivocal. More specifically, the effect of SMR training on both impulsive and inattentive aspects of attention disorders seems to be possible, through a direct impact on sensorimotor excitability and an indirect impact on sensory-cognitive integration by means of reduced motor interference (Egner, 2002). Previous research on the SMR protocol with no adequately designed control group has been an impediment to its

further development in clinical usage and research (Shouse and Lubar, 1979; Tansey, 1984, 1985, 1986).

Therefore firstly, this thesis has tried to bridge the gaps between the empirical literature and theoretical ideals, by attempting to enhance the specific effects of SMR training on the outcome EEG measurements for SMR training and improved perceptual sensitivity, with decreased errors of attention. Secondly, compared with a pseudo-neurofeedback control group, a significant increase in cortical activation is illustrated (see the Method section, section 5.2). Thus, Exps II and III provide evidence for the effect of SMR on behaviour and electrophysiology. The NF-related changes are more easily seen in EEG reactions (ERPs, ERDs and during NFT periods), but not in the resting EEG spectrograms (Kropotov, et al., 2007). Spectrograms are more variable than ERPs/ERDs, especially because of individual variations in spectrograms, and therefore significant changes in spectrograms may not be evident due to large standard deviation. In addition, NF may indeed change only the reactivity of the brain to certain stimuli in certain conditions (situation-specific preparation during training and immediately after training).

The implied links between attention and the increased resting beta activity in the dorsal attention (frontoparietal) networks and the decreased theta activity during training periods and the resting state are discussed in the following paragraphs.

Importantly, an increase in beta activity subsequent to SMR training has been reported in clinical studies, as well as in studies of healthy individuals. Another type of NFT was developed by Congedo et al. (2004), which used low resolution brain electromagnetic tomography (LORETA) – NF, to increase beta power in the area of the anterior cingulate cortex (ACC) after training (Cannon, et al., 2009; Cannon, et al.,

2007; Congedo, et al., 2004). The results indicated that the subjects were able to increase beta power in the ACC as well as in adjacent areas, but no increase was detected in more distant locations (Cannon, et al., 2009).

In contrast to the control condition in Exp III, the NFT with actual SMR was accompanied by a significant reduction in theta activity in the central region of the resting EEG (e.g., theta/beta training with a tendency toward a decrease in the posterior-midline theta activity; Gevensleben, et al., 2009b). In addition, a recent study related to ADHD has reported that impaired functional connectivity within brain attention networks may contribute to this disorder (Mazaheri, et al., 2010). More results from EEG spectra also support a re-conceptualization of ADHD, based on the CNS abnormality that underlies the disorder, rather than the behavioural profile of the child (Clarke, et al., 2002). ADHD patients' distinct EEG clusters are characterized by increased high amplitude theta, with a deficiency in beta activity (Chabot, et al., 2005; Clarke, et al., 2001). Evidently, in terms of beta and theta activity, the straightforward effect of SMR training on these relevant frequency bands may alter the EEG rhythmic bands, allowing the theoretical application of SMR training to treat ADHD in clinics.

With regard to the role of theta in the resting EEG, a significantly decreased theta activity in the central region was also found in real SMR groups, but not in the pseudo-NF group. Some previous SMR studies have already reported that the same setting of the SMR/theta protocol is associated with significantly increased perceptual sensitivity in the attention task (e.g., Egner, 2002; Egner and Gruzelier, 2004; Egner, et al., 2004). In fact compared to SMR with theta activity in the training period, the decreased theta amplitude has a greater contribution to the SMR/Theta ratio than the increased SMR. Therefore, the significant decrease in theta activity in the resting EEG

and during the NFT period is considered to be a characteristic of wakefulness in healthy subjects (Bertini, et al., 2007; Strijkstra, et al., 2003). Several studies of patients with ADHD have shown that less stable vigilance and a worse continuous performance test associated with an elevation of theta activity and a decrease in the power of fast (i.e. beta) frequencies (e.g., Arns, et al., 2009; Barry, et al., 2003; Sander, et al., 2010). Therefore, in line with the theory that NFT reverses the ratio (to increase fast and decrease low frequency activity), the concept is an elementary rule for the treatment of subjects with ADHD. Based on the hypothesis of insufficient cortical arousal in those patients, NF as a generic tool to stimulate cerebral arousal regulation for ADHD is "Efficacious and Specific" (Level 5) in a meta-analysis (Arns, et al., 2009).

The SMR/theta ratio in the SMR training should be considered as an index of cortical arousal level, based on the description of vigilance stages (Sander, et al., 2010). The vigilance stages refer to distinct states of global brain activation (Olbrich, et al., 2009), observable on the continuum ranging from full wakefulness to sleep onset (e.g., Sander, et al., 2010). Importantly, during the transition from resting conditions, from eyes-closed to sleeping, a gradual reduction in alpha power and a gradual increase in theta power occurs (Strijkstra, et al., 2003). Therefore, even a simple awake eyes-closed EEG could demonstrate a positive relation between theta power and sleepiness. In fact, high theta power may indicate a high motivation for sleep, because it follows the increase in alpha power that occurs during sleep entry (Bertini, et al., 2007; Strijkstra, et al., 2003; Tanaka, et al., 1997).

Surprisingly, it was found that SMR training is associated with a relative reduction in post-training SMR activity in the EC resting EEG, which implies a link

between this reduction in resting SMR activity and the reduction in the number of commission errors (Egner, 2002; Egner, et al., 2004). It has been suggested that rather than leading to permanently robust levels of SMR activity, this training may be correlated with an improvement in control or may facilitate more efficient circuitry to suppress motor and somatosensory interference in attentional processing. In addition, the total context of SMR activity before and during NFT also agrees with a report of the impossibility of maintaining a high amplitude mu (SMR) rhythm (Niedermeyer, et al., 2004). Therefore, any assumption concerning the long-term sustained effect of SMR training should consider its role in the attention network, motor preparation and execution, since the SMR rhythms reflect sensorimotor processing in frontoparietal networks (Pineda, 2005) and in SMR desynchronization (ERD) or synchronization (ERS) after SMR training. Further studies are required to prove this assumption, in accordance with the post-NF EEG activity with long-term effects in both healthy subjects and patients.

There may be an explanation for the decreased SMR in the central area (around bilateral somatosensory cortices) in the eyes-closed resting EEG. The observed findings could be explained by a reduction in μ -rhythms, during the subconscious “planning”, just before performance (Krepki, et al., 2007; Manoilov and Borodzhieva, 2008), representing preparation for movement accompanied by a power decrease in certain frequency bands, termed Event-Related Desynchronization (ERD) (Pfurtscheller, 2000; Pfurtscheller, et al., 1996). In fact, it is very difficult to discriminate between more than two mental states, when only imagery-induced ERD patterns are available (Klimesch, 1999). Therefore, those subjects (in the groups receiving actual SMR feedback protocols) may produce reduced SMR rhythms (with

profitably subconscious planning of the following NFT), during the period of the EC baseline state (the resting EEG recorded before the SMR training). Again, these novel findings in this thesis, with significant spectral changes in pre- vs. post-training assessment, are compatible with some previous research illustrating significant increases in SMR, during the actual training period, but depicting non-significant decreases in SMR, post-training in the EC resting EEG of healthy humans (Doppelmayr, et al., 2009; Egner, et al., 2004) and patients (e.g., Gevensleben, et al., 2009b; Pineda, et al., 2008).

In the view of exogenous stimulation, the outcome index of the AE group (receiving electrostimulation with high and low alternating frequencies) showed a greater decrease in theta amplitude than the index data for the SMR group, especially in the training period. A similar result was reported by Chen et al., in 2006, and they demonstrated decreased theta during high frequency EA stimulation of the hands (Chen, et al., 2006). Although this team reported only an instant effect from the EA stimulation, other acupuncture papers have mentioned a prolonged effect, due to stimulation of the CNS neurotransmitter, post acupuncture stimulation (e.g., Dhond, et al., 2008; Han, 2004). Other fMRI papers have documented the effect of acupuncture on the RSN or DMN (e.g., Dhond, et al., 2008) and provide a stimulus for the research of SMR training assisted with electroacustimulation.

In summary, this thesis provides new evidence for significant attention improvement due to SMR training, in healthy subjects. Compared with the pseudo-NFT, the enhanced perceptual sensitivity from actual SMR training agrees with previous research into the efficacy of SMR in improving attention performance (d'). Evidence for resting EEG activity at post-training has been interpreted as

demonstrating more flexible control over the SMR rhythm and meaningfully persuasive links between attention and a reduction in resting SMR activity and the increase in resting beta activity in the dorsal attention (frontoparietal) networks and links between wakefulness and a decrease in theta activity during the training period and the resting state.

Of course, in order to explain the precise relationship between the EEG changes during NFT process, it should be considered whether those subjects, after real SMR (several sessions), would have the same imaginary processing without real-time EEG feedback. Some fMRI studies have given positive reports for a similar design and results (e.g., Caria, et al., 2007; Rota, et al., 2009). Based on this hypothesis, a home program with a mimic feedback and a recorded on-line audiovisual clip from a real SMR training session could probably be considered for clinical use in the future.

6.2.3 The combination of NF assisted by EA

The SMR training produced a significant and reliable effect on both perceptual sensitivity and enhanced EEG beta power in the frontal cortex. Both of EA and NFT effects must be considered together because of to their similar neuromodulation, not just to demonstrate the ordinary effect of SMR training alone, but to further validate the assumption of the potential effect of exogenous stimulation on endogenous training. Although the results of Exp I provide a sensible rationale in terms of attention performance for the use of the EA stimulation, and as these data have already been appraised, the study of the integration of neurofeedback and EA stimulation is still largely unsatisfactory.

For the treatment of brain disorders, for instance, the US Food and Drug Administration (FDA) has approved devices such as a wrist electrical stimulator and a cranial electric stimulator (e.g., Hirshberg, et al., 2005). However, acupuncture and electroacustimulation may be the best form of treatment for altering the brain, providing peripheral stimulation of the brain via sensory inputs, not only because of its long history of application in humans, but also because of recent reports that provide persuasive reports of neuroimaging in brain function (e.g., Chen, et al., 2006; Dhond, et al., 2008). Thus, the advantages of this stimulation strategy to intervene and improve brain function are well presented in Exp I, but the study of the integration of neurofeedback and stimulation is still largely unsatisfactory due to the natural weakness of artefacts or bias in the EEG recording. Since fMRI is much more expensive and less widely available than EEG equipment, the refinement of EEG recording and analysis may support the use of EA as an adjuvant.

Based on Exp II, there is evidence for an efficient pipeline that eliminates most of the vagueness from volume conduction, so the ICA-based resting EEG power spectra can be used to study cortical activation in healthy subjects. The thirteen ICs identified by using ICA-based resting EEG analysis were grouped to construct five regions, depending on their correlation coefficient for EEG-alpha power in the EC state. The functional networks (connectivity) constructed by those five regions and thirteen independent components have also been demonstrated to be very similar to the BOLD signals that constitute the resting-state networks (RSNs) or default mode network (DMN) of the brain in the fMRI.

In Exp III the improved perceptual sensitivity (d') was increased by using SMR to significantly reduce the number of commission errors and to enhance a subject's

wakefulness by inhibiting theta activity during the SMR training period. The analysis of spectral changes in resting EEG, post-NFT, meaningfully explained the associated beta rhythmic activity in the frontal area, post actual SMR training (details in the section 6.2.2), compared with the pseudo-NFT. These associated links between enhanced cognitive function and changed rhythmic activity in the frontal region of the attention network in the resting EEG seem to show the same inclination as actual SMR training, which is a striking contrast to the results for pseudo-NFT.

In summary, this thesis demonstrates that protocols of SMR training and SMR training assisted by EA can facilitate operant enhancement of in-training SMR/theta ratios, a decrease in the number of commission errors, and an increase in perceptual sensitivity, post training, which endorses the use of the SMR EEG-biofeedback protocol. The results supplement present arguments for the use of an NFT protocol in healthy subjects and provide an electrophysiologically based rationale for empirical clinical applications for disorders characterised by lack of frontal beta band activity and excessive central theta band activity, such as ADHD. The findings of this thesis, showing replicable improvements and concurrent and relevant measures of electrophysiological activation, comply with the general clinical assumption that the combination of stimulation and feedback may be more effective than either alone (e.g., Hirshberg, et al., 2005).

6.3 Methodological Limitations and Future Directions

The major methodological limitations of the three studies in this thesis are presented in the interpretation of the results and the recommended modifications and additions for possible future studies, detailed in previous sections (6.1 and 6.2). Thus this section indicates primarily the limitations of data collection, and how this could be rectified in future studies.

In view of the data collected that showed the effects of SMR neurofeedback protocols and the likely explanation for its electrophysiological activity, it is apparent that there is still too little information pertaining to actual real-time training. Firstly, the in-training EEG data collected in this thesis consisted of single electrode records that only cover the ongoing activity in the frequency components involved in the feedback process, but not the entire head EEG recordings, which would show real-time possible connections. Furthermore, these data mainly consist of blocks of mean amplitude values for regular sampling intervals (i.e. 3-min or 2-min periods) in a recording channel (Cz). Taken together, the in-training data does not allow any possibility to explore the topographical and temporal spectral dynamics of the actual feedback learning process in the entire brain. However, this limitation of the in-training data collection in a Cz channel is partially solved by the double whole-scalp EEG recordings, prior and subsequent to the overall NFT courses. Nevertheless, this thesis does not provide real-time, whole-scalp EEG data to address the question of in-training EEG generation (and possible source localization analysis) or progressive changes in topographical EEG spectra. These limitations may prevent a more thorough understanding of how exactly various training protocols produce their effect during the period of feedback sessions. From the current data, the issue of

real-time determination of electrophysiological effective mediation has thus not been solved. Accordingly, in future investigations, the monitoring of whole-scalp EEG records during training sessions may be highly desirable, in order to provide evidence of effective NFT to brain interaction, regardless of the highly time consuming and intensive challenge in amassing whole-scalp EEG records.

Alternatively, during an early or a late session in the NFT program, the monitoring of such training data could provide valuable data to show a real-time NFT effect. Indeed for comprehensive research, the assessment of cognitive-behavioural dependent measures at pre- and post-training should also be performed using whole-scalp EEG recordings, simultaneously. These improvements for the future study of neurofeedback would likely allow the detection of a direct electrocortical linkage, for instance the process of functional connectivity within the training sessions and its consequences.

A further issue that has not been addressed fully in this thesis is the question of the long-term effect of NFT. The application of these techniques to normal subjects and to clinical cases is based on their potential to evoke long-term effects. The experimental work presented in this thesis implies inferences from the changed resting EEG power spectra. Accordingly, the setting of baseline resting EEG power spectra, analysed by ICA and using significant increases in beta power in the frontal region related to the DAN, could be used to investigate the long-term effects of NF on cortical activity. Therefore in the future, studies will need to involve regular follow-up assessments by EEG and behavioural measures over a long time interval, in order to evaluate the costs and efficacy of NFT (both in terms of time and money). As a

cognitive performance enhancement tool in clinics or for a particular purpose in education, NFT must be justified by long-term returns.

One more issue that arises from establishing NFT as a scientifically evidence-based clinical technique is the establishment of a control group, to demonstrate the significant effects on relevant behavioural outcome measures and a demonstrable illustration of the neurophysiological outcomes of such NFT effects. The control with pseudo-NFT, in Exp III, engages in similar audiovisual feedback technique training but there is no presentation of the subject's own real-time brain waves. Therefore, these actual NFT effects should not be attributed to practice or motivational factors, because there are no significant changes in any of the variables assessed in the attention task, for the control group. Evidently, future NFT research with an adequately designed control group will support further development in clinical usage and research

Finally, from the statistical point of view, increasing the statistical power of comparable investigations is highly recommended, especially in a study such as Exp III, with four groups. Sample sizes should be large enough to distinguish four groups with all related behavioural data, outcome dependent measures and resting EEG ICA power spectra.

6.4 Final Conclusions

The experimental work in this thesis provides evidence that SMR neurofeedback training enhanced perceptual sensitivity and attention, in healthy subjects, due to measurable differences in cognitive, electrocortical and outcome measures. These effects of NFT and EA stimulation, which were specific to the ICA-based EEG power spectra, clarify the theoretical conceptualization of SMR and the strategy for a combination of endogenous with exogenous methods, for training protocols in practice. The potential consequence of their combined applications may be better than SMR or EA stimulation alone in subjects with cognitive disorder. The results also ascribe the assumed effects to the intrinsic factors in the SMR training process with a possible assumption of a particular assistant role of EA stimulation. The underlying changes in resting EEG spectra, after NFT, in regard to actual operant training contingencies, is illustrated by the congruent evidence of enhanced beta power in the frontal cortex with the observed corresponding attentional performance, indicating an improvement in behaviour that is mediated by electrophysiological enhancement.

REFERENCES

- Abad-Alegria F, Galve JA, Martinez T. (1995): Changes of cerebral endogenous evoked potentials by acupuncture stimulation: a P300 study. *Am J Chin Med* 23(2):115-9.
- Alonso-Nanclares L, Gonzalez-Soriano J, Rodriguez J, DeFelipe J. (2008): Gender differences in human cortical synaptic density. *Proceedings of the National Academy of Sciences* 105(38):14615-14619.
- Andreassi, J. L. (2000). *Psychophysiology: Human behavior and physiological response*: Lawrence Erlbaum.
- Arns, M., de Ridder, S., Strehl, U., Breteler, M., & Coenen, A. (2009). Efficacy of neurofeedback treatment in ADHD: the effects on inattention, impulsivity and hyperactivity: a meta-analysis. *Clin EEG Neurosci*, 40(3), 180-189.
- Asada, H., Fukuda, Y., Tsunoda, S., Yamaguchi, M., & Tonoike, M. (1999). Frontal midline theta rhythms reflect alternative activation of prefrontal cortex and anterior cingulate cortex in humans. *Neurosci Lett*, 274(1), 29-32.
- Baddeley, A. D. (1997). *Human memory: Theory and practice*: Psychology Pr.
- Bai, L., Qin, W., Tian, J., Dong, M., Pan, X., Chen, P., . . . Liu, Y. (2009). Acupuncture modulates spontaneous activities in the anticorrelated resting brain networks. *Brain Res*, 1279, 37-49. doi: S0006-8993(09)00899-3 [pii]10.1016/j.brainres.2009.04.056
- Baillet, S., Mosher, J. C., & Leahy, R. M. (2001). Electromagnetic Brain Mapping. *IEEE Signal Processing Magazine*, 18, 14-30.
- Barry, M. (2000). Basic concepts and clinical findings in the treatment of seizure disorders with EEG operant conditioning. *Clinical Electroencephalography*, 31(1).
- Barry, R. J., Clarke, A. R., & Johnstone, S. J. (2003). A review of electrophysiology in attention-deficit/hyperactivity disorder: I. Qualitative and quantitative electroencephalography. *Clin Neurophysiol*, 114(2), 171-183. doi: S1388245702003620 [pii]
- Barry, R. J., Clarke, A. R., Johnstone, S. J., & Brown, C. R. (2009). EEG differences in children between eyes-closed and eyes-open resting conditions. *Clin Neurophysiol*. doi: S1388-2457(09)00489-1 [pii]10.1016/j.clinph.2009.08.006
- Barry, R. J., Clarke, A. R., Johnstone, S. J., Magee, C. A., & Rushby, J. A. (2007). EEG differences between eyes-closed and eyes-open resting conditions. *Clin Neurophysiol*, 118(12), 2765-2773. doi: S1388-2457(07)00400-2 [pii]10.1016/j.clinph.2007.07.028
- Barry, R. J., Rushby, J. A., Wallace, M. J., Clarke, A. R., Johnstone, S. J., & Zlojutro, I. (2005). Caffeine effects on resting-state arousal. *Clin Neurophysiol*, 116(11), 2693-2700. doi: S1388-2457(05)00318-4 [pii]10.1016/j.clinph.2005.08.008
- Basar E, Gnder A, Ungan P. (1980): Comparative frequency analysis of single EEG-evoked potential records. *Journal of biomedical engineering* 2(1):9-14.
- Bassett DS, Bullmore E. (2006): Small-world brain networks. *The neuroscientist* 12(6):512-523.
- Beatty, J., Greenberg, A., Deibler, W. P., & O'Hanlon, J. F. (1974). Operant control of occipital theta rhythm affects performance in a radar monitoring task. *Science*, 183(4127), 871.

- Beaussart, M., & Guieu, J. (1977). Artefacts. *Handbook of electroencephalography and clinical neurophysiology*. Amsterdam: Elsevier.
- Bechtereva N, Kropotov YD. (1984): Neurophysiological correlates of visual stimulus recognition in man. *International Journal of Psychophysiology* 1(4):317-324.
- Becker K, Holtmann M. (2006): Role of electroencephalography in attention-deficit hyperactivity disorder. *Expert review of neurotherapeutics* 6(5):731-739.
- Beckmann, C. F., DeLuca, M., Devlin, J. T., & Smith, S. M. (2005). Investigations into resting-state connectivity using independent component analysis. *Philosophical Transactions of the Royal Society B: Biological Sciences*, 360(1457), 1001.
- Beissner F, Henke C. (2009): Methodological Problems in fMRI Studies on Acupuncture: A Critical Review With Special Emphasis on Visual and Auditory Cortex Activations. *Evid Based Complement Alternat Med*.
- Bekker, E. M., Kenemans, J. L., & Verbaten, M. N. (2005). Source analysis of the N2 in a cued Go/NoGo task. *Cognitive Brain Research*, 22(2), 221-231.
- Bell, A. J., & Sejnowski, T. J. (1995). An information-maximization approach to blind separation and blind deconvolution. *Neural Comput*, 7(6), 1129-1159.
- Ben-Simon, E., Podlipsky, I., Arieli, A., Zhdanov, A., & Hendler, T. (2008). Never resting brain: simultaneous representation of two alpha related processes in humans. *PLoS one*, 3(12), e3984.
- Benesty J, Makino S, Chen J. (2005): *Speech enhancement*: Springer.
- Berman, B. M. (2001). Seminal studies in acupuncture research. *J Altern Complement Med*, 7 Suppl 1, S129-137.
- Berridge, K. C. (2004). Motivation concepts in behavioral neuroscience. *Physiology & Behavior*, 81(2), 179-209.
- Bertini, M., Ferrara, M., De Gennaro, L., Curcio, G., Moroni, F., Vecchio, F., . . . Babiloni, C. (2007). Directional information flows between brain hemispheres during presleep wake and early sleep stages. *Cerebral Cortex*, 17(8), 1970-1978.
- Biella, G., Sotgiu, M. L., Pellegata, G., Paulesu, E., Castiglioni, I., & Fazio, F. (2001). Acupuncture produces central activations in pain regions. *Neuroimage*, 14(1 Pt 1), 60-66. doi: S1053-8119(01)90798-0 [pii]10.1006/nimg.2001.0798
- Birbaumer, N., Weber, C., Neuper, C., Buch, E., Haapen, K., & Cohen, L. (2006). Physiological regulation of thinking: brain-computer interface (BCI) research. *Progress in Brain Research*, 159, 369-391.
- Biswal, B., Yetkin, F. Z., Haughton, V. M., & Hyde, J. S. (1995). Functional connectivity in the motor cortex of resting human brain using echo-planar MRI. *Magn Reson Med*, 34(4), 537-541.
- Biswal, B., Yetkin, F. Z., Haughton, V. M., & Hyde, J. S. (1995). Functional connectivity in the motor cortex of resting human brain using echo-planar MRI. *Magnetic resonance in medicine*, 34(4), 537-541.
- Bland BH, Oddie SD. (1998): Anatomical, electrophysiological and pharmacological studies of ascending brainstem hippocampal synchronizing pathways. *Neuroscience & Biobehavioral Reviews* 22(2):259-273.
- Bodnar, R. J. (2008). Endogenous opiates and behavior: 2007. *Peptides*, 29(12), 2292-2375.

- Bokura, H., Yamaguchi, S., & Kobayashi, S. (2001a). Electrophysiological correlates for response inhibition in a Go/NoGo task. *Clinical Neurophysiology*, *112*(12), 2224-2232.
- Bokura, H., Yamaguchi, S., & Kobayashi, S. (2001b). Electrophysiological correlates for response inhibition in a Go/NoGo task. *Clin Neurophysiol*, *112*(12), 2224-2232. doi: S1388-2457(01)00691-5 [pii]
- Bonnerman, R. (1979). Acupuncture: The World Health Organization view. *World Health*, *31*, 24-29.
- Bosch-Bayard J, Valdes-Sosa P, Virues-Alba T, Aubert-Vazquez E, John ER, Harmony T, Riera-Diaz J, Trujillo-Barreto N. (2001): 3D statistical parametric mapping of EEG source spectra by means of variable resolution electromagnetic tomography (VARETA). *Clinical EEG (electroencephalography)* *32*(2):47.
- Bossetti CA, Birdno MJ, Grill WM. (2007): Analysis of the quasi-static approximation for calculating potentials generated by neural stimulation. *Journal of neural engineering* *5*(1):44.
- Boulougouris, V., & Tsaltas, E. (2008). Serotonergic and dopaminergic modulation of attentional processes. *Prog Brain Res*, *172*, 517-542. doi: S0079-6123(08)00925-4 [pii]10.1016/S0079-6123(08)00925-4
- Bouyer, J. J., Montaron, M. F., Vahnee, J. M., Albert, M. P., & Rougeul, A. (1987). Anatomical localization of cortical beta rhythms in cat. *Neuroscience*, *22*(3), 863-869. doi: 0306-4522(87)92965-4 [pii]
- Bray PA, Mamiya N, Fann AV, Gellman H, Skinner RD, Garcia-Rill EE. (2005): Modulation of the sleep state-dependent P50 midlatency auditory-evoked potential by electric stimulation of acupuncture points. *Arch Phys Med Rehabil* *86*(10):2018-26.
- Bressler SL, Kelso J. (2001): Cortical coordination dynamics and cognition. *Trends in cognitive sciences* *5*(1):26-36.
- Briand, L. A., Gritton, H., Howe, W. M., Young, D. A., & Sarter, M. (2007). Modulators in concert for cognition: modulator interactions in the prefrontal cortex. *Progress in neurobiology*, *83*(2), 69-91.
- Bronzino, J. D. (1995). Principles of electroencephalography. In J. D. Bronzino (Ed.), *The Biomedical Engineering Handbook* (pp. 201-212). Florida: CRC Press.
- Brookes MJ, Gibson AM, Hall SD, Furlong PL, Barnes GR, Hillebrand A, Singh KD, Holliday IE, Francis ST, Morris PG. (2005): GLM-beamformer method demonstrates stationary field, alpha ERD and gamma ERS co-localisation with fMRI BOLD response in visual cortex. *NeuroImage* *26*(1):302-308.
- Brookes MJ, Woolrich M, Luckhoo H, Price D, Hale JR, Stephenson MC, Barnes GR, Smith SM, Morris PG. (2011): Investigating the electrophysiological basis of resting state networks using magnetoencephalography. *Proceedings of the National Academy of Sciences* *108*(40):16783-16788.
- Brown WS, Marsh JT, Smith JC. (1979): Principal component analysis of ERP differences related to the meaning of an ambiguous word. *Electroencephalography and clinical neurophysiology* *46*(6):709-714.
- Broyd, S. J., Demanuele, C., Debener, S., Helps, S. K., James, C. J., & Sonuga-Barke, E. J. (2009). Default-mode brain dysfunction in mental disorders: a systematic review.

- Neurosci Biobehav Rev*, 33(3), 279-296. doi: S0149-7634(08)00150-4 [pii]10.1016/j.neubiorev.2008.09.002
- Buckner, R. L., Sepulcre, J., Talukdar, T., Krienen, F. M., Liu, H., Hedden, T., . . . Johnson, K. A. (2009). Cortical hubs revealed by intrinsic functional connectivity: mapping, assessment of stability, and relation to Alzheimer's disease. *The Journal of neuroscience*, 29(6), 1860-1873.
- Bullmore, E., & Sporns, O. (2009). Complex brain networks: graph theoretical analysis of structural and functional systems. *Nature Reviews Neuroscience*, 10(3), 186-198.
- Buschman TJ, Miller EK. (2007): Top-down versus bottom-up control of attention in the prefrontal and posterior parietal cortices. *Science* 315(5820):1860-1862.
- Buzsaki G, Draguhn A. (2004): Neuronal oscillations in cortical networks. *Science* 304(5679):1926-1929.
- Bynum, J., & Stern, J. (1970). Analysis of visual search activity in skilled and novice helicopter pilots (Visual search activity decrease observed as function of time-on-task for skilled and unskilled helicopter pilots, recording eye movements and blinks). *AEROSPACE MEDICINE*, 41, 300-305.
- Cabyoglu, M. T., Ergene, N., & Tan, U. (2006). The mechanism of acupuncture and clinical applications. *Int J Neurosci*, 116(2), 115-125. doi: H41G22R466800466 [pii]10.1080/00207450500341472
- Calhoun, V. D., Adali, T., Pearlson, G. D., & Pekar, J. J. (2001). A method for making group inferences from functional MRI data using independent component analysis. *Hum Brain Mapp*, 14(3), 140-151. doi: 10.1002/hbm.1048 [pii]
- Calhoun, V. D., Adali, T., & Pekar, J. J. (2004). A method for comparing group fMRI data using independent component analysis: application to visual, motor and visuomotor tasks. *Magn Reson Imaging*, 22(9), 1181-1191. doi: S0730-725X(04)00277-2 [pii]10.1016/j.mri.2004.09.004
- Cannon, R., Congedo, M., Lubar, J., & Hutchens, T. (2009). Differentiating a network of executive attention: LORETA neurofeedback in anterior cingulate and dorsolateral prefrontal cortices. *Int J Neurosci*, 119(3), 404-441. doi: 907250775 [pii]10.1080/00207450802480325
- Cannon, R., Lubar, J., Congedo, M., Thornton, K., Towler, K., & Hutchens, T. (2007). The effects of neurofeedback training in the cognitive division of the anterior cingulate gyrus. *Int J Neurosci*, 117(3), 337-357. doi: 770423867 [pii]10.1080/00207450500514003
- Cantor, D. S. (1999). An Overview of Quantitative EEG and Its Applications to Neurofeedback. In J. R. Evans & A. Abarbanel (Eds.), *Introduction to quantitative EEG and Neurofeedback* (pp. 3-27). California, USA: Academic Press.
- Cao J, Murata N. (1999): A stable and robust ICA algorithm based on t-distribution and generalized Gaussian distribution models. *Neural Networks for Signal Processing IX*, 1999. Proceedings of the 1999 IEEE Signal Processing Society Workshop.: IEEE. p 283-292.
- Cardoso JF. (1998): Blind signal separation: statistical principles. *Proceedings of the IEEE* 86(10):2009-2025.
- Caria, A., Veit, R., Sitaram, R., Lotze, M., Weiskopf, N., Grodd, W., & Birbaumer, N. (2007). Regulation of anterior insular cortex activity using real-time fMRI. *Neuroimage*,

- 35(3), 1238-1246. doi: S1053-8119(07)00038-9
[pii]10.1016/j.neuroimage.2007.01.018
- Castellanos, F. X., Margulies, D. S., Kelly, C., Uddin, L. Q., Ghaffari, M., Kirsch, A., . . . Biswal, B. (2008). Cingulate-precuneus interactions: a new locus of dysfunction in adult attention-deficit/hyperactivity disorder. *Biological psychiatry*, 63(3), 332-337.
- Caton, R. (1875). Electrical Currents of the Brain. *The Journal of Nervous and Mental Disease*, 2(4), 610.
- Chabot, R. J., di Michele, F., & Prichep, L. (2005). The role of quantitative electroencephalography in child and adolescent psychiatric disorders. *Child Adolesc Psychiatr Clin N Am*, 14(1), 21-53, v-vi. doi: S1056-4993(04)00068-9 [pii]10.1016/j.chc.2004.07.005
- Chae Y, Kang OS, Lee HJ, Kim SY, Lee H, Park HK, Yang JS, Park HJ. (2010): Effect of acupuncture on selective attention for smoking-related visual cues in smokers. *Neurol Res* 32 Suppl 1:27-30.
- Chang S, Chang ZG, Li SJ, Chiang MJ, Ma CM, Cheng HY, Hsieh SH. (2009): Effects of Acupuncture at Neiguan (PC 6) on Electroencephalogram. *The Chinese Journal of Physiology*:1-7.
- Chao, A. S., Chao, A., Wang, T. H., Chang, Y. C., Peng, H. H., Chang, S. D., . . . Wong, A. M. (2007). Pain relief by applying transcutaneous electrical nerve stimulation (TENS) on acupuncture points during the first stage of labor: a randomized double-blind placebo-controlled trial. *Pain*, 127(3), 214-220. doi: S0304-3959(06)00421-0 [pii]10.1016/j.pain.2006.08.016
- Chen, A. C., Feng, W., Zhao, H., Yin, Y., & Wang, P. (2008). EEG default mode network in the human brain: spectral regional field powers. *Neuroimage*, 41(2), 561-574. doi: S1053-8119(07)01163-9 [pii]10.1016/j.neuroimage.2007.12.064
- Chen, A. C., Liu, F. J., Wang, L., & Arendt-Nielsen, L. (2006). Mode and site of acupuncture modulation in the human brain: 3D (124-ch) EEG power spectrum mapping and source imaging. *Neuroimage*, 29(4), 1080-1091. doi: S1053-8119(05)00624-5 [pii]10.1016/j.neuroimage.2005.08.066
- Chen, J-L., Ros, T., & Gruzelier, J. H. (2012). Dynamic changes of ICA-derived EEG functional connectivity in the resting state. *Human brain mapping*. doi: 10.1002/hbm.21475. epub, Feb 17, 2012.
- Chen, J-L., Thompson, T., Kropotov, J., & Gruzelier, J. (2011). Beneficial Effects of Electrostimulation Contingencies on Sustained Attention and Electrocortical Activity. *CNS Neuroscience & Therapeutics*, 17(5), 311.
- Chen, Y. C., Duann, J. R., Chuang, S. W., Lin, C. L., Ko, L. W., Jung, T. P., & Lin, C. T. (2010). Spatial and temporal EEG dynamics of motion sickness. *Neuroimage*, 49(3), 2862-2870. doi: S1053-8119(09)01076-3 [pii]10.1016/j.neuroimage.2009.10.005
- Cheng, R. S. S., & Pomeranz, B. (1979). Electroacupuncture analgesia could be mediated by at least two pain-relieving mechanisms; endorphin and non-endorphin systems. *Life Sciences*, 25(23), 1957-1962.
- Chesterton, L. S., Barlas, P., Foster, N. E., Lundeberg, T., Wright, C. C., & Baxter, G. D. (2002). Sensory stimulation (TENS): effects of parameter manipulation on mechanical pain thresholds in healthy human subjects. *Pain*, 99(1-2), 253-262.

- Cheyne, D., Gaetz, W., Garnero, L., Lachaux, J. P., Ducorps, A., Schwartz, D., & Varela, F. J. (2003). Neuromagnetic imaging of cortical oscillations accompanying tactile stimulation. *Cognitive Brain Research*, *17*(3), 599-611.
- Cho, M. K., Jang, H. S., Jeong, S. H., Jang, I. S., Choi, B. J., & Lee, M. G. (2008). Alpha neurofeedback improves the maintaining ability of alpha activity. *Neuroreport*, *19*(3), 315-317.
- Cho, M. K., Jang, H. S., Jeong, S. H., Jang, I. S., Choi, B. J., & Lee, M. G. T. (2008). Alpha neurofeedback improves the maintaining ability of alpha activity. *Neuroreport*, *19*(3), 315.
- Cho Z, Na C, Wong E, Lee S, Hong I. (2000): "Investigation of acupuncture using brain functional magnetic resonance imaging," in *Computer Controlled Acupuncture*, Litscher G and Cho Z, Eds., pp. 45–64, Pabst Scientific, Lengerich, Germany.
- Cho Z, Na C, Wong E, Lee S, Hong I. (2001): "Functional magnetic resonance imaging of the brain in the investigation of acupuncture," in *Clinical Acupuncture-Scientific Basis*, Stux G and Hammerschlag R, Eds., pp. 85–90, Springer, Berlin, Germany.
- Cho, Z. H., Chung, S. C., Jones, J. P., Park, J. B., Park, H. J., Lee, H. J., . . . Min, B. I. (1998). New findings of the correlation between acupoints and corresponding brain cortices using functional MRI. *Proceedings of the National Academy of Sciences*, *95*(5), 2670.
- Cho, Z. H., Hwang, S. C., Wong, E. K., Son, Y. D., Kang, C. K., Park, T. S., . . . Min, K. T. (2006). Neural substrates, experimental evidences and functional hypothesis of acupuncture mechanisms. *Acta Neurol Scand*, *113*(6), 370-377. doi: ANE600 [pii]10.1111/j.1600-0404.2006.00600.x
- Choi S, Cichocki A, Park HM, Lee SY. (2005): Blind source separation and independent component analysis: A review. *Neural Information Processing-Letters and Reviews* *6*(1):1-57.
- Chorlian, D. B., Rangaswamy, M., & Porjesz, B. (2009). EEG coherence: topography and frequency structure. *Experimental brain research*, *198*(1), 59-83.
- Clarke, A. R., Barry, R. J., McCarthy, R., & Selikowitz, M. (2001). EEG-defined subtypes of children with attention-deficit/hyperactivity disorder. *Clin Neurophysiol*, *112*(11), 2098-2105. doi: S1388-2457(01)00668-X [pii]
- Clarke, A. R., Barry, R. J., McCarthy, R., Selikowitz, M., & Brown, C. R. (2002). EEG evidence for a new conceptualisation of attention deficit hyperactivity disorder. *Clin Neurophysiol*, *113*(7), 1036-1044. doi: S1388245702001153 [pii]
- Claydon, L. S., Chesterton, L. S., Barlas, P., & Sim, J. (2008). Effects of simultaneous dual-site TENS stimulation on experimental pain. *European Journal of Pain*, *12*(6), 696-704.
- Claydon, L. S., Chesterton, L. S., Barlas, P., & Sim, J. (2008). Effects of simultaneous dual-site TENS stimulation on experimental pain. *Eur J Pain*, *12*(6), 696-704. doi: S1090-3801(07)00676-3 [pii]10.1016/j.ejpain.2007.10.014
- Coben, R., Linden, M., & Myers, T. E. (2010). Neurofeedback for autistic spectrum disorder: a review of the literature. *Applied Psychophysiology and Biofeedback*, *35*(1), 83-105.
- Coburn, K. L., Lauterbach, E. C., Boutros, N. N., Black, K. J., Arciniegas, D. B., & Coffey, C. E. (2006). The value of quantitative electroencephalography in clinical psychiatry: a report by the Committee on Research of the American Neuropsychiatric Association.

- J Neuropsychiatry Clin Neurosci*, 18(4), 460-500. doi: 18/4/460 [pii]10.1176/appi.neuropsych.18.4.460
- Codispoti, M., Ferrari, V., & Bradley, M. M. (2006). Repetitive picture processing: autonomic and cortical correlates. *Brain Research*, 1068(1), 213-220.
- Comon, P. (1994). Independent component analysis, A new concept. *Signal Processing*(36), 287-314.
- Congedo, M., John, R. E., De Ridder, D., Prichep, L., & Isenhardt, R. (2009). On the "Dependence" of "Independent" Group EEG Sources; an EEG Study on Two Large Databases. *Brain Topogr*. doi: 10.1007/s10548-009-0113-6
- Congedo, M., Lubar, J. F., & Joffe, D. (2004). Low-resolution electromagnetic tomography neurofeedback. *IEEE Trans Neural Syst Rehabil Eng*, 12(4), 387-397. doi: 10.1109/TNSRE.2004.840492
- Contreras, D., Destexhe, A., Sejnowski, J., & Steriade, M. (1996). Control of spatiotemporal coherence of a thalamic oscillation by corticothalamic feedback. *Science*, 274, 771-774.
- Cooper, N. R., Burgess, A. P., Croft, R. J., & Gruzelier, J. H. (2006). Investigating evoked and induced electroencephalogram activity in task-related alpha power increases during an internally directed attention task. *Neuroreport*, 17(2), 205-208. doi: 00001756-200602060-00019 [pii]
- Corbetta, M., Kincade, J. M., Ollinger, J. M., McAvoy, M. P., & Shulman, G. L. (2000). Voluntary orienting is dissociated from target detection in human posterior parietal cortex. *Nature neuroscience*, 3, 292-297.
- Corbetta, M., & Shulman, G. L. (2002). Control of goal-directed and stimulus-driven attention in the brain. *Nat Rev Neurosci*, 3(3), 201-215.
- Corsi-Cabrera, M., Ramos, J., Arce, C., & Guevara, M. (1992). Changes in the waking EEG as a consequence of sleep and sleep deprivation. *Sleep: Journal of Sleep Research & Sleep Medicine*.
- Costa, R. M. (2007). Plastic corticostriatal circuits for action learning. *Annals of the New York Academy of Sciences*, 1104(1), 172-191.
- Cuffin BN, Schomer DL, Ives JR, Blume H. (2001): Experimental tests of EEG source localization accuracy in spherical head models. *Clinical Neurophysiology* 112(1):46-51.
- Cvetkovic, D., & Cosic, I. (2009). EEG inter/intra-hemispheric coherence and asymmetric responses to visual stimulations. *Medical and Biological Engineering and Computing*, 47(10), 1023-1034.
- Dale AM, Halgren E. (2001): Spatiotemporal mapping of brain activity by integration of multiple imaging modalities. *Current opinion in neurobiology* 11(2):202-208.
- Dale AM, Liu AK, Fischl BR, Buckner RL, Belliveau JW, Lewine JD, Halgren E. (2000): Dynamic statistical parametric neurotechnique mapping: combining fMRI and MEG for high-resolution imaging of cortical activity. *Neuron* 26(1):55-67.
- Damoiseaux, J. S., Rombouts, S. A., Barkhof, F., Scheltens, P., Stam, C. J., Smith, S. M., & Beckmann, C. F. (2006). Consistent resting-state networks across healthy subjects. *Proc Natl Acad Sci U S A*, 103(37), 13848-13853. doi: 0601417103 [pii]10.1073/pnas.0601417103

- Davidson RJ, Jackson DC, Larson CL. (2000): Human electroencephalography. *Handbook of psychophysiology* 2:27-52.
- Davies, D. R., & Parasuraman, R. (1982). *The psychology of vigilance*: Academic Press London.
- De Luca, M., Beckmann, C. F., De Stefano, N., Matthews, P. M., & Smith, S. M. (2006). fMRI resting state networks define distinct modes of long-distance interactions in the human brain. *Neuroimage*, 29(4), 1359-1367. doi: S1053-8119(05)00625-7 [pii]10.1016/j.neuroimage.2005.08.035
- de Pasquale, F., Della Penna, S., Snyder, A. Z., Lewis, C., Mantini, D., Marzetti, L., . . . Romani, G. L. (2010). Temporal dynamics of spontaneous MEG activity in brain networks. *Proceedings of the National Academy of Sciences*, 107(13), 6040.
- De Vico Fallani, F., Astolfi, L., Cincotti, F., Mattia, D., Tocci, A., Marciani, M. G., . . . Babiloni, F. (2007). Extracting information from cortical connectivity patterns estimated from high resolution EEG recordings: a theoretical graph approach. *Brain Topogr*, 19(3), 125-136. doi: 10.1007/s10548-007-0019-0
- Debener, S., Ullsperger, M., Siegel, M., & Engel, A. K. (2006). Single-trial EEG-fMRI reveals the dynamics of cognitive function. *Trends Cogn Sci*, 10(12), 558-563. doi: S1364-6613(06)00272-5 [pii]10.1016/j.tics.2006.09.010
- deCharms, R. C. (2007). Reading and controlling human brain activation using real-time functional magnetic resonance imaging. *Trends in cognitive sciences*, 11(11), 473-481.
- Delorme A, Makeig S. (2004): EEGLAB: an open source toolbox for analysis of single-trial EEG dynamics including independent component analysis. *Journal of neuroscience methods* 134(1):9-21.
- Delorme, A., & Makeig, S. (2003). EEG changes accompanying learned regulation of 12-Hz EEG activity. *Neural Systems and Rehabilitation Engineering, IEEE Transactions on*, 11(2), 133-137.
- Delorme, A., Makeig, S., Fabre-Thorpe, M., & Sejnowski, T. (2002). From single-trial EEG to brain area dynamics. *Neurocomputing*, 44, 1057-1064.
- Delorme, A., Palmer, J., Onton, J., Oostenveld, R., & Makeig, S. (2012). Independent EEG Sources Are Dipolar. *PloS one*, 7(2), e30135.
- Delorme A, Sejnowski T, Makeig S. (2007): Enhanced detection of artifacts in EEG data using higher-order statistics and independent component analysis. *NeuroImage* 34(4):1443.
- Dhond, R. P., Kettner, N., & Napadow, V. (2007). Neuroimaging acupuncture effects in the human brain. *J Altern Complement Med*, 13(6), 603-616. doi: 10.1089/acm.2007.7040
- Dhond, R. P., Yeh, C., Park, K., Kettner, N., & Napadow, V. (2008). Acupuncture modulates resting state connectivity in default and sensorimotor brain networks. *Pain*, 136(3), 407-418. doi: S0304-3959(08)00020-1 [pii]10.1016/j.pain.2008.01.011
- Dierks T, Jelic V, Pascual-Marqui RD, Wahlund LO, Julin P, Linden DEJ, Maurer K, Winblad B, Nordberg A. (2000): Spatial pattern of cerebral glucose metabolism (PET) correlates with localization of intracerebral EEG-generators in Alzheimer's disease. *Clinical Neurophysiology* 111(10):1817-1824.

- Ding, J. R., Liao, W., Zhang, Z., Mantini, D., Xu, Q., Wu, G. R., . . . Chen, H. (2011). Topological Fractionation of Resting-State Networks. *PloS one*, 6(10), e26596.
- Ding L, Lai Y, He B. (2004): Low resolution brain electromagnetic tomography in a realistic geometry head model: a simulation study. *Physics in medicine and biology* 50(1):45.
- Donchin, E., & Coles, M. G. (1988). Is the P300 component a manifestation of context updating?
- Doppelmayr, M., Weber, E., Hoedlmoser, K., & Klimesch, W. (2009). Effects of SMR feedback on the EEG amplitude. *Human Cogn. Neurophysiol.*, 2, 21-32.
- Dosenbach, N. U., Fair, D. A., Miezin, F. M., Cohen, A. L., Wenger, K. K., Dosenbach, R. A., . . . Petersen, S. E. (2007). Distinct brain networks for adaptive and stable task control in humans. *Proc Natl Acad Sci U S A*, 104(26), 11073-11078. doi: 0704320104 [pii]10.1073/pnas.0704320104
- Dumermuth, G. and Molinari, L. Spectral analysis of the EEG: some fundamentals revisited and some open problems. *Neuropsychobiology*, 1987, 17:85-99
- Durstewitz, D., Seamans, J. K., & Sejnowski, T. J. (2000). Dopamine-mediated stabilization of delay-period activity in a network model of prefrontal cortex. *Journal of Neurophysiology*, 83(3), 1733.
- Eckart, M. T., Huelse-Matia, M. C., McDonald, R. S., & Schwarting, R. K. W. (2010). 6-Hydroxydopamine lesions in the rat neostriatum impair sequential learning in a serial reaction time task. *Neurotoxicity research*, 17(3), 287-298.
- Egner, T. (2002). *Learned self-regulation of EEG frequency components and its effects on electrocortical and cognitive performance measures*. Ph.D., Imperial College London, London.
- Egner, T., & Gruzelier, J. H. (2001). Learned self-regulation of EEG frequency components affects attention and event-related brain potentials in humans. *Neuroreport*, 12(18), 4155-4159.
- Egner, T., & Gruzelier, J. H. (2003). Ecological validity of neurofeedback: modulation of slow wave EEG enhances musical performance. *Neuroreport*, 14(9), 1221-1224. doi: 10.1097/01.wnr.0000081875.45938.d1
- Egner, T., & Gruzelier, J. H. (2004). EEG biofeedback of low beta band components: frequency-specific effects on variables of attention and event-related brain potentials. *Clin Neurophysiol*, 115(1), 131-139. doi: S1388245703003535 [pii]
- Egner, T., Zech, T. F., & Gruzelier, J. H. (2004). The effects of neurofeedback training on the spectral topography of the electroencephalogram. *Clin Neurophysiol*, 115(11), 2452-2460. doi: S1388245704002056 [pii]10.1016/j.clinph.2004.05.033
- Engel, A. K., Fries, P., & Singer, W. (2001). Dynamic predictions: oscillations and synchrony in top-down processing. *Nat Rev Neurosci*, 2(10), 704-716. doi: 10.1038/3509456535094565 [pii]
- Esposito, F., Scarabino, T., Hyvarinen, A., Himberg, J., Formisano, E., Comani, S., . . . Di Salle, F. (2005). Independent component analysis of fMRI group studies by self-organizing clustering. *Neuroimage*, 25(1), 193-205. doi: S1053-8119(04)00660-3 [pii]10.1016/j.neuroimage.2004.10.042
- Evans AC, Collins DL, Mills S, Brown E, Kelly R, Peters TM. (1993): 3D statistical neuroanatomical models from 305 MRI volumes. Nuclear Science Symposium and

- Medical Imaging Conference, 1993., 1993 IEEE Conference Record.: IEEE. p 1813-1817.
- Evans, J. R., & Abarbanel, A. (1999). *Introduction to quantitative EEG and neurofeedback*. San Diego: Academic Press.
- Ezzo, J., Streitberger, K., & Schneider, A. (2006). Cochrane systematic reviews examine P6 acupuncture-point stimulation for nausea and vomiting. *J Altern Complement Med*, 12(5), 489-495. doi: 10.1089/acm.2006.12.489
- Fair, D. A., Cohen, A. L., Dosenbach, N. U., Church, J. A., Miezin, F. M., Barch, D. M., . . . Schlaggar, B. L. (2008). The maturing architecture of the brain's default network. *Proc Natl Acad Sci U S A*, 105(10), 4028-4032. doi: 0800376105 [pii]10.1073/pnas.0800376105
- Falkenstein M, Hoormann J, Hohnsbein J. (1999a): ERP components in Go/Nogo tasks and their relation to inhibition. *Acta psychologica* 101(2):267-291.
- Falkenstein M, Hoormann J, Hohnsbein J. (1999b): ERP components in Go/Nogo tasks and their relation to inhibition. *Acta Psychol (Amst)* 101(2-3):267-91.
- Falkenstein M, Koshlykova NA, Kiroj VN, Hoormann J, Hohnsbein J. (1995): Late ERP components in visual and auditory Go/Nogo tasks. *Electroencephalogr Clin Neurophysiol* 96(1):36-43.
- Fan, J., Byrne, J., Worden, M. S., Guise, K. G., McCandliss, B. D., Fossella, J., & Posner, M. I. (2007). The relation of brain oscillations to attentional networks. *The Journal of neuroscience*, 27(23), 6197-6206.
- Fender, D. H. (1987). Source Localization of Brain Electrical Activity. In A.S. Gevins & A. Remond (Eds.), *Methods of Analysis of Brain Electrical and Magnetic Signals* (pp. 355-403). Amsterdam-New York-Oxford: Elsevier.
- Fernandez-Bouzas A, Harmony T, Bosch J, Aubert E, Fernández T, Valdes P, Silva J, Marosi E, Martínez-López M, Casián G. (1999): Sources of abnormal EEG activity in the presence of brain lesions. *Clinical EEG and Neuroscience* 30(2):46-52.
- Fernández-Bouzas A, Harmony T, Fernández T, Ricardo-Garcell J, Casián G, Sánchez-Conde R. (2001): Cerebral blood flow and sources of abnormal EEG activity (VARETA) in neurocysticercosis. *Clinical Neurophysiology* 112(12):2281-2287.
- Fernández T, Harmony T, Silva-Pereyra J, Fernández-Bouzas A, Gersenowies J, Galán L, Carbonell F, Marosi E, Otero G, Valdés SI. (2000): Specific EEG frequencies at specific brain areas and performance. *Neuroreport* 11(12):2663-2668.
- Fetz, E. E. (1969). Operant conditioning of cortical unit activity. *Science*, 163(3870), 955.
- Fetz, E. E. (2007). Volitional control of neural activity: implications for brain-computer interfaces. *The Journal of physiology*, 579(3), 571-579.
- Fiorino, D. F., Coury, A., Fibiger, H. C., & Phillips, A. G. (1993). Electrical stimulation of reward sites in the ventral tegmental area increases dopamine transmission in the nucleus accumbens of the rat. *Behavioural brain research*, 55(2), 131-141.
- Fisch, B. J. (1999). *Fisch and Spehlmann's EEG Primer: Basic Principles of Digital and Analog EEG* (Third revised and enlarged ed.). New York: Elsevier.
- Folstein, M. F., Folstein, S. E., & McHugh, P. R. (1975). Mini-mental state: A practical method for grading the cognitive state of patients for the clinician. *Journal of psychiatric research*.

- Forbes, G. B. (1998). Clinical utility of the test of variables of attention (TOVA) in the diagnosis of attention-deficit/hyperactivity disorder. *Journal of Clinical Psychology*, 54(4), 461-476.
- Fox, M. D., Corbetta, M., Snyder, A. Z., Vincent, J. L., & Raichle, M. E. (2006). Spontaneous neuronal activity distinguishes human dorsal and ventral attention systems. *Proceedings of the National Academy of Sciences*, 103(26), 10046.
- Fox, M. D., Snyder, A. Z., Vincent, J. L., Corbetta, M., Van Essen, D. C., & Raichle, M. E. (2005). The human brain is intrinsically organized into dynamic, anticorrelated functional networks. *Proc Natl Acad Sci U S A*, 102(27), 9673-9678. doi: 0504136102 [pii]10.1073/pnas.0504136102
- Fransson, P. (2006). How default is the default mode of brain function? Further evidence from intrinsic BOLD signal fluctuations. *Neuropsychologia*, 44(14), 2836-2845. doi: S0028-3932(06)00251-X [pii]10.1016/j.neuropsychologia.2006.06.017
- Freeman, W. J. (1999). *How brains make up their minds*. London: Weidenfeld & Nicolson.
- Freeman, W. J. (2000). *How brains make up their minds*: Columbia Univ Pr.
- Fuchs M, Ford MR, Sands S, Lew HL. (2004): Overview of dipole source localization. *Physical Medicine and Rehabilitation Clinics of North America* 15(1):251-262.
- Fuchs M, Wagner M, Köhler T, Wischmann HA. (1999): Linear and nonlinear current density reconstructions. *Journal of Clinical Neurophysiology* 16(3):267-295.
- Fuchs M, Wagner M, Kastner J. (2001): Boundary element method volume conductor models for EEG source reconstruction. *Clinical neurophysiology: official journal of the International Federation of Clinical Neurophysiology* 112(8):1400.
- Fuchs, T., Birbaumer, N., Lutzenberger, W., Gruzelier, J. H., & Kaiser, J. (2003). Neurofeedback treatment for attention-deficit/hyperactivity disorder in children: a comparison with methylphenidate. *Appl Psychophysiol Biofeedback*, 28(1), 1-12.
- Gamma A, Lehmann D, Frei E, Iwata K, Pascual-Marqui RD, Vollenweider FX. (2004): Comparison of simultaneously recorded [H215O]-PET and LORETA during cognitive and pharmacological activation. *Human brain mapping* 22(2):83-96.
- Gareus IK, Lacour M, Schulte AC, Hennig J. (2002): Is there a BOLD response of the visual cortex on stimulation of the vision-related acupoint GB 37? *Journal of Magnetic Resonance Imaging* 15(3):227-232.
- Garris, P., & Wightman, R. (1994). Different kinetics govern dopaminergic transmission in the amygdala, prefrontal cortex, and striatum: an in vivo voltammetric study. *The Journal of neuroscience*, 14(1), 442.
- Garrity, A. G., Pearlson, G. D., McKiernan, K., Lloyd, D., Kiehl, K. A., & Calhoun, V. D. (2007). Aberrant "default mode" functional connectivity in schizophrenia. *American Journal of Psychiatry*, 164(3), 450.
- Gasser T, Molinari L. (1996): The analysis of the EEG. *Statistical Methods in Medical Research* 5(1):67-99.
- Gaztelu, J. M., & Buno, W., Jr. (1982). Septo-hippocampal relationships during EEG theta rhythm. *Electroencephalogr Clin Neurophysiol*, 54(4), 375-387.
- Gemba H, Sasaki K. (1990): Potential related to no-go reaction in go/no-go hand movement with discrimination between tone stimuli of different frequencies in the monkey. *Brain research* 537(1):340-344.

- Gevensleben, H., Holl, B., Albrecht, B., Schlamp, D., Kratz, O., Studer, P., . . . Heinrich, H. (2010). Neurofeedback training in children with ADHD: 6-month follow-up of a randomised controlled trial. *European child & adolescent psychiatry*, *19*(9), 715-724.
- Gevensleben, H., Holl, B., Albrecht, B., Schlamp, D., Kratz, O., Studer, P., . . . Heinrich, H. (2009a). Distinct EEG effects related to neurofeedback training in children with ADHD: a randomized controlled trial. *International Journal of Psychophysiology*, *74*(2), 149-157.
- Gevensleben, H., Holl, B., Albrecht, B., Schlamp, D., Kratz, O., Studer, P., . . . Heinrich, H. (2009b). Distinct EEG effects related to neurofeedback training in children with ADHD: a randomized controlled trial. *Int J Psychophysiol*, *74*(2), 149-157. doi: S0167-8760(09)00198-6 [pii]10.1016/j.ijpsycho.2009.08.005
- Gillig, P. M., & Sanders, R. D. (2011). Higher Cortical Functions: Attention and Vigilance. *Innovations in clinical neuroscience*, *8*(1), 43.
- Gilmore PC, Brenner RP. (1981): Correlation of EEG, computerized tomography, and clinical findings: study of 100 patients with focal delta activity. *Archives of Neurology* *38*(6):371.
- Gleichmann, U., Ingvar, D., Lassen, N., Lübbers, D., Siesjö, B., & Thews, G. (1962). Regional cerebral cortical metabolic rate of oxygen and carbon dioxide, related to the EEG in the anesthetized dog. *Acta physiologica Scandinavica*, *55*(1), 82-94.
- Goldman, R. I., Stern, J. M., Engel, J., Jr., & Cohen, M. S. (2002). Simultaneous EEG and fMRI of the alpha rhythm. *Neuroreport*, *13*(18), 2487-2492. doi: 10.1097/01.wnr.0000047685.08940.d0
- Gollo, L. L., Mirasso, C. R., Atienza, M., Crespo-Garcia, M., & Cantero, J. L. (2011). Theta Band Zero-Lag Long-Range Cortical Synchronization via Hippocampal Dynamical Relaying. *PloS one*, *6*(3), e17756.
- Gomez-Herrero, G., Atienza, M., Egiazarian, K., & Cantero, J. L. (2008). Measuring directional coupling between EEG sources. *Neuroimage*, *43*(3), 497-508. doi: S1053-8119(08)00854-9 [pii]10.1016/j.neuroimage.2008.07.032
- Gonsalvez, C. J., & Polich, J. (2002). P300 amplitude is determined by target-to-target interval. *Psychophysiology*, *39*(03), 388-396.
- Gonsalvez, C. J., & Polich, J. (2002). P300 amplitude is determined by target to target interval. *Psychophysiology*, *39*(3), 388-396.
- Gorodnitsky IF, George JS, Rao BD. (1995): Neuromagnetic source imaging with FOCUSS: a recursive weighted minimum norm algorithm. *Electroencephalography and clinical neurophysiology* *95*(4):231-251.
- Gow RV, Rubia K, Taylor E, Vallée-Tourangeau F, Matsudaira T, Ibrahimovic A, Sumich A. (2012): Abnormal centroparietal ERP response in predominantly medication-naive adolescent boys with ADHD during both response inhibition and execution. *Journal of Clinical Neurophysiology* *29*(2):181.
- Grave de Peralta Menendez R, Gonzalez Andino SL. (2000): Discussing the capabilities of Laplacian minimization. *Brain topography* *13*(2):97-104.
- Green, D. M., & Swets, J. A. (1966). *Signal detection theory and psychophysics* (Vol. 1974): Wiley New York.
- Green, D. M., & Swets, J. A. (1966). *Signal detection theory and psychophysics*. London: J. Wiley.

- Green, D. M., & Swets, J. A. (1974). *Signal detection theory and psychophysics*: Robert E. Krieger.
- Greenberg, L. M. (1987). An objective measure of methylphenidate response: clinical use of the MCA. *Psychopharmacol Bull*, 23(2), 279-282.
- Greicius, M. (2008). Resting-state functional connectivity in neuropsychiatric disorders. *Curr Opin Neurol*, 21(4), 424-430.
- Greicius, M. D., Krasnow, B., Reiss, A. L., & Menon, V. (2003). Functional connectivity in the resting brain: a network analysis of the default mode hypothesis. *Proc Natl Acad Sci U S A*, 100(1), 253-258.
- Grin-Yatsenko, V. A., Baas, I., Ponomarev, V. A., & Kropotov, J. D. (2010). Independent component approach to the analysis of EEG recordings at early stages of depressive disorders. *Clinical Neurophysiology*, 121(3), 281-289.
- Gross D, Gotman J. (1999): Correlation of high-frequency oscillations with the sleep–wake cycle and cognitive activity in humans. *Neuroscience* 94(4):1005-1018.
- Gruzelier, J. (2009). A theory of alpha/theta neurofeedback, creative performance enhancement, long distance functional connectivity and psychological integration. *Cogn Process*, 10 Suppl 1, S101-109. doi: 10.1007/s10339-008-0248-5
- Gruzelier, J., Egner, T., & Vernon, D. (2006). Validating the efficacy of neurofeedback for optimising performance. *Prog Brain Res*, 159, 421-431. doi: S0079-6123(06)59027-2 [pii]10.1016/S0079-6123(06)59027-2
- Gruzelier, J., Inoue, A., Smart, R., Steed, A., & Steffert, T. (2010). Acting performance and flow state enhanced with sensory-motor rhythm neurofeedback comparing ecologically valid immersive VR and training screen scenarios. *Neuroscience Letters*, 480(2), 112-116.
- Gursoy E, Niebur D. (2009): Harmonic load identification using complex independent component analysis. *Power Delivery, IEEE Transactions on* 24(1):285-292.
- Gusnard, D. A., Akbudak, E., Shulman, G. L., & Raichle, M. E. (2001). Medial prefrontal cortex and self-referential mental activity: relation to a default mode of brain function. *Proc Natl Acad Sci U S A*, 98(7), 4259-4264. doi: 10.1073/pnas.071043098071043098 [pii]
- Gusnard, D. A., & Raichle, M. E. (2001). Searching for a baseline: functional imaging and the resting human brain. *Nat Rev Neurosci*, 2(10), 685-694. doi: 10.1038/3509450035094500 [pii]
- Haake, M., Muller, H. H., Schade-Brittinger, C., Basler, H. D., Schafer, H., Maier, C., . . . Molsberger, A. (2007). German Acupuncture Trials (GERAC) for chronic low back pain: randomized, multicenter, blinded, parallel-group trial with 3 groups. *Arch Intern Med*, 167(17), 1892-1898. doi: 167/17/1892 [pii]10.1001/archinte.167.17.1892
- Haalman I, Vaadia E. (1998): Dynamics of neuronal interactions: relation to behavior, firing rates, and distance between neurons. *Human brain mapping* 5(4):249-253.
- Haas, L. (2003). Hans Berger (1873–1941), Richard Caton (1842–1926), and electroencephalography. *Journal of Neurology, Neurosurgery & Psychiatry*, 74(1), 9.
- Halgren E, Baudena P, Heit G, Clarke M, Marinkovic K, Chauvel P. (1994): Spatio-temporal stages in face and word processing. 2. Depth-recorded potentials in the human frontal and Rolandic cortices. *Journal of Physiology-Paris* 88(1):51-80.

- Hamalainen MS, Ilmoniemi R. (1994): Interpreting magnetic fields of the brain: minimum norm estimates. *Medical and Biological Engineering and Computing* 32(1):35-42.
- Hampson, M., Peterson, B. S., Skudlarski, P., Gatenby, J. C., & Gore, J. C. (2002). Detection of functional connectivity using temporal correlations in MR images. *Human brain mapping*, 15(4), 247-262.
- Hamzei, F., Dettmers, C., Rijntjes, M., Glauche, V., Kiebel, S., Weber, B., & Weiller, C. (2002). Visuomotor control within a distributed parieto-frontal network. *Exp Brain Res*, 146(3), 273-281. doi: 10.1007/s00221-002-1139-0
- Han, J. S. (2003). Acupuncture: neuropeptide release produced by electrical stimulation of different frequencies. *Trends Neurosci*, 26(1), 17-22. doi: S0166223602000061 [pii]
- Han, J. S. (2004). Acupuncture and endorphins. *Neurosci Lett*, 361(1-3), 258-261. doi: 10.1016/j.neulet.2003.12.019S0304394003014009 [pii]
- Han, J. S., & Sun, S. L. (1990). Differential release of enkephalin and dynorphin by low and high frequency electroacupuncture in the central nervous system. *Acupunct Sci Int J*, 1, 19-27.
- Han, J. S., & Terenius, L. (1982). Neurochemical basis of acupuncture analgesia. *Annu Rev Pharmacol Toxicol*, 22, 193-220. doi: 10.1146/annurev.pa.22.040182.001205
- Hanslmayr S, Klimesch W, Sauseng P, Gruber W, Doppelmayr M, Freunberger R, Pecherstorfer T. (2005): Visual discrimination performance is related to decreased alpha amplitude but increased phase locking. *Neuroscience Letters* 375(1):64-68.
- Hanslmayr S, Klimesch W, Sauseng P, Gruber W, Doppelmayr M, Freunberger R, Pecherstorfer T, Birbaumer N. (2007): Alpha phase reset contributes to the generation of ERPs. *Cerebral cortex* 17(1):1-8.
- Hanslmayr, S., Sauseng, P., Doppelmayr, M., Schabus, M., & Klimesch, W. (2005). Increasing individual upper alpha power by neurofeedback improves cognitive performance in human subjects. *Applied Psychophysiology and Biofeedback*, 30(1), 1-10.
- Hasselmo, M. E. (2005). What is the function of hippocampal theta rhythm?--Linking behavioral data to phasic properties of field potential and unit recording data. *Hippocampus*, 15(7), 936-949.
- He, D., Veiersted, K. B., Hostmark, A. T., & Medbo, J. I. (2004). Effect of acupuncture treatment on chronic neck and shoulder pain in sedentary female workers: a 6-month and 3-year follow-up study. *Pain*, 109(3), 299-307.
- Heinze HJ, Mangun, G. R., Burchert, W., Hinrichs, H., Scholz, M., Munte, T. F. et al. (1994): Combined spatial and temporal imaging of brain activity during visual selective attention in humans. *Nature* 372:8.
- Hester R, Fassbender C, Garavan H. (2004): Individual differences in error processing: a review and reanalysis of three event-related fMRI studies using the GO/NOGO task. *Cerebral cortex* 14(9):986-994.
- Hilgetag, C. C., Burns, G. A. P. C., O'Neill, M. A., Scannell, J. W., & Young, M. P. (2000). Anatomical connectivity defines the organization of clusters of cortical areas in the macaque and the cat. *Philosophical Transactions of the Royal Society of London. Series B: Biological Sciences*, 355(1393), 91-110.

- Hipp JF, Hawellek DJ, Corbetta M, Siegel M, Engel AK. (2012): Large-scale cortical correlation structure of spontaneous oscillatory activity. *Nature neuroscience* 15(6):884-890.
- Hirshberg, L. M., Chiu, S., & Frazier, J. A. (2005). Emerging brain-based interventions for children and adolescents: overview and clinical perspective. *Child Adolesc Psychiatr Clin N Am*, 14(1), 1-19, v. doi: S1056-4993(04)00074-4 [pii]10.1016/j.chc.2004.07.011
- Hoedlmoser, K., Pecherstorfer, T., Gruber, G., Anderer, P., Doppelmayr, M., Klimesch, W., & Schabus, M. (2008). Instrumental conditioning of human sensorimotor rhythm (12-15 Hz) and its impact on sleep as well as declarative learning. *Sleep*, 31(10), 1401-1408.
- Hollerman, J. R., & Schultz, W. (1998). Dopamine neurons report an error in the temporal prediction of reward during learning. *Nat Neurosci*, 1(4), 304-309.
- Holper, L., Muehlemann, T., Scholkmann, F., Eng, K., Kiper, D., & Wolf, M. (2010). Testing the potential of a virtual reality neurorehabilitation system during performance of observation, imagery and imitation of motor actions recorded by wireless functional near-infrared spectroscopy (fNIRS). *Journal of NeuroEngineering and Rehabilitation*, 7(1), 57.
- Honey, C., Sporns, O., Cammoun, L., Gigandet, X., Thiran, J. P., Meuli, R., & Hagmann, P. (2009). Predicting human resting-state functional connectivity from structural connectivity. *Proceedings of the National Academy of Sciences*, 106(6), 2035.
- Honey, C. J., Kötter, R., Breakspear, M., & Sporns, O. (2007). Network structure of cerebral cortex shapes functional connectivity on multiple time scales. *Proceedings of the National Academy of Sciences*, 104(24), 10240.
- Hori E, Takamoto K, Urakawa S, Ono T, Nishijo H. (2010): Effects of acupuncture on the brain hemodynamics. *Autonomic Neuroscience* 157(1):74-80.
- Hsieh, J. C., Tu, C. H., Chen, F. P., Chen, M. C., Yeh, T. C., Cheng, H. C., . . . Ho, L. T. (2001). Activation of the hypothalamus characterizes the acupuncture stimulation at the analgesic point in human: a positron emission tomography study. *Neurosci Lett*, 307(2), 105-108. doi: S0304-3940(01)01952-8 [pii]
- Huang, C., Wang, Y., Han, J. S., & Wan, Y. (2002). Characteristics of electroacupuncture-induced analgesia in mice: variation with strain, frequency, intensity and opioid involvement. *Brain Res* 945(1):20-5
- Hui, K. K., Liu, J., Makris, N., Gollub, R. L., Chen, A. J., Moore, C. I., . . . Kwong, K. K. (2000). Acupuncture modulates the limbic system and subcortical gray structures of the human brain: evidence from fMRI studies in normal subjects. *Hum Brain Mapp*, 9(1), 13-25.
- Hui, K. K., Liu, J., Marina, O., Napadow, V., Haselgrove, C., Kwong, K. K., . . . Makris, N. (2005). The integrated response of the human cerebro-cerebellar and limbic systems to acupuncture stimulation at ST 36 as evidenced by fMRI. *Neuroimage*, 27(3), 479-496. doi: S1053-8119(05)00314-9 [pii]10.1016/j.neuroimage.2005.04.037
- Hui, K. K., Marina, O., Claunch, J. D., Nixon, E. E., Fang, J., Liu, J., . . . Rosen, B. R. (2009). Acupuncture mobilizes the brain's default mode and its anti-correlated network in healthy subjects. *Brain Res*, 1287, 84-103. doi: S0006-8993(09)01280-3 [pii]10.1016/j.brainres.2009.06.061

- Hui, K. K., Marina, O., Liu, J., Rosen, B. R., & Kwong, K. K. (2010). Acupuncture, the limbic system, and the anticorrelated networks of the brain. *Auton Neurosci*. doi: S1566-0702(10)00069-X [pii]10.1016/j.autneu.2010.03.022
- Hutsler, J., & Galuske, R. A. W. (2003). Hemispheric asymmetries in cerebral cortical networks. *Trends in Neurosciences*, 26(8), 429-435.
- Hyman, J. M., Zilli, E. A., Paley, A. M., & Hasselmo, M. E. (2005). Medial prefrontal cortex cells show dynamic modulation with the hippocampal theta rhythm dependent on behavior. *Hippocampus*, 15(6), 739-749.
- Hyvarinen, A., & Oja, E. (2000). Independent component analysis: algorithms and applications. *Neural Netw*, 13(4-5), 411-430. doi: S0893-6080(00)00026-5 [pii]
- Hyvarinen A, Karhunen J, Oja E. (2002): Frontmatter and Index: Wiley Online Library.
- Hyvarinen A. (1999): Fast and robust fixed-point algorithms for independent component analysis. *Neural Networks, IEEE Transactions on* 10(3):626-634.
- Hyvarinen A, Karhunen J, Oja E. (2001): Independent component analysis. Wiley, New York.
- Hyvarinen, A., Ramkumar, P., Parkkonen, L., & Hari, R. (2010). Independent component analysis of short-time Fourier transforms for spontaneous EEG/MEG analysis. *Neuroimage*, 49(1), 257-271. doi: S1053-8119(09)00940-9 [pii]10.1016/j.neuroimage.2009.08.028
- Ikemoto, S., & Wise, R. A. (2002). Rewarding effects of the cholinergic agents carbachol and neostigmine in the posterior ventral tegmental area. *The Journal of neuroscience*, 22(22), 9895.
- Imai, K., Ariga, H., Chen, C., Mantyh, C., Pappas, T. N., & Takahashi, T. (2008). Effects of electroacupuncture on gastric motility and heart rate variability in conscious rats. *Autonomic neuroscience: basic & clinical*, 138(1-2), 91.
- Innocenti, G. M. (1994). Some new trends in the study of the corpus callosum. *Behavioural brain research*, 64(1-2), 1-8.
- Ioannides, A. A. (2007). Dynamic functional connectivity. *Current opinion in neurobiology*, 17(2), 161-170.
- Ishii, R., Shinosaki, K., Ukai, S., Inouye, T., Ishihara, T., Yoshimine, T., . . . Robinson, S. E. (1999). Medial prefrontal cortex generates frontal midline theta rhythm. *Neuroreport*, 10(4), 675.
- Itoh, K., Hirota, S., Katsumi, Y., Ochi, H., & Kitakoji, H. (2008). A pilot study on using acupuncture and transcutaneous electrical nerve stimulation (TENS) to treat knee osteoarthritis (OA). *Chin Med*, 3, 2. doi: 1749-8546-3-2 [pii]10.1186/1749-8546-3-2
- Itoh, K., Katsumi, Y., Hirota, S., & Kitakoji, H. (2006). Effects of trigger point acupuncture on chronic low back pain in elderly patients--a sham-controlled randomised trial. *Acupunct Med*, 24(1), 5-12.
- James, C. J., & Hesse, C. W. (2005). Independent component analysis for biomedical signals. *Physiol Meas*, 26(1), R15-39.
- Jann, K., Dierks, T., Boesch, C., Kottlow, M., Strik, W., & Koenig, T. (2009). BOLD correlates of EEG alpha phase-locking and the fMRI default mode network. *Neuroimage*, 45(3), 903-916.

- Jasper, H. H., & Carmichael, L. (1935). Electrical potentials from the intact human brain. *Science*.
- Jeffs B, Leahy R, Singh M. (1987): An evaluation of methods for neuromagnetic image reconstruction. *Biomedical Engineering, IEEE Transactions on*(9):713-723.
- Jensen, O., & Tesche, C. D. (2002). Frontal theta activity in humans increases with memory load in a working memory task. *European Journal of Neuroscience*, 15(8), 1395-1399.
- Jervis BW, Nichols MJ, Johnson TE, Allen E, Hudson NR. (1983): A fundamental investigation of the composition of auditory evoked potentials. *Biomedical Engineering, IEEE Transactions on*(1):43-50.
- John E. (1980): Developmental equations for the electroencephalogram. *Science*.
- Jones, B. E., Bobillier, P., Pin, C., & Jouvet, M. (1973). The effect of lesions of catecholamine-containing neurons upon monoamine content of the brain and EEG and behavioral waking in the cat. *Brain research*, 58(1), 157-177.
- Jonsdottir, S., Bouma, A., Sergeant, J. A., & Scherder, E. J. (2004). Effects of transcutaneous electrical nerve stimulation (TENS) on cognition, behavior, and the rest-activity rhythm in children with attention deficit hyperactivity disorder, combined type. *Neurorehabil Neural Repair*, 18(4), 212-221. doi: 18/4/212 [pii]10.1177/1545968304270759
- Jung, T. P., Makeig, S., Humphries, C., Lee, T. W., McKeown, M. J., Iragui, V., & Sejnowski, T. J. (2000). Removing electroencephalographic artifacts by blind source separation. *Psychophysiology*, 37(2), 163-178.
- Jung, T. P., Makeig, S., Stensmo, M., & Sejnowski, T. J. (1997). Estimating alertness from the EEG power spectrum. *Biomedical Engineering, IEEE Transactions on*, 44(1), 60-69.
- Jung, T. P., Makeig, S., Westerfield, M., Townsend, J., Courchesne, E., & Sejnowski, T. J. (2000). Removal of eye activity artifacts from visual event-related potentials in normal and clinical subjects. *Clin Neurophysiol*, 111(10), 1745-1758. doi: S1388-2457(00)00386-2 [pii]
- Kahneman, D. (1973). Attention and effort.
- Kaiser, D. (2000). QEEG: state of the art, or state of confusion. *Journal of Neurotherapy*, 4(2), 57-76.
- Kamiya, J. (1968). Conscious control of brain waves. *Psychology Today*, 1(11), 56-60.
- Kamp, A., & da Silva, F. L. (1999). Technological Basis of EEG Recording. In E. Niedermeyer & F. H. Lopes da Silva (Eds.), *Electroencephalography, Basic Principles, Clinical Applications, and Related Fields: Basic Principles, Clinical Applications and Related Fields* (pp. 110-121). Baltimore: Williams & Wilkins.
- Kaptchuk, T. J. (2002). Acupuncture: theory, efficacy, and practice. *Ann Intern Med*, 136(5), 374-383. doi: 200203050-00010 [pii]
- Kato, Y., Endo, H., & Kizuka, T. (2009). Mental fatigue and impaired response processes: Event-related brain potentials in a Go/NoGo task. *International Journal of Psychophysiology*, 72(2), 204-211.
- Kaufman, J. N., Ross, T. J., Stein, E. A., & Garavan, H. (2003). Cingulate hypoactivity in cocaine users during a GO-NOGO task as revealed by event-related functional magnetic resonance imaging. *The Journal of neuroscience*, 23(21), 7839.

- Keck, M., Welt, T., Müller, M., Erhardt, A., Ohl, F., Toschi, N., . . . Sillaber, I. (2002). Repetitive transcranial magnetic stimulation increases the release of dopamine in the mesolimbic and mesostriatal system. *Neuropharmacology*, 43(1), 101-109.
- Keizer, A. W., Verschoor, M., Verment, R. S., & Hommel, B. (2010). The effect of gamma enhancing neurofeedback on the control of feature bindings and intelligence measures. *International Journal of Psychophysiology*, 75(1), 25-32.
- Kincade, J. M., Abrams, R. A., Astafiev, S. V., Shulman, G. L., & Corbetta, M. (2005). An event-related functional magnetic resonance imaging study of voluntary and stimulus-driven orienting of attention. *The Journal of neuroscience*, 25(18), 4593.
- Kincses WE, Braun C, Kaiser S, Elbert T. (1999): Modeling extended sources of event-related potentials using anatomical and physiological constraints. *Human brain mapping* 8(4):182-193.
- Kirmizi-Alsan E, Bayraktaroglu Z, Gurvit H, Keskin Y, Emre M, Demiralp T. (2006): Comparative analysis of event-related potentials during Go/NoGo and CPT: decomposition of electrophysiological markers of response inhibition and sustained attention. *Brain Res* 1104(1):114-28.
- Kiviniemi, V., Starck, T., Remes, J., Long, X., Nikkinen, J., Haapea, M., . . . Tervonen, O. (2009). Functional segmentation of the brain cortex using high model order group PICA. *Hum Brain Mapp*, 30(12), 3865-3886. doi: 10.1002/hbm.20813
- Klimesch, W. (1999). EEG alpha and theta oscillations reflect cognitive and memory performance: a review and analysis. *Brain Res Brain Res Rev*, 29(2-3), 169-195.
- Klimesch, W., Doppelmayr, M., Rohm, D., Pollhuber, D., & Stadler, W. (2000). Simultaneous desynchronization and synchronization of different alpha responses in the human electroencephalograph: a neglected paradox? *Neurosci Lett*, 284(1-2), 97-100. doi: S0304-3940(00)00985-X [pii]
- Klimesch, W., Sauseng, P., & Hanslmayr, S. (2007). EEG alpha oscillations: the inhibition-timing hypothesis. *Brain Res Rev*, 53(1), 63-88. doi: S0165-0173(06)00083-X [pii]10.1016/j.brainresrev.2006.06.003
- Klimesch, W., Sauseng, P., Hanslmayr, S., Gruber, W., & Freunberger, R. (2007). Event-related phase reorganization may explain evoked neural dynamics. *Neurosci Biobehav Rev*, 31(7), 1003-1016. doi: S0149-7634(07)00033-4 [pii]10.1016/j.neubiorev.2007.03.005
- Koepp, M., Gunn, R., Lawrence, A., Cunningham, V., Dagher, A., Jones, T., . . . Grasby, P. (1998). Evidence for striatal dopamine release during a video game. *Nature*, 393(6682), 266-267.
- Koles ZJ. (1998): Trends in EEG source localization. *Electroencephalography and clinical neurophysiology* 106(2):127-137.
- Kong, J., Ma, L., Gollub, R. L., Wei, J., Yang, X., Li, D., . . . Zhuang, D. (2002). A pilot study of functional magnetic resonance imaging of the brain during manual and electroacupuncture stimulation of acupuncture point (LI-4 Hegu) in normal subjects reveals differential brain activation between methods. *J Altern Complement Med*, 8(4), 411-419. doi: 10.1089/107555302760253603
- Kopp B, Rist F, Mattler U. (2007): N200 in the flanker task as a neurobehavioral tool for investigating executive control. *Psychophysiology* 33(3):282-294.

- Kotchoubey, B., Strehl, U., Uhlmann, C., Holzapfel, S., König, M., Froscher, W., . . . Birbaumer, N. (2001). Modification of slow cortical potentials in patients with refractory epilepsy: a controlled outcome study. *Epilepsia*, *42*(3), 406-416.
- Kotz, A., & Simpson, K. H. (2008). Stimulation-produced analgesia: acupuncture, TENS and related techniques. *Anaesthesia & Intensive Care Medicine*, *9*(1), 29-32.
- Kouijzer, M. E. J., de Moor, J. M. H., Gerrits, B. J. L., Buitelaar, J. K., & van Schie, H. T. (2009). Long-term effects of neurofeedback treatment in autism. *Research in Autism Spectrum Disorders*, *3*(2), 496-501.
- Krakow K, Woermann F, Symms M, Allen P, Lemieux L, Barker G, Duncan J, Fish D. (1999): EEG-triggered functional MRI of interictal epileptiform activity in patients with partial seizures. *Brain* *122*(9):1679-1688.
- Krepki, R., Blankertz, B., Curio, G., & Müller, K. R. (2007). The Berlin Brain-Computer Interface (BBCI) - Towards a new communication channel for online control in gaming applications. *Multimedia Tools and Applications*, *33*(1), 73-90.
- Kropotov JD, Ponomarev VA, Hollup S, Mueller A. (2011): Dissociating action inhibition, conflict monitoring and sensory mismatch into independent components of event related potentials in GO/NOGO task. *NeuroImage* *57*(2):565-575.
- Kropotov JD. (2009a): Attention Networks. *Quantitative EEG, Event-Related Potentials and Neurotherapy*. San Diego: Academic Press. p 231-252.
- Kropotov, J. D. (2009b). Executive System *Quantitative EEG, Event-Related Potentials and Neurotherapy*. San Diego: Academic Press. p 253-291.
- Kropotov, J. D. (2009c). Methods of Analysis of Background EEG *Quantitative EEG, Event-Related Potentials and Neurotherapy*. San Diego: Academic Press. p 116-160.
- Kropotov, J. D. (2009d). Methods: Neuronal Networks and Event-Related Potentials *Quantitative EEG, Event-Related Potentials and Neurotherapy*. San Diego: Academic Press. p 325-365.
- Kropotov, J. D., & Etlinger, S. C. (1999). Selection of actions in the basal ganglia-thalamocortical circuits: review and model. *International Journal of Psychophysiology*, *31*(3), 197-217.
- Kropotov, J. D., Grin-Yatsenko, V. A., Ponomarev, V. A., Chutko, L. S., Yakovenko, E. A., & Nikishena, I. S. (2005). ERPs correlates of EEG relative beta training in ADHD children. *Int J Psychophysiol*, *55*(1), 23-34. doi: S0167876004001011 [pii]10.1016/j.ijpsycho.2004.05.011
- Kropotov, J. D., Grin-Yatsenko, V. A., Ponomarev, V. A., Chutko, L. S., Yakovenko, E. A., & Nikishena, I. S. (2007). Changes in EEG spectrograms, event-related potentials and event-related desynchronization induced by relative beta training in ADHD children. *Journal of Neurotherapy*, *11*(2), 3-11.
- Kropotov JD, NÄÄÄNEN R, Sevostianov A, Alho K, Reinikainen K, Kropotova O. (1995): Mismatch negativity to auditory stimulus change recorded directly from the human temporal cortex. *Psychophysiology* *32*(4):418-422.
- Kuhnpast N. (2008): Neural correlates of emotional face processing in bulimia nervosa.
- Kulichenko, A., Fokina, Y. O., & Pavlenko, V. (2009). Changes in EEG Rhythms and Spike Activity of Brainstem Dopaminergic Neurons Induced by Neurofeedback Sessions in Cats. *Neurophysiology*, *41*(3), 196-200.

- Laibow, R. (1999). Medical Applications of NeuroBioFeedback. In J. R. Evans & A. Abarbanel (Eds.), *Introduction to Quantitative EEG and Neurofeedback* (pp. 83-102). London: Academic Press.
- Lapish, C. C., Kroener, S., Durstewitz, D., Lavin, A., & Seamans, J. K. (2007). The ability of the mesocortical dopamine system to operate in distinct temporal modes. *Psychopharmacology*, *191*(3), 609-625.
- Laufs, H. (2008). Endogenous brain oscillations and related networks detected by surface EEG-combined fMRI. *Hum Brain Mapp*, *29*(7), 762-769. doi: 10.1002/hbm.20600
- Laufs, H., Daunizeau, J., Carmichael, D. W., & Kleinschmidt, A. (2008). Recent advances in recording electrophysiological data simultaneously with magnetic resonance imaging. *Neuroimage*, *40*(2), 515-528. doi: S1053-8119(07)01073-7 [pii]10.1016/j.neuroimage.2007.11.039
- Laufs, H., Kleinschmidt, A., Beyerle, A., Eger, E., Salek-Haddadi, A., Preibisch, C., & Krakow, K. (2003). EEG-correlated fMRI of human alpha activity. *Neuroimage*, *19*(4), 1463-1476. doi: S1053811903002866 [pii]
- Laufs, H., Krakow, K., Sterzer, P., Eger, E., Beyerle, A., Salek-Haddadi, A., & Kleinschmidt, A. (2003). Electroencephalographic signatures of attentional and cognitive default modes in spontaneous brain activity fluctuations at rest. *Proc Natl Acad Sci U S A*, *100*(19), 11053-11058. doi: 10.1073/pnas.18316381001831638100 [pii]
- Lavric A, Pizzagalli D, Forstmeier S, Rippon G. (2001): A double-dissociation of English past-tense production revealed by event-related potentials and low-resolution electromagnetic tomography (LORETA). *Clinical Neurophysiology* *112*(10):1833-1849.
- Lee, J. D., Chon, J. S., Jeong, H. K., Kim, H. J., Yun, M., Kim, D. Y., . . . Yoo, H. S. (2003). The cerebrovascular response to traditional acupuncture after stroke. *Neuroradiology*, *45*(11), 780-784. doi: 10.1007/s00234-003-1080-3
- Lee, J. H., Kim, J., & Yoo, S. S. (2012). Real-time fMRI-based neurofeedback reinforces causality of attention networks. *Neuroscience Research*.
- Lee TW, Girolami M, Bell AJ, Sejnowski TJ. (2000): A unifying information-theoretic framework for independent component analysis. *Computers & Mathematics with Applications* *39*(11):1-21.
- Levesque, J., Beauregard, M., & Mensour, B. (2006). Effect of neurofeedback training on the neural substrates of selective attention in children with attention-deficit/hyperactivity disorder: A functional magnetic resonance imaging study. *Neuroscience Letters*, *394*(3), 216-221.
- Lewis, B. L., & O'Donnell, P. (2000). Ventral tegmental area afferents to the prefrontal cortex maintain membrane potential 'up' states in pyramidal neurons via D1 dopamine receptors. *Cerebral cortex*, *10*(12), 1168.
- Lewis, D., Campbell, M., Foote, S., Goldstein, M., & Morrison, J. (1987). The distribution of tyrosine hydroxylase-immunoreactive fibers in primate neocortex is widespread but regionally specific. *The Journal of neuroscience*, *7*(1), 279.
- Li, L., Yao, D., & Yin, G. (2009). Spatio-temporal dynamics of visual selective attention identified by a common spatial pattern decomposition method. *Brain Research*, *1282*, 84-94.

- Liang, X. B., Liu, X. Y., Li, F. Q., Luo, Y., Lu, J., Zhang, W. M., . . . Han, J. S. (2002). Long-term high-frequency electro-acupuncture stimulation prevents neuronal degeneration and up-regulates BDNF mRNA in the substantia nigra and ventral tegmental area following medial forebrain bundle axotomy. *Molecular brain research*, *108*(1-2), 51-59.
- Liang, X. B., Luo, Y., Liu, X. Y., Lu, J., Li, F. Q., Wang, Q., . . . Han, J. S. (2003). Electro-acupuncture improves behavior and upregulates GDNF mRNA in MFB transected rats. *Neuroreport*, *14*(8), 1177.
- Liao TJ, Nakanishi H, Nishikawa H. (1993): The effect of acupuncture stimulation of the middle latency auditory evoked potential. *Tohoku J Exp Med* *170*(2):103-12.
- Lin, Y. C. (2006). Perioperative usage of acupuncture. *Pediatric Anesthesia*, *16*(3), 231-235.
- Litscher, G. (2004). Effects of acupressure, manual acupuncture and Laserneedle acupuncture on EEG bispectral index and spectral edge frequency in healthy volunteers. *Eur J Anaesthesiol*, *21*(1), 13-19.
- Liu AK, Belliveau JW, Dale AM. (1998): Spatiotemporal imaging of human brain activity using functional MRI constrained magnetoencephalography data: Monte Carlo simulations. *Proceedings of the National Academy of Sciences* *95*(15):8945-8950.
- Llinas, R. R. (1988). The intrinsic electrophysiological properties of mammalian neurons: insights into central nervous system function. *Science*, *242*(4886), 1654-1664.
- Lloyd, M. A., & Appel, J. B. (1976). Signal detection theory and the psychophysics of pain: an introduction and review. *Psychosomatic medicine*, *38*(2), 79.
- Lopes da Silva F. (2004): Functional localization of brain sources using EEG and/or MEG data: volume conductor and source models. *Magnetic resonance imaging* *22*(10):1533-1538.
- Lowe, M. J., Mock, B. J., & Sorenson, J. A. (1998). Functional connectivity in single and multislice echoplanar imaging using resting-state fluctuations. *Neuroimage*, *7*(2), 119-132. doi: S1053-8119(97)90315-3 [pii]10.1006/nimg.1997.0315
- Lu, G. W. (1983). Characteristics of afferent fiber innervation on acupuncture points zusanli. *American Journal of Physiology- Regulatory, Integrative and Comparative Physiology*, *245*(4), 606.
- Lubar, J. F., & Shouse, M. N. (1976). EEG and behavioral changes in a hyperkinetic child concurrent with training of the sensorimotor rhythm (SMR). *Applied Psychophysiology and Biofeedback*, *1*(3), 293-306.
- Lubar, J. F., Swartwood, M. O., Swartwood, J. N., & O'Donnell, P. H. (1995). Evaluation of the effectiveness of EEG neurofeedback training for ADHD in a clinical setting as measured by changes in T.O.V.A. scores, behavioral ratings, and WISC-R performance. *Biofeedback Self Regul*, *20*(1), 83-99.
- Lubar, J. O., & Lubar, J. F. (1984). Electroencephalographic biofeedback of SMR and beta for treatment of attention deficit disorders in a clinical setting. *Biofeedback Self Regul*, *9*(1), 1-23.
- Luijpen, M. W., Swaab, D. F., Sergeant, J. A., van Dijk, K. R., & Scherder, E. J. (2005). Effects of transcutaneous electrical nerve stimulation (TENS) on memory in elderly with mild cognitive impairment. *Behav Brain Res*, *158*(2), 349-357. doi: S0166-4328(04)00375-4 [pii], 10.1016/j.bbr.2004.09.017

- Lund, I., & Lundeberg, T. (2006). Are minimal, superficial or sham acupuncture procedures acceptable as inert placebo controls? *Acupunct Med*, 24(1), 13-15.
- Lutzenberger, W., Birbaumer, N., Elbert, T., Rockstroh, B., Bippus, W., & Breidt, R. (1980). Self-regulation of slow cortical potentials in normal subjects and patients with frontal lobe lesions. *Progress in Brain Research*, 54, 427-430.
- Luu, P., Tucker, D. M., Derryberry, D., Reed, M., & Poulsen, C. (2003). Electrophysiological responses to errors and feedback in the process of action regulation. *Psychol Sci*, 14(1), 47-53.
- MacDonald KD, Brett B, Barth DS. (1996): Inter-and intra-hemispheric spatiotemporal organization of spontaneous electrocortical oscillations. *Journal of Neurophysiology* 76(1):423-437.
- Mackworth, J. F. (1964). Performance decrement in vigilance, threshold, and high-speed perceptual motor tasks. *Canadian Journal of Psychology/Revue canadienne de psychologie*, 18(3), 209.
- Makeig, S., Bell, A.J., Jung, T.P., Sejnowski, B. (1996). Independent component analysis of electroencephalographic data. *Adv. Neural Inf. Process Syst.*, 8, 145-151.
- Makeig, S., Delorme, A., Westerfield, M., Jung, T. P., Townsend, J., Courchesne, E., & Sejnowski, T. J. (2004). Electroencephalographic brain dynamics following manually responded visual targets. *PLoS Biol*, 2(6), e176. doi: 10.1371/journal.pbio.0020176
- Makeig, S., & Jung, T. P. (1996). Tonic, phasic, and transient EEG correlates of auditory awareness in drowsiness. *Cognitive Brain Research*, 4(1), 15-25.
- Makeig, S., Jung, T. P., Bell, A. J., Ghahremani, D., & Sejnowski, T. J. (1997). Blind separation of auditory event-related brain responses into independent components. *Proc Natl Acad Sci U S A*, 94(20), 10979-10984.
- Makeig, S., Westerfield, M., Jung, T. P., Enghoff, S., Townsend, J., Courchesne, E., & Sejnowski, T. J. (2002). Dynamic brain sources of visual evoked responses. *Science*, 295(5555), 690-694. doi: 10.1126/science.1066168295/5555/690 [pii]
- Mann, F. (2000). *Reinventing acupuncture: a new concept of ancient medicine*: Butterworth-Heinemann Medical.
- Manoilov, P. K., & Borodzhieva, A. N. (2008). *Studying Eye-Blinking Artefacts Power Spectrum*. Paper presented at the International Scientific Conference Computer Science.
- Mantini, D., Perrucci, M. G., Del Gratta, C., Romani, G. L., & Corbetta, M. (2007). Electrophysiological signatures of resting state networks in the human brain. *Proc Natl Acad Sci U S A*, 104(32), 13170-13175.
- Marco-Pallares, J., Grau, C., & Ruffini, G. (2005). Combined ICA-LORETA analysis of mismatch negativity. *Neuroimage*, 25(2), 471-477.
- Marken, R. S. (2009). You say you had a revolution: Methodological foundations of closed-loop psychology. *Review of General Psychology*, 13(2), 137.
- Markram, H., Gupta, A., Uziel, A., Wang, Y., & Tsodyks, M. (1998). Information Processing with Frequency-Dependent Synaptic Connections* 1,* 2,* 3. *Neurobiology of learning and memory*, 70(1-2), 101-112.
- Markram, H., Tsodyks, M., Wang, Y., & Uziel, A. (1999). Frequency-dependent synaptic transmission in the neocortex. *Advances in Synaptic Plasticity*. MIT Press, Cambridge, MA, 239-264.

- Marwick, C. (1997). Acceptance of Some Acupuncture Applications. *JAMA*, 278(21), 1725-a-1727. doi: 10.1001/jama.1997.03550210021013
- Marx, E., Stephan, T., Nolte, A., Deutschlander, A., Seelos, K. C., Dieterich, M., & Brandt, T. (2003). Eye closure in darkness animates sensory systems. *Neuroimage*, 19(3), 924-934. doi: S1053811903001502 [pii]
- Maurer K, Dierks T. (1992): Functional imaging procedures in dementias: mapping of EEG and evoked potentials. *Acta Neurologica Scandinavica* 85(S139):40-46.
- Mason, M. F., Norton, M. I., Van Horn, J. D., Wegner, D. M., Grafton, S. T., & Macrae, C. N. (2007). Wandering minds: the default network and stimulus-independent thought. *Science*, 315(5810), 393.
- Mayer, D. J., Price, D. D., & Rafii, A. (1977). Antagonism of acupuncture analgesia in man by the narcotic antagonist naloxone. *Brain Res*, 121(2), 368-372. doi: 0006-8993(77)90161-5 [pii]
- Mazaheri, A., Coffey-Corina, S., Mangun, G. R., Bekker, E. M., Berry, A. S., & Corbett, B. A. (2010). Functional disconnection of frontal cortex and visual cortex in attention-deficit/hyperactivity disorder. *Biol Psychiatry*, 67(7), 617-623.
- McCarthy G, Wood CC, Williamson PD, Spencer DD. (1989): Task-dependent field potentials in human hippocampal formation. *J Neurosci* 9(12):4253-68.
- McEvoy LK, Smith ME, Gevins A. (2000): Test-retest reliability of cognitive EEG. *Clin Neurophysiol* 111(3):457-63.
- McNab, F., Varrone, A., Farde, L., Jucaite, A., Bystritsky, P., Forssberg, H., & Klingberg, T. (2009). Changes in cortical dopamine D1 receptor binding associated with cognitive training. *Science*, 323(5915), 800-802. doi: 323/5915/800 [pii]10.1126/science.1166102
- McNicol, D. (1972). *A primer of signal detection theory* (Vol. 569): Allen & Unwin Australia.
- Melzack, R. (1976). Acupuncture and pain mechanisms (author's transl). *Der Anaesthetist*, 25(5), 204.
- Melzack, R., & Wall, P. D. (1967). Pain mechanisms: a new theory. *Survey of Anesthesiology*, 11(2), 89.
- Mesulam, M. (1990). Large-scale neurocognitive networks and distributed processing for attention, language, and memory. *Annals of neurology*, 28(5), 597-613.
- Michel CM, Murray MM, Lantz G, Gonzalez S, Spinelli L, Grave de Peralta R. (2004): EEG source imaging. *Clinical Neurophysiology* 115(10):2195-2222.
- Miller, E., Maimon, Y., Rosenblatt, Y., Mendler, A., Hasner, A., Barad, A., . . . Lev-Ari, S. (2009). Delayed Effect of Acupuncture Treatment in OA of the Knee: A Blinded, Randomized, Controlled Trial. *Evid Based Complement Alternat Med*. doi: nen080 [pii]10.1093/ecam/nen080
- Miltner, W. H., Braun, C., Arnold, M., Witte, H., & Taub, E. (1999). Coherence of gamma-band EEG activity as a basis for associative learning. *Nature*, 397(6718), 434-436. doi: 10.1038/17126
- Mink, J. W. (1996). The basal ganglia: focused selection and inhibition of competing motor programs. *Progress in neurobiology*, 50(4), 381-425.
- Mizuhara, H., Wang, L. Q., Kobayashi, K., & Yamaguchi, Y. (2004). A long-range cortical network emerging with theta oscillation in a mental task. *Neuroreport*, 15(8), 1233.

- Moffitt MA, Grill WM. (2004): Electrical localization of neural activity in the dorsal horn of the spinal cord: a modeling study. *Annals of biomedical engineering* 32(12):1694-1709.
- Molina-Luna, K., Pekanovic, A., Röhrich, S., Hertler, B., Schubring-Giese, M., Rioult-Pedotti, M. S., & Luft, A. R. (2009). Dopamine in motor cortex is necessary for skill learning and synaptic plasticity. *PloS one*, 4(9), e7082.
- Monastra, V. J., Lubar, J. F., & Linden, M. (2001). The development of a quantitative electroencephalographic scanning process for attention deficit–hyperactivity disorder: Reliability and validity studies. *Neuropsychology*, 15(1), 136.
- Monastra, V. J., Monastra, D. M., & George, S. (2002). The effects of stimulant therapy, EEG biofeedback, and parenting style on the primary symptoms of attention-deficit/hyperactivity disorder. *Appl Psychophysiol Biofeedback*, 27(4), 231-249.
- Montaron, M. F., Bouyer, J. J., Rougeul, A., & Buser, P. (1982). Ventral mesencephalic tegmentum (VMT) controls electrocortical beta rhythms and associated attentive behaviour in the cat. *Behavioural brain research*, 6(2), 129-145.
- Moran LV, Hong LE. (2011): High vs low frequency neural oscillations in schizophrenia. *Schizophrenia bulletin* 37(4):659-663.
- Mosher JC, Leahy RM. (1998): Recursive MUSIC: a framework for EEG and MEG source localization. *Biomedical Engineering, IEEE Transactions on* 45(11):1342-1354.
- Mosher JC, Leahy RM. (1999): Source localization using recursively applied and projected (RAP) MUSIC. *Signal Processing, IEEE Transactions on* 47(2):332-340.
- Mosher JC, Lewis PS, Leahy RM. (1992): Multiple dipole modeling and localization from spatio-temporal MEG data. *Biomedical Engineering, IEEE Transactions on* 39(6):541-557.
- Mulert C, Jager L, Schmitt R, Bussfeld P, Pogarell O, Moller HJ, Juckel G, Hegerl U. (2004): Integration of fMRI and simultaneous EEG: towards a comprehensive understanding of localization and time-course of brain activity in target detection. *NeuroImage* 22(1):83-94.
- Muller, N., & Knight, R. (2006). The functional neuroanatomy of working memory: contributions of human brain lesion studies. *Neuroscience*, 139(1), 51-58.
- Muller, U., & Carew, T. J. (1998). Serotonin induces temporally and mechanistically distinct phases of persistent PKA activity in Aplysia sensory neurons. *Neuron*, 21(6), 1423-1434.
- Munakata, Y., & Pfaffly, J. (2004). Hebbian learning and development. *Developmental Science*, 7(2), 141-148.
- Murthy, V. N., & Fetz, E. E. (1992). Coherent 25- to 35-Hz oscillations in the sensorimotor cortex of awake behaving monkeys. *Proc Natl Acad Sci U S A*, 89(12), 5670-5674.
- Napadow, V., Makris, N., Liu, J., Kettner, N. W., Kwong, K. K., & Hui, K. K. (2005). Effects of electroacupuncture versus manual acupuncture on the human brain as measured by fMRI. *Hum Brain Mapp*, 24(3), 193-205. doi: 10.1002/hbm.20081
- Neiss, R. (1988). Reconceptualizing arousal: Psychobiological states in motor performance. *Psychological Bulletin*, 103(3), 345.
- Neuhaus AH, Trempler NR, Hahn E, Luborzewski A, Karl C, Hahn C, Opgen-Rhein C, Urbanek C, Schaub R, Dettling M. (2010): Evidence of specificity of a visual P3

- amplitude modulation deficit in schizophrenia. *Schizophrenia research* 124(1):119-126.
- Neuper, C., & Pfurtscheller, G. (1992). (event-related negativity and alpha band desynchronization in motor reactions]. *EEG EMG Z Elektroenzephalogr Elektromyogr Verwandte Geb*, 23(2), 55-61.
- Neuper, C., Wortz, M., & Pfurtscheller, G. (2006). ERD/ERS patterns reflecting sensorimotor activation and deactivation. *Prog Brain Res*, 159, 211-222. doi: S0079-6123(06)59014-4 [pii]10.1016/S0079-6123(06)59014-4
- Niedermeyer, E., & Da Silva, F. H. L. (2005). *Electroencephalography: basic principles, clinical applications, and related fields*: Lippincott Williams & Wilkins.
- Niedermeyer, E., Goldszmidt, A., & Ryan, D. (2004). "Mu rhythm status" and clinical correlates. *Clin EEG Neurosci*, 35(2), 84-87.
- Niedermeyer, E., & Lopes da Silva, F. (1999). *Electroencephalography Basic Principles, Clinical Applications and Related Fields*.: Williams and Wilkins, Baltimore, MD.
- Niedermeyer. (1987). *Electroencephalography* (4 ed.). Baltimore: Lippincott, Williams & Wilkins.
- Niehaus, J. L., Cruz-Bermúdez, N. D., & Kauer, J. A. (2009). Plasticity of Addiction: A Mesolimbic Dopamine Short-Circuit? *The American Journal on Addictions*, 18(4), 259-271.
- Nieuwenhuis S, Yeung N, van den Wildenberg W, Ridderinkhof KR. (2003): Electrophysiological correlates of anterior cingulate function in a go/no-go task: effects of response conflict and trial type frequency. *Cogn Affect Behav Neurosci* 3(1):17-26.
- Nowlis, D. P., & Kamiya, J. (1970). The control of electroencephalographic alpha rhythms through auditory feedback and the associated mental activity. *Psychophysiology*, 6(4), 476-484.
- Nunez, P. L. (1987). Removal of reference electrode and volume conduction effects by spatial deconvolution of evoked potentials using a three-concentric sphere model of the head. *Electroencephalogr Clin Neurophysiol Suppl*, 39, 143-148.
- Nunez, P. L. (1995). *Neocortical Dynamics and Human EEG Rhythms*. New York: Oxford University Press.
- Nunez, P. L., & Srinivasan, R. (2006). A theoretical basis for standing and traveling brain waves measured with human EEG with implications for an integrated consciousness. *Clin Neurophysiol*, 117(11), 2424-2435. doi: S1388-2457(06)01367-8 [pii]10.1016/j.clinph.2006.06.754
- Nunez, P. L., Srinivasan, R., Westdorp, A. F., Wijesinghe, R. S., Tucker, D. M., Silberstein, R. B., & Cadusch, P. J. (1997). EEG coherency. I: Statistics, reference electrode, volume conduction, Laplacians, cortical imaging, and interpretation at multiple scales. *Electroencephalogr Clin Neurophysiol*, 103(5), 499-515. doi: S0013469497000667 [pii]
- Nuwer MR, Lehman D, Da Silva FL, Matsuoka S, Sutherling W, Vibert JF. (1999). IFCN guidelines for topographic and frequency analysis of EEGs and EPs. The International Federation of Clinical Neurophysiology. *Electroencephalogr Clin Neurophysiol Suppl* 52: 15-20.

- O'Reilly, R. C., Noelle, D. C., Braver, T. S., & Cohen, J. D. (2002). Prefrontal cortex and dynamic categorization tasks: representational organization and neuromodulatory control. *Cerebral cortex*, *12*(3), 246.
- Oakes, T. R., Pizzagalli, D. A., Hendrick, A. M., Horras, K. A., Larson, C. L., Abercrombie, H. C., . . . Davidson, R. J. (2004). Functional coupling of simultaneous electrical and metabolic activity in the human brain. *Human brain mapping*, *21*(4), 257-270.
- Oken, B., Salinsky, M., & Elsas, S. (2006). Vigilance, alertness, or sustained attention: physiological basis and measurement. *Clinical Neurophysiology*, *117*(9), 1885-1901.
- Olbrich H, Maes H, Valerius G, Langosch J, Feige B. (2005): Event-related potential correlates selectively reflect cognitive dysfunction in schizophrenics. *Journal of neural transmission* *112*(2):283-295.
- Olbrich, S., Mulert, C., Karch, S., Trenner, M., Leicht, G., Pogarell, O., & Hegerl, U. (2009). EEG-vigilance and BOLD effect during simultaneous EEG/fMRI measurement. *Neuroimage*, *45*(2), 319-332. doi: S1053-8119(08)01213-5 [pii]10.1016/j.neuroimage.2008.11.014
- Olofsson, J. K., & Polich, J. (2007). Affective visual event-related potentials: Arousal, repetition, and time-on-task. *Biological psychology*, *75*(1), 101-108.
- Onton, J., Delorme, A., & Makeig, S. (2005). Frontal midline EEG dynamics during working memory. *Neuroimage*, *27*(2), 341-356. doi: S1053-8119(05)00267-3 [pii]10.1016/j.neuroimage.2005.04.014
- Onton, J., & Makeig, S. (2006). Information-based modeling of event-related brain dynamics. *Prog Brain Res*, *159*, 99-120. doi: S0079-6123(06)59007-7 [pii]10.1016/S0079-6123(06)59007-7
- Onton, J., Westerfield, M., Townsend, J., & Makeig, S. (2006). Imaging human EEG dynamics using independent component analysis. *Neurosci Biobehav Rev*, *30*(6), 808-822. doi: S0149-7634(06)00050-9 [pii]10.1016/j.neubiorev.2006.06.007
- Packard, M. G., & White, N. M. (1991). Dissociation of hippocampus and caudate nucleus memory systems by posttraining intracerebral injection of dopamine agonists. *Behavioral Neuroscience*, *105*(2), 295.
- Paisley, A., & Summerlee, A. (1984). Relationships between behavioural states and activity of the cerebral cortex. *Progress in neurobiology*, *22*(2), 155-184.
- Panych, L. P., Wada, J. A., & Beddoes, M. P. (1989). Practical digital filters for reducing EMG artefact in EEG seizure recordings. *Electroencephalography and clinical neurophysiology*, *72*(3), 268-276.
- Parasuraman, R., Warm, J. S., & See, J. E. (1998). Brain systems of vigilance.
- Pariante, J., White, P., Frackowiak, R. S., & Lewith, G. (2005). Expectancy and belief modulate the neuronal substrates of pain treated by acupuncture. *Neuroimage*, *25*(4), 1161-1167. doi: S1053-8119(05)00029-7 [pii]10.1016/j.neuroimage.2005.01.016
- Pascual-Marqui, R. D. (2002). Standardized low-resolution brain electromagnetic tomography (sLORETA): technical details. *Methods Find Exp Clin Pharmacol*, *24 Suppl D*, 5-12. doi: 846 [pii]
- Pascual-Marqui, R. D., Esslen, M., Kochi, K., & Lehmann, D. (2002). Functional imaging with low-resolution brain electromagnetic tomography (LORETA): a review. *Methods Find Exp Clin Pharmacol*, *24 Suppl C*, 91-95. doi: 841 [pii]

- Pascual-Marqui RD, Lehmann D, Koenig T, Kochi K, Merlo MCG, Hell D, Koukkou M. (1999): Low resolution brain electromagnetic tomography (LORETA) functional imaging in acute, neuroleptic-naive, first-episode, productive schizophrenia. *Psychiatry Research: Neuroimaging* 90(3):169-179.
- Pascual-Marqui RD, Michel CM, Lehmann D. (1994): Low resolution electromagnetic tomography: a new method for localizing electrical activity in the brain. *International Journal of Psychophysiology* 18(1):49-65.
- Pashler, H. E. (1999). *The psychology of attention*: The MIT Press.
- Patel SH, Azzam PN. (2005): Characterization of N200 and P300: selected studies of the event-related potential. *International Journal of Medical Sciences* 2(4):147.
- Pfefferbaum A, Ford JM, Weller BJ, Kopell BS. (1985): ERPs to response production and inhibition. *Electroencephalogr Clin Neurophysiol* 60(5):423-34.
- Pfefferbaum A, Ford, J.M., Weller, B.J., Kopell, B.S. (1985): ERPs to response production and inhibition. *Electroencephalogr. Clin. Neurophysiol* 60:423-434.
- Pfurtscheller, G. (2000). Spatiotemporal ERD/ERS patterns during voluntary movement and motor imagery. *Suppl Clin Neurophysiol*, 53, 196-198.
- Pfurtscheller, G., Brunner, C., Schlogl, A., & Lopes da Silva, F. H. (2006). Mu rhythm (de)synchronization and EEG single-trial classification of different motor imagery tasks. *Neuroimage*, 31(1), 153-159. doi: S1053-8119(05)02514-0 [pii]10.1016/j.neuroimage.2005.12.003
- Pfurtscheller, G., & Neuper, C. (1992). Simultaneous EEG 10 Hz desynchronization and 40 Hz synchronization during finger movements. *Neuroreport*, 3(12), 1057-1060.
- Pfurtscheller, G., Stancak, A., Jr., & Neuper, C. (1996). Event-related synchronization (ERS) in the alpha band--an electrophysiological correlate of cortical idling: a review. *Int J Psychophysiol*, 24(1-2), 39-46.
- Phillips C, Rugg MD, Friston KJ. (2002a): Anatomically informed basis functions for EEG source localization: combining functional and anatomical constraints. *NeuroImage* 16(3):678-695.
- Phillips C, Rugg MD, Friston KJ. (2002b): Systematic regularization of linear inverse solutions of the EEG source localization problem. *NeuroImage* 17(1):287-301.
- Pilloni, C., Caracausi, R. S., Tognali, F., & Sbarbaro, V. (1980). EEG evaluation of patients undergoing extracorporeal circulation under analgesic and electrohypoaesthesia with auricular acupuncture. *Minerva anesthesiologica*, 46(3), 371.
- Pineda, J. A. (2005). The functional significance of mu rhythms: translating "seeing" and "hearing" into "doing". *Brain Res Brain Res Rev*, 50(1), 57-68. doi: S0165-0173(05)00057-3 [pii]10.1016/j.brainresrev.2005.04.005
- Pineda, J. A., Brang, D., Hecht, E., Edwards, L., Carey, S., Bacon, M., . . . Rork, A. (2008). Positive behavioral and electrophysiological changes following neurofeedback training in children with autism. *Research in Autism Spectrum Disorders*, 2(3), 557-581.
- Pivik R, Broughton R, Coppola R, Davidson R, Fox N, Nuwer M. (1993): Guidelines for the recording and quantitative analysis of electroencephalographic activity in research contexts. *Psychophysiology* 30(6):547-558.

- Pizzagalli, DA. (2007). Electroencephalography and high-density electrophysiological source localization. In J. T. T. Cacioppo, Louis G. ; Berntson, Gary G. (Ed.), *Handbook of psychophysiology* (pp. 56-84). New York, US: Cambridge University Press.
- Pizzagalli DA, Peccoralo LA, Davidson RJ, Cohen JD. (2005): Resting anterior cingulate activity and abnormal responses to errors in subjects with elevated depressive symptoms: A 128-channel EEG study. *Human brain mapping* 27(3):185-201.
- Pizzagalli DA, Oakes TR, Davidson RJ. (2003): Coupling of theta activity and glucose metabolism in the human rostral anterior cingulate cortex: an EEG/PET study of normal and depressed subjects. *Psychophysiology* 40(6):939-949.
- Polich, J. (1989). Frequency, intensity, and duration as determinants of P300 from auditory stimuli. *Journal of Clinical Neurophysiology*, 6(3), 277.
- Polich, J. (2007). Updating P300: an integrative theory of P3a and P3b. *Clinical Neurophysiology*, 118(10), 2128-2148.
- Polich J, Herbst KL. (2000): P300 as a clinical assay: rationale, evaluation, and findings. *Int J Psychophysiol* 38(1):3-19.
- Polich J, Kok A. (1995): Cognitive and biological determinants of P300: an integrative review. *Biol Psychol* 41(2):103-46.
- Polich, J., & McIsaac, H. K. (1994). Comparison of auditory P300 habituation from active and passive conditions. *International Journal of Psychophysiology*, 17(1), 25-34.
- Pollen, D. A., & Trachtenberg, M. C. (1972). Some problems of occipital alpha block in man. *Brain Res*, 41(2), 303-314. doi: 0006-8993(72)90504-5 [pii]
- Posner, M. I. (1989). The attention system of the human brain: DTIC Document.
- Posner MI, Dehaene S. (1994): Attentional networks. *Trends in Neurosciences* 17(2):75-79.
- Poulos, C. X., & Cappell, H. (1991). Homeostatic theory of drug tolerance: A general model of physiological adaptation. *Psychological review*, 98(3), 390.
- Proakis JG. (2003): Spread spectrum signals for digital communications: Wiley Online Library.
- Protzner, A. B., Cortese, F., Alain, C., & McIntosh, A. R. (2009). The temporal interaction of modality specific and process specific neural networks supporting simple working memory tasks. *Neuropsychologia*, 47(8-9), 1954-1963.
- Raichle, M. E., MacLeod, A. M., Snyder, A. Z., Powers, W. J., Gusnard, D. A., & Shulman, G. L. (2001). A default mode of brain function. *Proc Natl Acad Sci U S A*, 98(2), 676-682. doi: 10.1073/pnas.98.2.676, 98/2/676 [pii]
- Raichle, M. E., & Snyder, A. Z. (2007). A default mode of brain function: a brief history of an evolving idea. *Neuroimage*, 37(4), 1083-1090; discussion 1097-1089. doi: S1053-8119(07)00130-9 [pii]10.1016/j.neuroimage.2007.02.041
- Rakic, P. (2002). Neurogenesis in adult primate neocortex: an evaluation of the evidence. *Nature Reviews Neuroscience*, 3(1), 65-71.
- Rao H, Zhou T, Zhuo Y, Fan S, Chen L. (2002): Spatiotemporal activation of the two visual pathways in form discrimination and spatial location: a brain mapping study. *Human brain mapping* 18(2):79-89.
- Ravden, D., & Polich, J. (1998). Habituation of P300 from visual stimuli. *International Journal of Psychophysiology*, 30(3), 359-365.

- Raymond, J., Sajid, I., Parkinson, L. A., & Gruzelier, J. H. (2005). Biofeedback and dance performance: A preliminary investigation. *Applied Psychophysiology and Biofeedback*, *30*(1), 65-73.
- Raymond, J., Varney, C., Parkinson, L. A., & Gruzelier, J. H. (2005). The effects of alpha/theta neurofeedback on personality and mood. *Brain Res Cogn Brain Res*, *23*(2-3), 287-292. doi: S0926-6410(04)00315-5 [pii]10.1016/j.cogbrainres.2004.10.023
- Reynolds, G. S. (1975). A primer of operant conditioning. (Rev ed).
- Robbins, T. W., & Everitt, B. J. (1996). Neurobehavioural mechanisms of reward and motivation. *Current opinion in neurobiology*, *6*(2), 228-236.
- Rockstroh, B., Elbert, T., Birbaumer, N., Wolf, P., Dürching-Röth, A., Reker, M., . . . Dichgans, J. (1993). Cortical self-regulation in patients with epilepsies. *Epilepsy Research*, *14*(1), 63-72.
- Roelfsema, P. R., Engel, A. K., Konig, P., & Singer, W. (1997). Visuomotor integration is associated with zero time-lag synchronization among cortical areas. *Nature*, *385*, 157-161.
- Roopun, A. K., Middleton, S. J., Cunningham, M. O., LeBeau, F. E., Bibbig, A., Whittington, M. A., & Traub, R. D. (2006). A beta2-frequency (20-30 Hz) oscillation in nonsynaptic networks of somatosensory cortex. *Proc Natl Acad Sci U S A*, *103*(42), 15646-15650.
- Ros, T., Moseley, M. J., Bloom, P. A., Benjamin, L., Parkinson, L. A., & Gruzelier, J. H. (2009). Optimizing microsurgical skills with EEG neurofeedback. *BMC Neurosci*, *10*, 87. doi: 1471-2202-10-87 [pii]10.1186/1471-2202-10-87
- Ros, T., Munneke, M. A., Ruge, D., Gruzelier, J. H., & Rothwell, J. C. (2010). Endogenous control of waking brain rhythms induces neuroplasticity in humans. *Eur J Neurosci*, *31*(4), 770-778. doi: EJM7100 [pii]10.1111/j.1460-9568.2010.07100.x
- Ros, T., Theberge, J., Frewen, P. A., Kluetsch, R., Densmore, M., Calhoun, V. D., & Lanius, R. A. (2012). Mind over chatter: plastic up-regulation of the fMRI alertness network by EEG neurofeedback.
- Rosas, H. D., Lee, S. Y., Bender, A. C., Zaleta, A. K., Vangel, M., Yu, P., . . . Pappu, V. (2010). Altered white matter microstructure in the corpus callosum in Huntington's disease: Implications for cortical. *NeuroImage*, *49*(4), 2995-3004.
- Rosser, N., Heuschmann, P., Wersching, H., Breitenstein, C., Knecht, S., & Flöel, A. (2008). Levodopa improves procedural motor learning in chronic stroke patients. *Archives of physical medicine and rehabilitation*, *89*(9), 1633-1641.
- Rossiter, T. R., & LaVaque, T. J. (1995). A Comparison of EEG Biofeedback and Psychostimulants in Treating Attention Deficit Hyperactivity Disorders. *Journal of Neurotherapy*, 48-59.
- Rosted, P., Griffiths, P. A., Bacon, P., & Gravill, N. (2001). Is there an effect of acupuncture on the resting EEG? *Complementary therapies in medicine*, *9*(2), 77-81.
- Rota, G., Sitaram, R., Veit, R., Erb, M., Weiskopf, N., Dogil, G., & Birbaumer, N. (2009). Self-regulation of regional cortical activity using real-time fMRI: the right inferior frontal gyrus and linguistic processing. *Hum Brain Mapp*, *30*(5), 1605-1614. doi: 10.1002/hbm.20621

- Roth, S., Sterman, M., & Clemente, C. (1967). Comparison of EEG correlates of reinforcement, internal inhibition and sleep. *Electroencephalography and clinical neurophysiology*, 23(6), 509-520.
- Rowan, A. J., & Tolunsky, E. (2003). *Primer of EEG: with a mini-atlas*: Butterworth-Heinemann.
- Rubinov, M., & Sporns, O. (2010). Complex network measures of brain connectivity: uses and interpretations. *NeuroImage*, 52(3), 1059-1069.
- Sakai S, Hori E, Umeno K, Kitabayashi N, Ono T, Nishijo H. (2007): Specific acupuncture sensation correlates with EEGs and autonomic changes in human subjects. *Autonomic neuroscience: basic & clinical* 133(2):158.
- Salvador, R., Suckling, J., Coleman, M. R., Pickard, J. D., Menon, D., & Bullmore, E. (2005). Neurophysiological architecture of functional magnetic resonance images of human brain. *Cereb Cortex*, 15(9), 1332-1342. doi: bhi016 [pii]10.1093/cercor/bhi016
- Samar, V. J., Bopardikar, A., Rao, R., & Swartz, K. (1999). Wavelet Analysis of Neuroelectric Waveforms: A Conceptual Tutorial* 1,* 2. *Brain and Language*, 66(1), 7-60.
- Sanchez, A., & David, V. (2002). Frontiers of research in BSS/ICA. *Neurocomputing*, 49(1-4), 7-23.
- Sander, C., Arns, M., Olbrich, S., & Hegerl, U. (2010). EEG-vigilance and response to stimulants in paediatric patients with attention deficit/hyperactivity disorder. *Clin Neurophysiol*. doi: S1388-2457(10)00309-3 [pii]10.1016/j.clinph.2010.03.021
- Sander, R. D. (2010). Motor examinations in psychiatry. *Psychiatry (Edgmont)*, 7(11), 37.
- Sasaki K, Gemba H, Nambu A, Matsuzaki R. (1993): No-go activity in the frontal association cortex of human subjects. *Neuroscience Research* 18(3):249-252.
- Sasaki K, Gemba H, Tsujimoto T. (1989): Suppression of visually initiated hand movement by stimulation of the prefrontal cortex in the monkey. *Brain research* 495(1):100-107.
- Sauseng P, Klimesch W, Gruber W, Hanslmayr S, Freunberger R, Doppelmayr M. (2007): Are event-related potential components generated by phase resetting of brain oscillations? A critical discussion. *Neuroscience* 146(4):1435-1444.
- Sayers BMA, Beagley H, Henshall W. (1974): The mechanism of auditory evoked EEG responses. *Nature*.
- Schachter, S. C., & Schomer, D. L. (2005). *Atlas of Ambulatory EEG*: Academic Press.
- Scheeringa, R., Bastiaansen, M. C., Petersson, K. M., Oostenveld, R., Norris, D. G., & Hagoort, P. (2008). Frontal theta EEG activity correlates negatively with the default mode network in resting state. *Int J Psychophysiol*, 67(3), 242-251. doi: S0167-8760(07)00163-8 [pii]10.1016/j.ijpsycho.2007.05.017
- Scherder, E. J., Van Someren, E. J., Bouma, A., & v d Berg, M. (2000). Effects of transcutaneous electrical nerve stimulation (TENS) on cognition and behaviour in aging. *Behav Brain Res*, 111(1-2), 223-225. doi: S0166432800001704 [pii]
- Schnitzler A, Gross J. (2005): Normal and pathological oscillatory communication in the brain. *Nature Reviews Neuroscience* 6(4):285-296.
- Schreckenberger, M., Lange-Asschenfeld, C., Lochmann, M., Mann, K., Siessmeier, T., Buchholz, H. G., . . . Grunder, G. (2004). The thalamus as the generator and modulator of EEG alpha rhythm: a combined PET/EEG study with lorazepam challenge in humans. *NeuroImage*, 22(2), 637-644.

- Schulteis, G., & Martinez, J. L. (1992). Peripheral modulation of learning and memory: enkephalins as a model system. *Psychopharmacology*, *109*(3), 347-364.
- Schultz, W. (2002). Getting formal with dopamine and reward. *Neuron*, *36*(2), 241-263.
- Schultz, W., Dayan, P., & Montague, P. R. (1997). A neural substrate of prediction and reward. *Science*, *275*(5306), 1593.
- Schurmann, M., & Basar, E. (1999). Alpha oscillations shed new light on relation between EEG and single neurons. *Neurosci Res*, *33*(2), 79-80. doi: S0168-0102(98)00116-3 [pii]
- Seeck M, Lazeyras F, Michel C, Blanke O, Gericke C, Ives J, Delavelle J, Golay X, Haenggeli C, De Tribolet N. (1998): Non-invasive epileptic focus localization using EEG-triggered functional MRI and electromagnetic tomography. *Electroencephalography and clinical neurophysiology* *106*(6):508-512.
- Sereno, M. I., Pitzalis, S., & Martinez, A. (2001). Mapping of contralateral space in retinotopic coordinates by a parietal cortical area in humans. *Science*, *294*(5545), 1350-1354. doi: 10.1126/science.1063695294/5545/1350 [pii]
- Shackman, A. J., McMenamin, B. W., Slagter, H. A., Maxwell, J. S., Greischar, L. L., & Davidson, R. J. (2009). Electromyogenic artifacts and electroencephalographic inferences. *Brain Topogr*, *22*(1), 7-12. doi: 10.1007/s10548-009-0079-4
- Shah AS, Bressler SL, Knuth KH, Ding M, Mehta AD, Ulbert I, Schroeder CE. (2004): Neural dynamics and the fundamental mechanisms of event-related brain potentials. *Cerebral cortex* *14*(5):476-483.
- Sharp, S. I., McQuillin, A., & Gurling, H. (2009). Genetics of attention-deficit hyperactivity disorder (ADHD). *Neuropharmacology*, *57*(7-8), 590-600.
- Shaw, C. A., McEachern, J. C., & McEachern, J. (2001). *Toward a theory of neuroplasticity: Psychology Pr.*
- Shen, J. (2001). Research on the neurophysiological mechanisms of acupuncture: review of selected studies and methodological issues. *J Altern Complement Med*, *7 Suppl 1*, S121-127. doi: 10.1089/107555301753393896
- Shen, J., Wenger, N., Glaspy, J., Hays, R. D., Albert, P. S., Choi, C., & Shekelle, P. G. (2000). Electroacupuncture for control of myeloablative chemotherapy-induced emesis: A randomized controlled trial. *JAMA*, *284*(21), 2755-2761. doi: jci00080 [pii]
- Shen, Y., & Li, R. (1995). The role of neuropeptides in learning and memory: possible mechanisms. *Medical hypotheses*, *45*(6), 529-538.
- Sher, L. (1998). The role of the endogenous opioid system in the effects of acupuncture on mood, behavior, learning, and memory. *Medical hypotheses*, *50*(6), 475-478.
- Sher, L. (2001). Role of endogenous opioids in the effects of light on mood and behavior. *Medical hypotheses*, *57*(5), 609-611.
- Shouse, M. N., & Lubar, J. F. (1979). Operant conditioning of EEG rhythms and ritalin in the treatment of hyperkinesis. *Biofeedback Self Regul*, *4*(4), 299-312.
- Shulman, G. L., Fiez, J. A., Corbetta, M., Buckner, R. L., Miezin, F. M., Raichle, M. E., & Petersen, S. E. (1997). Common blood flow changes across visual tasks: II. Decreases in cerebral cortex. *Journal of Cognitive Neuroscience*, *9*(5), 648-663.
- Shulman, G. L., McAvoy, M. P., Cowan, M. C., Astafiev, S. V., Tansy, A. P., d'Avossa, G., & Corbetta, M. (2003). Quantitative analysis of attention and detection signals during visual search. *Journal of Neurophysiology*, *90*(5), 3384.

- Sluka, K. A., & Walsh, D. (2003). Transcutaneous electrical nerve stimulation: Basic science mechanisms and clinical effectiveness* 1. *The Journal of Pain*, 4(3), 109-121.
- Smallwood J, Davies JB, Heim D, Finnigan F, Sudberry M, O'Connor R, Obonsawin M. (2004): Subjective experience and the attentional lapse: Task engagement and disengagement during sustained attention. *Consciousness and cognition* 13(4):657-690.
- Smith EE, Jonides J. (1999): Storage and executive processes in the frontal lobes. *Science* 283(5408):1657-1661.
- Smith, J. L., Johnstone, S. J., & Barry, R. J. (2008). Movement-related potentials in the Go/NoGo task: The P3 reflects both cognitive and motor inhibition. *Clinical Neurophysiology*, 119(3), 704-714.
- Smith, J. L., Johnstone, S. J., & Barry, R. J. (2008). Movement-related potentials in the Go/NoGo task: the P3 reflects both cognitive and motor inhibition. *Clin Neurophysiol*, 119(3), 704-714. doi: S1388-2457(07)00728-6 [pii]10.1016/j.clinph.2007.11.042
- Snyder E, Hillyard SA. (1976): Long-latency evoked potentials to irrelevant, deviant stimuli. *Behav Biol* 16(3):319-31.
- Somers, D. L., & Clemente, F. R. (2009). Contralateral high or a combination of high-and low-frequency transcutaneous electrical nerve stimulation reduces mechanical allodynia and alters dorsal horn neurotransmitter content in neuropathic rats. *The Journal of Pain*, 10(2), 221-229.
- Stam CJ. (2004): Functional connectivity patterns of human magnetoencephalographic recordings: a'small-world'network? *Neuroscience Letters* 355(1-2):25-28.
- Stam CJ, de Bruin EA. (2004): Scale-free dynamics of global functional connectivity in the human brain. *Human brain mapping* 22(2):97-109.
- Stam, C. J., Nolte, G., & Daffertshofer, A. (2007). Phase lag index: assessment of functional connectivity from multi channel EEG and MEG with diminished bias from common sources. *Human brain mapping*, 28(11), 1178-1193.
- Stam CJ, Reijneveld JC. (2007): Graph theoretical analysis of complex networks in the brain. *Nonlinear biomedical physics* 1(1):3.
- Steriade, M. (1993). Cellular substrates of brain rhythms. *Electroencephalography. Basic Principles, Clinical Applications, and Related Fields* 4:28-75.
- Steriade, M. (1999). Coherent oscillations and short-term plasticity in corticothalamic networks. *Trends in Neurosciences*.
- Steriade, M. (2000). Corticothalamic resonance, states of vigilance and mentation. *Neuroscience*, 101(2), 243-276.
- Steriade, M. (2001). Impact of network activities on neuronal properties in corticothalamic systems. *J Neurophysiol*, 86(1), 1-39.
- Steriade, M. (2006). Grouping of brain rhythms in corticothalamic systems. *Neuroscience*, 137(4), 1087-1106.
- Steriade, M., Gloor, P., Llinas, R. R., Lopes da Silva, F. H., & Mesulam, M. M. (1990). Basic mechanisms of cerebral rhythmic activities. *Electroencephalography and Clinical Neurophysiology*, 76, 481-508.
- Steriade, M., & Llinas, R. R. (1988). The functional states of the thalamus and the associated neuronal interplay. *Physiol Rev*, 68(3), 649-742.

- Steriade, M., McCormick, D. A., & Sejnowski, T. J. (1993). Thalamocortical oscillations in the sleeping and aroused brain. *Science*, *262*, 679-685.
- Sterman, M., & Friar, L. (1972). Suppression of seizures in an epileptic following sensorimotor EEG feedback training. *Electroencephalography and clinical neurophysiology*, *33*(1), 89-95.
- Sterman, M., & Wyrwicka, W. (1967). EEG correlates of sleep: evidence for separate forebrain substrates. *Brain research*, *6*(1), 143.
- Sterman, M., Wyrwicka, W., & Howe, R. (1969). Behavioral and neurophysiological studies of the sensorimotor rhythm in the cat. *Electroencephalography and clinical neurophysiology*, *27*(7), 678.
- Sterman, M. B. (1996). Physiological origins and functional correlates of EEG rhythmic activities: implications for self-regulation. *Biofeedback Self Regul*, *21*(1), 3-33.
- Sterman, M. B., & Egner, T. (2006). Foundation and practice of neurofeedback for the treatment of epilepsy. *Appl Psychophysiol Biofeedback*, *31*(1), 21-35. doi: 10.1007/s10484-006-9002-x
- Sterman, M. B., Goodman, S. J., & Kovalesky, R. A. (1978). Effects of sensorimotor EEG feedback training on seizure susceptibility in the rhesus monkey. *Exp Neurol*, *62*(3), 735-747.
- Sterman, M. B., Howe, R. C., & Macdonald, L. R. (1970). Facilitation of spindle-burst sleep by conditioning of electroencephalographic activity while awake. *Science*, *167*(3921), 1146.
- Sterman, M. B., Wyrwicka, W., & Roth, S. (1969). Electrophysiological correlates and neural substrates of alimentary behavior in the cat. *Ann NY Acad Sci*, *157*(2), 723-739.
- Strafella, A. P., Paus, T., Barrett, J., & Dagher, A. (2001). Repetitive transcranial magnetic stimulation of the human prefrontal cortex induces dopamine release in the caudate nucleus. *The Journal of neuroscience: the official journal of the Society for Neuroscience*, *21*(15), RC157.
- Strafella, A. P., Paus, T., Fraraccio, M., & Dagher, A. (2003). Striatal dopamine release induced by repetitive transcranial magnetic stimulation of the human motor cortex. *Brain*, *126*(12), 2609-2615.
- Streitberger, K., Ezzo, J., & Schneider, A. (2006). Acupuncture for nausea and vomiting: an update of clinical and experimental studies. *Auton Neurosci*, *129*(1-2), 107-117. doi: S1566-0702(06)00221-9 [pii]10.1016/j.autneu.2006.07.015
- Strijkstra, A. M., Beersma, D. G., Drayer, B., Halbesma, N., & Daan, S. (2003). Subjective sleepiness correlates negatively with global alpha (8-12 Hz) and positively with central frontal theta (4-8 Hz) frequencies in the human resting awake electroencephalogram. *Neurosci Lett*, *340*(1), 17-20. doi: S0304394003000338 [pii]
- Sutton S, Tueting P, Zubin J. (1967): Information delivery and the sensory evoked potential. *Science*.
- Swainson R, Cunnington R, Jackson GM, Rorden C, Peters AM, Morris PG, Jackson SR. (2003): Cognitive control mechanisms revealed by ERP and fMRI: evidence from repeated task-switching. *Journal of Cognitive Neuroscience* *15*(6):785-799.
- Takeshige, C., Sato, T., Mera, T., Hisamitsu, T., & Fang, J. (1992). Descending pain inhibitory system involved in acupuncture analgesia. *Brain Res Bull*, *29*(5), 617-634. doi: 0361-9230(92)90131-G [pii]

- Takeshige, C., Tanaka, M., Sato, T., & Hishida, F. (1990). Mechanism of individual variation in effectiveness of acupuncture analgesia based on animal experiment. *Eur J Pain*, *11*, 109-113.
- Talairach, J., Tournoux, P. (1988). *Co-planar Stereotaxic Atlas of the Human Brain. 3-dimensional Proportional System: An Approach to Cerebral Imaging*. New York: Georg Thieme Verlag/Thieme Medical Publishers, Stuttgart.
- Tallon-Baudry, C., Mandon, S., Freiwald, W. A., & Kreiter, A. K. (2004). Oscillatory synchrony in the monkey temporal lobe correlates with performance in a visual short-term memory task. *Cereb Cortex*, *14*(7), 713-720.
- Tan, G., Thornby, J., Hammond, D. C., Strehl, U., Canady, B., Arnemann, K., & Kaiser, D. A. (2009). Meta-analysis of EEG biofeedback in treating epilepsy. *Clin EEG Neurosci*, *40*(3), 173-179.
- Tanaka, H., Hayashi, M., & Hori, T. (1997). Topographical characteristics and principal component structure of the hypnagogic EEG. *Sleep*, *20*(7), 523-534.
- Tanaka, Y., Koyama, Y., Jodo, E., Kayama, Y., Kawachi, A., Ukimura, O., & Miki, T. (2002). Effects of acupuncture to the sacral segment on the bladder activity and electroencephalogram. *Psychiatry and Clinical Neurosciences*, *56*(3), 249-250.
- Tansey, M. A. (1984). EEG sensorimotor rhythm biofeedback training: some effects on the neurologic precursors of learning disabilities. *Int J Psychophysiol*, *1*(2), 163-177.
- Tansey, M. A. (1985). Brainwave signatures--an index reflective of the brain's functional neuroanatomy: further findings on the effect of EEG sensorimotor rhythm biofeedback training on the neurologic precursors of learning disabilities. *Int J Psychophysiol*, *3*(2), 85-99.
- Tansey, M. A. (1986). A simple and a complex tic (Gilles de la Tourette's syndrome): their response to EEG sensorimotor rhythm biofeedback training. *Int J Psychophysiol*, *4*(2), 91-97. doi: 0167-8760(86)90002-4 [pii]
- Tass, P., Silchenko, A., Hauptmann, C., Barnikol, U., & Speckmann, E. J. (2009). Long-lasting desynchronization in rat hippocampal slice induced by coordinated reset stimulation. *Physical Review E*, *80*(1), 011902.
- Thakor, N. V., & Tong, S. (2004). Advances in quantitative electroencephalogram analysis methods. *Annu. Rev. Biomed. Eng.*, *6*, 453-495.
- Thatcher, R. W., Krause, P. J., & Hrybyk, M. (1986). Cortico-cortical associations and EEG coherence: A two-compartmental model. *Electroencephalogr Clin Neurophysiol*, *64*, 123-143.
- Thompson, J. W., & Cummings, M. (2008). Investigating the safety of electroacupuncture with a Picoscope. *Acupunct Med*, *26*(3), 133-139.
- Thompson, J. W., & Cummings, M. (2008). Investigating the safety of electroacupuncture with a Picoscope(tm). *Acupuncture in Medicine*, *26*(3), 133.
- Thompson, L., & Thompson, M. (1998). Neurofeedback combined with training in metacognitive strategies: effectiveness in students with ADD. *Applied Psychophysiology and Biofeedback*, *23*(4), 243-263.
- Thompson, M., & Thompson, L. (2003). *The Neurofeedback Book - An Introduction to Basic Concepts in Applied Psychophysiology*. Colorado: The Association for Applied Psychophysiology and Biofeedback.

- Thompson, T., Steffert, T., Ros, T., Leach, J., & Gruzelier, J. (2008). EEG applications for sport and performance. *Methods*, 45(4), 279-288. doi: S1046-2023(08)00116-3 [pii]10.1016/j.ymeth.2008.07.006
- Tiitinen H, Sinkkonen J, Reinikainen K, Alho K, Lavikainen J, Näätänen R. (1993): Selective attention enhances the auditory 40-Hz transient response in humans. *Nature* 364, 59 - 60 (01 July 1993); doi:10.1038/364059a0
- Tinguely, G., Finelli, L. A., Landolt, H. P., Borbély, A. A., & Achermann, P. (2006). Functional EEG topography in sleep and waking: state-dependent and state-independent features. *NeuroImage*, 32(1), 283-292.
- Tong, K. C., Lo, S. K., & Cheing, G. L. (2007). Alternating frequencies of transcutaneous electric nerve stimulation: does it produce greater analgesic effects on mechanical and thermal pain thresholds? *Arch Phys Med Rehabil*, 88(10), 1344-1349. doi: S0003-9993(07)01291-9 [pii]10.1016/j.apmr.2007.07.017
- Torgerson, W. S. (1952). Multidimensional scaling: Theory and method. *Psychometrika*, 17(4), 401-419.
- Toro, R., Fox, P. T., & Paus, T. (2008). Functional coactivation map of the human brain. *Cerebral cortex*, 18(11), 2553.
- Towle VL, Syed I, Berger C, Grzesczczuk R, Milton J, Erickson RK, Cogen P, Berkson E, Spire JP. (1998): Identification of the sensory/motor area and pathologic regions using ECoG coherence. *Electroencephalography and clinical neurophysiology* 106(1):30-39.
- Trujillo-Barreto NJ, Aubert-Vazquez E, Valdes-Sosa PA. (2004): Bayesian model averaging in EEG/MEG imaging. *Neuroimage* 21(4):1300-19.
- Tsigos, C., & Chrousos, G. P. (2002). Hypothalamic-pituitary-adrenal axis, neuroendocrine factors and stress. *Journal of Psychosomatic Research*, 53(4), 865-871.
- Uchida, Y., Nishigori, A., Takeda, D., Ohshiro, M., Ueda, Y., Ohshima, M., & Kashiba, H. (2003). Electroacupuncture induces the expression of Fos in rat dorsal horn via capsaicin-insensitive afferents. *Brain Res*, 978(1-2), 136-140. doi: S0006899303028002 [pii]
- Uchida S, Nakayama H, Maehara T, Hirai N, Arakaki H, Nakamura M, Nakabayashi T, Shimizu H. (2000): Suppression of gamma activity in the human medial temporal lobe by sevoflurane anesthesia. *Neuroreport* 11(1):39-42.
- Uddin, L. Q., Kelly, A. M., Biswal, B. B., Xavier Castellanos, F., & Milham, M. P. (2009). Functional connectivity of default mode network components: correlation, anticorrelation, and causality. *Hum Brain Mapp*, 30(2), 625-637. doi: 10.1002/hbm.20531
- Ulett, G. A. (1992). *Beyond Yin and Yang: How Acupuncture Really Works*; St Louis, MO: Warren H. Green: Inc.
- Ulett, G. A. (1996). Conditioned healing with electroacupuncture. *Altern Ther Health Med*, 2(5), 56-60.
- Ulett, G. A., Han, J., & Han, S. (1998a). Traditional and evidence-based acupuncture: history, mechanisms, and present status. *South Med J*, 91(12), 1115-1120.
- Ulett, G. A., Han, S., & Han, J. S. (1998b). Electroacupuncture: mechanisms and clinical application. *Biol Psychiatry*, 44(2), 129-138. doi: S0006-3223(97)00394-6 [pii]

- Ungerleider SKLG. (2000): Mechanisms of visual attention in the human cortex. *Annual review of neuroscience* 23(1):315-341.
- Ursin, H., & Eriksen, H. R. (2004). The cognitive activation theory of stress. *Psychoneuroendocrinology*, 29(5), 567-592.
- Vaadia E, Haalman I, Abeles M, Bergman H, Prut Y, Slovin H, Aertsen A. (1995): Dynamics of neuronal interactions in monkey cortex in relation to behavioural events. *Nature* 373(6514):515-518.
- Valdes-Sosa P, Marti F, Garcia F, Casanova R. (2000): Variable resolution electric-magnetic tomography. Cuban Neuroscience Center, Havana Cuba.
- Van De Ven, V. G., Formisano, E., Prvulovic, D., Roeder, C. H., & Linden, D. E. J. (2004). Functional connectivity as revealed by spatial independent component analysis of fMRI measurements during rest. *Human brain mapping*, 22(3), 165-178.
- Van Den Heuvel, M. P., & Hulshoff Pol, H. E. (2010). Exploring the brain network: a review on resting-state fMRI functional connectivity. *European Neuropsychopharmacology*, 20(8), 519-534.
- Van Dijk, K. R., Scherder, E. J., Scheltens, P., & Sergeant, J. A. (2002). Effects of transcutaneous electrical nerve stimulation (TENS) on non-pain related cognitive and behavioural functioning. *Rev Neurosci*, 13(3), 257-270.
- Van Veen V, Carter CS. (2002): The anterior cingulate as a conflict monitor: fMRI and ERP studies. *Physiology and Behavior* 77(4):477-482.
- Veltman, J., & Gaillard, A. (1996). Physiological indices of workload in a simulated flight task. *Biological psychology*, 42(3), 323-342.
- Vernon, D., Egner, T., Cooper, N., Compton, T., Neilands, C., Sheri, A., & Gruzelier, J. (2003). The effect of training distinct neurofeedback protocols on aspects of cognitive performance. *Int J Psychophysiol*, 47(1), 75-85. doi: S0167876002000910 [pii]
- Vigario, R., & Oja, E. (2000). Independence: a new criterion for the analysis of the electromagnetic fields in the global brain? *Neural Netw*, 13(8-9), 891-907. doi: S0893-6080(00)00073-3 [pii]
- Vinogradova O. (1995): Expression, control, and probable functional significance of the neuronal theta-rhythm. *Progress in neurobiology* 45(6):523-583.
- Viola, F. C., Thorne, J., Edmonds, B., Schneider, T., Eichele, T., & Debener, S. (2009). Semi-automatic identification of independent components representing EEG artifact. *Clin Neurophysiol*, 120(5), 868-877. doi: S1388-2457(09)00233-8 [pii]10.1016/j.clinph.2009.01.015
- Virji-Babul, N., Cheung, T., Weeks, D., Herdman, A. T., & Cheyne, D. (2007). Magnetoencephalographic analysis of cortical activity in adults with and without Down syndrome. *J Intellect Disabil Res*, 51(Pt 12), 982-987. doi: JIR999 [pii]10.1111/j.1365-2788.2007.00999.x
- Vitacco D, Brandeis D, Pascual-Marqui R, Martin E. (2002): Correspondence of event-related potential tomography and functional magnetic resonance imaging during language processing. *Human brain mapping* 17(1):4-12.
- Wagner M, Fuchs M, Kastner J. (2004): Evaluation of sLORETA in the presence of noise and multiple sources. *Brain topography* 16(4):277-280.

- Wang, J. Q., Mao, L., & Han, J. S. (1992). Comparison of the antinociceptive effects induced by electroacupuncture and transcutaneous electrical nerve stimulation in the rat. *Int J Neurosci*, 65(1-4), 117-129.
- Wang, K., Svensson, P., & Arendt-Nielsen, L. (2007). Effect of acupuncture-like electrical stimulation on chronic tension-type headache: a randomized, double-blinded, placebo-controlled trial. *Clin J Pain*, 23(4), 316-322. doi: 10.1097/AJP.0b013e318030c90400002508-200705000-00005 [pii]
- Wang, Y., Cao, X., & Wu, G. (1999). Role of dopamine receptors and the changes of the tyrosine hydroxylase mRNA in acupuncture analgesia in rats. *Acupuncture & electro-therapeutics research*, 24(2), 81.
- Watkins, L. R., & Mayer, D. J. (1982). Organization of endogenous opiate and nonopiate pain control systems. *Science*, 216(4551), 1185.
- Weiss, S., & Mueller, H. M. (2003). The contribution of EEG coherence to the investigation of language. *Brain and Language*, 85(2), 325-343.
- Weizman, R., Dick, J., Gil-Ad, I., Weitz, R., Tyano, S., & Laron, Z. (1987). Effects of acute and chronic methylphenidate administration on beta-endorphin, growth hormone, prolactin and cortisol in children with attention deficit disorder and hyperactivity. *Life Sci*, 40(23), 2247-2252.
- White, P., Lewith, G., Prescott, P., & Conway, J. (2004). Acupuncture versus placebo for the treatment of chronic mechanical neck pain: a randomized, controlled trial. *Ann Intern Med*, 141(12), 911-919. doi: 141/12/911 [pii]
- Winter, W. R., Nunez, P. L., Ding, J., & Srinivasan, R. (2007). Comparison of the effect of volume conduction on EEG coherence with the effect of field spread on MEG coherence. *Stat Med*, 26(21), 3946-3957. doi: 10.1002/sim.2978
- Woldorff M, Liotti M, Seabolt M, Busse L, Lancaster J, Fox P. (2002): The temporal dynamics of the effects in occipital cortex of visual-spatial selective attention. *Cognitive Brain Research* 15:1-15.
- Wong, A. M., Su, T. Y., Tang, F. T., Cheng, P. T., & Liaw, M. Y. (1999). Clinical trial of electrical acupuncture on hemiplegic stroke patients. *Am J Phys Med Rehabil*, 78(2), 117-122.
- Worrell GA, Lagerlund TD, Sharbrough FW, Brinkmann BH, Busacker NE, Cicora KM, O'Brien TJ. (2000): Localization of the epileptic focus by low-resolution electromagnetic tomography in patients with a lesion demonstrated by MRI. *Brain topography* 12(4):273-282.
- Wu, M. T., Sheen, J. M., Chuang, K. H., Yang, P., Chin, S. L., Tsai, C. Y., . . . Yang, C. F. (2002). Neuronal specificity of acupuncture response: a fMRI study with electroacupuncture. *Neuroimage*, 16(4), 1028-1037. doi: S1053811902911456 [pii]
- Wyrwicka, W., & Sterman, M. B. (1968). Instrumental conditioning of sensorimotor cortex EEG spindles in the waking cat. *Physiology & Behavior*, 3(5), 703-707.
- Wyrwicka, W., Sterman, M. B., & Clemente, C. D. (1962). Conditioning of induced electroencephalographic sleep patterns in the cat. *Science*, 137, 616-618.
- Yan, B., Li, K., Xu, J., Wang, W., Liu, H., Shan, B., & Tang, X. (2005). Acupoint-specific fMRI patterns in human brain. *Neurosci Lett*, 383(3), 236-240. doi: S0304-3940(05)00402-7 [pii]10.1016/j.neulet.2005.04.021

- Yan, C., Liu, D., He, Y., Zou, Q., Zhu, C., Zuo, X., . . . Zang, Y. (2009). Spontaneous brain activity in the default mode network is sensitive to different resting-state conditions with limited cognitive load. *PLoS One*, 4(5), e5743. doi: 10.1371/journal.pone.0005743
- Yano, T., Kato, B., Fukuda, F., Shinbara, H., Yoshimoto, K., Ozaki, A., & Kuriyama, K. (2004). Alterations in the function of cerebral dopaminergic and serotonergic systems following electroacupuncture and moxibustion applications: possible correlates with their antistress and psychosomatic actions. *Neurochemical research*, 29(1), 283-293.
- Yao J, Dewald J. (2005): Evaluation of different cortical source localization methods using simulated and experimental EEG data. *NeuroImage* 25(2):369-382.
- Yu H, Xu G, Yang R, Yang S, Geng Y, Chen Y, Li W, Sun H. (2009): Somatosensory-evoked potentials and cortical activities evoked by magnetic stimulation on acupoint in human. p 3445.
- Zeng, Y., Liang, X. C., Dai, J. P., Wang, Y., Yang, Z. L., Li, M., . . . Shi, J. (2006). Electroacupuncture modulates cortical activities evoked by noxious somatosensory stimulations in human. *Brain Res*, 1097(1), 90-100. doi: S0006-8993(06)00800-6 [pii]10.1016/j.brainres.2006.03.123
- Zhang, W. T., Jin, Z., Cui, G. H., Zhang, K. L., Zhang, L., Zeng, Y. W., . . . Han, J. S. (2003). Relations between brain network activation and analgesic effect induced by low vs. high frequency electrical acupoint stimulation in different subjects: a functional magnetic resonance imaging study. *Brain Res*, 982(2), 168-178. doi: S0006899303029834 [pii]
- Zhang, W. T., Jin, Z., Luo, F., Zhang, L., Zeng, Y. W., & Han, J. S. (2004). Evidence from brain imaging with fMRI supporting functional specificity of acupoints in humans. *Neurosci Lett*, 354(1), 50-53. doi: S0304394003011625 [pii]
- Zhang, Y., Chen, Y., Bressler, S. L., & Ding, M. (2008). Response preparation and inhibition: the role of the cortical sensorimotor beta rhythm. *Neuroscience*, 156(1), 238-246.
- Zhao, Z. Q. (2008). Neural mechanism underlying acupuncture analgesia. *Progress in neurobiology*, 85(4), 355-375.
- Zoefel, B., Huster, R. J., & Herrmann, C. S. (2011). Neurofeedback training of the upper alpha frequency band in EEG improves cognitive performance. *NeuroImage*, 54(2), 1427-1431.

APPENDICES

THE PUBLICATION LIST

1. Chen, J-L., Thompson, T., Kropotov, J., & Gruzelier, J. (2011). Beneficial Effects of Electrostimulation Contingencies on Sustained Attention and Electrocortical Activity. *CNS Neuroscience & Therapeutics*, 17(5), 311.

Impact Factor: 4.43

2. Chen, J-L., Ros, T., & Gruzelier, J. H. (2012). Dynamic changes of ICA-derived EEG functional connectivity in the resting state. *Human brain mapping*. 2012 Feb 17. doi: 10.1002/hbm.21475.

Impact Factor: 5.88

Beneficial Effects of Electrostimulation Contingencies on Sustained Attention and Electrocortical Activity

Max Jean-Lon Chen,^{1,2} Trevor Thompson,³ Juri Kropotov^{4,5} & John H. Gruzelier¹

1 Department of Psychology, Goldsmiths, University of London, London, UK

2 Department of Physical Medicine & Rehabilitation, Chang Gung Memorial Hospital and College of Medicine, Chang Gung University, Tao-Yuan, Taiwan

3 Department of Psychology and Counselling, University of Greenwich, London, UK

4 Institute of the Human Brain of Russian Academy of Sciences, 12 a ul. Academica Pavlova, St. Petersburg, Russia

5 Institute of Psychology, Norwegian University of Science and Technology, Dragvoll, Trondheim, Norway

Keywords

Acustimulation; Attention; Controlled trial; Event-related potentials (ERPs); Frequency modulation; Independent component analysis (ICA); sLORETA; Topographic EEG.

Correspondence

Max Jean-Lon Chen, Department of Psychology, Goldsmiths, University of London, New Cross, London SE14 6NW, UK.

Tel.: +44 0207 919 7870;

Fax: +44 0207 919 7873, or +886-3-3274850;

E-mail: m.chen@gold.ac.uk, or

bigmac1479@gmail.com

doi: 10.1111/j.1755-5949.2010.00190.x

SUMMARY

Introduction: Chinese acupuncture therapy has been practiced for more than 3000 years. According to neuroimaging studies, electroacupuncture has been demonstrated to be effective via control of the frequency parameter of stimulation, based on the theory of frequency modulation of brain function. **Aims:** To investigate the following: (1) possible sustained effects of acustimulation in improving perceptual sensitivity in attention by comparing before, during, and 5 min following stimulation; (2) relations between commission errors and the motor inhibition event-related potential (ERP) component measured with independent component analysis (ICA); (3) whether habituation would be demonstrated in the sham control group and would be mitigated by acustimulation in the experimental groups. **Results:** Twenty-seven subjects were divided into three groups ($n = 9$). d-Prime (d') derived from signal detection theory was used as an index of perceptual sensitivity in the visual continuous performance attention test. Increased d' was found during both alternating frequency (AE) and low frequency (LE) stimulation, but with no change in the sham control group (SE). However, only following AE was there a sustained poststimulation effect. Spatial filtration-based independent components (ICs) in the AE group revealed significantly decreased amplitudes of the motor inhibition ICs both during and poststimulation. There was a significant habituation effect from task repetition in the sham group with decreased amplitudes of ICs as follows: the visual comparison component difference between go (correct response) and nogo cues (correct withheld response), the P400 action monitoring and the working memory component in the nogo condition, and the passive auditory component on control trials. **Conclusion:** The results showed associations between acustimulation and improved perceptual sensitivity with sustained improvements following AE, but not LE stimulation. Improvements in commission errors in the AE group were related to the motor inhibition IC. The activational effects of acustimulation apparently attenuated the across-task habituation that characterized the control group.

Introduction

Acupuncture therapy has been practiced in Chinese medicine for more than 3000 years with applications including treating headache, recovering from stroke, and controlling pain [1–4]. Acupuncture can be considered an important complementary medicine practice, with increasing interest from the public, and both the National Institute of Health (USA) and the World Health Organization have summarized guidelines on acupuncture therapy [5,6]. Recent years have seen increased interest in acupuncture therapy in neuroscience including (1) mechanisms of action [7], (2) respondent brain areas [8,9,10], and (3) temporal dynam-

ics such as immediate and/or delayed effects [11,12]. With the increasing development of acustimulation methods for cognition, reliability requirements have become more critical.

Peripheral electrical stimulation may be elicited via electrodes located on the skin (transcutaneous electrical nerve stimulation, [TENS]), and the process is usually named electroacupuncture stimulation or acustimulation [13]. Wang et al. have demonstrated that TENS operates through very similar mechanisms to traditional acupuncture [14], with the mechanism of therapeutic action thought to involve neurotransmitter and opioid peptide systems [1,13–16]. To facilitate the release of neuropeptides in the central nervous system (CNS), the stimulus

parameters of electroacupuncture (intensity, mode, frequency, etc.) can be controlled more precisely than by manual acupuncture. Furthermore, the uncomfortable pain sensation induced by needle manipulation is undesirable and an invasive procedure may also carry the risks of hematoma formation and infection. Electroacupuncture has been the procedure of choice for its comfort, convenience and high repeatability during an individual stimulus program.

Different types of endorphins for analgesia have been selectively released by low- and high-frequency acustimulation [13,17]. Low-frequency stimulation has induced the release of enkephalins, whereas high-frequency stimulation has increased the release of dynorphins in both animal and human experiments [13,18]. Therefore acustimulation in specific frequencies can facilitate the release of specific endogenous opioid peptides for acupuncture-induced analgesia in the CNS. Furthermore, through increases in the level of enkephalins and serotonin in the CNS and plasma acupuncture could affect psychological processes, hence applications for the treatment of depression and anxiety [18–20].

Regarding the temporal effects, both short-term and long-term impact has been examined. It has been proposed that the basic mechanism of the former involves immediate frequency modulation of neuroplasticity [7], and of the latter gene transformation of protein synthesis in specific cortical areas as shown with neuroimaging [8,9]. Dhond *et al.* have claimed that acupuncture can “enhance the post-stimulation spatial extent of resting brain networks to include anti-nociceptive, memory, and affective brain regions” [11]. It follows from the neuroimaging results, summarized in the Discussion, that there is a likely impact of acustimulation on cognitive functions aside from therapeutic outcome.

There has been limited research showing differential effects between low- versus high-frequency stimulation on cognitive function. With the electroencephalograph (EEG), scalp maps of high-versus low-frequency effects have been investigated in a resting eyes-closed condition, but not in cognitive tasks [12]. In general the relationship between acustimulation and task-evoked brain activity is a neglected area.

As a behavioral task we utilized a continuous performance visual attention test, which has a venerable history in applications in psychopharmacology [21–25] and neurochemistry [26–28]. For about half a century variants of the task have been used to locate impairments and monitor the efficacy of treatments. Applications have ranged from aging [29,30] to sleep deprivation [31], neurobiological disorders including amnesia [32,33], dementia [34], traumatic brain injury [35], and HIV infection [36], and most widely psychopathology including attention deficit hyperactivity disorder (ADHD) [37–39], obsessive compulsive disorder [40,41], depression [42–44], posttraumatic stress disorder [45], and most of all the schizophrenia spectrum [46–52]. The application of signal detection theory [53] to extract a d' index of sensory sensitivity has been long established in studies of psychopathology [54,55]. This study also uses methods of EEG and event-related potential (ERP) topographic mapping, independent component analysis (ICA), and standardized low-resolution electromagnetic tomography (sLORETA) to study acustimulation and sustained attention.

Our main goals were to investigate the impact of electroacupuncture stimulation on attention and to compare alternat-

ing versus low frequencies on behavioral performance, the perceptual sensitivity in attention, topographic EEG, and ERPs for both immediate and poststimulation effects. According to previous research we expected to find that the alternating frequency electroacupuncture was superior to low-frequency stimulation [13,56]. In addition, due to a repeated task design, we hypothesized that habituation would be found in the control group, but not in the two acustimulation groups who would be resistant to habituation because of the activation effects of stimulation. In order to examine if specific cortical areas were affected by electroacupuncture and habituation, we used topographical EEG examination with the ICA method, and applied spatial filtration from a normal database.

Materials and Methods

Subjects

Data were recorded from 30 individuals, but because of technical problems or excessive artifacts, three data sets were excluded from further analysis. Twenty-seven healthy volunteers (20 female, 7 male), mean age = 22.5 (SD = 1.56, range 18–30 years) from Goldsmiths, University of London, participated in the study. Subjects were excluded if they had any history of epilepsy, drug abuse, head injury, or psychiatric disorders. Those participants currently having any sore, pain, cut, skin problems on the hands or receiving psychoactive medication were also screened out. All subjects had not experienced acustimulation before our testing. All had normal hearing and normal (or corrected-to-normal) eyesight. Written consent was obtained prior to the start of the experiment in accordance with the Helsinki Declaration, and the current investigation received the ethical approval from the College Research Ethics Committee.

Participants were randomly assigned to one of three experimental groups of equal size ($N = 9$) with the method of randomly permuted blocks <http://www.randomization.com>. Group 1 (alternating frequency, AE) who received stimulation with alternating low (5 Hz) and high (100 Hz) frequencies; Group 2 (low frequency, LE) received stimulation with the low frequency (5 Hz) only; Group 3 (sham electrostimulation, SE) received a control condition with the minimal intensity for electroacupuncture.

Experimental Design

Each subject was asked to perform a continuous performance visual attention task and sat in a comfortable armchair throughout the duration of the experiment in a quiet room. They were seated facing a computer screen, 100 cm in front of them, and were instructed to press a response button whenever a visual target stimulus picture occurred and to withhold responses to other stimuli. Detection accuracy and response time were recorded during the repetitive tasks. All subjects were blind to the stimulation mode and effect. They were told that the machine could stimulate acupuncture points through high-frequency or low-frequency stimulation, and this may or may not give a sensation. Transcutaneous electric acupoint stimulation (Han's acupoint

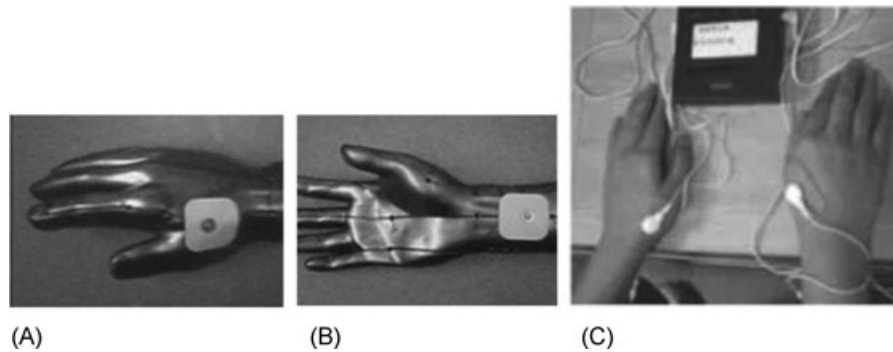


Figure 1 The location of two acupoints. (A) HeGu, (B) NeiGuan, and (C) the application of the stimulator device on both acupoints.

nerve stimulator [HANS], Wearnes Technology, Singapore) was applied. The selected acupoints were LI-4 (HeGu point) and P-6 (NeiGuan point) of both hands. The HeGu point is located at the first inter-interosseous muscle of the hand. The NeiGuan point is located on the anterior surface of the wrist between the tendons of the flexor carpi radialis and the palmaris longus, next to the median nerve, and on average 3–5 cm proximal to the flexor crease. The two acupoints of each hand were stimulated at the same time as a circuit in one output channel of HANS (Figure 1) in order to prevent unusual current overflowing across the body inducing arrhythmia. Subjects received stimulation via four adhesive surface electrodes (size: 4 cm × 5 cm) at the aforementioned bilateral acupoints. The stimulation intensity for the real acustimulation was adjusted to a maximal but comfortable level, slightly below the pain or discomfort threshold, ranging from 7 to 15 mA. For the sham acustimulation the intensity was set at less than 5 mA [57]. Based on the literature review [57–64], we selected sham acustimulation applied to the same points with minimal intensity as our control placebo model, and only the intensity parameter of stimulation was different from the real stimulation groups.

Each subject was instructed to pay no attention to the sensation induced at the stimulated site, and to focus on the attention task. All 27 subjects were assessed by evaluating their behavioral results from the attention task and the event-related EEG measures in the three study stages (before stimulation, during stimulation, and 5 min poststimulation). Each study stage consisted of 5 min eyes closed baseline EEG, 5 min eyes open baseline EEG, and 20 min of the attention task.

Attention Paradigm

The two-stimuli go and nogo task is a subtype of the general go and nogo paradigm. When the “go” stimulus is presented a manual response is required whereas when a “nogo” stimulus is presented the response is to be withheld. The purpose of this design is to examine two types of errors, namely those representing inattentiveness and impulsivity. The task presents stimuli in pairs so that the subject would implicitly be ready to make a decision after the first stimulus in the pair and to respond as fast as possible after the second stimulus is shown on the screen. Here the im-

ages were flashed on the screen in pairs within 3 seconds with the instruction to press a button when the target pair occurred. The stimuli were nonlanguage based and consisted of a total of 20 different images of animals (A), plants (P), or humans (H). In addition, each human picture was presented together with a pure tone of 500 Hz of 20 ms duration. Four different categories of trials were shown: “Animal-Animal (A-A),” “Animal-Plant (A-P),” “Plant-Plant (P-P),” and “Plant-Human (P-H).” The duration of the stimuli was 100 ms, and trials were presented in a random order with equal probability. Interstimulus intervals were 1400 ms, and long enough for subjects to prepare their responses; the total interval between trials was 3100 ms. The task consisted of 400 trials, divided into four sessions with 100 trials each, and took around 20 min. The subject had to press a button as fast as possible when the A-A pairs were presented on a screen and ignore other pairs of stimuli (A-P, P-P, P-H, Figure 2) (Psytask user manual, <http://www.mitsar-medical.com>) [65].

Electroencephalographic (EEG) Recordings and Pretreatment of EEG

Topographical EEG and ERP data of all participants were recorded during the attention task. All neuroelectric data were recorded using the Mitsar 21-channel EEG system, the “Mitsar-201” (CE 0537) manufactured by Mitsar, Ltd. (<http://www.mitsar-medical.com>), with a 19-channel electrode cap with silver-chloride electrodes that included Fz, Cz, Pz, Fp1/2, F3/4, F7/8, T3/4, T5/6, C3/4, P3/4, O1/2. The cap was placed on the scalp according to the standard 10–20 system (Electro-cap International, Inc. <http://www.electro-cap.com/caps.htm>). Electrodes were referenced to linked earlobes (off-line) and the input signals were sampled at a rate of 250 Hz (bandpass 0.5–30 Hz). The ground electrode was placed on the forehead. Impedance was kept below 5 k Ω . Electro-oculogram (EOG) data were recorded from electrodes (Fp1/2) placed above the frontal muscles to monitor eye blinking or movements. An EOG correction procedure to remove artifacts was performed and nonspecific artifacts were rejected off-line. ERP waveforms were averaged and computed off line and trials with omission and commission errors were automatically

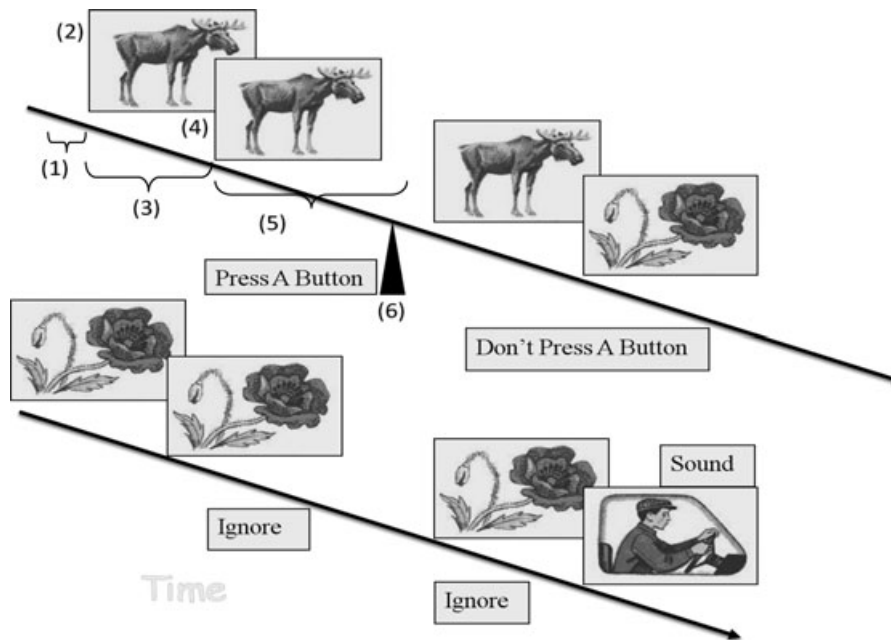


Figure 2 Stimulus presentation in the visual attention task: (1) prestimulus interval, (2) first stimulus, (3) interstimulus interval, (4) second stimulus, (5) poststimulus interval, (6) subject response. Two arrows and lines represent the continuous time axis during the task with four pairs of pictures randomly shown. The first pair, the Animal-Animal (A-A) pair, represents the

“go” cue, to which the subject should press the button. The second pair, the Animal-Plant (A-P) pair, represents a “nogo” cue, and the subject should not respond. The remaining two Plant-Plant (P-P) and Plant-Human (P-H) pairs are control condition trials, and the subject should ignore them.

excluded from analysis. All participants performed the attention task three times: before, during, and 5 min poststimulation.

Data management and Statistical Analysis

EEG data analysis was performed using WinEEG 2.83, the commercial software from the Mitsar, Ltd. (<http://www.mitsar-medical.com>). First, data were digitally filtered using a linear filter to minimize drifts and line noise. ERP data epochs were extracted (0 to 3000 ms) and baseline corrected (−100 to 0 ms). Epochs containing unique, nonstereotyped artifacts (e.g., swallowing, extreme muscle activities with amplitudes over 35 μ V, electrode cable movements) were automatically rejected from further analysis, whereas epochs containing repeatedly occurring artifacts (e.g., eye blinks, heart beat artifacts) were corrected using ICA [66,67]. The ICA method [68] (<http://scn.ucsd.edu/eeglab>) was implemented in the software, WinEEG, and written by Ponomarev [65]. sLORETA imaging for locating cortical generators provided source computations for the independent components (ICs) using freeware provided by the Key Institute for Brain-Mind Research in Zurich, Switzerland (<http://www.uzh.ch/keyinst/loreta.htm>) [69].

The behavioral parameters included errors of omission (indicative of inattentiveness), errors of commission (indicative of impulsivity), reaction time (RT) and reaction time variability (RTV). We also introduced the parameter “d-prime” (d') derived from signal

detection theory [53,70]. This takes into account both the ratio of hit rate (H) and the false alarm rate (F) and is used as measure of perceptual sensitivity. Conventionally in calculating d' , H is defined as (“H” = 1 - [number of omission errors/number of targets]), and F as (“F” = number of commission errors/number of non-targets). From these formulas, however, the d' is not simply [H-F], rather, it is the difference between the z-transforms of these two rates and were calculated as [$d' = z(H) - z(F)$]. In other words, d' measures both of these two error types as an index of perceptual sensitivity [71,72].

To evaluate the effectiveness of acustimulation relative to the sham procedure, a mixed-design ANOVA was used to examine the effects of Group (AE, LE, SE) and Time (before, during, after acustimulation) on behavioral measures. Separate ANOVAs were performed on each of the five measures: omission errors, commission errors, RT and RTV, and d' with the Bonferroni correction for *post hoc* comparisons. Given the exploratory nature of the study, an uncorrected significance threshold of $P = 0.05$ was used for each of the five ANOVAs in order to preserve a reasonable sensitivity for detecting real effects (i.e., to maintain a reasonable type I error rate). Given this, caution must be used in interpreting each effect, with greater credence given to those effects specifically predicted *a priori*, as outlined in the Introduction. So that the reader can judge which effects would survive a harsher significance criterion, an adjusted alpha of 0.01 was also calculated using a Bonferroni adjustment based on the number of tests (i.e., 0.05/5). The nature of any significant interactions that emerged were explored using

Table 1 Scores (mean \pm standard deviations) for attention test measures before, during, and after electrostimulation (3 groups)

Group	go/nogo Variables	Before	During	After
AE	Omission errors	1.22 \pm 0.83	1.67 \pm 1.66	1.33 \pm 1.87
	Commission errors	1.22 \pm 0.67	0.11 \pm 0.33	0.22 \pm 0.67
	d' (d-prime)	5.09 \pm 1.01	6.63 \pm 1.36	6.88 \pm 1.47
	RT (ms)	401.00 \pm 62.92	372.56 \pm 65.28	358.22 \pm 52.94
	RTV (ms)	8.68 \pm 2.23	8.23 \pm 2.30	8.64 \pm 2.65
LE	Omission errors	4.33 \pm 3.94	1.89 \pm 1.69	4.11 \pm 3.95
	Commission errors	1.44 \pm 1.33	0.56 \pm 0.88	1.00 \pm 0.71
	d' (d-prime)	4.47 \pm 1.03	6.27 \pm 1.13	4.79 \pm 1.12
	RT (ms)	379.00 \pm 53.70	379.67 \pm 54.35	378.89 \pm 56.37
	RTV (ms)	9.51 \pm 3.22	10.67 \pm 3.16	9.90 \pm 3.15
SE	Omission errors	5.67 \pm 5.05	4.78 \pm 3.96	5.67 \pm 4.36
	Commission errors	0.33 \pm 0.71	0.67 \pm 0.71	0.89 \pm 1.17
	d' (d-prime)	5.79 \pm 1.41	5.15 \pm 1.23	5.23 \pm 1.27
	RT (ms)	349.22 \pm 70.76	345.78 \pm 44.53	353.67 \pm 56.49
	RTV (ms)	8.58 \pm 4.46	9.56 \pm 2.94	9.97 \pm 4.18

AE, alternating frequency; LE, low frequency; SE, sham electrostimulation; RT, response time; RTV, response time variability.

contrast tests comparing mean scores across time periods (i.e., before vs. after, before vs. during, after vs. during) for each of the three groups, in line with the primary goals of the study, including parameters of ERP and ICs (latencies and amplitudes) in both conditions (go and nogo cues).

Results

Behavioral Performance

Table 1 shows the means and standard deviations of the d' , commission errors, omission errors, RT, and RTV scores of the attention task for the three groups, and in Table 2 the results of ANOVA with repeated measures.

The results for d' are shown in Figure 3 and Table 2. There were significant main effects for Group ($F[2,27] = 7.394$, $P = 0.003$) and Time ($F[2,27] = 3.487$, $P = 0.048$), and importantly there was a Group \times Time interaction ($F[4,27] = 3.554$, $P = 0.013$) whereby relative to the control group stimulation in both AE and LE groups resulted in higher d' , which indicates increased perceptual sensitivity (contrast tests, $t[24] = 2.538$, $P = 0.018$ and $t[24] = 1.926$, $P = 0.066$, respectively). Furthermore with AE the increase in d' with stimulation ($t[24] = 2.532$, $P = 0.018$; in Figure 3, t1) was sustained poststimulation ($t[24] = 2.932$, $P = 0.007$; in Figure 3, t2), whereas with LE the increase with stimulation ($t[24] = 3.494$, $P = 0.002$; in Figure 3, t3) was not sustained poststimulation ($t[24] = -2.884$, $P = 0.008$; in Figure 3, t4; nonsignificant before vs. after stimulation, $t[24] = 0.611$, $P = 0.547$; in Figure 3, t5). Moreover, the consequent difference between the AE and SE groups poststimulation showed higher d' scores following AE stimulation ($t[24] = 2.695$, $P = 0.013$, contrast test).

For omission errors there was only a Group effect ($F[2,27] = 4.347$, $P < 0.024$), without significant effects of Time ($F[2,27] = 1.727$, $P = 0.189$) or a Group \times Time interaction ($F[4,27] = 1.210$,

Table 2 The effects of Group and Time (before, during, after electrostimulation) on the attention task with two-way repeated measures ANOVA

	Source	df	F	P
d' (d-prime)	Group	2	7.394	0.003**
	Time	2	3.487	0.048*
	Group \times Time	4	3.554	0.013*
Commission errors	Group	2	2.090	0.146
	Time	2	3.166	0.051
	Group \times Time	4	2.857	0.033*
Omission errors	Group	2	4.347	0.024*
	Time	2	1.727	0.189
	Group \times Time	4	1.210	0.319
RT (ms)	Group	2	0.809	0.457
	Time	2	2.013	0.157
	Group \times Time	4	2.347	0.068
RTV (ms)	Group	2	0.605	0.554
	Time	2	1.034	0.364
	Group \times Time	4	0.928	0.456

Group \times Time indicates the interaction between group and time period.

*significance level: $P < 0.05$; **significance level: $P < 0.01$; according to Bonferroni correction.

AE, alternating frequency; LE, low frequency; SE, sham electrostimulation.

$P = 0.319$). The Group effect was attributable to the higher omission errors overall in the control group, as shown in Table 1, which were also higher at baseline ($P = 0.055$, Bonferroni). On the other hand, the commission errors, shown in Figure 4, disclosed both a tendency toward an effect of Time ($F[2,27] = 3.166$, $P = 0.051$) and importantly a significant Group \times Time interaction ($F[4,27] = 2.857$, $P = 0.033$), which was due to a reduction in errors with repetition in both electroacupuncture groups. The effects of

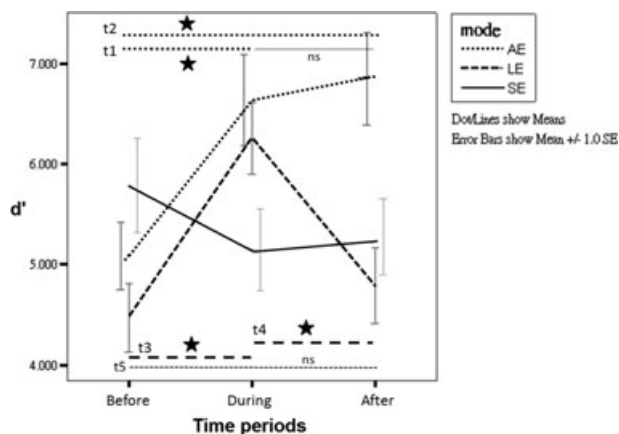


Figure 3 Electrostimulation changes on mean d' scores (\pm SEM) in the attention task for both AE and LE groups relative to the SE control group (\star denotes $P < 0.05$; AE, alternating frequency; LE, low frequency; SE, sham electrostimulation; t1, the contrast test during vs. before stimulation in the AE group; t2, the contrast test after vs. before stimulation in the AE group; ns, not significant during vs. after stimulation in the AE group; t3, the contrast test during vs. before LE stimulation; t4, after vs. during LE stimulation; t5, before vs. after LE stimulation, ns, not significant).

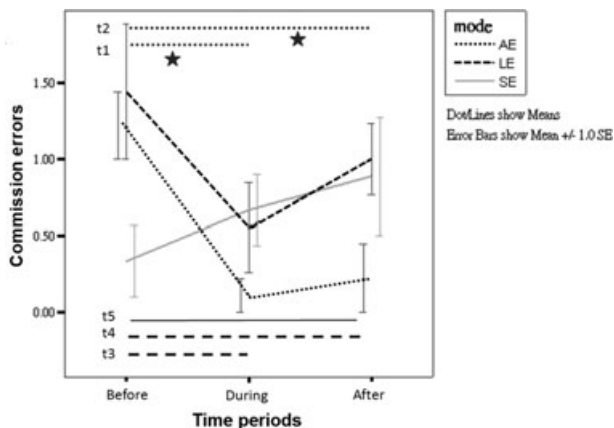


Figure 4 Electrostimulation changes on mean commission errors (\pm SEM) in the attention task for both AE and LE groups relative to the SE control group (\star denotes $P < 0.05$; t1, the contrast test during vs. before stimulation in the AE group; t2, the contrast test after vs. before stimulation in the AE group; t3, the contrast test during vs. before LE stimulation; t4, after vs. before LE stimulation; t5, after vs. before SE stimulation).

stimulation on d' were found largely attributable to reductions in commission errors (in Figure 4 and Table 1). Then underscoring the pattern of results with d' , whereas with AE stimulation there was a decrease in commission errors (contrast test, $t[24] = -4.082$, $P = 0.0004$, in Figure 4, t1) which was sustained poststimulation (contrast test, $t[24] = -3.674$, $P = 0.001$, in Figure 4, t2), with LE there was a tendency toward a decrease in errors with stimulation (contrast test, $t[24] = -1.868$, $P = 0.074$, in Figure 4, t3) which was not sustained poststimulation (contrast test, $t[24] = -0.934$, $P = 0.360$, in Figure 4, t4).

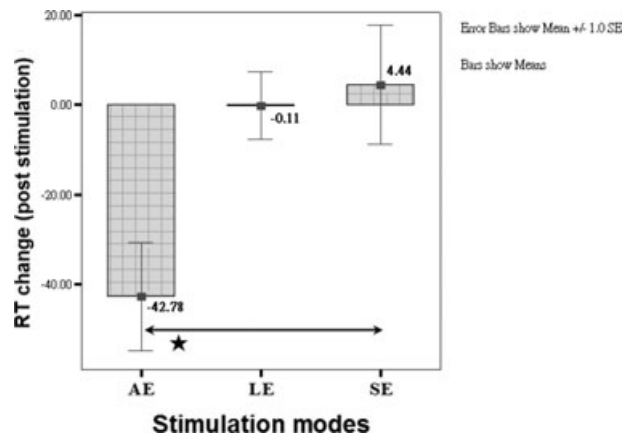


Figure 5 Postelectrostimulation changes on mean response times (\pm SEM) in the attention task for the AE, LE, and SE control groups (\star denotes $P < 0.05$; RT, response time).

Turning to the RT measures there were no significant effects of Group (Table 2, $F[2,27] = 0.809$, $P = 0.457$), Time ($F[2,27] = 2.013$, $P = 0.157$) nor was there a Group \times Time interaction ($F[4,27] = 2.347$, $P = 0.068$). However, as can be seen in Table 1 and Figure 5, there was a mean reduction in RTs poststimulation in the AE group compared with the SE group. Exploratory *post hoc* analyses with the Bonferroni correction indicated that the reduction in RT differed significantly between the SE and AE groups poststimulation ($P = 0.023$). Regarding response time variability (RTV), there were no significant effects of Group ($F[2,27] = 0.605$, $P = 0.554$), Time ($F[2,27] = 1.034$, $P = 0.364$) nor was there a Group \times Time interaction ($F[4,27] = 0.928$, $P = 0.456$).

ERP Data

The group grand averages of the two conditions (go and nogo) in the attention task for the midline electrodes for each time period (before, during, and after stimulation) are illustrated in Figure 6. All three groups showed no statistically reliable changes in the early ERP components (with latencies of 80–180 ms), or in the late positive components (180–420 ms), and all groups displayed a trend of decreasing amplitude, but with no statistically significant findings (see also Table 3).

Extracting Late ERP Components by Means of the ICA Method and Spatial Filters

Motor Inhibition Component

Analysis of the grand mean ERPs in response to the difference between go and nogo cues revealed a relatively large frontocentral positive deflection in all groups, especially in the AE group (left columns of Figures 7A and 8A). Interestingly, for the AE group at Fz, Cz, and Pz, the motor inhibition component extracted by the ICA method and spatial filters had a significantly decreased peak

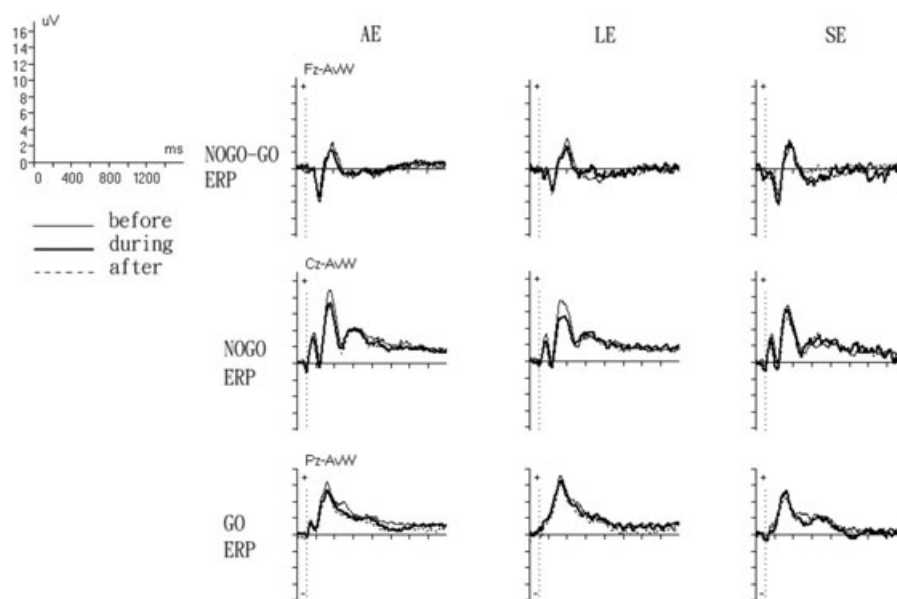


Figure 6 Grand average ERPs for each group and time block for the midline electrodes in the attention paradigm. A frontally distributed negative ERP component had greater amplitude for nogo in comparison to go stimuli and was associated with response inhibition in go-nogo paradigms (upper panel).

No significant changes in amplitudes and latencies among three groups and three time periods (before, during, and after stimulation) were found. (See also Table 3.)

Table 3 Means and standard deviations for the visual attention ERP measures in each group before, during, and after electrostimulation

Group	go/nogo	Before variables	During	After
AE	Pz go amplitude	6.07 ± 2.20	4.96 ± 2.28	4.77 ± 2.12
	Pz go latency	323.78 ± 10.60	321.56 ± 13.33	322.44 ± 8.82
	Cz nogo amplitude	9.22 ± 3.59	7.23 ± 2.49	7.21 ± 2.19
	Cz nogo latency	348.67 ± 17.89	348.22 ± 16.38	344.67 ± 24.49
LE	Pz go amplitude	7.10 ± 3.23	6.39 ± 2.78	6.24 ± 2.95
	Pz go latency	321.56 ± 21.49	320.22 ± 24.13	317.56 ± 24.29
	Cz nogo amplitude	8.39 ± 5.35	6.37 ± 4.33	6.76 ± 3.81
	Cz nogo latency	362.44 ± 31.52	363.78 ± 31.31	355.33 ± 33.97
SE	Pz go amplitude	5.20 ± 2.95	5.40 ± 2.28	4.36 ± 1.80
	Pz go latency	324.44 ± 16.49	328.67 ± 19.34	326.22 ± 24.05
	Cz nogo amplitude	7.01 ± 4.52	6.71 ± 3.88	5.37 ± 4.27
	Cz nogo latency	354.00 ± 15.17	351.33 ± 22.05	342.44 ± 15.61

AE, alternating frequency; LE, low frequency; SE, sham electrostimulation.

from 372 ms to 396 ms, compared with the prestimulation stage (during vs. before stimulation, $P = 0.0156$ in Figure 7; after vs. before stimulation, $P = 0.0143$ in Figure 8) [73–75].

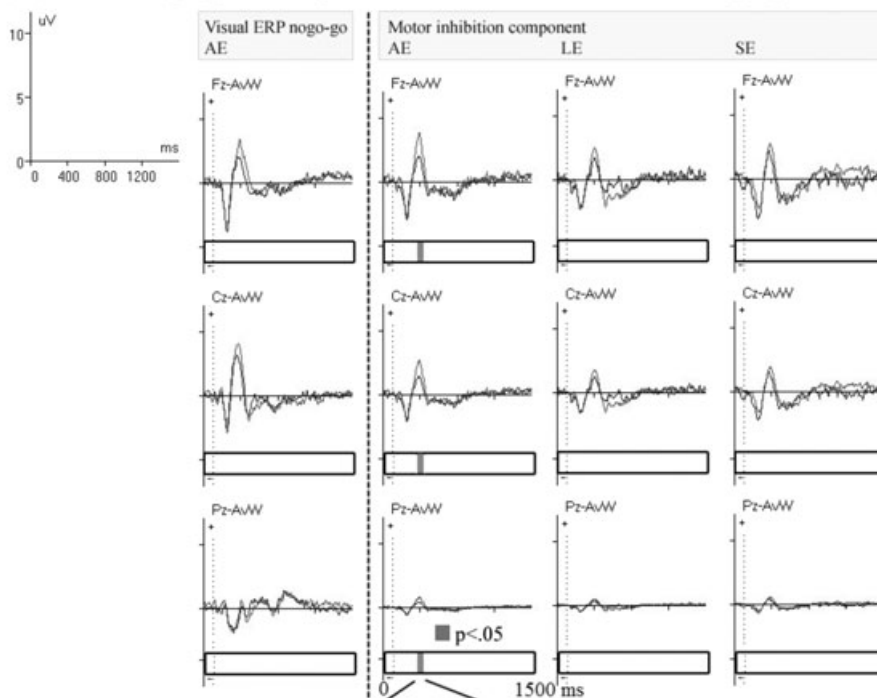
Analysis of ICs Related to Habituation/Inattention

To evaluate if a putative habituation effect in controls would be inhibited by the stimulation with task repetition, we used the ICA method to reveal the fundamental components in the ERPs. The related ICs of ERPs were compared for the first and last task in

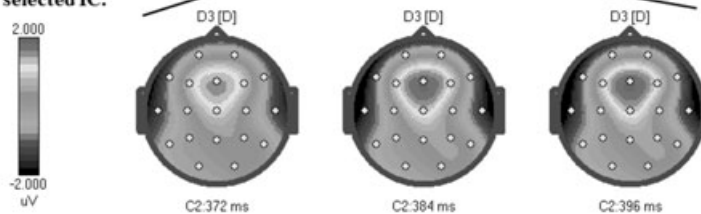
each group. Of 11 components that were identified by the spatial filters based on the ICA from the Human Brain Indices (HBI) reference database. (<http://www.mitsar-medical.com>) [65], seven components responding to the “go and nogo” cues were meaningfully related to the visual attention task as follows: visual comparison component at the left temporal area, visual comparison component at right temporal area, P400 working memory component at the frontal area, P300b component at the parietal area, slow wave component at the hippocampus, P300 suppression component at the frontal area, and P400 action monitoring component at the anterior cingulate cortex (ACC) [65]. However, only

During vs. before stimulation

(A) The curves display grand average visual ERPs and the motor inhibition IC in 3 groups.



(B) The 2D topographies of the selected IC.



(C) The perspective views of the selected IC in sLORETA.

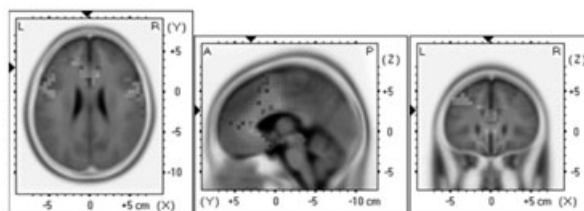
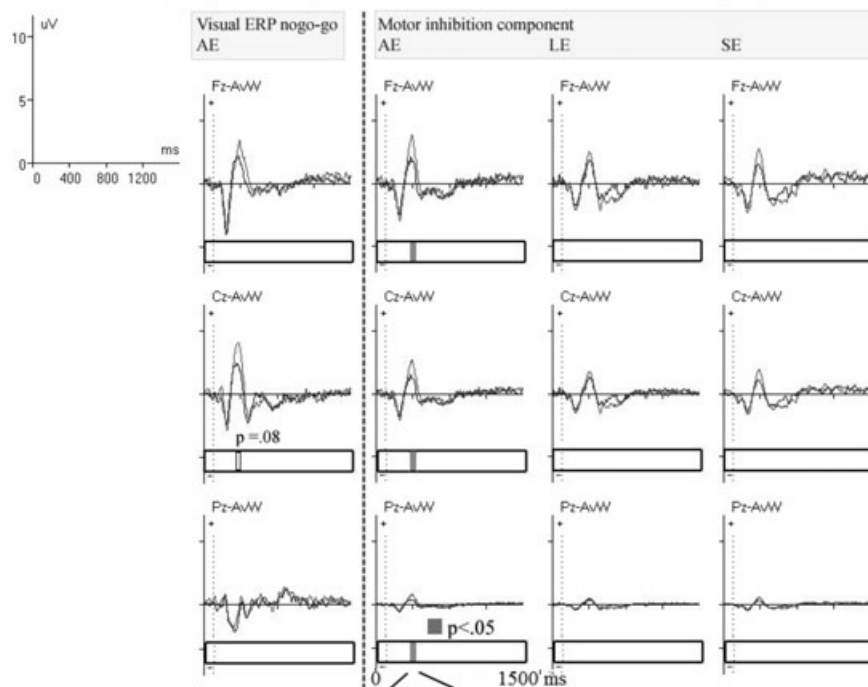


Figure 7 (A) Grand mean extracted motor inhibition ICs at midline scalp sites and correlated ERP of nogo-go cues, during stimulation (blue lines) compared with prestimulation (red lines) in the three groups. Red lines showed the prestimulation baseline of grand mean ERPs and grand mean motor inhibition components in the three groups. The animal pairs were the targets of the manual responses (GO cues), and nogo-go means the component difference between go and nogo cues. Superimposed blue lines gave the grand mean ERPs and grand mean motor inhibition components during

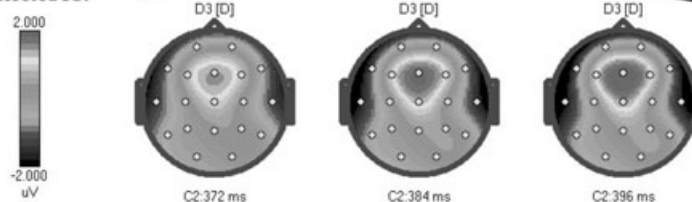
electrostimulation in the three groups. **(B)** Horizontal bars below each trace represent *t*-test results from 0–1500 ms after the second stimulus onset, with values *P* < 0.05 represented in gray between 372 and 396 ms, to illustrate the time course of significant differences from the baseline in the 2D scalp maps. **(C)** The perspective views (top, sagittal, and coronal views) showed the highest density of the motor inhibition component, according to sLORETA images for cortical generators.

After vs. before stimulation

(A) The curves display grand average visual ERPs and the motor inhibition IC in 3 groups.



(B) The 2D topographies of the selected IC.



(C) The perspective views of the selected IC in sLORETA.

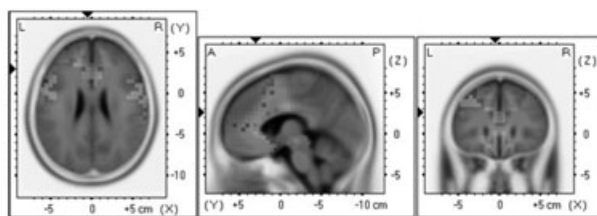


Figure 8 (A) Grand mean extracted motor inhibition ICs at midline scalp sites and correlated ERP of nogo-go cues, after stimulation (blue lines) compared with prestimulation (red lines) in the three groups. Layout as for Figure 7(A)–(C).

significantly changed ICs were considered further, as the goal of this report was to describe and investigate the ICA features that significantly changed by applying electroacupuncture and/or attention task repetition (details in the next paragraphs).

The ICA decomposition of the attention task revealed similar components in the three conditions. Between-group differences in mean IC topographies in the prestimulation stage were barely

visible, suggesting a good reproducibility of the component characteristics [76]. However, only with the control group did the differences between the first and the third repetition in mean IC topographies show fatigue according to time-on-task effects showing significantly decreased amplitudes of the components [77–79,80]. Four components showed obvious differences, including the left visual comparison component, the P400 action-monitoring

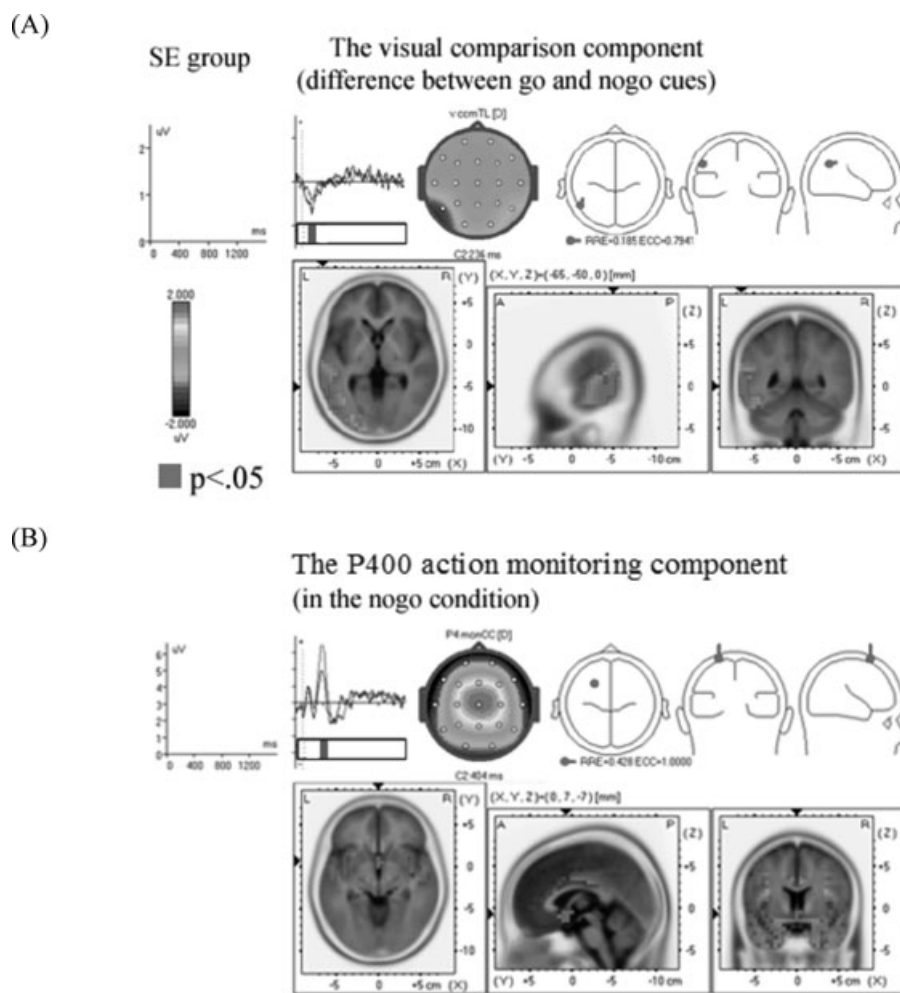


Figure 9 The independent components difference between the first and third task repetition in the sham stimulation group. **(A)** The visual comparison component difference between go and nogo cues. **(B)** The P400 action monitoring component in the nogo condition. The upper row of the panel for each component shows the grand mean component in amplitude-time plot at Cz (upper left), the scalp topographic map (upper middle), and the single equivalent current dipole locations for each component (upper right). The lower row shows the highest density of each component, according to

sLORETA images, from three different perspectives (top, sagittal and coronal views). Each red line shows the grand mean component of the first attention task. Each superimposed blue line gives the grand mean component of the repeated third task. Horizontal bars below each trace represent *t*-test results from 0–1500 ms post second stimulus onset, with values $P < 0.05$ represented in gray, to illustrate the time course of significant differences between the first and the third repeated tasks.

component, the P400 working memory component, and the passive auditory P300 component. The average characteristics of the components as identified in the control group from the beginning to the end of the three tasks are shown in Figures 9 and 10, with details in the next paragraphs.

Visual Comparison Component, Left: The normalized grand-mean component in Figure 9, (Figure 9A, upper row), revealed a large negative deflection between 100 and 400 ms post second stimulus onset, peaking around 236 ms ($P < 0.05$), with a left temporal topography. The significant change of this component in left temporal topography was also projected on to a mean- magnetic resonance imaging (MRI) brain image (Montreal Neurological In-

stitute, Canada), according to the sLORETA images of the components (Figure 9A, bottom row) [65,81].

P400 Action Monitoring Component: As illustrated in Figure 9(B), the second component of interest was labeled the P400 action monitoring component in the ACC area due to its time course and topography, which was characterized by a later and slower ERP positivity from 260 to 520 ms with a peak latency around 400 ms (Figure 9B, upper row). The P400 action monitoring component location was in deep brain frontocentral regions through the ACC area (Figure 9B, bottom row) [65,82]. The characteristics of the significantly decreased amplitude of the P400 action monitoring component ($P < 0.05$, around the peak) outlined in Figure 9(B)

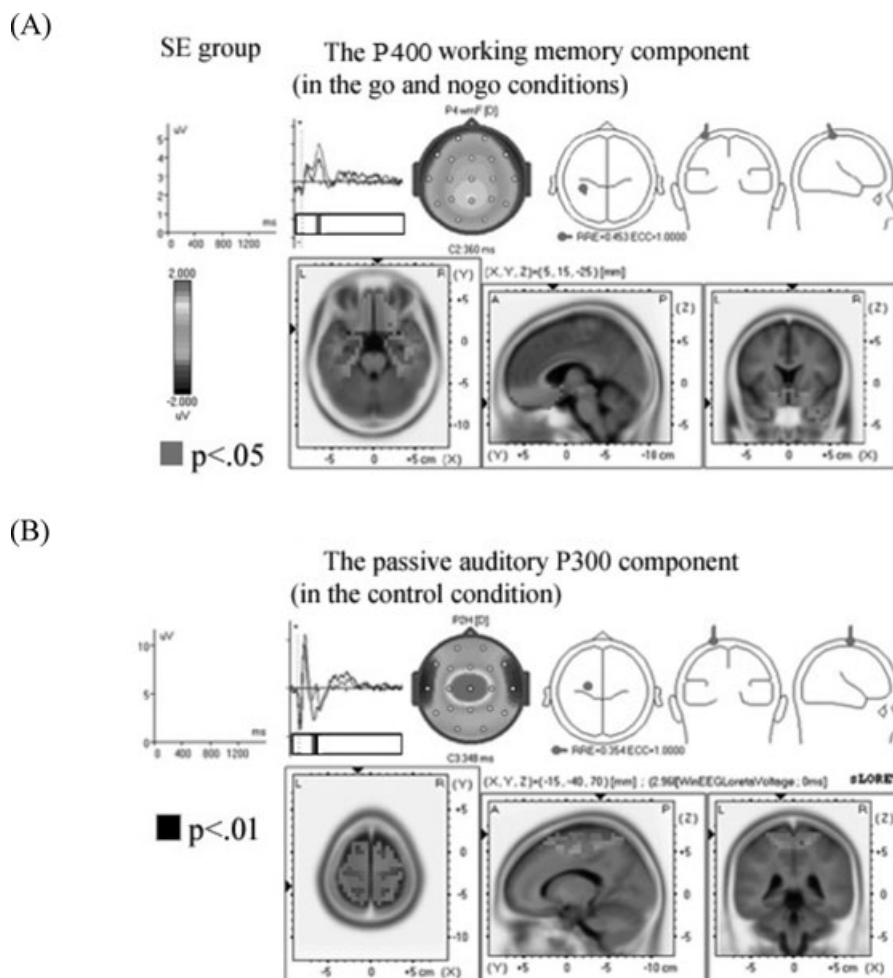


Figure 10 The independent components difference between the first and third task repetition in the sham stimulation group. **(A)** The P400 working memory component in both the go and nogo conditions. **(B)** The passive auditory P300 component in the control condition. Same layout as for the

panels in Figure 9(A) and (B) with values $P < 0.05$ and $P < 0.01$ represented in gray and black, to illustrate the time course of significant differences between the first and the third repeated tasks.

strongly suggested a relation between fatigue with task repetition, a time-on-task effect [76,80].

P400 Working Memory Component: The P400 working memory component presented with a positive double-peak morphology between 148 and 540 ms post second stimulus onset (peak latency around 360 ms; Figure 10A, upper row). This projected component on sLORETA images appeared to be more accurate than the 2D scalp map for assessing the spatial distributions of current density in deep sources. The P400 working memory component location was in the deep inferior prefrontal region, around the hippocampal area (Figure 10A, bottom row) [65,83]. The characteristics of the P400 working memory component mostly demonstrated a relation between fatigue with task repetition with a decline in amplitude ($P < 0.05$, around the peak).

Passive Auditory P300 Component: As illustrated in Figure 10(B), the passive auditory P300 component includes auditory N1/P2 peaks

[84], thus serving as a good indicator of the functioning of the auditory system in the visual attention task [85]. The peak of the passive auditory P300 component is around 348 ms and lasting roughly 900 ms. The passive auditory P300 responding to deviant auditory stimuli can be elicited without active attention. The 2D topography and the sLORETA images showed the highest density over the central scalp electrodes (Figure 10B, bottom row) [65,84,85]. The characteristics of the passive auditory P300 component possibly showed a significant relation between fatigue with task repetition with a declined amplitude of the passive auditory P300 component ($P < 0.01$, around the peak) in the present study, also as a function of time-on-task [76,80].

Discussion

The primary purpose was to explore the effects of electroacupuncture stimulation on a repetitive visual continuous performance

attention test and accompanying attention-related ERPs using behavioral performance indexes and ERP components extracted by the ICA method. Whereas a number of EEG studies have explored acupuncture effects without the popular ERP methodology [12,86–89], our current investigation was designed to complement these through the neglected field of topographical EEG, and also to learn more about the recent development of electrical stimulation. It was of particular interest to determine whether putative benefits would outlast stimulation, and whether stimulation with alternating high and low frequencies would be superior to low-frequency stimulation. It was hypothesized that stimulation would result in a significant behavioral change with increased sensory sensitivity (d'), largely due to a decrease in errors of commission, as found previously with university students performing the visual continuous performance task [71,90]. Students tend to be highly motivated to attend, producing few errors of omission, whereas the motivation to achieve may lead to over eagerness, resulting in impulsive errors of commission. It was further hypothesized that their performance would be reflected in ERP components with different types of ERPs generated on 'go' versus 'nogo' trials. Another purpose of this study was to examine if a putative habituation effect in controls would be inhibited by stimulation with task repetition. For this purpose response synchronized ICs of ERPs were compared for the first and last task in each group.

Behavioral Results

There was some suggestion of differences in commission errors, but given that the P -value was not significant with the conservative Bonferroni adjustment, caution must be applied and further research is warranted. However, d' was significantly changed differentially by parameters of stimulation (Table 2), particularly in relation to attention during and after stimulation with alternating frequencies (Figure 3).

The findings overall indicated that stimulation with alternating frequencies was superior to low-frequency stimulation in having sustained effects during the task, benefits which continued poststimulation. In contrast, low-frequency stimulation while effective during stimulation did not produce sustained benefits. These effects on the visual sustained attention task were disclosed through higher d' scores [53,91]. As anticipated, the improved d' score was largely due to a reduction in commission errors. RT was less definitively influenced, though exploratory *post hoc* tests confirmed shorter RTs following alternating frequency stimulation in the poststimulation condition when compared with sham stimulation.

ERPs to the Go and Nogo Stimuli

Compared to the prestimulation stage, the grand average ERPs showed a trend of decreasing peak amplitudes of the late components because of task repetition, but no changes in those early components having latencies between 80 to 180 ms. Previous studies using nonaffective targets have reported decreased P300 amplitudes at fronto-central sites both as a function of time-on-task and with sequence repetition, [77–79,80]. Another study em-

ploying unpleasant, neutral, and pleasant stimuli has reported that P300 amplitude decreased with repetitive picture processing [92]. In the current study the stimuli were mainly nonemotional and hence the results were in line with previous studies, notwithstanding the novel introduction of acustimulation

Application of ICA, Spatial Filter, and sLORETA

Applying ICA with spatial filtration disclosed a variety of interesting results, which confirm and extend efforts to decompose ERP components recorded during the visual attention task [93]. Mathematically, ICs are often characterized by scalp maps fitting the projection of a single equivalent current dipole, which is compatible with each presumed component reflecting synchronous cortical local field activity of a connected network. However, only a few components can be approximately calculated by a single dipole because some components are most likely to be generated by distributed neuronal circuits. Therefore standardized sLORETA images were used instead of dipole approximations. Overall the present findings strongly suggest that the main features of averaged ERP components can be successfully decomposed from ERP data via ICA decomposition combined with spatial filters (from HBI database) for each group and each time period, especially for the pre- versus poststimulation comparison. The components reflected motor inhibition, visual comparison, P400 action monitoring, working memory, and passive auditory P300 components.

Acupuncture Effect Induced by Stimulation in the Real versus the Sham Group

The typical HeGu and NeiGuan (LI-4 and P-6) acupoints are among the traditional points used in modulating cortical plasticity, relieving pain, and treating nausea and vomiting [12,57,94]. The HeGu acupoint lies at the midpoint between the first and second carpal bones of the first web space on the dorsal side, and the NeiGuan acupoint is located on the anterior surface of the wrist, approximately 3 cm proximal to the wrist between the tendons of the flexor carpi radialis and the palmaris longus, next to the median nerve. These junctures are full of peripheral nerve extensions from the sensory nerve and muscle tendons [95], and with lower focal transcutaneous resistance they can provide effective electrical stimulation without much current. In contrast, the sham (fake) electroacupuncture at the same acupoints (placebo electrostimulation), generates insufficient sensory input to cortex. Thus the observed changes of behavior and the motor inhibition component in the ERP could be due to the differences in the nerve conduction and excitability of stimulated acupoints of the two real electroacupuncture groups and the selected minimal stimulation in the sham group [57]. Certainly the differential stimulation effects between real versus sham stimulation on the same sites in behavioral performance and changes in ICs encourage the use of sham stimulation as a control for the study of brain function and associated acupuncture effects.

Acupuncture Effect Induced by Stimulation in Alternating Frequency Mode versus Low-Frequency Mode

Our study confirmed that only stimulation with alternating frequencies (5/100 Hz), but not with a low frequency delivered at 5 Hz, had the sustained poststimulation effect in improving *d'* scores and decreasing mean commission errors. Low stimulation at 5 Hz had only short-lived benefits. In addition, compared to the baseline without stimulation, alternating stimulation induced a significantly decreased motor inhibition component during stimulation and poststimulation, which theoretically was compatible with improvements in commission errors, which reflect motor impulsivity.

For clinical practice, the result of a prolonged effect due to alternating high and low frequencies has become an important issue for treatment [56]. A recent study with resting functional magnetic resonance imaging (fMRI) data using a probabilistic ICA method demonstrated for the first time that the poststimulation effects of acupuncture can enhance the spatial extent of resting brain networks [11]. Interestingly, such sustained poststimulation effects have been hypothesized to alleviate pain by altering neurotransmission in the CNS in both animals and man [1,96]. Differential release of opioid peptides in the CNS by electroacupuncture stimulation has been noted, with a low frequency of 2–15 Hz triggering the release of enkephalins and Beta endorphins, and a high frequency of 100 Hz stimulation increasing the release of dynorphin at the spinal cord level [1]. A combination of both frequencies with an alternating current of 2 and 100 Hz may allow synergistic interaction among the neurotransmitters and so provide a more powerful effect than sham stimulation [57,94]. Napadow *et al.* with fMRI have claimed that the limbic system is central to acupuncture effects regardless of the specific acupuncture modality, although some differences do exist in the underlying neurobiologic mechanisms for different modalities. The findings may also provide hints for optimizing acupuncture in clinical applications [97].

Further Potential Clinical Applications

Although most of the studies of electroacupuncture stimulation have explored the role of acupuncture in analgesia, neuroimaging research has also revealed possible brain networks and regions for potential influence on attention and memory [11,12,63,64,97]. Manual stimulation showed increased regional cerebral blood flow (rCBF) mainly in the parahippocampal gyrus, premotor area, frontal and temporal areas bilaterally, and the ipsilateral globus pallidus [98]. In a recent report of electroacupuncture-induced analgesia examined by fMRI, several areas with positive correlation of analgesic effects for low-frequency stimulation included the contralateral motor area, the supplementary motor area, and the ipsilateral superior temporal gyrus. In contrast with high-frequency stimulation the response occurred in the contralateral inferior parietal lobule, ipsilateral ACC, nucleus accumbens, and pons [64,99]. Functional MRI has demonstrated the CNS pathways involved in acupuncture stimulation. Even the subcortical gray structures, hypothalamus-limbic system, and hypothalamus-

pituitary-adrenal (HPA) axis have been related to electroacupuncture stimulation [63,100,101]. In the case of low-frequency stimulation, high activation has been elicited over the hypothalamus and primary somatosensory-motor cortex, with deactivation over the rostral segment of ACC [63].

The findings of our study also support the assumption that electroacupuncture stimulation has an effect on specific brain areas, and the improved performance in cognition is possibly related to enhanced cortical activity. While previous studies have demonstrated a sustained poststimulation effect for pain relief, gastric mobility, and heart rate variability (HRV) [102–104], to our knowledge no prior published research has examined sustained attention during stimulation and poststimulation periods in healthy young adults. This conclusion followed a search of nine bibliographic databases for the effects of TENS on nonpain related cognitive and behavior which found only reports on patients [105].

The Guidelines for Electroacupuncture Safe Practice in Dual-Site Electroacupuncture Stimulation of the Experimental Design

In clinical practice, the more distal acupoint location of the electrodes on hands and wrists seems much more practical than the proximal location of the limbs, paraspinal muscles, and neck or head regions. Our design with a pair of acupoints on each hand followed the guidelines for safe practice recommended by the British Medical Acupuncture Society (BMAS) to avoid adverse events. Especially, electroacupuncture should not be applied such that the current is likely to traverse the heart. If the application of electrostimulation is likely to cross the heart (e.g., from one shoulder to the other shoulder [106]), this placement is prohibited. A study has also reported that electrical fields generated by pairs of needles below the knee or elbow do not create a detectable spread of the currents along the limb or into the chest [106]. The safety guidelines are rarely mentioned in scientific reports.

Limitations and Recommendations for Future Research

Notwithstanding the beneficial outcome on sustained attention that we have demonstrated, our study has potential limitations or at least issues warranting further examination. First, an optimal washout period of the neurobiological effects generated by stimulation remains unknown. The effective poststimulation period was for a minimum of 30 min in our study, similar to the report of Claydon *et al.* using pressure pain threshold [102]. Second, the optimal sites for influencing cognition have not been systematically examined. HeGu (Li4) and NeiGuan (P6) are the well-studied acupoints, but other acupoints such as Zusanli (St36) and Taichong (Liv3) might be helpful adjuncts for improving cognitive function. Third, the relative contribution of the mechanism for the synergistic action produced by different combinations of neuropeptides is still not well understood, and therefore, the effectiveness of alternating frequency stimulation must be verified with neuroimaging. Meanwhile, various stimulation frequencies may involve different mechanisms. Several neurotransmitters such as serotonin and

dopamine are also believed to contribute to attention and memory systems [107–109]. It is not clear, however, to what extent these neurotransmitters are involved and how they are affected during and after electrical stimulation. Further research should be conducted to combine the behavioral, electrophysiological, and neurochemical modulation data.

Regarding the blinding of participants, first, we asked them to perform and focus on the repetitive visual attention task, and not pay attention to the sensation induced at the stimulated site. Second, the requirement of recruiting subjects was that all subjects had no experience about electroacupuncture prior to our testing. Complying with ethical considerations, although all subjects were blind to the stimulation mode and effect, they were told that the machine could generate transcutaneous stimulation on the acupoints of the hands with various frequencies, which may or may not give a sensation. However, because subjects had no experience of electrostimulation, they were blinded to the relationship of stimulation modes and effects. Importantly, only the intensity parameter of stimulation in the sham group was different from the real electroacupuncture groups, and possibly any emotional reaction to the thought of minimal tactile sensation was unlikely to influence responding; as mentioned earlier the sham stimulation itself has been shown not to affect sensory cortex [57,63].

Finally, electroacupuncture stimulation presented in this study is one method for modulating neuronal processing in order to improve cognitive performance. This may be useful in the range of neurological and psychopathological conditions mentioned above where the continuous performance paradigm has disclosed deficits [37,39,105]. Two studies related to the effects of TENS on cognition and behavior showed a moderate beneficial influence on cognitive functions in children with ADHD [110] and in aging [111].

EEG-neurofeedback is another approach [37,90,112]. In addition, recent emerging approaches combine feedback techniques and stimulation strategies for exploring more effective training protocols than either alone [113,114]. A just completed unpublished study has disclosed evidence for electroacupuncture stimulation assisting EEG-biofeedback training in the improvement of attention and memory performance and fundamental cortical electrophysiological activities as shown previously [71,72,115].

Conclusions

This single-blind randomized placebo-controlled study showed that electroacupuncture stimulation with alternating frequencies on pairs of acupoints of both hands resulted in significantly better sustained behavioral performance and sustained cortical activation in a repeated visual continuous attentional performance task than low-frequency stimulation, which in turn was superior to placebo. No obvious adverse effect in healthy subjects was noted. Evidence was provided that ICA with spatial filtration, applied to ERP data, successfully decomposed the spatiotemporally overlapping ERPs into a range of underlying EEG processes whose localization was congruent with a range of behavioral functions: visual comparison, P400 action monitoring, working memory, and passive auditory P300. The alternating frequency stimulation could be an adjunct for helping adults successfully enhance their sustained attention and inhibit competing motor responses both during and

poststimulation, indicating its potential therapeutic benefit for psychiatric disorders with compromised attention and cognition. When the baseline was compared with the prestimulation and poststimulation period in the control group with the placebo stimulation, the IC-derived ICs disclosed evidence of habituation. The absence of habituation in the experimental groups suggests a potentially successful activation for preventing fatigue. Further randomized trials with a larger sample size will be conducted to compare and combine electroacupuncture stimulation with a more established modality, such as EEG-biofeedback. Interestingly, these further trials will clarify the role of applied acustimulation on self-regulation, cognitive function, and cortical activation.

Acknowledgments

This research was supported by Grants from School of Medicine, Chang Gung University and the Department of Physical Medicine and Rehabilitation, Chang Gung Memorial Hospital, Taiwan (CMRPG350811, CMRPG350812).

Conflict of Interest

The authors have no conflict of interest.

References

- Han JS. Acupuncture and endorphins. *Neurosci Lett* 2004;**361**:258–261.
- He D, Veiersted KB, Hostmark AT, Medbo JI. Effect of acupuncture treatment on chronic neck and shoulder pain in sedentary female workers: A 6-month and 3-year follow-up study. *Pain* 2004;**109**:299–307.
- Huang C, Wang Y, Han JS, Wan Y. Characteristics of electroacupuncture-induced analgesia in mice: Variation with strain, frequency, intensity and opioid involvement. *Brain Res* 2002;**945**:20–25.
- Wong AM, Su TY, Tang FT, Cheng PT, Liaw MY. Clinical trial of electrical acupuncture on hemiplegic stroke patients. *Am J Phys Med Rehabil* 1999;**78**:117–122.
- Berman BM. Seminal studies in acupuncture research. *J Altern Complement Med* 2001;**7**(Suppl):S129–S137.
- Bonnerman R. Acupuncture: The World Health Organization view. *World Health* 1979;**31**:24–29.
- Kapchuk TJ. Acupuncture: Theory, efficacy, and practice. *Ann Intern Med* 2002;**136**:374–383.
- Biella G, Sotgiu ML, Pellegata G, Paulesu E, Castiglioni I, Fazio F. Acupuncture produces central activations in pain regions. *Neuroimage* 2001;**14**(1 Pt 1):60–66.
- Uchida Y, Nishigori A, Takeda D, et al. Electroacupuncture induces the expression of Fos in rat dorsal horn via capsaicin-insensitive afferents. *Brain Res* 2003;**978**:136–140.
- Dhond RP, Kettner N, Napadow V. Neuroimaging acupuncture effects in the human brain. *J Altern Complement Med* 2007;**13**:603–616.
- Dhond RP, Yeh C, Park K, Kettner N, Napadow V. Acupuncture modulates resting state connectivity in default and sensorimotor brain networks. *Pain* 2008;**136**:407–418.
- Chen AC, Liu FJ, Wang L, Arendt-Nielsen L. Mode and site of acupuncture modulation in the human brain: 3D (124-ch) EEG power spectrum mapping and source imaging. *Neuroimage* 2006;**29**:1080–1091.
- Han JS. Acupuncture: Neuropeptide release produced by electrical stimulation of different frequencies. *Trends Neurosci.* 2003;**26**:17–22.
- Wang JQ, Mao L, Han JS. Comparison of the antinociceptive effects induced by electroacupuncture and transcutaneous electrical nerve stimulation in the rat. *Int J Neurosci* 1992;**65**:117–129.
- Mayer DJ, Price DD, Rafii A. Antagonism of acupuncture analgesia in man by the narcotic antagonist naloxone. *Brain Res* 1977;**121**:368–372.
- Cheng RS, Pomeranz B. Electroacupuncture analgesia could be mediated by at least two pain-relieving mechanisms: Endorphin and non-endorphin systems. *Life Sci* 1979;**25**:1957–1962.
- Shen J. Research on the neurophysiological mechanisms of acupuncture: Review of selected studies and methodological issues. *J Altern Complement Med* 2001;**7**(Suppl):S121–S127.
- Ulett GA, Han S, Han JS. Electroacupuncture: Mechanisms and clinical application. *Biol Psychiatry* 1998;**44**:129–138.

19. Cabyoglu MT, Ergene N, Tan U. The mechanism of acupuncture and clinical applications. *Int J Neurosci*. 2006;**116**:115–125.
20. Ulett GA. Conditioned healing with electroacupuncture. *Altern Ther Health Med* 1996;**2**:56–60.
21. Cohen JD, Servan-Schreiber D. A theory of dopamine function and its role in cognitive deficits in schizophrenia. *Schizophr Bull* 1993;**19**:85–104.
22. Friedman JI, Adler DN, Howanitz E, et al. A double blind placebo controlled trial of donepezil adjunctive treatment to risperidone for the cognitive impairment of schizophrenia. *Biol Psychiatry* 2002;**51**:349–357.
23. Pietras CJ, Cherek DR, Lane SD, Theremissine OV, Steinberg JL. Effects of methylphenidate on impulsive choice in adult humans. *Psychopharmacology (Berl)* 2003;**170**:390–398.
24. Foldi NS, White RE, Schaefer LA. Detecting effects of donepezil on visual selective attention using signal detection parameters in Alzheimer's disease. *Int J Geriatr Psychiatry* 2005;**20**:485–488.
25. Keefe RS, Sweeney JA, Gu H, et al. Effects of olanzapine, quetiapine, and risperidone on neurocognitive function in early psychosis: A randomized, double-blind 52-week comparison. *Am J Psychiatry* 2007;**164**:1061–1071.
26. Kopelman MD, Corn TH. Cholinergic 'blockade' as a model for cholinergic depletion. A comparison of the memory deficits with those of Alzheimer-type dementia and the alcoholic Korsakoff syndrome. *Brain* 1988;**111**(Pt 5):1079–1110.
27. Walderhaug E, Lunde H, Nordvik JE, Landro NI, Refsum H, Magnusson A. Lowering of serotonin by rapid tryptophan depletion increases impulsiveness in normal individuals. *Psychopharmacology (Berl)* 2002;**164**:385–391.
28. Aston-Jones G, Cohen JD. Adaptive gain and the role of the locus coeruleus-norepinephrine system in optimal performance. *J Comp Neurol* 2005;**493**:99–110.
29. Paolo AM, Troster AI, Ryan JJ. Continuous Visual Memory Test performance in healthy persons 60 to 94 years of age. *Arch Clin Neuropsychol* 1998;**13**:333–337.
30. Daselaar SM, Fleck MS, Dobbins IG, Madden DJ, Cabeza R. Effects of healthy aging on hippocampal and rhinal memory functions: An event-related fMRI study. *Cereb Cortex* 2006;**16**:1771–1782.
31. Wu JC, Gillin JC, Buchsbaum MS, et al. Sleep deprivation PET correlations of Hamilton symptom improvement ratings with changes in relative glucose metabolism in patients with depression. *J Affect Disord* 2008;**107**:181–186.
32. Morris MK, Bowers D, Chatterjee A, Heilman KM. Amnesia following a discrete basal forebrain lesion. *Brain* 1992;**115**(Pt 6):1827–1847.
33. Shuren JE, Jacobs DH, Heilman KM. Diencephalic temporal order amnesia. *J Neurol Neurosurg Psychiatry* 1997;**62**:163–168.
34. Dysken MW, Katz R, Stallone F, Kuskowski M. Oxiracetam in the treatment of multi-infarct dementia and primary degenerative dementia. *J Neuropsychiatry Clin Neurosci* 1989;**1**:249–252.
35. Gale SD, Baxter L, Roundy N, Johnson SC. Traumatic brain injury and grey matter concentration: A preliminary voxel based morphometry study. *J Neurol Neurosurg Psychiatry* 2005;**76**:984–988.
36. Goethe KE, Mitchell JE, Marshall DW, et al. Neuropsychological and neurological function of human immunodeficiency virus seropositive asymptomatic individuals. *Arch Neurol* 1989;**46**:129–133.
37. Lubar JF, Swartwood MO, Swartwood JN, O'Donnell PH. Evaluation of the effectiveness of EEG neurofeedback training for ADHD in a clinical setting as measured by changes in T.O.V.A. scores, behavioral ratings, and WISC-R performance. *Biofeedback Self Regul* 1995;**20**:83–99.
38. Oades RD. Differential measures of 'sustained attention' in children with attention-deficit/hyperactivity or tic disorders: Relations to monoamine metabolism. *Psychiatry Res* 2000;**93**:165–178.
39. Arns M, de Ridder S, Strehl U, Breteler M, Coenen A. Efficacy of neurofeedback treatment in ADHD: The effects on inattention, impulsivity and hyperactivity: A meta-analysis. *Clin EEG Neurosci* 2009;**40**:180–189.
40. Mataix-Cols D, Junque C, Vallejo J, Sanchez-Turet M, Verger K, Barrios M. Hemispheric functional imbalance in a sub-clinical obsessive-compulsive sample assessed by the Continuous Performance Test. Identical Pairs version. *Psychiatry Res* 1997;**72**:115–126.
41. de Geus F, Denys D, Westenberg HG. Effects of quetiapine on cognitive functioning in obsessive-compulsive disorder. *Int Clin Psychopharmacol* 2007;**22**:77–84.
42. King DA, Cox C, Lyness JM, Caine ED. Neuropsychological effects of depression and age in an elderly sample: A confirmatory study. *Neuropsychology* 1995;**9**:399–408.
43. Lockwood KA, Alexopoulos GS, van Gorp WG. Executive dysfunction in geriatric depression. *Am J Psychiatry* 2002;**159**:1119–1126.
44. Schrijvers D, de Bruijn ER, Maas Y, De Grave C, Sabbe BG, Hulstijn W. Action monitoring in major depressive disorder with psychomotor retardation. *Cortex* 2008;**44**:569–579.
45. Litz BT, Weathers FW, Monaco V, et al. Attention, arousal, and memory in posttraumatic stress disorder. *J Trauma Stress* 1996;**9**:497–519.
46. Wohlberg GW, Kornetsky C. Sustained attention in remitted schizophrenics. *Arch Gen Psychiatry* 1973;**28**:533–537.
47. Gruzelier JH, Venables PH. Two-flash threshold, sensitivity and beta in normal subjects and schizophrenics. *Q J Exp Psychol* 1974;**26**:594–604.
48. Nuechterlein KH. Signal detection in vigilance tasks and behavioral attributes among offspring of schizophrenic mothers and among hyperactive children. *J Abnorm Psychol* 1983;**92**:4–28.
49. Cornblatt B, Obuchowski M, Schnur DB, O'Brien JD. Attention and clinical symptoms in schizophrenia. *Psychiatr Q* 1997;**68**:343–359.
50. Malla AK, Norman RM, Takhar J, et al. Can patients at risk for persistent negative symptoms be identified during their first episode of psychosis? *J Nerv Ment Dis* 2004;**192**:455–463.
51. Snitz BE, Macdonald AW, 3rd, Carter CS. Cognitive deficits in unaffected first-degree relatives of schizophrenia patients: A meta-analytic review of putative endophenotypes. *Schizophr Bull* 2006;**32**:179–194.
52. Umbricht DS, Bates JA, Lieberman JA, Kane JM, Javitt DC. Electrophysiological indices of automatic and controlled auditory information processing in first-episode, recent-onset and chronic schizophrenia. *Biol Psychiatry* 2006;**59**:762–772.
53. Green DM, Swets JA. *Signal detection theory and psychophysics*. London: J. Wiley, 1966.
54. Gruzelier JH, Corballis MC. Effects of instructions and drug administration on temporal resolution of paired flashes. *Q J Exp Psychol* 1970;**22**:115–124.
55. Nuechterlein KH. Vigilance in schizophrenia and related disorders. In: Steinhauer S, Zubin J, Gruzelier JH, editors. *Handbook of schizophrenia: Neuropsychology, psychophysiology and information processing*, vol. 5. Amsterdam: Elsevier Science Publishers, 1991.
56. Tong KC, Lo SK, Cheing GL. Alternating frequencies of transcutaneous electric nerve stimulation: Does it produce greater analgesic effects on mechanical and thermal pain thresholds? *Arch Phys Med Rehabil* 2007;**88**:1344–1349.
57. Chao AS, Chao A, Wang TH, et al. Pain relief by applying transcutaneous electrical nerve stimulation (TENS) on acupuncture points during the first stage of labor: A randomized double-blind placebo-controlled trial. *Pain* 2007;**127**:214–220.
58. Hsieh JC, Tu CH, Chen FP, et al. Activation of the hypothalamus characterizes the acupuncture stimulation at the analgesic point in human: A positron emission tomography study. *Neurosci Lett* 2001;**307**:105–108.
59. Itoh K, Katsumi Y, Hirota S, Kitakoji H. Effects of trigger point acupuncture on chronic low back pain in elderly patients: A sham-controlled randomised trial. *Acupunct Med* 2006;**24**:5–12.
60. Lund J, Lundeberg T. Are minimal, superficial or sham acupuncture procedures acceptable as inert placebo controls? *Acupunct Med* 2006;**24**:13–15.
61. Shen J, Wenger N, Gaspy J, et al. Electroacupuncture for control of myeloablative chemotherapy-induced emesis: A randomized controlled trial. *JAMA* 2000;**284**:2755–2761.
62. White P, Lewith G, Prescott P, Conway J. Acupuncture versus placebo for the treatment of chronic mechanical neck pain: A randomized, controlled trial. *Ann Intern Med* 2004;**141**:911–919.
63. Wu MT, Sheen JM, Chuang KH, et al. Neuronal specificity of acupuncture response: A fMRI study with electroacupuncture. *Neuroimage* 2002;**16**:1028–1037.
64. Zhang WT, Jin Z, Cui GH, et al. Relations between brain network activation and analgesic effect induced by low vs. high frequency electrical acupoint stimulation in different subjects: A functional magnetic resonance imaging study. *Brain Res* 2003;**982**:168–178.
65. Kropotov JD. *Quantitative EEG, event related potentials and neurotherapy*. San Diego: Academic Press, Elsevier, 2009.
66. Jung TP, Makeig S, Humphries C, et al. Removing electroencephalographic artifacts by blind source separation. *Psychophysiology* 2000;**37**:163–178.
67. Jung TP, Makeig S, Westfield M, Townsend J, Courchesne E, Sejnowski TJ. Removal of eye activity artifacts from visual event-related potentials in normal and clinical subjects. *Clin Neurophysiol* 2000;**111**:1745–1758.
68. Makeig S, Jung TP, Bell AJ, Ghahremani D, Sejnowski TJ. Blind separation of auditory event-related brain responses into independent components. *Proc Natl Acad Sci U S A* 1997;**94**:10979–10984.
69. Pascual-Marqui RD. Standardized low-resolution brain electromagnetic tomography (SLORETA): Technical details. *Methods Find Exp Clin Pharmacol* 2002;**24**(Suppl D):5–12.
70. McNicol D. *A primer of signal detection theory*. London: Allen & Unwin, 1972.
71. Egner T, Gruzelier JH. Learned self-regulation of EEG frequency components affects attention and event-related brain potentials in humans. *Neuroreport* 2001;**12**:4155–4159.
72. Egner T, Gruzelier JH. EEG biofeedback of low beta band components: Frequency-specific effects on variables of attention and event-related brain potentials. *Clin Neurophysiol* 2004;**115**:131–139.
73. Bekker EM, Kenemans JL, Verbaten MN. Source analysis of the N2 in a cued Go/NoGo task. *Brain Res Cogn Brain Res* 2005;**22**:221–231.
74. Bokura H, Yamaguchi S, Kobayashi S. Electrophysiological correlates for response inhibition in a Go/NoGo task. *Clin Neurophysiol* 2001;**112**:2224–2232.
75. Smith JL, Johnstone SJ, Barry RJ. Movement-related potentials in the Go/NoGo task: The P3 reflects both cognitive and motor inhibition. *Clin Neurophysiol* 2008;**119**:704–714.
76. Olofsson JK, Polich J. Affective visual event-related potentials: Arousal, repetition, and time-on-task. *Biol Psychol* 2007;**75**:101–108.
77. Polich J. Frequency, intensity, and duration as determinants of P300 from auditory stimuli. *J Clin Neurophysiol* 1989;**6**:277–286.
78. Ravden D, Polich J. Habituation of P300 from visual stimuli. *Int J Psychophysiol* 1998;**30**:359–365.
79. Gonsalvez CL, Polich J. P300 amplitude is determined by target-to-target interval. *Psychophysiology* 2002;**39**:388–396.
80. Kato Y, Endo H, Kizuka T. Mental fatigue and impaired response processes: Event-related brain potentials in a Go/NoGo task. *Int J Psychophysiol* 2009;**72**:204–211.
81. Protzner AB, Cortese F, Alain C, McIntosh AR. The temporal interaction of modality specific and process specific neural networks supporting simple working memory tasks. *Neuropsychologia* 2009;**47**:1954–1963.

82. Kaufman JN, Ross TJ, Stein EA, Garavan H. Cingulate hypoactivity in cocaine users during a GO-NOGO task as revealed by event-related functional magnetic resonance imaging. *J Neurosci* 2003;**23**:7839–7843.
83. Muller NG, Knight RT. The functional neuroanatomy of working memory: Contributions of human brain lesion studies. *Neuroscience* 2006;**139**:51–58.
84. Polich J. Updating P300: An integrative theory of P3a and P3b. *Clin Neurophysiol* 2007;**118**:2128–2148.
85. Polich J, McIsaac HK. Comparison of auditory P300 habituation from active and passive conditions. *Int J Psychophysiol* 1994;**17**:25–34.
86. Litscher G. Effects of acupressure, manual acupuncture and Laserneedle acupuncture on EEG bispectral index and spectral edge frequency in healthy volunteers. *Eur J Anaesthesiol* 2004;**21**:13–19.
87. Tanaka Y, Koyama Y, Jodo E, et al. Effects of acupuncture to the sacral segment on the bladder activity and electroencephalogram. *Psychiatry Clin Neurosci* 2002;**56**:249–250.
88. Rosted P, Griffiths PA, Bacon P, Gravill N. Is there an effect of acupuncture on the resting EEG? *Complement Ther Med* 2001;**9**:77–81.
89. Pilloni C, Caracausi RS, Tognali F, Sbarbaro V. EEG evaluation of patients undergoing extracorporeal circulation under analgesic and electrohypoalgesia with auricular acupuncture. *Minerva Anestesiol* 1980;**46**:371–386.
90. Gruzeliier J, Egner T, Vernon D. Validating the efficacy of neurofeedback for optimising performance. *Prog Brain Res* 2006;**159**:421–431.
91. Lloyd MA, Appel JB. Signal detection theory and the psychophysics of pain: An introduction and review. *Psychosom Med* 1976;**38**:79–94.
92. Codispoti M, Ferrari V, Bradley MM. Repetitive picture processing: Autonomic and cortical correlates. *Brain Res* 2006;**1068**:213–220.
93. Li L, Yao D, Yin G. Spatio-temporal dynamics of visual selective attention identified by a common spatial pattern decomposition method. *Brain Res* 2009;**1282**:84–94.
94. Streitberger K, Ezzo J, Schneider A. Acupuncture for nausea and vomiting: An update of clinical and experimental studies. *Auton Neurosci* 2006;**129**:107–117.
95. Lu GW. Characteristics of afferent fiber innervation on acupuncture points zusanli. *Am J Physiol* 1983;**245**:R606–R612.
96. Somers DL, Clemente FR. Contralateral high or a combination of high- and low-frequency transcutaneous electrical nerve stimulation reduces mechanical allodynia and alters dorsal horn neurotransmitter content in neuropathic rats. *J Pain* 2009;**10**:221–229.
97. Napadow V, Makris N, Liu J, Kettner NW, Kwong KK, Hui KK. Effects of electroacupuncture versus manual acupuncture on the human brain as measured by fMRI. *Hum Brain Mapp* 2005;**24**:193–205.
98. Lee JD, Chon JS, Jeong HK, et al. The cerebrovascular response to traditional acupuncture after stroke. *Neuroradiology* 2003;**45**:780–784.
99. Zhang WT, Jin Z, Luo F, Zhang L, Zeng YW, Han JS. Evidence from brain imaging with fMRI supporting functional specificity of acupoints in humans. *Neurosci Lett* 2004;**354**:50–53.
100. Cho ZH, Hwang SC, Wong EK, et al. Neural substrates, experimental evidences and functional hypothesis of acupuncture mechanisms. *Acta Neurol Scand* 2006;**113**:370–377.
101. Zeng Y, Liang XC, Dai JP, et al. Electroacupuncture modulates cortical activities evoked by noxious somatosensory stimulations in human. *Brain Res* 2006;**1097**:90–100.
102. Claydon LS, Chesterton LS, Barlas P, Sim J. Effects of simultaneous dual-site TENS stimulation on experimental pain. *Eur J Pain* 2008;**12**:696–704.
103. Chesterton LS, Barlas P, Foster NE, Lundeberg T, Wright CC, Baxter GD. Sensory stimulation (TENS): Effects of parameter manipulation on mechanical pain thresholds in healthy human subjects. *Pain* 2002;**99**:253–262.
104. Imai K, Ariga H, Chen C, Mantyh C, Pappas TN, Takahashi T. Effects of electroacupuncture on gastric motility and heart rate variability in conscious rats. *Auton Neurosci* 2008;**138**:91–98.
105. van Dijk KR, Scherder EJ, Scheltens P, Sergeant JA. Effects of transcutaneous electrical nerve stimulation (TENS) on non-pain related cognitive and behavioural functioning. *Rev Neurosci* 2002;**13**:257–270.
106. Thompson JW, Cummings M. Investigating the safety of electroacupuncture with a Picoscope. *Acupunct Med* 2008;**26**:133–139.
107. McNab F, Varrone A, Farde L, et al. Changes in cortical dopamine D1 receptor binding associated with cognitive training. *Science* 2009;**323**:800–802.
108. Muller U, Carew TJ. Serotonin induces temporally and mechanistically distinct phases of persistent PKA activity in Aplysia sensory neurons. *Neuron* 1998;**21**:1423–1434.
109. Boulougouris V, Tsaltas E. Serotonergic and dopaminergic modulation of attentional processes. *Prog Brain Res* 2008;**172**:517–542.
110. Jonsdottir S, Bouma A, Sergeant JA, Scherder EJ. Effects of transcutaneous electrical nerve stimulation (TENS) on cognition, behavior, and the rest-activity rhythm in children with attention deficit hyperactivity disorder, combined type. *Neurorehabil Neural Repair* 2004;**18**:212–221.
111. Scherder EJ, Van Someren EJ, Bouma A, v d Berg M. Effects of transcutaneous electrical nerve stimulation (TENS) on cognition and behaviour in aging. *Behav Brain Res* 2000;**111**:223–225.
112. Gruzeliier J. A theory of alpha/theta neurofeedback, creative performance enhancement, long distance functional connectivity and psychological integration. *Cogn Process* 2009;**10**(Suppl):S101–S109.
113. Hirshberg LM, Chiu S, Frazier JA. Emerging brain-based interventions for children and adolescents: Overview and clinical perspective. *Child Adolesc Psychiatr Clin N Am* 2005;**14**:1–19, v.
114. Ros T, Munneke MA, Ruge D, Gruzeliier JH, Rothwell JC. Endogenous control of waking brain rhythms induces neuroplasticity in humans. *Eur J Neurosci* 2010;**31**:770–778.
115. Vernon D, Egner T, Cooper N, et al. The effect of training distinct neurofeedback protocols on aspects of cognitive performance. *Int J Psychophysiol* 2003;**47**:75–85.

Dynamic Changes of ICA-Derived EEG Functional Connectivity in the Resting State

Jean-Lon Chen,^{1,2*} Tomas Ros,^{1,3} and John H. Gruzelier¹

¹Department of Psychology, Goldsmiths, University of London, London, United Kingdom

²Department of Physical Medicine & Rehabilitation, Chang Gung Memorial Hospital and College of Medicine, Chang Gung University, Tao-Yuan, Taiwan

³Department of Psychiatry, University of Western Ontario, London, Ontario, Canada

Abstract: An emerging issue in neuroscience is how to identify baseline state(s) and accompanying networks termed “resting state networks” (RSNs). Although independent component analysis (ICA) in fMRI studies has elucidated synchronous spatiotemporal patterns during cognitive tasks, less is known about the changes in EEG functional connectivity between eyes closed (EC) and eyes open (EO) states, two traditionally used baseline indices. Here we investigated healthy subjects ($n = 27$) in EC and EO employing a four-step analytic approach to the EEG: (1) group ICA to extract independent components (ICs), (2) standardized low-resolution tomography analysis (sLORETA) for cortical source localization of IC network nodes, followed by (3) graph theory for functional connectivity estimation of epochwise IC band-power, and (4) circumscribing IC similarity measures via hierarchical cluster analysis and multidimensional scaling (MDS). Our proof-of-concept results on alpha-band power demonstrate five statistically clustered groups with frontal, central, parietal, occipitotemporal, and occipital sources. Importantly, during EO compared with EC, graph analyses revealed two salient functional networks with frontoparietal connectivity: a more medial network with nodes in the mPFC/precuneus which overlaps with the “default-mode network” (DMN), and a more lateralized network comprising the middle frontal gyrus and inferior parietal lobule, coinciding with the “dorsal attention network” (DAN). Furthermore, a separate MDS analysis of ICs supported the emergence of a pattern of increased proximity (shared information) between frontal and parietal clusters specifically for the EO state. We propose that the disclosed component groups and their source-derived EEG functional connectivity maps may be a valuable method for elucidating direct neuronal (electrophysiological) RSNs in healthy people and those suffering from brain disorders. *Hum Brain Mapp* 00:000–000, 2012. © 2012 Wiley Periodicals, Inc.

Key words: EEG; alpha rhythm; independent component analysis (ICA); resting-state network (RSN); functional connectivity; default mode network (DMN); dorsal attention network; multi-dimensional scaling (MDS); standardized low-resolution tomography analysis (sLORETA)

Contract grant sponsors: School of Medicine, Chang Gung University, Department of Physical Medicine and Rehabilitation, Chang Gung Memorial Hospital, Taiwan; Contract grant numbers: CMRPG350813, .CMRPG350814.

*Correspondence to: Jean-Lon Chen, Department of Psychology, Goldsmiths, University of London, New Cross, London SE14 6NW, UK. E-mail: bigmac1479@gmail.com

Received for publication 7 December 2010; Revised 4 September 2011; Accepted 5 September 2011

DOI: 10.1002/hbm.21475

Published online in Wiley Online Library (wileyonlinelibrary.com).

INTRODUCTION

The identification of a resting baseline state is an essential issue in neuroscience in order to interpret brain activation and to disentangle the mechanisms behind neuronal cooperative activity, which form the core of all cognitive, perceptive and motor-driven activities. Since its discovery by Hans Berger in the 1930s, electroencephalography (EEG) has been a reliable method for monitoring brain dynamics, witnessing an early focus on the electrophysiological changes from the eyes-closed (EC) to the eyes-open (EO) resting states. This transition has traditionally been characterized by a suppression of occipital alpha activity via visual stimulation in the EO state, classically termed “alpha blocking” [Pollen and Trachtenberg, 1972], or more recently “alpha desynchronization” [Klimesch et al., 2000; Neuper and Pfurtscheller, 1992]. Both EC and EO resting conditions, either alone or in combination, have commonly served as a standard baseline estimate in cognitive tasks as well as resting (or “spontaneous”) conditions.

Modern advances in neuroimaging technology have provided new insights about the spontaneous activity of the resting awake brain. With the use of blood oxygen level-dependent (BOLD) functional MRI (fMRI), several resting state networks (RSNs) and a default-mode network (DMN) have been discovered [Gusnard and Raichle, 2001; Gusnard et al., 2001; Raichle and Snyder, 2007; Raichle et al., 2001]. RSNs comprise clusters of brain regions involving mainly cortical interconnection across widely distributed brain areas [Honey et al., 2009], reflecting intrinsic functional cross-talk. The DMN is one of the RSNs described as a task-negative network given that it is most active during “task-free” conditions [Biswal et al., 1995; Broyd et al., 2009; De Luca et al., 2006; Fransson, 2006; Lowe et al., 1998; Mantini et al., 2007]. These fMRI investigations are supported by studies with Positron Emission Tomography (PET) comparing tasks against resting conditions with eyes closed [Fox et al., 2005; Fransson, 2006].

Recently however, the study of RSNs has shifted its focus from the localization of specialized brain activations to the interpretation of interrelationships in brain dynamics. In parallel, a host of EEG rhythms have been documented in the network operations of corticothalamic systems [Steriade, 2006], where several rhythms have been found to coexist in the same area or interact among different structures [Steriade, 2001]. These discoveries have led to the suggestion that the EEG could be combined with fMRI to study baseline functions and oscillations within a more dynamic architecture of the human brain [Gusnard et al., 2001; Laufs, 2008; Mantini et al., 2007], by spatiotemporally decomposing the complex dynamics associated with multiple EEG frequencies simultaneously [Laufs et al., 2003a; Mantini et al., 2007].

The main advantage of EC and EO conditions is that they may be carried out without requiring subjects to perform a specific task, and therefore be easily deployed in EEG clinical settings. Barry et al. examined the possible

arousal and topography differences during the transition from EC to EO conditions in adults [Barry et al., 2007] and children [Barry et al., 2009]. These were associated with significant reductions in mean activity in the delta, theta, and alpha bands whilst accompanied by increased beta activity in frontal hemispheric regions. Others such as Chen et al. [2008] have used scalp EEG spectral regional field power to study the distribution of RSN activity at rest. The possibility still exists that the frequent disparities between EEG and fMRI studies may be due to the well-known inadequacy of conventional scalp recordings to resolve EEG source locations, for scalp voltage is a mixture of underlying source activity and volume conduction [Congedo et al., 2008; Nunez, 1987; Nunez et al., 1997; Winter et al., 2007].

As a potential solution, an approach termed Blind Source Separation (BSS) has been developed, originating from the engineering field of signal processing [Bell and Sejnowski, 1995; Comon, 1994; Hyvarinen, 2000]. Independent component analysis (ICA) is a special case of BSS methods that has been applied to EEG and fMRI data [Calhoun et al., 2001, 2004; Makeig, 1996; Makeig et al., 2002] as a tool to remove artifacts [e.g. Jung et al., 2000] and to separate physiological sources [e.g. Makeig et al., 2004]. One of the advantages of ICA is that individual-subject EEG epochs (or fMRI voxels) can be concatenated across subjects along the time axis to apply the ICA algorithm to group data [e.g. Calhoun et al., 2001, 2004].

Therefore, we propose here to utilize group-ICA as a valid approach to decompose resting EEG signals into a number of independent components (ICs). Then, using an inverse localization tool such as sLORETA, the cortical location of these ICs may be resolved into spatially well-defined nodes or “sources” [Pascual-Marqui et al. 2002]. Finally, through estimation of the cross-correlation of spectral power between different ICs within subjects, a functional relationship between such EEG source “nodes” can be established, analogous to approaches that have been adopted to calculate functional connectivity from BOLD signal strength in fMRI data [e.g. Buckner et al. 2009].

In summary, our results on dynamic changes in alpha-band connectivity between EC and EO demonstrate the feasibility of studying neuronal resting-state networks according to the existence of functional relationships between ICA components in EEG data. We also replicate the previously reported spectral power changes in alpha band power from the EC to the EO state.

MATERIALS AND METHODS

Participants

Participants were 27 healthy volunteers from Goldsmiths, University of London (20 females and 7 males) with ages ranging from 18 to 30 years, mean = 22.5. All subjects had normal hearing and normal or corrected-to-normal vision and were not receiving psychoactive medication. Subjects were excluded if they had any history of epilepsy, drug

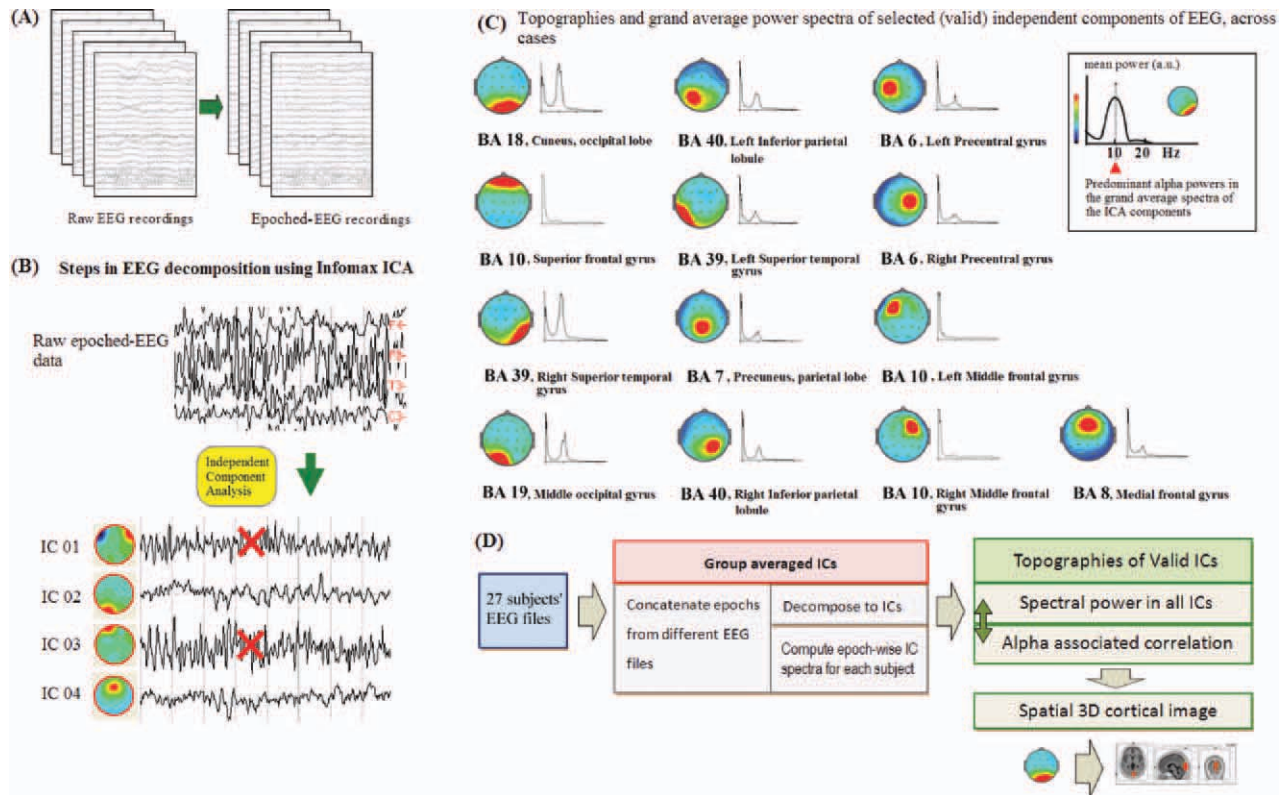


Figure 1.

Schematic representation of the different pipeline steps from (A) raw EEG to epoched-EEG recordings, from a single subject's EEG, (B) EEG concatenation and decomposition using Infomax ICA and artefact rejection, which excludes large amplitudes from muscular activity and eye-blinking, (C) the construction of mean power spectra of each valid independent component (IC)

and its topography. (D) General schema of deriving the alpha power correlation matrices from back-reconstructed Fourier spectra of all ICs to estimate functional connectivity in both EC and EO states. Then, three-dimensional cortical images are presented for visualizing related ICs within the cortical source-level map.

abuse, or head injury. They were recruited by advertisement and signed an informed consent form before the start of the experiment in accordance with the Helsinki Declaration. The current investigation received ethical approval from the College Research Ethics Committee.

Experimental Design

Each subject was asked to sit in an armchair in a quiet room with stable temperature and shaded daylight. The experiment began with a 3-min EC condition, followed by 3 min with EO. Each subject was given instructions to stay fully relaxed without eye movements to avoid motion artifacts in the eyes-closed condition. During the EO condition, participants were instructed to visually fixate on a small cross presented on a table below eye level in front of them, in order to reduce blinking and lateral eye movement artifacts.

Independent Component (ICA) and Spectral Power Analysis

The general scheme of this approach is illustrated in Figure 1. Artifact-free EEG epochs from all subjects in the EC and EO conditions were concatenated into one file, which was then decomposed into independent sources by the group ICA procedure [Jung, 2001; Makeig, 1996] using WinEEG 2.83 software (Mitsar, Ltd.; available at: <http://www.mitsar-medical.com>), which uses the Infomax ICA algorithm [Bell and Sejnowski, 1995]. Here, a temporal concatenation approach allows for unique time-courses for each subject, but assumes common group maps across conditions [Calhoun et al., 2001]. Theoretically, ICA is able to separate N source components from N channels of EEG signals in each subject. This is represented by the rows of an inverse unmixing matrix, W in $u = Wx$, where u is the source matrix and x is the scalp-recorded EEG. The time-courses of the sources are assumed to be statistically independent. Then, for each subject, epochwise spectral power of the back-reconstructed ICs was computed by short-time

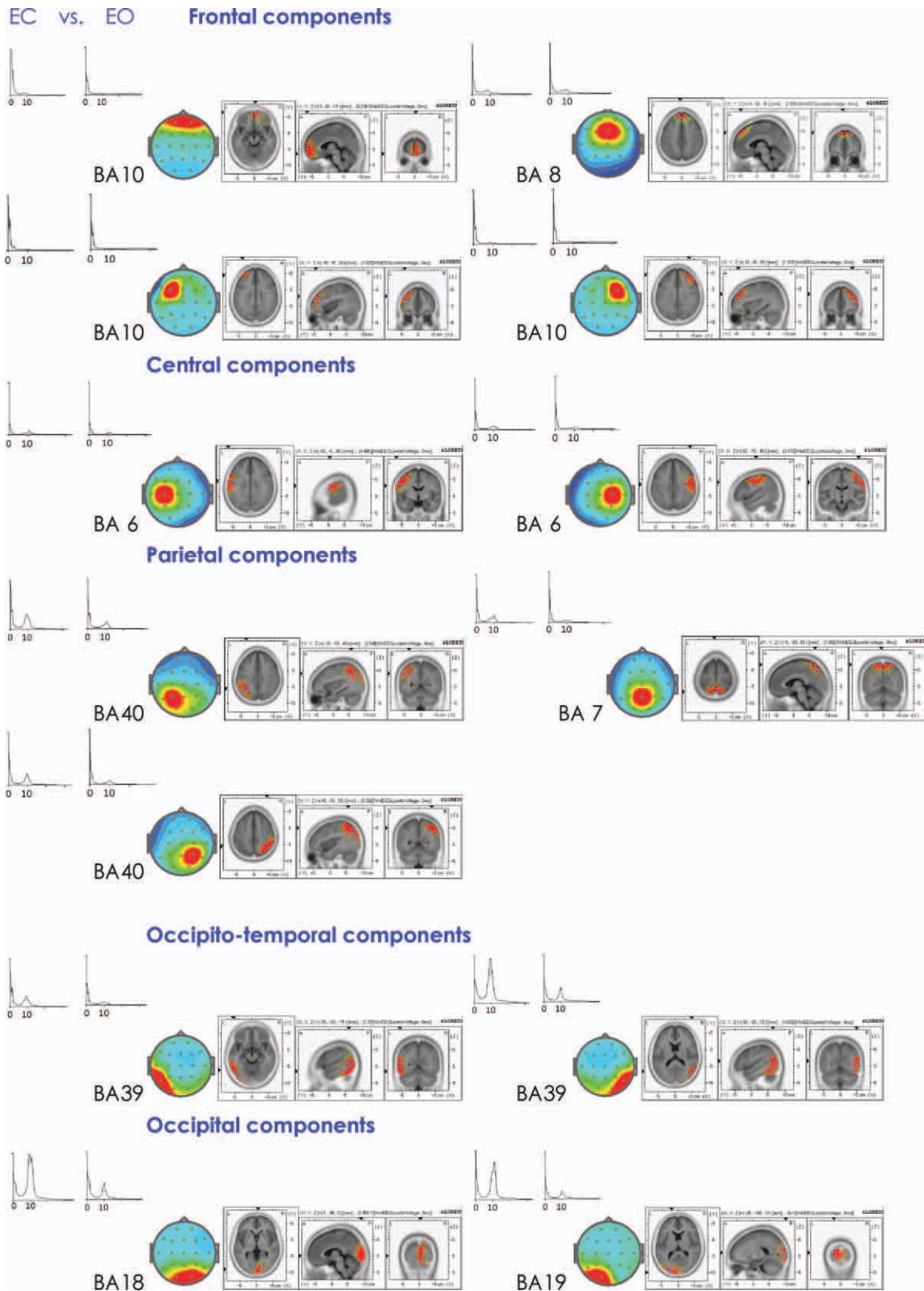


Figure 2.

Fourier Transform (STFT) across the EO and EC conditions (4-s epochs with a 50% overlapping Hanning time window). As may be seen in Figure 1C, the predominant frequency of ICs is alpha (8–12 Hz) in almost 70% or 9 ICs/13 ICs. Subsequently, for each resting condition and within each subject, we specifically cross-correlated the alpha-band (8–12 Hz) epochwise powers between all 13 ICs, yielding a square 13×13 connectivity matrix. Individual connectivity matrix r^2 values were then averaged across subjects to give a group-wise matrix for each resting condition. Through this time-frequency analysis we were able to show that several grouped components exhibit strong coupling with alpha-frequency dynamics in the resting state.

EEG Recording and Preprocessing of EEG

Scalp voltages were recorded using a 19 Ag/AgCl electrode cap according to the 10 to 20 international system: Fp1, Fp2, F7, F3, Fz, F4, F8, T3, C3, Cz, C4, T4, T5, P3, Pz, P4, T6, O1, O2 (Electro-cap International, Inc.; available at: <http://www.electro-cap.com>). The ground electrode was placed on the scalp, at a site equidistant between Fpz and Fz. Electrodes were referenced to linked earlobes, and then the common average reference was calculated offline before further analysis. Electro-oculogram (EOG) data were recorded from electrodes (Fp1/2) placed to monitor eye movements and eye blinking. Electrical signals were amplified with the Mitsar 21-channel EEG system (Mitsar-201, CE0537, Mitsar, Ltd.; available at: <http://www.mitsar-medical.com>) and electrode impedance was kept under 5 K Ω . The EEG was recorded continuously, digitized at a sampling rate of 250 Hz, and stored on hard disk for offline analyses. EEG data were filtered with a 0.5 to 60 Hz bandpass filter offline [e.g. Mantini et al., 2007]. Artifact rejection methods consisted of the exclusion of epochs with large amplitudes (over $\pm 80 \mu\text{V}$), eye-blinking, DC bias, physiologically unresolvable noise [Onton et al., 2006], muscular activity of frontal muscles defined by fast activity over 20 Hz [Shackman et al., 2009], and slow eye movements coincident with the EOG [c.f. Viola et al., 2009]. Moreover, it has been shown that ICA itself is capable of reliably separating blinking, such as blinking and lateral eye movement [e.g. Jung et al., 2000]. In general, each 3 minute resting-state period of EEG was analyzed in 4-s epochs (50% overlapping with Hanning time window), resulting in 89 epochs. On average around 60 to 70 valid epochs without artifacts from each of the 27 subjects were analyzed.

ICA decomposition yielded a total of 19 ICs, from which epochwise spectral power analysis was applied to 13 physiologically-relevant ICs (recognised as non-artifactual and with high single-dipole fit) to examine the dynamics of EEG-alpha power from the EC to EO state. This evaluation allowed a more direct comparison of the present results with previous literature [for a review see Klimesch, 1999].

Source Localization Analysis

sLORETA (standardized low-resolution brain electromagnetic tomography) analysis was performed on scalp maps of selected ICA components to find the maximal densities of their cortical sources [Pascual-Marqui et al., 2002]. sLORETA imaging provided source computations for the ICs using software provided from the Key Institute for Brain-Mind Research in Zurich, Switzerland (available at: <http://www.uzh.ch/keyinst/loreta.htm>). sLORETA is an inverse solution technique that estimates the distribution of the electrical neuronal activity in three-dimensional space. Specifically, sLORETA computes three-dimensional linear solutions for the EEG inverse problem within a head model co-registered to the Talairach probability brain atlas [Talairach, 1988] and viewed within MNI (Montreal Neurological Institute) 152 coordinates at 5 mm resolution. Valid ICA components were defined by their single dipole fitting having satisfactory relative residual energy below 10% [e.g. Grin-Yatsenko et al., 2010], meaning that over 90% of the component's power may be represented by a single dipole and indicating each was clearly generated by a strong locally circumscribed cortical source (Fig. 2).

Computation of Mean Regional Correlation Matrix and Graph Analysis

According to graph theory, and within any chosen frequency information exchange may be measured by the (nonrandom) cross-correlation coefficients in the band-power spectrum, reflecting functional connectivity. Graph theory defines a graph as a set of nodes (in this study, ICs) and edges (connections between nodes) [Bullmore and Sporns, 2009; Rubinov and Sporns, 2010]. Within each subject, ICs were cross-correlated region by region according to their alpha-power across epochs during the full length of two resting time series (more than 60 epochs in each), thus creating two square correlation matrices in the EC and EO states, respectively. The individual within-subject

Figure 2.

The topographies, power spectra, and source localization of 13 independent components (ICs) in the EO and EC states. For cortical localization of generators the sLORETA equivalent source current density (5 mm resolution) for each extracted IC was estimated using component topographies as input data

[Pascual-Marqui, 2002]. For each IC, its spectral power (left panel, EC vs. EO state, same scale for all ICs), scalp topography (middle panel), and three-dimensional spatial maps (right panel) are illustrated.

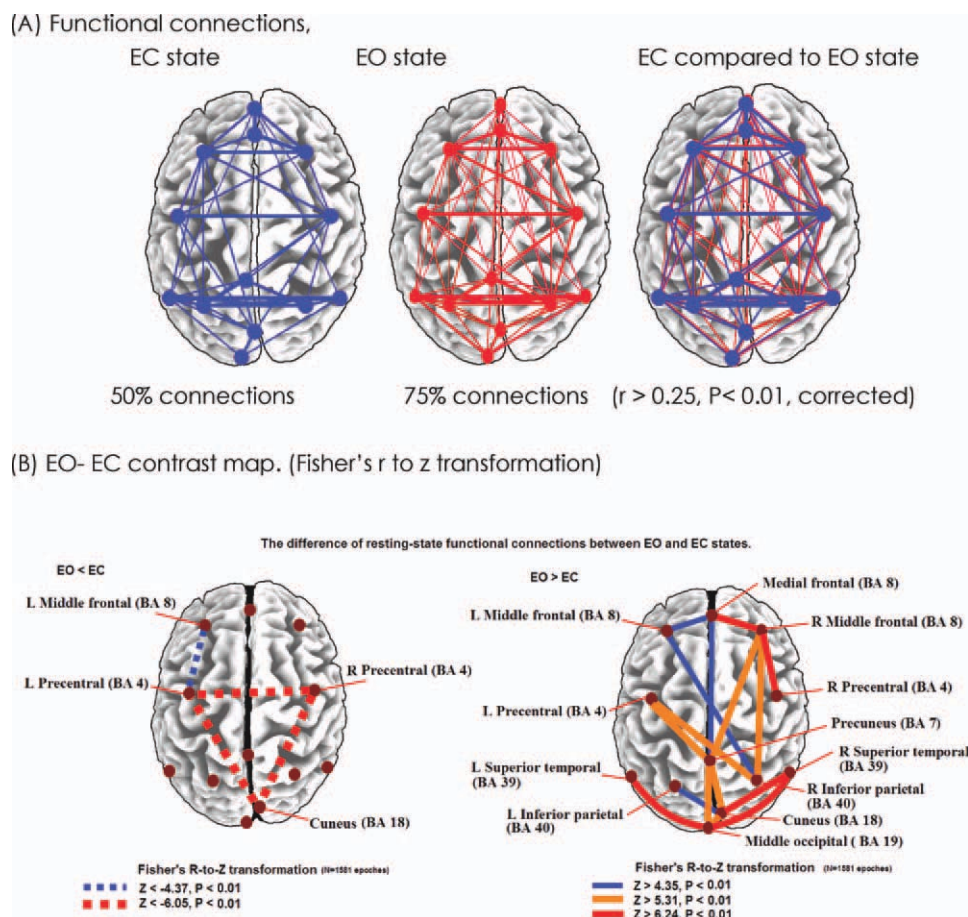


Figure 3.

Resting-state functional connections revealed by EEG-alpha power spectra, compared between EC and EO states. **(A)** Significantly enhanced connections of DAN between frontal and parietal regions (anterior to posterior) are demonstrated during the EO state, compared to the EC state. The significantly enhanced connections in the EO state (75%) are depicted, more than those connections in the EC state (50%). **(B)** Statistically significant connections of DMN, DAN, and visual networks are depicted by top 15%, 10%, 8% pairs of z scores, compared EO with EC state

(two-tailed t -tests, Bonferroni corrected). Visual networks are enhanced in the parietal, occipital, and occipitotemporal regions in the EO state. Increased connection strength between medial prefrontal cortex and precuneus regions, strong DMN in the EO state, is still noted in line with Yan et al. [2009]. The significantly decreased functional connectivity among left precentral, right precentral, and cuneus from EC to EO state ensures that the improvement of intrinsic networks' activity does not come from the general improved signal-to-noise ratio between states.

connectivity matrix r^2 values were then averaged across subjects to give a group-wise matrix for each resting state. We then performed one-sample t -tests (two-tailed) on the Fisher's r to Z -transformed (normally distributed) correlation coefficients to test whether they were significantly different from zero [Salvador et al., 2005]. To account for multiple comparisons, Bonferroni's correction was applied to eliminate false-positive errors ($P = 0.01/78 \text{ connections} = 0.000128$), and statistically significant results with P values < 0.000128 were accepted as significant. All graph analysis calculations were performed in Matlab 7.04 (Mathworks, MA). This allowed the computation of weighted undirected graphs (Fig. 3).

Clustering of ICA Components

The goal of IC clustering is in order to group together highly similar activity from multiple subjects in order to express their characteristic activities. Alpha desynchronisation upon visual input from EC to EO is generally considered to reflect activation of the entire cortex [Schurmann and Basar, 1999]. Therefore, in order to extend the ICA analysis from single to multicomponent dynamics, the estimated components were clustered according to mutual similarities in their EEG alpha-power correlation coefficients. A variety of frameworks has been used to summarize relevant components at the group level in fMRI

TABLE I. Coordinates of the main ICs of the circumscribed groups in the resting state, as shown in Fig. 2, the stereotactic space of Talairach and Tournoux [1988]

Group	<i>x</i>	<i>y</i>	<i>z</i>	Brodman area	Anatomical region
Group F	5	63	-7	BA10	Superior frontal gyrus
	-40	45	25	BA10	Middle frontal gyrus
	40	45	25	BA10	Middle frontal gyrus
	-5	51	39	BA8	Medial frontal gyrus
Group C	-59	-3	32	BA6	Precentral gyrus
	50	-8	37	BA6	Precentral gyrus
Group P	-40	-47	39	BA40	Inferior parietal lobule
	-5	-60	63	BA7	Precuneus, parietal lobe
	40	-51	49	BA40	Inferior parietal lobule
Group OT	54	-62	22	BA39	Superior temporal gyrus
	-54	-62	22	BA39	Superior temporal gyrus
Group O	5	-87	14	BA18	Cuneus, occipital lobe
	-20	-96	14	BA19	Middle occipital gyrus

Brain regions are identified by putative Brodmann area (BA). Group F, C, P, OT, O, and mean the circumscribed frontal, central, parietal, occipitotemporal, and occipital components.

studies [Esposito et al., 2005; Jann et al., 2009; Mantini et al., 2007]. In this study, in order to circumscribe the alpha power-associated components, agglomerative hierarchical cluster analysis was performed on the components' alpha power correlation coefficients with the statistical software package, SPSS (SPSS Inc, Chicago). Each component measure was normalized by Z-transformation prior to cluster analysis. Then, to assess mutual similarity, all pairs of components were compared by calculating the Pearson correlation of their alpha power, and classified into a hierarchical cluster tree according to their proximity (dendrogram). A dendrogram consists of mirrored C-shape lines, where the length of the mirrored C indicates the distance between objects (components). To calculate the distance between clusters, the Average Linkage method (Pearson correlation) was used. Here a "distance" matrix was calculated, namely the-Euclidean distances in the original space of the components using multidimensional scaling (MDS) in order to fit an optimal configuration of groups of components in a two-dimensional space by minimizing the mismatch of the distances between the components in the MDS plot [Esposito et al., 2005; Torgerson, 1952]. From these components five groups were qualitatively selected by the similarity matrix, the dendrogram, the MDS plot, and visual inspection, as anatomically relevant areas across subjects, potentially depicting functionally related groups in the EC and EO resting states.

RESULTS

Alpha-Band Power Cortical Sources (ICA)

As illustrated in Figure 1, Infomax ICA was applied to extract ICs from the concatenated EEG data of the 27 participants in both EC and EO states. The EEG data was decomposed into 13 spatially fixed and maximally-ICs. Only six artifact ICs were excluded (horizontal and vertical eye

movements $\times 2$, temporal muscle artifacts $\times 2$, and ICs with unspecific muscle artifacts $\times 2$). Our results in each resting state were calculated using more than 60 epochs in each condition for each subject. All components in EC/EO states (Fig. 2) exhibited a high repeatability across subjects with strong cortical source locations. Moreover, we suggest that the consistency in the cortical localization of components in healthy individuals in both EC and EO states is due to the absence of experimental stimuli [for review see Onton et al., 2006], although some unsuccessfully represented artifact components may always be caused by participant confounds such as drowsiness, muscle activity, or eye movements. The cortical location and Brodmann area number of source locations of each IC are illustrated in Figure 2. The Talairach coordinates are further listed in Table I.

Functional Connectivity (Graph Analysis)

In accordance with the traditional graph theoretical approach, the square correlation matrix was used, to create weighted undirected binary graph such that nodes (ICs) were either connected or not connected. The distribution of *r*-values suggested significantly enhanced connections in the EO state (75%) compared with those in the EC state (50%, in Fig. 3A). For the EO to EC state contrast (two-tailed *t*-tests, Bonferroni corrected) the top 8% of all possible connections, were defined by Fisher's $z > 6.24$, $P < 0.01$ [e.g. Dosenbach et al., 2007].

By lowering the graph definition threshold more potential connection patterns to other parts of the brain were revealed, indicating that the findings were robust to small changes in the graph-definition threshold. Hence for visualization purposes, we made the *z*-score threshold vary from the top 8% to 15% of all interregional correlations (top 15% of all possible compared connections, $z > 4.35$, $P < 0.01$). Figure 3A,B illustrate the top 15% *z*-score pairs for the functional connections between cortical nodes.

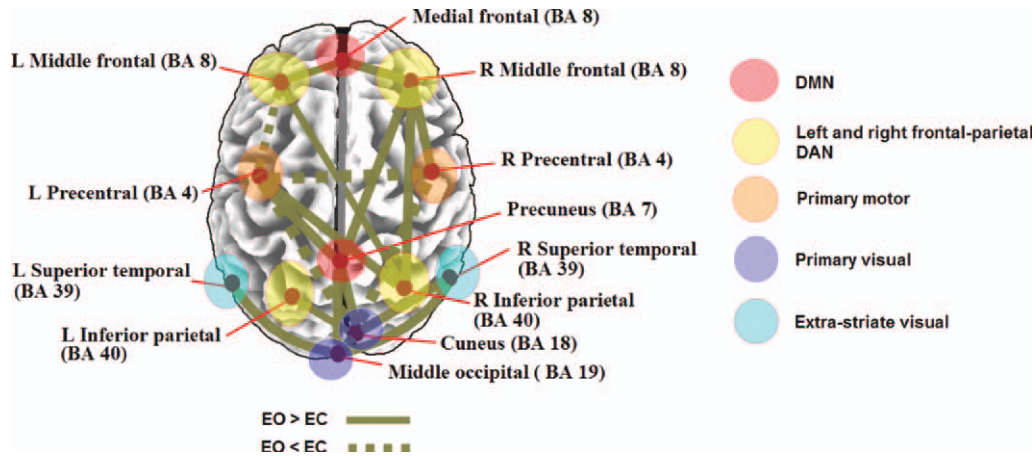


Figure 4.

Resting-state functional connections revealed by EEG-alpha power spectra, compared with other fMRI-RSN reports. The illustrated cortical node locations and their membership(s) within previously identified resting-state networks with fMRI are presented together with the results of the current study [Beckmann et al., 2005; Biswal et al., 1995; Damoiseaux et al., 2006; De Luca et al., 2006; Salvador et al., 2005; Van den Heuvel et al., 2008].

Significant correlations occurred (1) intrahemispherically in the EO state superior to the EC state (right BA40-BA8, $z > 5.31$, $P < 0.01$; right BA4-BA8, $z > 6.24$, $P < 0.01$); (2) interhemispherically between homologous region pairs (precentral BA4, $z < -6.05$, $P < 0.01$, in the EO state inferior to the EC state); and (3) interhemispherically between nonhomologous regions (left frontal BA8-right parietal BA40, $z > 4.35$, $P < 0.01$; left precentral BA4-right parietal BA40, $z > 5.31$, $P < 0.01$) in the EO state superior to the EC state. In other words, within-DAN correlations were generally greater than other cross-network correlations in the EO condition. Thus, DAN is always at least partially engaged and intrahemispheric connectivities become as strong as interhemispheric ones when the eyes are open. Furthermore, comparing functional connectivity value pairs revealed a significant between-condition difference within the midline connectivity of the DMN, specifically between medial prefrontal cortex (mPFC) and precuneus (medial frontal BA 8-precuneus BA7, $z > 4.35$, $P < 0.01$, Fig. 3B).

Figure 4 depicts these nodes within RSNs related in recent fMRI studies, including the primary sensorimotor network, the primary visual and extra-striate visual network, left and right lateralized networks consisting of superior parietal and superior frontal regions (DAN, reported as one single inset) as well as the so-called default mode network (DMN) consisting of precuneus, medial frontal, and inferior parietal cortical regions.

Resting-State Clusters With Well-Defined Functional-Anatomical Regions (Dendrogram Analysis)

Hierarchical cluster analysis of cross-correlations between alpha power ICs identified a consistent set of five

spatiotemporally distinct groups from 27 subjects in each resting condition, in line with resting state networks disclosed by fMRI studies [van den Heuvel and Hulshoff Pol, 2010; Toro et al., 2008]. Importantly, the five grouped-ICs were explained by the correlation coefficient in each clustered group ($P < 0.0005$, corrected), and may be considered as a good signature of the resting EEG in both EC and EO states. This is represented by the dendrogram plots in Figure 5, revealing distinct grouping patterns for components in both EC and EO states. Five groups were thus classified on the basis of coordinates in Talairach space and by regional anatomy (see also Table I):

1. Frontal group (F): a network involving predominantly lateral and middle prefrontal cortices, as well as the anterior pole of the prefrontal lobe.
2. Central group (C): a lateral network involving the precentral gyri.
3. Parietal group (P): a posterior-lateral and midline network involving primarily the parietal regions.
4. Occipitotemporal group (OT): a lateral network dominated by the bilateral middle temporal cortices in the occipitotemporal regions.
5. Occipital group (O): a posterior network involving predominantly the occipital cortex.

All of the group spatial maps were found in both EC and EO states. As illustrated in Figure 4, our results are consistent with fMRI resting-state network (RSN) reports of regions showing functional connectivity patterns across resting states [Fox et al., 2005; Fransson, 2005; Yan et al., 2009] as well as strong anatomical connectivities [Honey et al., 2007, 2009].

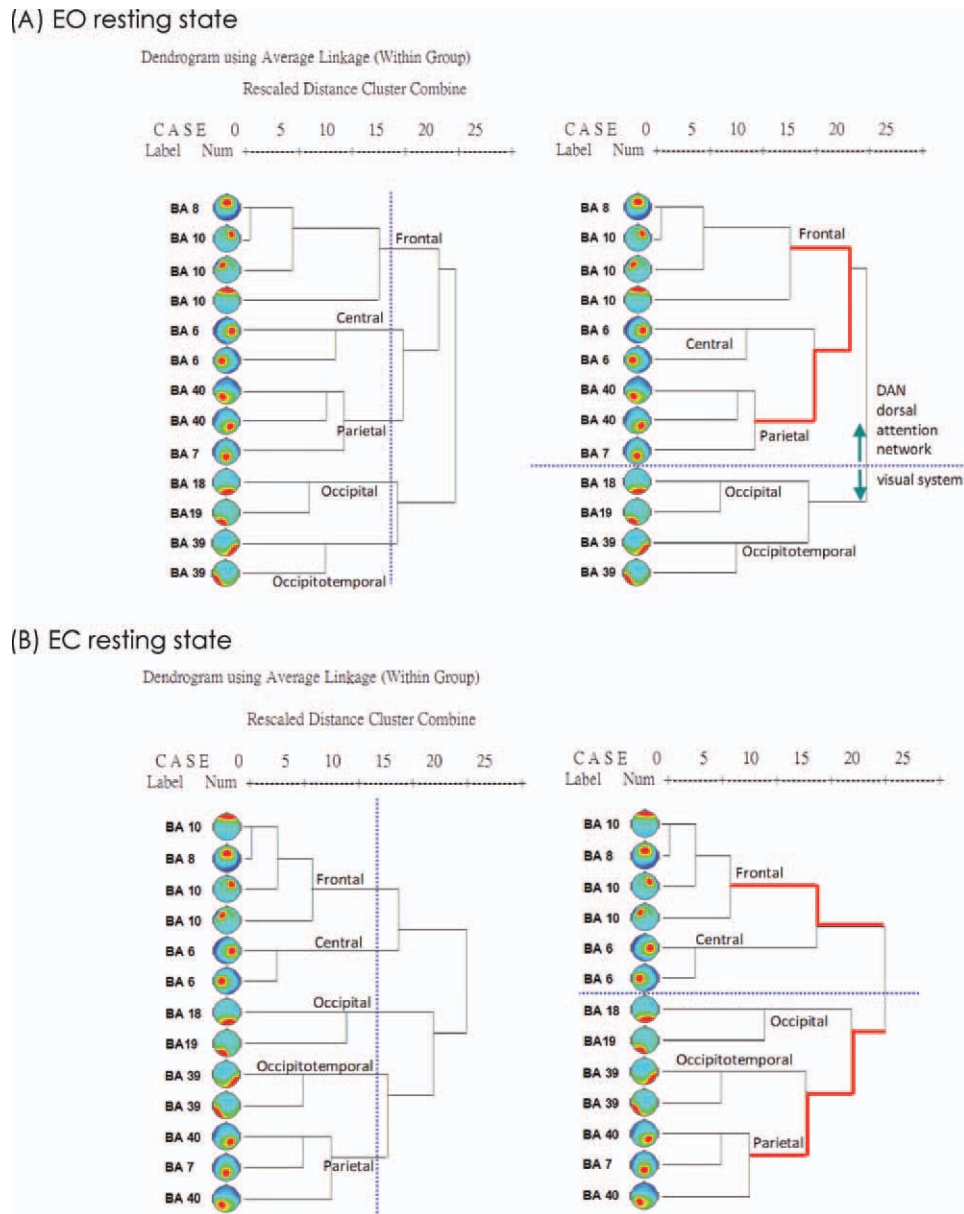


Figure 5.

The Dendrogram was performed to illustrate the grouping of the 13 ICs, suggested by Pearson correlations (r values) of alpha power spectra (from 1581 epochs) among all ICs; (A) in the EO condition and (B) in the EC condition (EC, eyes-closed; EO, eyes-open; BA, brain regions are identified by putative Brodmann area;

vertical blue-dot lines, instruction lines to help illustrate five groups according to the dendrogram and similarity; horizontal blue-dot lines, lines to help differentiate the dorsal attention network from the visual system in both states; red lines, indicating the distance (relationship) between the frontal and parietal groups).

In addition, the dorsal attention network (DAN) most evident in the frontal and parietal groups in the EO state, rather than the EC state, depicted by the dendrogram (Fig. 5). This effect is reinforced by the observation of enhanced correlation between nodes belonging to Groups F, C and P in the functional connectivity correlation matrix for the EO compared to EC condition (Fig. 6).

Functional Clustering Changes Between EC and EO States (Multidimensional Scaling Analysis)

Here, the functional distances between IC groups within the two conditions were represented by graphical distances in two-dimensional space, as depicted in Figure 7. Multidimensional-scaling (MDS) provides an interpretable map of

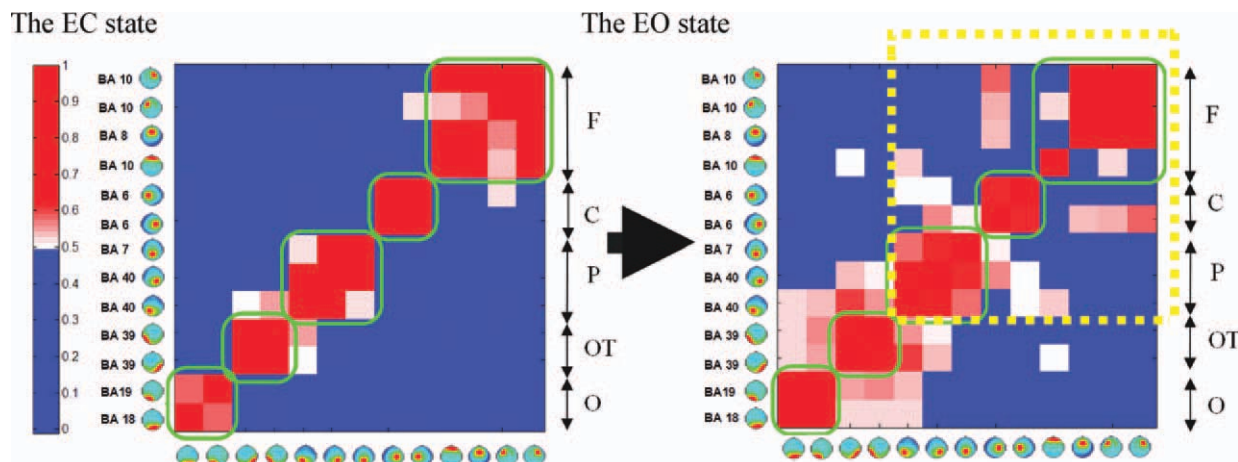


Figure 6.

Illustrative functional connectivity correlation matrices from the EC to EO state. Functional connectivity correlation matrix (unweighted undirected network) represents the cross-correlation of the independent component (IC) pairs for alpha-band spectral power, significant threshold, and arranged by the similarity among components. Green boxes depict circumscribed IC groups according to their significant functional connectivity ($r >$

0.50, $P < 0.01$ corrected), please refer to the dendrogram and MDS plots (Figs. 5 and 7). The yellow box indicates enhanced correlation of the Group F, C, and P in the dorsal attention network (DAN) during the EO condition (F: frontal, C: central, P: parietal, OT: occipitotemporal, O: occipital; r : Pearson's correlation coefficient).

the relations between all ICs whose similarity has been determined by Pearson correlations (r values) and whose IC group membership was revealed by dendrogram cluster analysis (Fig. 5). Hence, corepresentation of the clustered ICs' group membership may aid in highlighting differences in functional associations from EC to EO states on a network level. Here, functionally similar IC components, represented by topographical icons, are plotted in closer proximity within the MDS plot (Fig. 7). This analysis confirms many of the organizational features already highlighted in Figure 5 with symmetrically paired regions in cortical space, reflecting anatomical relations and functional similarity among the five principal IC groups (Table I). In accordance with some prior studies reporting stronger alpha-band similarities posteriorly rather than anteriorly in the EC condition [Barry et al., 2007; Chorlian et al., 2009], the components within Group F were more segregated than those in Group P and Group OT (Fig. 7). Moreover, comparing the relationship between Groups F and P in the EC versus EO conditions, the closer distance between the two groups in the MDS plot in the EO state suggests tighter coupling within the DAN [e.g. Mantini et al., 2007].

source separation (BSS) methods have been exploited to analyze resting-state EEG activity in healthy subjects [Chen et al., 2008; Congedo et al., 2010; Gomez-Herrero et al., 2008; Scheeringa et al., 2008], and in those with clinical disorders [Chen et al., 2009; De Vico Fallani et al.,

DISCUSSION

To our knowledge, this is the first study to combine EEG-ICA and graph theory to investigate spectral power functional connectivity of cortically localized sources from the eyes-closed to the eyes-open state. Although blind

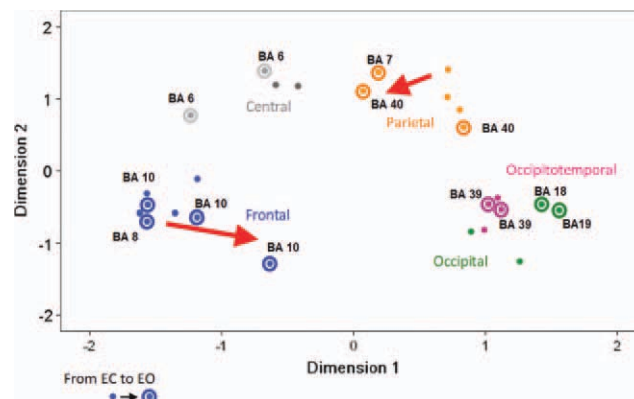


Figure 7.

The Euclidean distances matrix of the 13 ICs in the resting state was visualized in a two-dimensional space using multidimensional scaling (MDS). Five groups (frontal, central, parietal, occipital, and occipitotemporal groups) were presented by five different color according to the dendrogram and Pearson correlations of 13 ICs (please see Fig. 5). The distance between groups shows their relationship, and the connectivity of frontal and parietal groups is increased from EC to EO state, and the same as the visual system (occipital and occipitotemporal groups).

2007; Grin-Yatsenko et al., 2010], the present study demonstrates the feasibility and potential of using spectral analysis of ICA components to estimate EEG resting-state connectivity by representing the spatially-segregated, unmixed EEG sources as functional nodes within electrocortical networks, in accordance with graph theory [Bullmore and Sporns, 2009]. Compared with previous source-space attempts to provide a global pattern of electrocortical connectivity, our multistep approach effectively integrates information about functional interactions and provides a parsimonious procedure to describe dynamic state-changes in EEG resting-state networks (RSNs). Our principal findings indicate there is an increase in functional connectivity from EC to EO states, particularly between posterior and anterior regions, and that the electrophysiological network of the resting brain (without stimulation or task) is composed of five well-defined clusters of EEG activity: frontal, central, parietal, occipitotemporal, and occipital. Moreover, the alpha-band topographical maps and connectivity patterns are consistent with the estimated resting patterns from previous fMRI-RSN studies, such as the default-mode network (DMN) and dorsal attention network (DAN) [for a review see Toro et al., 2008; van den Heuvel and Hulshoff Pol, 2010]. In addition, the occipital group (O) and the occipitotemporal group (OT) appear similar to the reported primary visual and extra-striate visual networks. Given that cortical localization of ICA components and connectivity maps exhibit a high degree of consistency in spatial and frequency parameters within and between subjects during rest [e.g. van de Ven et al., 2004], it may be beneficial to implement this EEG-ICA functional connectivity approach to clinical populations during resting-state baseline recordings.

Functional Connectivity Changes From EC to EO

Interhemispheric connectivity varied both as a function of the resting state (from EC to EO) and cortical areas. During the EC state, we observed that alpha power-associated correlations of spatially localized sources conveyed a preferred interhemispheric direction (Fig. 3A, the EC state). Moreover, these alpha power-related associations showed a more distinct posterior than anterior focus [e.g. Chorlian et al., 2009]. Given that prior published fMRI-RSN studies revealed significant patterns of correlated spontaneous activity between homologous regions in opposite hemispheres [e.g. Fair et al., 2008; Salvador et al., 2005], the corpus callosum could act as the major conduit for information transfer between the cerebral hemispheres [Innocenti, 1994; Rosas et al., 2010]. In addition, connectivity strength emerged more significantly between posterior regions within the left hemisphere (left temporoparietal junction (TPJ), BAs 39/40) than between regions in the right hemisphere (Fig. 3A). In line with traditional findings, increased communication within the left TPJ may be reflective of a lateralized language processing network

[Hutsler and Galuske, 2003]. This feature has also been reported in spontaneous MEG activity of brain networks, indicating that coupling of spontaneous oscillations occurs predominantly within the left intrahemispheric parietal pathway [de Pasquale et al., 2010]. While most cortical sources manifested interhemispheric connections in the EC state between bilateral homologous regions, in the EO state significant correlations emerged most frequently intrahemispherically, demonstrated by the increased dynamic linkage between ipsilateral frontal and parietal regions (Fig. 3A, the EO state). Here, the frontal sources (F) were localized to Brodmann areas (BA) 8 and 10 (medial, right, and left middle frontal gyri), while the parietal sources (P) consisted of BA 7 and BA 40 (precuneus, right, and left inferior parietal lobules).

Importantly, the dorsal attention network (DAN) and default-mode network (DMN) appeared to become more prominent in the EO state (Fig. 3B, EO > EC). This observation is directly in line with reports of increased fMRI coupling between medial prefrontal cortex and precuneus (BA7) in the EO versus EC condition [Yan et al., 2009], and multimodal associations between alpha-power fluctuations and DMN activity [Ben-Simon et al., 2008, Jann et al., 2010; Mantini et al., 2007]. Amongst others, these RSNs have been reported in the work by Biswal et al. [1995], Beckmann et al. [2005], De Luca et al. [2006], Damoiseaux et al. [2006], and Salvador et al. [2005] (Fig. 4). Although the aforementioned studies made use of different groups of subjects, methods (e.g. seed, ICA, or clustering) and MRI acquisition protocols, they coincide with the EEG-based results of the present study, suggesting the robust formation of functionally and consistently linked networks in the brain during resting conditions.

Neurophysiological Implications of the Five Functionally Clustered Groups

Although the RSN and DMN concepts have come from important fMRI-BOLD evidence demonstrating consistent activation patterns across distinct brain regions [Greicius et al., 2003; Raichle et al., 2001], it is as yet unclear how these relate to the concurrent coupling and degree of neuronal activity [Debener et al., 2006]. In contrast, EEG has excellent temporal resolution and is a direct electrophysiological correlate of spontaneous and task-related neuronal activity. ICA has been extensively used for the analysis of electromagnetic brain signals [James and Hesse, 2005; Vigario and Oja, 2000], and provides a statistical estimation of maximally independent EEG sources. Several earlier studies have demonstrated the application of ICA to multichannel EEG data for distinguishing artifacts and functional brain sources [e.g. Jung et al., 2000; Makeig et al., 2004; Marco-Pallares et al., 2005]. Interestingly, about 20% of all grey matter neurons, nonpyramidal type, express metabolic activity well reflected in the BOLD signal, but not in the EEG [Broyd et al., 2009]. To solve the problem originating from a

degree of incongruence between hemodynamic and electrophysiological signals, more recent research has tried combining different modalities, such as EEG-fMRI, to better understand which portions of BOLD activity are reflected in the EEG [Jann et al., 2009; Mantini et al., 2007]. Here we examined directly the spatial characteristics of the five hierarchically clustered groups based on the EEG alpha-band spectral power of each IC, with the aim of validating this approach in relation to previous reports of EEG and fMRI default patterns.

An important question is whether these groups directly reflect anatomical connectivity. We selected the alpha rhythm, the most prominent EEG rhythm during the conscious resting state, as the basis of the ICA-based EEG cluster groups. In previous reports [Barry et al., 2005, 2007; Chen et al., 2008] the distribution of scalp EEG power in relation to anatomical sources within the RSN was unresolved due to the masking of underlying source activity through volume conduction [Nunez and Srinivasan, 2006]. Compared with blood-oxygenation level fMRI recordings, our combined ICA and sLORETA based results suggest an electrophysiological, and therefore neuronal, functional connectivity amongst well-specified anatomical regions.

Visual versus parietal system

A good example is the separation of the dorsal parietal cluster (Group P, parietal clustered group in both EC and EO) from the rest of the visual system (Group O and Group OT, in Table I and Fig. 5) [De Luca et al., 2006; Gusnard et al., 2001; Mantini et al., 2007]. The visual system is organized into two parallel anatomical pathways—the dorsal (occipitoparietal) pathway related to spatial vision and visually guided actions, and the ventral (occipitotemporal) pathway associated with identification of visual objects [Corbetta and Shulman, 2002; Sereno et al., 2001]. Interestingly these three groups are shown to be separated by alpha power-associated IC clustering, compared to similar results of correlations between EEG rhythms and fMRI RSNs reported by Mantini et al. in 2007, and a weak interaction between two EEG-alpha generators (precuneus and cuneus) found by Gomez-Herrero et al. [2008].

Frontal and parietal subdivisions

Previous work has shown that the DMN can be divided into at least two subnetworks, with anterior and posterior (frontal and parietal) subdivisions [Damoiseaux et al., 2006; Kiviniemi et al., 2009]. Similarly, based on cluster analyses of alpha power-associated ICs, we were also able to demonstrate a parietal sub-network (Group P in Table I and Fig. 5) and a frontal sub-network (Group F in Table I and Fig. 5). Crucially, during EEG-fMRI coregistration, Mantini et al. [2007] observed that both the DMN and the dorsal attention network (DAN) were coupled to changes in EEG power. The DMN and DAN are two of the most

robust and well-studied RSNs, and are associated with task-negative and task-positive functions, respectively [Shulman et al., 1997]. Earlier reports have suggested that default and attention networks show considerable correlation with EEG-alpha band power [Laufs et al., 2003a,b). In particular, a study of the temporal dynamics of spontaneous MEG activity has also demonstrated strong correlations in the alpha-band in both the DAN and the DMN [de Pasquale et al., 2010]. The results of the present study underline the prominence of the DMN and DAN particularly in the EO state, and our findings of relevant circumscribed regions are consistent with the idea that the DAN as well as the DMN appear to exhibit more functional coupling during the EO versus EC condition; the DMN being characterized by increased connection strength between medial prefrontal cortex (MPFC) and precuneus (PCu) regions (Figs. 3B and 4), in line with Yan et al. [2009].

Group Interactions Visualized With Multidimensional Scaling (MDS)

By way of a two-dimensional plot, the MDS method facilitates visualizing the similarity matrices of the alpha power-associated correlation coefficients and the proximity of the EEG components. During the shift from EC to EO, the frontal and parietal clusters appear to become closer in the EO state, suggesting more tightly coupled activities among the regions of both the DAN and DMN, potentially to increase contextual integration and evaluation of visual information [Hamzei et al., 2002; Mason et al., 2007; Yan et al., 2009]. Interestingly, we also discovered a number of symmetrical interhemispheric connections that were stronger than would be predicted by the anatomical distance between bilaterally homologous regions in both EC and EO states [Salvador et al., 2005]; for example the coupling between left and right occipitotemporal areas (BA 39; Figs. 3A and 5). Another example is the visual system in the MDS plot (Fig. 7). The distance from the occipital group (Group O) to the parietal group (Group P) was approximately similar to the distance from the occipital group to the occipitotemporal group (Group OT) in the EC state, suggesting a similar strength of coupling of the two parallel visual pathways in keeping with the relatively more inactivated visual cortex. In contrast, in EO with fixation (Fig. 7), the components of occipital and occipitotemporal groups move more closely, respectively, showing increased functional connectivity (Fig. 3B), but not with the parietal group, suggesting a more pronounced coupling of the prevalent ventral pathway, putatively activated during visual object detection (a cross presented in the EO fixation condition), rather than the dorsal pathway which is used during visually guided actions [e.g. e.g. Virji-Babul et al., 2007]. Together, this is consistent with reports that the oculomotor and attentional systems appear to be activated upon eyes opening, showing an “exteroceptive mental state,” as indicated by Marx et al. [2003] in an

fMRI study. On the other hand, it is evident that the sensorimotor group (Group C) remained closer to the occipital group in the EC state (Figs. 5B and 7), possibly reflecting stronger coactivation of the visual and somatosensory systems in the “interoceptive mental state” with eyes closed, and characterized by imagination and sensory activity [Marx et al., 2003].

Methodological Limitations

The principal drawback of the present study was the use of a limited number of electrodes. Although the results found with the ICA-sLORETA method seem encouraging, they could be refined with the use of a greater number of electrodes (given that the number of resolved ICs is numerically equal to the number of recording electrodes used). There is a limit to this nevertheless, since owing to volume conduction, high-density EEG channels close to each other tend to be increasingly influenced by activity from similar brain regions. Nevertheless, volume conduction is a widely recognized problem that pervades almost all functional connectivity analyses of the EEG. In this case, EEG signal changes occurring at one location may “spread” and be detected at another, and thus be (erroneously) interpreted as evidence of altered synchrony *between* locations (sensors). One proposed workaround has been to utilize strictly phase-lagged signals in connectivity analyses (given that volume conduction is instantaneous) [Stam et al., 2007]. However, this may also run the risk of “throwing the baby out with the bathwater,” as there is evidence that considerable cortico-cortical coupling occurs with zero phase-lag in the brain, independent of volume conduction [Gollo et al., 2011; Roelfsema et al., 1997]. In this study we have proposed an alternative approach in the frequency-domain which, although phase-insensitive, explicitly defines independent “sources” (ICs) of EEG activity. Here, the time-course of each IC is defined individually from the source-space matrix, thereby minimizing the source “spread” which manifests itself in sensor-space. Moreover, since ICA was performed before frequency-domain transformation, it would be comparatively easy to translate this processing pipeline to phase-sensitive measures (such as phase synchrony) by likewise taking advantage of maximal signal independence in ICA source-space. Importantly, ICA source-space is qualitatively different from the source-space of inverse-source localization methods (minimum-norm or dipole-fitting methods). The latter may be envisaged as computing “virtually implanted electrodes,” which can detect distinct but potentially spatiotemporally overlapping activities within the same anatomical location. ICA, in contrast, employs higher-order statistical methods to linearly unmix the sources in the signal a priori, which may be followed by a subsequent step of cortical source localization (e.g. sLORETA). This may be additionally useful in view of the fact that volume conduction is expressed through linear summation

of the signal. On the other hand the principal limitation of ICA is that it is designed to separate mixtures of principally non-Gaussian activities. In this respect, we tested an alternative approach of performing ICA on prefiltered alpha-band data; however, this approach yielded a lower number of valid extracted cerebral components (about 50% less), many of which had high residual variance, indicating poor localization of electrocortical activity. We speculate that this may be due to the fact that the standalone alpha rhythm has been reported to have near-Gaussian properties [Dick and Vaughn, 1970]. Nevertheless, patches of cortex that generate the EEG naturally oscillate at multiple frequencies simultaneously (frequency nesting) and ICA is apparently able to best estimate the maximal independence of EEG generators according to a wider distribution of frequencies; thus our original pipeline retains the property of being physiologically realistic. Almost all previous EEG studies have traditionally applied ICA on broadband data before filtration to individual frequencies of interest [Chen et al., 2009; Grin-Yatsenko et al., 2010].

Notwithstanding, the most obvious limitation may be the cortical nature of the EEG signal itself, which reflects widespread synchrony of pyramidal neurons in cortical grey matter, and is more problematic for resolving activity from deeper brain structures, as can be done with fMRI. Therefore more EEG-fMRI studies should be encouraged, with efforts also directed toward standardizing methods for ICA-based EEG networks and their differentiation between different behavioral states. For example, future studies could be carried out to determine the functional connectivity of theta or beta-power clustered ICs, compared with networks demonstrated by previous fMRI studies. Likewise, studies could be designed to reveal how connectivities within/between RSNs vary with pharmacological intake or relate to brain-related pathologies, and to clarify whether observed clustered IC patterns are equivalent during altered brain states [e.g. for sleep: Tinguely et al., 2006; for motion sickness: Chen et al., 2009].

CONCLUSIONS

In conclusion, this work demonstrates the feasibility and addresses the potential of using a multistep, data-driven approach for source-based EEG functional connectivity analysis, based on the combined advantages of ICA, source localization, graph theory, and multidimensional scaling in order to reveal the spatiotemporal dynamics of EEG changes from EC to EO states. Our results suggest that cerebral processing underlying eyes-closed and eyes-open baseline states consists of statistically clustered groups within spatially and functionally related cortical regions (frontal, central, parietal, occipitotemporal, and occipital), clearly identified in two-dimensional and three-dimensional space. From EC to EO resting states, and in line with previous fMRI studies, graph analyses and MDS plots indicated enhanced functional connectivity of frontal

and parietal groups putatively subserved by the dorsal attentional network (DAN) and default-mode network (DMN); there was moreover a tight coupling of occipito-temporal groups associated with processing in more ventral areas, in keeping with the dichotomy of the dorsal/ventral stream hypothesis of the visual information system [Hilgetag et al., 2000; Salvador et al., 2005]. These results suggest that two physiological mechanisms (ventral and dorsal attention networks) functionally coexist during simple resting states such as EO fixation. Since resting-state connectivity has been shown to correlate with behavioral performance and cognitive measures in a host of published studies [for a review, see Greicius et al., 2008], EEG spectral-power based RSNs, resolved with ICA, may provide a useful measure with which to directly quantify neuronal functional connectivity during resting state and/or task-related conditions, in healthy subjects and those with mental illness.

ACKNOWLEDGMENTS

This research was supported by grants from School of Medicine, Chang Gung University & Department of Physical Medicine and Rehabilitation, Chang Gung Memorial Hospital, Taiwan (CMRPG350813, CMRPG350814). Trevor Thompson is thanked for helpful suggestions.

REFERENCES

- Alper KR, John ER, Brodie J, Gunther W, Daruwala R, Prichep LS (2006): Correlation of PET and qEEG in normal subjects. *Psychiatry Res* 146:271–282.
- Arieli A, Sterkin A, Grinvald A, Aertsen A (1996): Dynamics of ongoing activity: Explanation of the large variability in evoked cortical responses. *Science* 273:1868–1871.
- Barry RJ, Clarke AR, Johnstone SJ, Brown CR (2009): EEG differences in children between eyes-closed and eyes-open resting conditions. *Clin Neurophysiol* 120:1806–1811.
- Barry RJ, Clarke AR, Johnstone SJ, Magee CA, Rushby JA (2007): EEG differences between eyes-closed and eyes-open resting conditions. *Clin Neurophysiol* 118:2765–2773.
- Barry RJ, Rushby JA, Wallace MJ, Clarke AR, Johnstone SJ, Zlojutro I (2005): Caffeine effects on resting-state arousal. *Clin Neurophysiol* 116:2693–2700.
- Bell AJ, Sejnowski TJ (1995): An information-maximization approach to blind separation and blind deconvolution. *Neural Comput* 7:1129–1159.
- Ben-Simon E, Podlipsky I, Arieli A, Zhdanov A, Hendler T (2008): Never resting brain: Simultaneous representation of two alpha related processes in humans. *PLoS one* 3:e3984.
- Bertrand O, Tallon-Baudry C (2000): Oscillatory gamma activity in humans: A possible role for object representation. *Int J Psychophysiol* 38:211–223.
- Biswal B, Yetkin FZ, Haughton VM, Hyde JS (1995): Functional connectivity in the motor cortex of resting human brain using echo-planar MRI. *Magn Reson Med* 34:537–541.
- Buckner RL, Sepulcre J, Talukdar T, Krienen FM, Liu H, Hedden T, Andrews-Hanna JR, Sperling RA, Johnson KA. (2009): Cortical hubs revealed by intrinsic functional connectivity: Mapping, assessment of stability, and relation to Alzheimer's disease. *J Neurosci* 29:1860–1873.
- Bullmore E, Sporns O (2009): Complex brain networks: Graph theoretical analysis of structural and functional systems. *Nat Rev Neurosci* 10:186–198.
- Brookes MJ, Gibson AM, Hall SD, Furlong PL, Barnes GR, Hillebrand A, Singh KD, Holliday IE, Francis ST, Morris PG (2005): GLM-beamformer method demonstrates stationary field, alpha ERD and gamma ERS co-localisation with fMRI BOLD response in visual cortex. *Neuroimage* 26:302–308.
- Broyd SJ, Demanuele C, Debener S, Helps SK, James CJ, Sonuga-Barke EJ (2009): Default-mode brain dysfunction in mental disorders: A systematic review. *Neurosci Biobehav Rev* 33:279–296.
- Buccino G, Binkofski F, Fink GR, Fadiga L, Fogassi L, Gallese V, Seitz RJ, Zilles K, Rizzolatti G, Freund HJ (2001): Action observation activates premotor and parietal areas in a somatotopic manner: An fMRI study. *Eur J Neurosci* 13:400–404.
- Calhoun VD, Adali T, Pearlson GD, Pekar JJ (2001): A method for making group inferences from functional MRI data using independent component analysis. *Hum Brain Mapp* 14:140–151.
- Calhoun VD, Adali T, Pekar JJ (2004): A method for comparing group fMRI data using independent component analysis: Application to visual, motor and visuomotor tasks. *Magn Reson Imaging* 22:1181–1191.
- Chen AC, Feng W, Zhao H, Yin Y, Wang P (2008): EEG default mode network in the human brain: Spectral regional field powers. *Neuroimage* 41:561–574.
- Chen YC, Duann JR, Chuang SW, Lin CL, Ko LW, Jung TP, Lin CT (2009): Spatial and temporal EEG dynamics of motion sickness. *Neuroimage* 49:2862–2870.
- Chorlian DB, Rangaswamy M, Porjesz B (2009): EEG coherence: Topography and frequency structure. *Exp Brain Res* 198:59–83.
- Comon P (1994): Independent component analysis: A new concept. *Signal Processing* 36:287–314.
- Congedo M, Gouy-Pailler C, Jutten C (2008): On the blind source separation of human electroencephalogram by approximate joint diagonalization of second order statistics. *Clin Neurophysiol* 119:2677–2686.
- Congedo M, John RE, De Ridder D, Prichep L, Isenhardt R (2010). On the "dependence" of "independent" group EEG sources; an EEG study on two large databases. *Brain Topogr* 23:134–138.
- Corbetta M, Shulman GL (2002): Control of goal-directed and stimulus-driven attention in the brain. *Nat Rev Neurosci* 3:201–215.
- Damoiseaux JS, Beckmann CF, Arigita EJ, Barkhof F, Scheltens P, Stam CJ, Smith SM, Rombouts SA (2008): Reduced resting-state brain activity in the "default network" in normal aging. *Cereb Cortex* 18:1856–1864.
- Damoiseaux JS, Rombouts SA, Barkhof F, Scheltens P, Stam CJ, Smith SM, Beckmann CF (2006): Consistent resting-state networks across healthy subjects. *Proc Natl Acad Sci USA* 103:13848–13853.
- De Luca M, Beckmann CF, De Stefano N, Matthews PM, Smith SM (2006): fMRI resting state networks define distinct modes of long-distance interactions in the human brain. *Neuroimage* 29:1359–1367.
- De Vico Fallani F, Astolfi L, Cincotti F, Mattia D, Tocci A, Marciani MG, Colosimo A, Salinari S, Gao S, Cichocki A, Babiloni F (2007): Extracting information from cortical connectivity patterns estimated from high resolution EEG recordings: A theoretical graph approach. *Brain Topogr* 19:125–136.
- Debener S, Ullsperger M, Siegel M, Engel AK (2006): Single-trial EEG-fMRI reveals the dynamics of cognitive function. *Trends Cogn Sci* 10:558–563.

- Dick DE, Vaughn AO (1970): Mathematical description and computer detection of alpha waves. *Math Biosci* 7:81–95.
- Dosenbach NU, Fair DA, Miezin FM, Cohen AL, Wenger KK, Dosenbach RA, Fox MD, Snyder AZ, Vincent JL, Raichle ME, Schlaggar BL, Petersen SE (2007): Distinct brain networks for adaptive and stable task control in humans. *Proc Natl Acad Sci USA* 104:11073–11078.
- de Pasquale F, Della Penna S, Snyder AZ, Lewis C, Mantini D, Marzetti L, Belardinelli P, Ciancetta L, Pizzella V, Romani GL, et al. (2010): Temporal dynamics of spontaneous MEG activity in brain networks. *Proc Natl Acad Sci USA* 107:6040–6045.
- Egner T, Gruzelier JH (2001): Learned self-regulation of EEG frequency components affects attention and event-related brain potentials in humans. *Neuroreport* 12:4155–4159.
- Egner T, Gruzelier JH (2004): EEG biofeedback of low beta band components: Frequency-specific effects on variables of attention and event-related brain potentials. *Clin Neurophysiol* 115:131–139.
- Esposito F, Scarabino T, Hyvarinen A, Himberg J, Formisano E, Comani S, Tedeschi G, Goebel R, Seifritz E, Di Salle F (2005): Independent component analysis of fMRI group studies by self-organizing clustering. *Neuroimage* 25:193–205.
- Fox MD, Snyder AZ, Vincent JL, Corbetta M, Van Essen DC, Raichle ME (2005): The human brain is intrinsically organized into dynamic, anticorrelated functional networks. *Proc Natl Acad Sci USA* 102:9673–9678.
- Fransson P (2005): Spontaneous low-frequency BOLD signal fluctuations: An fMRI investigation of the resting-state default mode of brain function hypothesis. *Hum Brain Mapp* 26:15–29.
- Fransson P (2006): How default is the default mode of brain function? Further evidence from intrinsic BOLD signal fluctuations. *Neuropsychologia* 44:2836–2845.
- Grin-Yatsenko VA, Baas I, Ponomarev VA, Kropotov JD (2010): Independent component approach to the analysis of EEG recordings at early stages of depressive disorders. *Clin Neurophysiol* 121:281–289.
- Gobbele R, Waberski TD, Simon H, Peters E, Klostermann F, Curio G, Buchner H (2004): Different origins of low- and high-frequency components (600 Hz) of human somatosensory evoked potentials. *Clin Neurophysiol* 115:927–937.
- Goldman RI, Stern JM, Engel J Jr, Cohen MS (2002): Simultaneous EEG and fMRI of the alpha rhythm. *Neuroreport* 13:2487–2492.
- Gollo LL, Mirasso CR, Atienza M, Crespo-Garcia M, Cantero JL (2011): Theta band zero-lag long-range cortical synchronization via hippocampal dynamical relaying. *PLoS One* 6:e17756.
- Gomez-Herrero G, Atienza M, Egiazarian K, Cantero JL (2008): Measuring directional coupling between EEG sources. *Neuroimage* 43:497–508.
- Goncharova II, McFarland DJ, Vaughan TM, Wolpaw JR (2003): EMG contamination of EEG: Spectral and topographical characteristics. *Clin Neurophysiol* 114:1580–1593.
- Grech R, Cassar T, Muscat J, Camilleri KP, Fabri SG, Zervakis M, Xanthopoulos P, Sakkalis V, Vanrumste B (2008): Review on solving the inverse problem in EEG source analysis. *J Neuroeng Rehabil* 5:25.
- Greicius M (2008): Resting-state functional connectivity in neuropsychiatric disorders. *Curr Opin Neurol* 21:424–430.
- Greicius MD, Krasnow B, Reiss AL, Menon V (2003): Functional connectivity in the resting brain: A network analysis of the default mode hypothesis. *Proc Natl Acad Sci USA* 100:253–258.
- Grin-Yatsenko VA, Baas I, Ponomarev VA, Kropotov JD (2010): Independent component approach to the analysis of EEG recordings at early stages of depressive disorders. *Clin Neurophysiol* 121:281–289.
- Gruzelier J, Egner T, Vernon D (2006): Validating the efficacy of neurofeedback for optimising performance. *Prog Brain Res* 159:421–431.
- Gusnard DA, Akbudak E, Shulman GL, Raichle ME (2001): Medial prefrontal cortex and self-referential mental activity: Relation to a default mode of brain function. *Proc Natl Acad Sci USA* 98:4259–4264.
- Gusnard DA, Raichle ME (2001): Searching for a baseline: Functional imaging and the resting human brain. *Nat Rev Neurosci* 2:685–694.
- Hagmann P, Cammoun L, Gigandet X, Meuli R, Honey CJ, Wedeen VJ, Sporns O (2008): Mapping the structural core of human cerebral cortex. *PLoS Biol* 6:e159.
- Hamzei F, Dettmers C, Rijntjes M, Glauche V, Kiebel S, Weber B, Weiller C (2002): Visuomotor control within a distributed parieto-frontal network. *Exp Brain Res* 146:273–281.
- Hilgetag CC, Burns GA, O'Neill MA, Scannell JW, Young MP (2000): Anatomical connectivity defines the organization of clusters of cortical areas in the macaque monkey and the cat. *Philos Trans R Soc Lond B Biol Sci* 355:91–110.
- Hoedlmoser K, Pecherstorfer T, Gruber G, Anderer P, Doppelmayr M, Klimesch W, Schabus M (2008): Instrumental conditioning of human sensorimotor rhythm (12–15 Hz) and its impact on sleep as well as declarative learning. *Sleep* 31:1401–1408.
- Honey CJ, Kotter R, Breakspear M, Sporns O (2007): Network structure of cerebral cortex shapes functional connectivity on multiple time scales. *Proc Natl Acad Sci USA* 104:10240–10245.
- Honey CJ, Sporns O, Cammoun L, Gigandet X, Thiran JP, Meuli R, Hagmann P (2009): Predicting human resting-state functional connectivity from structural connectivity. *Proc Natl Acad Sci USA* 106:2035–2040.
- Hutsler J, Galuske RAW (2003): Hemispheric asymmetries in cerebral cortical networks. *Trends Neurosci* 26:429–435.
- Hyvarinen A, Oja E (2000): Independent component analysis: Algorithms and applications. *Neural Netw* 13:411–430.
- Hyvarinen A, Ramkumar P, Parkkonen L, Hari R (2010): Independent component analysis of short-time Fourier transforms for spontaneous EEG/MEG analysis. *Neuroimage* 49:257–271.
- Innocenti GM (1994): Some new trends in the study of the corpus callosum. *Behav Brain Res* 64:1–8.
- Isaichev SA, Derevyankin VT, Koptelov Yu M, Sokolov EN (2001): Rhythmic alpha-activity generators in the human EEG. *Neurosci Behav Physiol* 31:49–53.
- James CJ, Hesse CW (2005): Independent component analysis for biomedical signals. *Physiol Meas* 26:R15–R39.
- Jann K, Dierks T, Boesch C, Kottlow M, Strik W, Koenig T (2009): BOLD correlates of EEG alpha phase-locking and the fMRI default mode network. *Neuroimage* 45:903–916.
- Jung TP, Makeig S, Westerfield M, Townsend J, Courchesne E, Sejnowski TJ (2000): Removal of eye activity artifacts from visual event-related potentials in normal and clinical subjects. *Clin Neurophysiol* 111:1745–1758.
- Jung TP, Makeig S, Mckeown MJ, Bell AJ, Lee TW, Sejnowski TJ (2001): Imaging brain dynamics using independent component analysis. *Proc IEEE* 89:1107–1122.
- Kilner JM, Mattout J, Henson R, Friston KJ (2005): Hemodynamic correlates of EEG: A heuristic. *Neuroimage* 28:280–286.
- Kiviniemi V, Starck T, Remes J, Long X, Nikkinen J, Haapea M, Veijola J, Moilanen I, Isohanni M, Zang YF, Tervonen O (2009): Functional segmentation of the brain cortex using high model order group PICA. *Hum Brain Mapp* 30:3865–3886.

- Klimesch W (1999): EEG alpha and theta oscillations reflect cognitive and memory performance: A review and analysis. *Brain Res Brain Res Rev* 29:169–195.
- Klimesch W, Doppelmayr M, Rohm D, Pollhuber D, Stadler W (2000): Simultaneous desynchronization and synchronization of different alpha responses in the human electroencephalograph: A neglected paradox? *Neurosci Lett* 284:97–100.
- Klimesch W, Sauseng P, Hanslmayr S (2007): EEG alpha oscillations: The inhibition-timing hypothesis. *Brain Res Rev* 53:63–88.
- Lachaux JP, Fonlupt P, Kahane P, Minotti L, Hoffmann D, Bertrand O, Bacia M (2007): Relationship between task-related gamma oscillations and BOLD signal: New insights from combined fMRI and intracranial EEG. *Hum Brain Mapp* 28:1368–1375.
- Laufs H (2008): Endogenous brain oscillations and related networks detected by surface EEG-combined fMRI. *Hum Brain Mapp* 29:762–769.
- Laufs H, Daunizeau J, Carmichael DW, Kleinschmidt A (2008): Recent advances in recording electrophysiological data simultaneously with magnetic resonance imaging. *Neuroimage* 40:515–528.
- Laufs H, Hamandi K, Walker MC, Scott C, Smith S, Duncan JS, Lemieux L (2006): EEG-fMRI mapping of asymmetrical delta activity in a patient with refractory epilepsy is concordant with the epileptogenic region determined by intracranial EEG. *Magn Reson Imaging* 24:367–371.
- Laufs H, Kleinschmidt A, Beyerle A, Eger E, Salek-Haddadi A, Preibisch C, Krakow K (2003a): EEG-correlated fMRI of human alpha activity. *Neuroimage* 19:1463–1476.
- Laufs H, Krakow K, Sterzer P, Eger E, Beyerle A, Salek-Haddadi A, Kleinschmidt A (2003b): Electroencephalographic signatures of attentional and cognitive default modes in spontaneous brain activity fluctuations at rest. *Proc Natl Acad Sci USA* 100:11053–11058.
- Lin CT, Wu RC, Liang SF, Chao WH, Chen YJ, Jung TP (2005): EEG-based drowsiness estimation for safety driving using independent component analysis. *IEEE Trans Circuits Syst* 52:12.
- Lowe MJ, Mock BJ, Sorenson JA (1998): Functional connectivity in single and multislice echoplanar imaging using resting-state fluctuations. *Neuroimage* 7:119–132.
- Lu H, Zuo Y, Gu H, Waltz JA, Zhan W, Scholl CA, Rea W, Yang Y, Stein EA (2007): Synchronized delta oscillations correlate with the resting-state functional MRI signal. *Proc Natl Acad Sci USA* 104:18265–18269.
- Makeig S, Bell AJ, Jung TP, Sejnowski B (1996): Independent component analysis of electroencephalographic data. *Adv Neural Inf Process Syst* 8:145–151.
- Makeig S, Delorme A, Westerfield M, Jung TP, Townsend J, Courchesne E, Sejnowski TJ (2004): Electroencephalographic brain dynamics following manually responded visual targets. *PLoS Biol* 2:e176.
- Makeig S, Jung TP, Bell AJ, Ghahremani D, Sejnowski TJ (1997): Blind separation of auditory event-related brain responses into independent components. *Proc Natl Acad Sci USA* 94:10979–10984.
- Makeig S, Westerfield M, Jung TP, Covington J, Townsend J, Sejnowski TJ, Courchesne E (1999): Functionally independent components of the late positive event-related potential during visual spatial attention. *J Neurosci* 19:2665–2680.
- Makeig S, Westerfield M, Jung TP, Enghoff S, Townsend J, Courchesne E, Sejnowski TJ (2002): Dynamic brain sources of visual evoked responses. *Science* 295:690–694.
- Mantini D, Perrucci MG, Del Gratta C, Romani GL, Corbetta M (2007): Electrophysiological signatures of resting state networks in the human brain. *Proc Natl Acad Sci USA* 104:13170–13175.
- Marco-Pallares J, Grau C, Ruffini G (2005): Combined ICA-LOR-ETA analysis of mismatch negativity. *Neuroimage* 25:471–477.
- Marx E, Deutschlander A, Stephan T, Dieterich M, Wiesmann M, Brandt T (2004): Eyes open and eyes closed as rest conditions: Impact on brain activation patterns. *Neuroimage* 21:1818–1824.
- Marx E, Stephan T, Nolte A, Deutschlander A, Seelos KC, Dieterich M, Brandt T (2003): Eye closure in darkness animates sensory systems. *Neuroimage* 19:924–934.
- Meltzer JA, Negishi M, Mayes LC, Constable RT (2007): Individual differences in EEG theta and alpha dynamics during working memory correlate with fMRI responses across subjects. *Clin Neurophysiol* 118:2419–2436.
- Miwakeichi F, Martinez-Montes E, Valdes-Sosa PA, Nishiyama N, Mizuhara H, Yamaguchi Y (2004): Decomposing EEG data into space-time-frequency components using Parallel Factor Analysis. *Neuroimage* 22:1035–1045.
- Mizuhara H, Wang LQ, Kobayashi K, Yamaguchi Y (2004): A long-range cortical network emerging with theta oscillation in a mental task. *Neuroreport* 15:1233–1238.
- Neuper C, Pfurtscheller G (1992): [Event-related negativity and alpha band desynchronization in motor reactions]. *EEG EMG Z Elektroenzephalogr Elektromyogr Verwandte Geb* 23:55–61.
- Neuper C, Wortz M, Pfurtscheller G (2006): ERD/ERS patterns reflecting sensorimotor activation and deactivation. *Prog Brain Res* 159:211–222.
- Niessing J, Ebisch B, Schmidt KE, Niessing M, Singer W, Galuske RA (2005): Hemodynamic signals correlate tightly with synchronized gamma oscillations. *Science* 309:948–951.
- Nunez PL (1987): Removal of reference electrode and volume conduction effects by spatial deconvolution of evoked potentials using a three-concentric sphere model of the head. *Electroencephalogr Clin Neurophysiol Suppl* 39:143–148.
- Nunez PL, Silberstein RB (2000): On the relationship of synaptic activity to macroscopic measurements: Does co-registration of EEG with fMRI make sense? *Brain Topogr* 13:79–96.
- Nunez PL, Srinivasan R (2006): A theoretical basis for standing and traveling brain waves measured with human EEG with implications for an integrated consciousness. *Clin Neurophysiol* 117:2424–2435.
- Nunez PL, Srinivasan R, Westdorp AF, Wijesinghe RS, Tucker DM, Silberstein RB, Cadusch PJ (1997): EEG coherency. I: Statistics, reference electrode, volume conduction, Laplacians, cortical imaging, and interpretation at multiple scales. *Electroencephalogr Clin Neurophysiol* 103:499–515.
- Nuwer MR, Lehmann D, da Silva FL, Matsuoka S, Sutherling W, Vibert JF (1999): IFCN guidelines for topographic and frequency analysis of EEGs and EPs. *The International Federation of Clinical Neurophysiology. Electroencephalogr Clin Neurophysiol Suppl* 52:15–20.
- Oishi N, Mima T, Ishii K, Bushara KO, Hiraoka T, Ueki Y, Fukuyama H, Hallett M (2007): Neural correlates of regional EEG power change. *Neuroimage* 36:1301–1312.
- Onton J, Westerfield M, Townsend J, Makeig S (2006): Imaging human EEG dynamics using independent component analysis. *Neurosci Biobehav Rev* 30:808–822.
- Pascual-Marqui RD, Esslen M, Kochi K, Lehmann D (2002): Functional imaging with low-resolution brain electromagnetic tomography (LORETA): A review. *Methods Find Exp Clin Pharmacol* 24(Suppl C):91–95.
- Pfurtscheller G, Flotzinger D, Mohl W, Peltoranta M (1992): Prediction of the side of hand movements from single-trial multi-channel EEG data using neural networks. *Electroencephalogr Clin Neurophysiol* 82:313–315.

- Pfurtscheller G, Neuper C, Krausz G (2000): Functional dissociation of lower and upper frequency mu rhythms in relation to voluntary limb movement. *Clin Neurophysiol* 111:1873–1879.
- Pfurtscheller G, Stancak A Jr, Neuper C (1996): Event-related synchronization (ERS) in the alpha band—An electrophysiological correlate of cortical idling: a review. *Int J Psychophysiol* 24: 39–46.
- Pineda JA (2005): The functional significance of mu rhythms: translating seeing and hearing into doing. *Brain Res Brain Res Rev* 50:57–68.
- Pollen DA, Trachtenberg MC (1972): Some problems of occipital alpha block in man. *Brain Res* 41:303–314.
- Raichle ME, MacLeod AM, Snyder AZ, Powers WJ, Gusnard DA, Shulman GL (2001): A default mode of brain function. *Proc Natl Acad Sci USA* 98:676–682.
- Raichle ME, Snyder AZ (2007): A default mode of brain function: A brief history of an evolving idea. *Neuroimage* 37:1083–1090; discussion 1097–1089.
- Roelfsema PR, Engel AK, König P, Singer W (1997): Visuomotor integration is associated with zero time-lag synchronization among cortical areas. *Nature* 385:157–161.
- Rosas HD, Lee SY, Bender AC, Zaleta AK, Vangel M, Yu P, Fischl B, Pappu V (2010): Altered white matter microstructure in the corpus callosum in Huntington’s disease: Implications for cortical. *Neuroimage* 49:2995–3004.
- Rubinov M, Sporns O (2010): Complex network measures of brain connectivity: Uses and interpretations. *Neuroimage* 52:1059–1069.
- Salvador R, Suckling J, Coleman MR, Pickard JD, Menon D, Bullmore E (2005): Neurophysiological architecture of functional magnetic resonance images of human brain. *Cereb Cortex* 15:1332–1342.
- Scheeringa R, Bastiaansen MC, Petersson KM, Oostenveld R, Norris DG, Hagoort P (2008): Frontal theta EEG activity correlates negatively with the default mode network in resting state. *Int J Psychophysiol* 67:242–251.
- Schmithorst VJ, Holland SK (2004): Comparison of three methods for generating group statistical inferences from independent component analysis of functional magnetic resonance imaging data. *J Magn Reson Imaging* 19:365–368.
- Schurmann M, Basar E (1999): Alpha oscillations shed new light on relation between EEG and single neurons. *Neurosci Res* 33:79–80.
- Sereno MI, Pitzalis S, Martinez A (2001): Mapping of contralateral space in retinotopic coordinates by a parietal cortical area in humans. *Science* 294:1350–1354.
- Shackman AJ, McMenamin BW, Slagter HA, Maxwell JS, Greischar LL, Davidson RJ (2009): Electromyogenic artifacts and electroencephalographic inferences. *Brain Topogr* 22:7–12.
- Shulman GL, Fiez JA, Corbetta M, Buckner RL, Miezin FM, Raichle ME, Petersen SE (1997): Common blood flow changes across visual tasks: II. Decreases in cerebral cortex. *J Cogn Neurosci* 9:648–663.
- Sridharan D, Levitin DJ, Menon V (2008): A critical role for the right fronto-insular cortex in switching between central-executive and default-mode networks. *Proc Natl Acad Sci USA* 105: 12569–12574.
- Stam CJ, Nolte G, Daffertshofer A (2007): Phase lag index: Assessment of functional connectivity from multi channel EEG and MEG with diminished bias from common sources. *Hum Brain Mapp* 28:1178–1193.
- Steriade M (2001): Impact of network activities on neuronal properties in corticothalamic systems. *J Neurophysiol* 86:1–39.
- Steriade M (2006): Grouping of brain rhythms in corticothalamic systems. *Neuroscience* 137:1087–1106.
- Sun M (1997): An efficient algorithm for computing multishell spherical volume conductor models in EEG dipole source localization. *IEEE Trans Biomed Eng* 44:1243–1252.
- Talairach J, Tournoux P (1988): Co-planar stereotaxic atlas of the human brain. 3-Dimensional proportional system: An approach to cerebral imaging. Stuttgart, New York: Georg Thieme Verlag/Thieme Medical Publishers.
- Tinguely G, Finelli LA, Landolt HP, Borbely AA, Achermann P (2006): Functional EEG topography in sleep and waking: state-dependent and state-independent features. *Neuroimage* 32:283–292.
- Torgerson WS (1952): Multidimensional scaling: Theory and method. *Psychometrika* 17:401–419.
- Trujillo-Barreto NJ, Aubert-Vazquez E, Valdes-Sosa PA (2004): Bayesian model averaging in EEG/MEG imaging. *Neuroimage* 21:1300–1319.
- Tyvaert L, Levan P, Grova C, Dubeau F, Gotman J (2008): Effects of fluctuating physiological rhythms during prolonged EEG-fMRI studies. *Clin Neurophysiol* 119:2762–2774.
- Uddin LQ, Kelly AM, Biswal BB, Xavier Castellanos F, Milham MP (2009): Functional connectivity of default mode network components: Correlation, anticorrelation, and causality. *Hum Brain Mapp* 30:625–637.
- Vanni S, Portin K, Virsu V, Hari R (1999): Mu rhythm modulation during changes of visual percepts. *Neuroscience* 91:21–31.
- Vigario R, Oja E (2000): Independence: a new criterion for the analysis of the electromagnetic fields in the global brain? *Neural Netw* 13:891–907.
- Viola FC, Thorne J, Edmonds B, Schneider T, Eichele T, Debener S (2009): Semi-automatic identification of independent components representing EEG artifact. *Clin Neurophysiol* 120:868–877.
- Virji-Babul N, Cheung T, Weeks D, Herdman AT, Cheyne D (2007): Magnetoencephalographic analysis of cortical activity in adults with and without Down syndrome. *J Intellect Disabil Res* 51:982–987.
- van den Heuvel MP, Hulshoff Pol HE (2010): Exploring the brain network: A review on resting-state fMRI functional connectivity. *Eur Neuropsychopharmacol* 20:519–534.
- van de Ven VG, Formisano E, Prvulovic D, Roeder CH, Linden DEJ (2004): Functional connectivity as revealed by spatial independent component analysis of fMRI measurements during rest. *Hum Brain Mapp* 22:165–178.
- von Stein A, Chiang C, König P (2000): Top-down processing mediated by interareal synchronization. *Proc Natl Acad Sci USA* 97:14748–14753.
- Winter WR, Nunez PL, Ding J, Srinivasan R (2007): Comparison of the effect of volume conduction on EEG coherence with the effect of field spread on MEG coherence. *Stat Med* 26:3946–3957.
- Yan C, Liu D, He Y, Zou Q, Zhu C, Zuo X, Long X, Zang Y (2009): Spontaneous brain activity in the default mode network is sensitive to different resting-state conditions with limited cognitive load. *PLoS One* 4:e5743.